RICE UNIVERSITY

Characterization of the Temporomandibular Joint Disc and Fibrocartilage Engineering using Human Embryonic Stem Cells
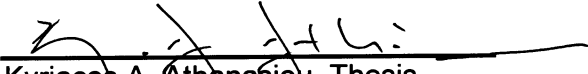
by

Vincent P. Willard

A THESIS SUBMITTED
IN PARTIAL FULFILLMENT OF THE
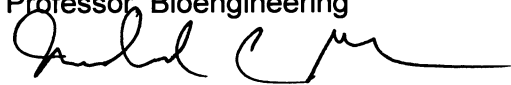REQUIREMENTS FOR THE DEGREE

Doctor of Philosophy
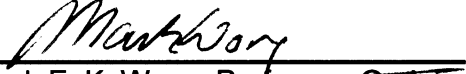
APPROVED, THESIS COMMITTEE:

Kyriacos A. Athanasiou, Thesis
Director, Distinguished Professor,
Biomedical Engineering, UC Davis

Antonios G. Mikos, Committee
Chair, Louis Calder Professor,
Bioengineering

K. Jane Grande-Allen, Associate
Professor, Bioengineering

Michael C. Gustin, Professor,
Biochemistry and Cell Biology

Jerry C. Hu, Development Engineer,
Biomedical Engineering, UC Davis

Mark E. K. Wong, Professor, Oral
and Maxillofacial Surgery, UT Dental
Branch at Houston

HOUSTON, TEXAS
MAY, 2011

Abstract

Characterization of the Temporomandibular Joint Disc and Fibrocartilage

Engineering using Human Embryonic Stem Cells

by

Vincent P. Willard

Fibrocartilages in the body, including the temporomandibular joint (TMJ) disc and knee meniscus, lack intrinsic healing capacity following trauma or disease. Current treatments only address the symptoms of fibrocartilage damage and do nothing to prevent further degradation of the joint. A tissue engineered replacement, with biochemical and biomechanical properties approaching those of native tissue, could provide a solution. This thesis investigates two components critical to the generation of a tissue engineered TMJ disc: 1) characterization of the native disc to identify a suitable animal model and create design parameters, and 2) development of approaches to use human embryonic stem cells (hESCs) in fibrocartilage tissue engineering.

The first step to achieving this goal was to identify an animal model for the human TMJ disc based on quantitative biochemical and biomechanical properties. To this end, rabbit, goat, pig, cow, and human discs were analyzed, and the pig disc was shown to possess properties most similar to the human. The next step was to further characterize the pig TMJ, as many aspects of the joint were still poorly understood. Though the TMJ disc is anchored to the surrounding bony tissue on all sides by discal attachments, little was known about their properties. Biochemical and histological analysis was performed on

these attachments and indicated that they are similar to the disc but possess distinct regional matrix content related to joint biomechanics. Finally, though the contribution of collagen to the mechanical properties of the TMJ disc was well characterized, the contribution of the glycosaminoglycans (GAGs) was unknown. By removing sulfated GAGs with chondroitinase ABC, it was found that these molecules contribute to the viscoelastic compressive properties of the disc, but only in regions with the highest native GAG content.

The second aspect of this thesis involved producing fibrocartilage tissue from hESCs. The pluripotency and unlimited self-renewal of these cells makes them ideally suited for producing fibrocartilages that contain a spectrum of matrix components. This work began by investigating what factors are necessary for fibrochondrogenic differentiation of hESCs in embryoid bodies (EBs). Growth factors and co-cultures with primary fibrochondrocytes were both shown to be potent modulators of fibrochondrogenesis, although differentiation of hESCs consistently produced a heterogeneous cell population. To purify populations of fibrochondrocytes differentiated form hESCs, two inexpensive and novel techniques were investigated. First, density gradient separation was the first technique attempted. This technique was able to isolate distinct subpopulations of cells, some of which were mechanically similar to native chondrocytes. Second, a chondrogenic tuning technique was applied to differentiated hESCs. Following fibrochondrogenesis in EBs, cells were expanded in monolayer in chondrocyte specific media before being used for tissue engineering. Chondrogenic tuning produced several distinct cell populations during expansion,

and, as a result, a spectrum of different cartilaginous tissues was achieved for tissue engineering. Three of the cell populations produced tissues similar to the native TMJ disc, outer meniscus, and inner meniscus.

Overall, this thesis identified an animal model for TMJ characterization and *in vivo* studies, furthered understanding of structure-function relationships of the TMJ disc and its attachments, and developed a technique for producing a spectrum of engineered fibrocartilages from hESCs.

Acknowledgements

The completion of this thesis has been a transforming process both personally and professionally. It has been a long road over the last six years and I am extremely grateful for all of those who have helped me along the way. I would first like to thank my thesis director, Dr. Kyriacos Athanasiou. I am eternally grateful for his mentorship and training, both related to science and life. I would also like to thank the other members of my thesis committee, Dr. Antonios Mikos, Dr. Jane Grande-Allen, Dr. Michael Gustin, Dr. Jerry Hu, and Dr. Mark Wong for their insightful comments on my research and willingness to support me along the way.

There is no way I could have completed this thesis without those who came before me. Although I can't list all of them here, I would like express extreme gratitude to all members of the Athanasiou lab past, present, and future. In particular I would like to thank Ms. Johannah Sanchez-Adams; our professional and personal collaborations mean everything to me. To my mentors (Drs. Dierdre Anderson, Gwen Hoben and Eugene Koay), thank you for your time and patience. I would like to thank Dr. Jerry Hu for always being a skeptic, but also for being a wizard with grant submissions. To my fellow Athanasiou class of 2005 members (Drs. Kerem Kalpakci, Dan Huey, Gidon Ofek, and Ben Elder), it was quite a ride and there is no way I would have made it through without you. I would like to thank Sriram and Donald for being crazy enough to move to CA and always inspiring me with your artistic talents. I have also worked with several

talented undergraduates over the last few years (Andrew, Wendy, and Raymond) and I'm always appreciative of their hard work.

Finally, I would like to thank my family, for without them I most certainly would not be in a position to write this thesis. In particular, I would like to thank my mom for being there for me every second of my life, but always letting me make my own decisions. Dad, Lisa, and Pops, thanks for always being a positive support for me, you can't ask for more from a parent. To my brothers, Zane and Jake, thank you for keeping me young. I also want to thank my extended family and friends for being such wonderful people whom I cherish dearly.

Table of Contents

Table of Figures

Chapter 6: Fibrochondrogenesis of hESCs: Growth factor combinations and co-cultures

Chapter 7: Mechanical Characterization of Differentiated Human Embryonic Stem Cells

Chapter 8: Producing a Spectrum of Cartilages from Human Embryonic Stem Cells by Employing a Chondrogenic Tuning Process

Table of Tables

Introduction

The fibrocartilaginous temporomandibular joint (TMJ) disc in the jaw is critical for such basic activities as talking and chewing. Unfortunately, displacement and degradation of this tissue is associated with chronic pathologies in millions of Americans. A functional tissue engineered TMJ disc replacement may finally provide relief for this patient population. Towards this end, this thesis had two global objectives: 1) to create a set of design parameters for tissue engineering of the TMJ disc, and 2) to use human embryonic stem cells (hESCs) for tissue engineering of the TMJ disc and other fibrocartilages. These two objectives were conducted under the following governing hypotheses. First, *the TMJ disc and its attachments possess distinct regional and interspecies variations based on functional requirements.* Second, *fibrocartilage can be engineered using human embryonic stem cells.* These overall hypotheses were investigated via the following specific aims:

1. <u>To identify an appropriate large animal model for the human TMJ disc.</u> To complete this aim, regional quantitative biochemical and biomechanical properties of rabbit, goat, pig, and cow discs were compared to those of human discs. *It was hypothesized that: 1) TMJ discs from all species would possess distinct regional variations, and 2) the pig disc would be most similar to the human, based on previously observed anatomical resemblances.* In this aim, regional biochemical (collagen, GAG, and DNA content), biomechanical (tension and compression), and histological (GAG and cell distribution) assessments were performed.

2. <u>To understand the TMJ disc attachments and structure-function relationships within the disc</u>. This aim was initiated by characterizing the biochemical and histological properties of the TMJ attachments and comparing them to the disc itself. *It was hypothesized that the attachments of the disc would show biochemical similarity to the disc itself, but that regional variations in biochemical content would be observed.* Next, structure-function relationships within the disc were investigated by probing the role of sulfated GAGs in disc compressive properties. *It was hypothesized that sulfated GAG depletion in the TMJ disc would have minimal impact on the tissue's compressive moduli.* Stress-relaxation compressive testing, biochemical examinations, and histological assessments were used in this aim.

3. <u>To use human embryonic stem cells as a cell source for fibrocartilage tissue engineering</u>. This aim was initiated by investigating the use of growth factors and hESC co-cultures with primary cells for fibrochondrogenesis. *It was hypothesized that growth factors and co-cultures would differentially regulate fibrochondrogenesis of hESCs.* Next, purification of differentiated hESCs using density gradient separation was investigated. *It was hypothesized that one gradient layer would contain a cell population that is phenotypically and mechanically similar to native chondrocytes.* Finally, a chondrogenic tuning technique was applied between the differentiation and tissue engineering steps. *It was hypothesized that the phenotype of EB derived chondroprogenitors would*

be modified during the course of the chondrogenic tuning process, resulting in a variety of tissue engineered cartilages. Flow cytometry, qRT-PCR, and single cell mechanical testing were used to evaluate cell phenotype in this aim. Biochemical and histological assessments were used to evaluate tissue created by differentiated hESCs.

The following chapters provide background for this work and explain the experimental results related to the specific aims of this thesis. Chapter 1 provides an introduction to the TMJ disc. The etiology of TMJ disorders and motivation for engineering of the TMJ disc are described. Additionally, all prior work to characterize and engineer the disc is detailed, as they are a stepping off point for the experimental work completed in this thesis.

All work related to the first global objective, to create a set of design parameters for tissue engineering of the TMJ disc, is described in chapters 2 – 4. Chapter 2 describes the work related to Specific Aim 1. This chapter details quantitative biochemical and biomechanical comparisons between TMJ discs from rabbits, goats, pigs, cows, and humans. This work allowed for further investigation of the TMJ disc in Aim 2, as described in chapters 3 and 4. Chapter 3 provides a description of the biochemical and histological characterization of the TMJ disc attachments. Chapter 4 investigates the contribution of sulfated GAGs to the regional viscoelastic compressive properties of the TMJ disc.

Chapter 5 provides a detailed introduction to the TMJ as a whole. The current anatomical, characterization, and tissue engineering studies related to all cartilages and bones are described. There is a complete description of prior work

related to all three fibrocartilages of the TMJ: the disc, fossa cartilage, and condylar cartilage. This chapter provided a useful introduction to the work in Specific Aim 3, because fibrocartilage engineered from hESCs could potentially be used not only for replacing the TMJ disc, but also the condylar and fossa cartilages.

Experimental work related to the second global objective, to use human embryonic stem cells (hESCs) for tissue engineering of the TMJ disc and other fibrocartilages, is described in chapters 6 – 8. These chapters also detail all work related to Specific Aim 3. Chapter 6 investigates growth factor combinations and co-culture with primary cells towards fibrochondrogenesis of hESCs. Chapters 7 and 8 look at two distinct ways of isolating fibrochondrogenic cells from hESCs with enhanced homogeneity. Chapter 7 describes the use of density gradient separation for isolating subpopulations of differentiated cells. Chapter 8 investigates the application of a chondrogenic tuning process to differentiated hESCs to modulate the engineered fibrocartilage that they produce.

The cumulative knowledge obtained in these studies is summarized in the Conclusions chapter. Overarching principles of this work are discussed, and directions for future studies are described.

Chapter 1: Is tissue engineering of the TMJ disc a feasible process?

Abstract

Temporomandibular joint (TMJ) disorders are common and difficult to remedy. Tissue engineering is one alternative that seeks to improve TMJ surgical treatment options. Tissue engineering aims to replace diseased or injured tissue with biologically engineered constructs. These constructs should reproduce native function and limit an immune response. To achieve tissue engineering success, it is important to first understand the tissue's cellular, biochemical, and mechanical properties in order to create validation and design criteria. Reviewed herein are the known properties of the TMJ disc and initial attempts toward TMJ disc tissue engineering. Important aspects of tissue engineering are scaffold selection, cell source, biochemical factors, and mechanical stimuli.

Motivation

The temporomandibular joint (TMJ), or jaw joint, is used throughout normal everyday functions such as eating or talking. Thus, disease or injury of this joint greatly decreases a patient's quality of life. Common activities become difficult and painful for patients with a TMJ disorder (TMD). The prevalence of

TMJ dysfunction is surprisingly high; based on various epidemiological studies, 28-88% of the population exhibit some physical sign or symptom of a TMJ dysfunction.[4]

Around one-fifth of patients exhibiting symptoms seek medical treatment for TMDs.[5] In the United States, there is an estimated 10 million TMD patients[6]; around 70% of patients seeking treatment exhibit a displaced TMJ disc.[7] Figure 1 illustrates the five stages of TMJ disc internal derangement as described by Wilkes[8]; the patient population from this study had an average age of 31 years and a female to male ratio of 7:1, common characteristics of the TMD patient population.

In addition to joint pain, TMD symptoms include headaches, earaches, jaw clicking, limited jaw opening, and jaw lock.[4, 7, 9] Unfortunately, TMD symptoms offer little aid in understanding the cause of TMDs. Numerous treatment options for TMD patients exist, but standard approaches and treatments are rarely agreed upon, even among experts. TMJ treatments and surgical approaches are presented in greater detail in reviews by Wong et al.[10] and Dimitroulis.[11] Briefly, non-surgical options are the first treatment modality and include pain medication and physical therapy. Minimally invasive surgery, like arthrocentesis or arthroplasty, may be attempted in dysfunctional joints with limited tissue degradation; these procedures aim to reduce inflammation or repair the disc/attachments. When the disc is beyond repair, it may be removed (discectomy). Post-discectomy the joint may be left empty or replaced with autologous tissue. Synthetic discs are no longer implanted due to extensive wear

and immune response.[12] In the most extreme cases of degeneration, patients may opt for total joint replacement. Unfortunately, many TMDs are progressive, leading to extensive joint remodeling. Treatments primarily focus on the reduction of pain. This leaves the field of TMJ research primed for tissue engineering alternatives that have the potential to reduce pain and restore total function.

Disc characteristics

The TMJ disc is located between the mandibular condyle and fossa-eminence of the temporal bone (Figure 2). The joint is enclosed in a synovial capsule; the synovium serves to nourish and lubricate the joint.[13] The TMJ is a ginglymo-diarthrodial joint, meaning it exhibits both hinge-like and rotational motions. During normal movements, the disc translates anteriorly during jaw opening and posteriorly during closing. The presence of the disc's fibrous attachments is important to joint motions, but their exact mechanical function and location is heavily debated. The disc is believed to aid in joint lubrication as well as load distribution, jaw stabilization, and shock absorption.

The TMJ disc is divided into three regions: anterior band, posterior band, and intermediate zone (Figure 2). The posterior band is thicker than the anterior band; both bands are significantly thicker than the intermediate zone.[14] The disc is generally divided into these three regions for characterization purposes. The bilaminar zone, a fourth element of the disc, exists between the posterior band and the posterior attachments, but generally, is not considered part of the disc.

This region possesses some vasculature and is difficult to discern from the posterior attachment tissue.

While the disc is cartilaginous, it is very different from hyaline articular cartilage or even the knee meniscus.[15] A healthy TMJ disc is primarily avascular, although some vasculature can be found near the attachment regions. It is well hydrated, containing 70% water.[16] Similar to the knee meniscus, the TMJ disc exhibits a mixed population of cell types. In the porcine disc, there are approximately 70% fibroblast-like cells and 30% chondrocyte-like cells.[16] The percent of chondrocyte-like cells increases in the intermediate zone and decreases in the bands. This cell population is indicative of the disc's proper characterization as fibrocartilage.

The extracellular matrix (ECM) of the disc is essential to tissue function and important to thoroughly understand before attempting to engineer a construct. The TMJ disc is primarily collagen, and the collagen of the TMJ disc is nearly all collagen type I. Collagen type I makes up the majority of the disc's dry weight, approximately 85%.[17] Trace amounts of types II, III, VI, IX, and XII can be found in various animal models.[18-23] The fibers of the disc are primarily oriented circumferentially around the outer regions of the disc.[24] In the intermediate zone, fibers are more random but possess a primarily anteroposterior alignment. Collagen fibers in the porcine disc have an average diameter of 18 ± 9 μm with a range of 2.9 to 37.4 μm.[25] Parallel to the collagen fibers are elastin fibers, which are found in all regions.[20, 25-27]

Glycosaminoglycans (GAGs) and proteoglycans (PGs) are also important components of tissue ECM. The TMJ disc contains approximately 5% GAGs on a dry weight basis.[17, 25, 28] Chondroitin sulfate is the most prevalent GAG in the disc, comprising 70-80% of the total GAG content.[17, 25, 29] Aggrecan is an example of a chondroitin sulfate PG that is present in the disc and is important in hydration, lubrication, and compressive strength.[30] Dermatan sulfate is the next most abundant GAG in the disc, making up 15-25% of total GAG content.[17, 29, 31] Dermatan sulfate PGs include decorin and biglycan, which are important in controlling the collagen fiber lateral packing ability and diameter size.[30] Hyaluronic acid, which binds non-convanently to aggrecan, has been found in the range of 2.8-10% of the total GAG content.[17, 28, 29, 32] Heparan sulfate was found as 4.3% of total GAG content in the human disc.[28] Keratan sulfate GAGs are generally considered a trace component of the TMJ disc but have been measured up to 2% of the total GAGs.[17, 25, 29, 31]

Mechanical properties of the TMJ disc are important to understand since engineered constructs must support the necessary load imparted on the native tissue. The tensile elastic modulus of the porcine TMJ disc is higher in the anteroposterior direction than the mediolateral direction at 76.4 MPa and 3.2 MPa, respectively.[33] In the mediolateral direction, Detamore and Athanasiou[34] found significant differences between the posterior band, anterior band, and intermediate zone with relaxation moduli of 23.4 MPa, 9.5 MPa, and 0.58 MPa, respectively. In the anteroposterior direction, the stiffest region was the central section followed by the medial section and then lateral section.[34, 35]

Several methods have proved useful in modeling the compressive properties of the TMJ disc. An elastic, compressive modulus for human discs was observed in the range of 211 kPa to 514 kPa, dependent on the strain rate.[36] The biphasic theory has been employed frequently since its conception to illustrate a tissue's viscoelastic characteristics.[37] Biphasic modeling of the porcine TMJ disc yielded properties of 20.1 kPa for the aggregate modulus, 0.45 for the Poisson's ratio, and 24.1×10^{-15} m^4/Ns for the permeability.[38] Most recently, unconfined compression, stress relaxation tests were performed to give the surface-regional instantaneous and relaxation moduli of the porcine disc. These values were found to be strain dependent, ranging from 90-3870 kPa (instantaneous modulus) and from 16.9-74.6 kPa (relaxation modulus) for 10%-30% strain, respectively. The coefficient of viscosity was also strain dependent, ranging from 1.3-13.8 MPa*s.[39]

Shear properties of the TMJ disc have recently received due attention. Tanaka et al.[40] found a storage modulus between 0.78-2.0 MPa depending on the compressive strain and percent shear. A loss modulus near 0.4 MPa and loss tangent ranging from 0.2-0.25 MPa was observed.

Tissue engineering

Tissue engineering is a potential option for the future treatment of diseased or injured discs. The general approach to tissue engineering involves selection of a cell source, seeding these cells on an appropriate scaffold, and applying external stimuli to encourage ECM production and organization. These

external stimuli may be grouped into two general categories: biochemical and mechanical. Tissue engineering approaches may commence *ex vivo* or *in vivo* and may exclude one or more of the aforementioned factors (cells, scaffold, and stimuli). For example, skin therapies have been successful using acellular collagen scaffolds. However, all tissue engineering therapies aim to replace the native tissue characteristics through tissue remodeling or regeneration. TMJ tissue engineering has focused on the combination of scaffolds, cells, and stimuli *in vitro* as illustrated in figure 3.

Scaffolds

Scaffolds, an important part of a construct's initial mechanical integrity, provide surface area for cell attachment. The earliest tissue engineering study used a porous collagen scaffold; after two weeks the construct appeared similar to the disc in gross morphology and cell shape.[41] Later, researchers attempting to create a replacement for the TMJ disc used fibers of polyglycolic acid (PGA) and polylactid acid (PLA) and concluded that both scaffold materials were able to support cell attachment, matrix production, and retain testable mechanical properties after 12 weeks.[42] Another study compared PGA, polyamide filaments, expanded polytetrafluoroethylene (ePTFE) filaments, and bone blocks.[43] While all these scaffolds supported cell attachment and a small amount of collagen production, they were unable to form neotissue after 4 or 8 weeks. Tissue engineering studies in our lab have primarily used PGA non-woven meshes.[44-48] While PGA supports cell attachment and matrix production, it degrades very

rapidly, leaving constructs with limited mechanical integrity after only a few weeks. PLA non-woven mesh, however, has shown promise in retaining tensile and compressive integrity over a similar time scale.[49]

Some researchers have investigated novel materials for TMJ disc engineering that would allow custom-shaped scaffolds to be implanted through minimally invasive surgery.[50] Acrylated collagen type I scaffolds were successfully photopolymerized through a layer of rat skin; in this study, viability of osteoblasts in a photopolymerized poly(ethylene oxide) dimethacrylate was demonstrated, suggesting this process could be accomplished with other cell types. However, corresponding data for TMJ disc cells encapsulated in alginate showed a drastic decrease is cell numbers at 4 and 8 weeks of culture with no ECM production at any time point, suggesting TMJ disc cells may not survive an encapsulated environment.[51]

Cell source

The cell source for a tissue engineering study is tremendously important, but limited research has been conducted in TMJ disc engineering studies. The most commonly used cells for these experiments are derived from the TMJ disc[41, 43-48, 51, 52] or articular cartilage.[42, 43, 53] A major hurdle to overcome in tissue engineering is that tissue engineering generally requires a large cell population to create a construct. While passaged cells may seem appealing, chondrocytes have been found to de-differentiate to a more fibroblastic phenotype after only a couple of passages.[1] Additionally, TMJ disc cells showed a decreased

expression for ECM proteins with the exception of decorin and biglycan due to passage (Figure 4).[2] Thus, for the future of TMJ disc engineering, a cell source that can yield a large population of TMJ disc cells, or a population of cells that rapidly fill a scaffold, must be identified.

As mentioned previously, after a discectomy, surgeons may replace the disc with some type of autologous tissue, such as skin, auricular cartilage, dura mater, temporalis muscle, or temporalis fascia.[42] Any of these tissues may serve as potential cell sources for the TMJ disc, but one of the most appealing in terms of clinical feasibility and patient comfort is dermis. Adult dermal fibroblasts have been shown to produce matrix indicative of a chondrocytic phenotype when seeded on aggrecan-coated plates (Figure 4).[3]

Biochemical factors

Growth factors are commonly used in tissue engineering studies. Four studies have demonstrated the potential of growth factors for TMJ disc tissue engineering. This potential was first observed using transforming growth factor-β_1 (TGF-β_1) and prostaglandin E_2 (PGE$_2$) on bovine TMJ disc cells in monolayer. TGF-β_1 increased cell proliferation by 250%, while PGE$_2$ had no significant effect.[23] Also in monolayer, the effects of platelet derived growth factor (PDGF), insulin like growth factor (IGF) and basic fibroblast growth factor (bFGF) on porcine TMJ disc cells demonstrated that lower concentrations of these growth factors favored biosynthesis, while higher concentrations favored proliferation.[47] The most beneficial growth factors were IGF-I and bFGF, which both showed

significant increases in collagen synthesis and cell proliferation. The effects of IGF-I, bFGF and TGF-β_1 on porcine TMJ disc cells in PGA scaffolds showed increased collagen production when exposed to low concentrations of IGF-I and TGF-β_1[48], but no other significant differences between the experimental groups existed. In the end, IGF-I was recommended for future tissue engineering studies due to low cost and beneficial collagen production. Of course, the native tissue is exposed to a variety of growth factors; so, it is possible growth factor combinations will be more beneficial than any single factor. IGF-I, bFGF, and TGF-β_1 have been investigated in combinations of two to determine if synergistic effects exist.[45] All constructs exposed to growth factor combinations improved in structural integrity compared to a no growth factor control, but no combination was statistically significant in terms of biochemical or mechanical properties. While synergistic effects were not observed, improved overall cellularity of the constructs was noted when both growth factors were used at a high concentration.

Although growth factors have received the most attention, positive biochemical stimulation is also likely to come from culture conditions and cellular interactions as well. An ascorbic acid concentration of 25 µg/mL has been shown to produce constructs with higher total collagen content and higher aggregate modulus relative to concentrations of 0 µg/mL or 50 µg/mL.[46] This was likely associated with improved seeding observed for the constructs cultured in 25 µg/mL of ascorbic acid. Initial cell seeding is another important consideration in any tissue engineering construct due to cell-to-cell interactions and signaling.

Almarza and Athanasiou[44] showed that PGA scaffolds seeded at saturation increased cellularity and ECM content relative to scaffolds seeded below saturation.

Mechanical stimulation

The native TMJ disc undergoes significant loading, which is often broken down into compression, tension, and shear components.[54] While cells proliferate and produce ECM in static culture, mechanical stimuli may be required to produce an optimal tissue engineered construct. A variety of mechanical stimuli may be beneficial including compression, tension, hydrostatic pressure, and fluid shear stress. Darling and Athanasiou[55] have published an extensive review of the mechanical bioreactors that have been used in engineering cartilaginous tissues.

Three recent studies have investigated the effects of mechanical stimulation on TMJ disc constructs. A low-shear fluid environment by means of a rotating wall bioreactor created constructs with dense matrix and cell composition[56]; however, when the biochemical content of these constructs was compared to those grown in static culture, no clear benefit of the bioreactor was observed. When disc cells were exposed to hydrostatic pressure in monolayer or PGA scaffolds, constant hydrostatic pressure at 10 MPa increased collagen production compared to static culture.[52] In contrast, intermittent hydrostatic pressure from 0 to 10 MPa at 1 Hz frequency was detrimental to the constructs, producing less collagen and GAGs than unloaded controls. These results were consistent in both two and three-dimensional culture. In another recent study,

dynamic tensile strain significantly reduced interleukin-1β induced up regulation of matrix metalloproteinase.[57] This may have implications on future tissue engineering studies since MMPs play an important role in ECM degradation and remodeling.

Future directions for TMJ disc tissue engineering

While TMJ disc tissue engineering is in its infancy, other musculoskeletal tissues have been studied to a greater extent. These tissues include articular cartilage, bone, and tendon. TMJ disc tissue engineering should build on not only past TMJ research but also successes in these other tissues, while keeping in mind the disc's structural and functional differences.

The issue of scaffold certainly requires further investigation. Scaffolds that degrade too quickly are unable to provide the necessary mechanical integrity; thus, future research may focus on polymers with longer degradation times or that encourage rapid ECM production. Alternatively, using natural polymers like collagen may be effective since cells would simply remodel existing matrix instead of forming a new collagen network, thereby decreasing the time until the scaffold reaches a functional state. A third option is a scaffoldless or self-assembling process. Such approaches have been examined in both tendon and articular cartilage.[58, 59] While these methods require refinement to increase mechanical strength, data suggest these approaches may offer a new direction in soft tissue engineering. Furthermore, by eliminating the scaffold material within

an engineering construct, concerns over mechanical integrity and cell toxicity due to the scaffold degradation process are diminished.

An optimal cell source is necessary for tissue engineering to be realized. To date, no such source has been identified that is likely to be clinically sound. However, research in other musculoskeletal tissues like cartilage, tendon, and bone has explored the possibility of using mesenchymal stem cells for tissue engineering.[60-71] Using progenitor cells may also be desirable for the TMJ disc, since bone marrow or adipose tissue could potentially yield a large population of autologous, pluripotent cells. Alternatively, research on other potential cell sources, such as embryonic stem cells and dermis-derived fibroblasts, continues to demonstrate promise.

The inclusion of biochemical signaling will be an integral part of producing a TMJ disc tissue engineering construct. Significant work has been performed in both two- and three-dimensional cultures to determine optimal growth factor signaling for TMJ disc engineering. Recent work showed the growth factors IGF-I and TGF-β_1 used alone produced increases in collagen production.[48] This provides a basis for growth factor selection in future TMJ disc tissue engineering studies. Beyond growth factors, the media used for culturing should also be further investigated. Ascorbic acid concentration has influenced the outcome of engineered constructs[46]; thus, other media supplements may need further optimization as well. Cell-to-cell interactions are important, and seeding the cells in scaffolds at saturation was shown to produce constructs with significant

increases in ECM production[44]. This is clearly vital for fabrication of an optimal TMJ disc construct.

Cartilage is a mechanical tissue; thus, mechanical stimulation should be expected for regeneration of any cartilaginous tissue. The most successful mechanical stimulation used to date for the TMJ disc has been constant hydrostatic pressure.[52] Hydrostatic pressure should certainly be pursued further, because there are likely to be other beneficial loading regiments. Tension has shown promise in monolayer culture and should be pursued for future three-dimensional tissue engineering studies.[57] Success in engineering the knee meniscus has been seen using direct compression; these results may apply to the TMJ disc due to the fibrocartilaginous nature of both tissues.[72] Additionally, perfusion increased cellularity and ECM production in articular chondrocytes and may hold the same potential for the TMJ disc.[73] Perfusion may also create larger constructs due to increased nutrient circulation.

In conclusion, while the field of TMJ disc engineering remains young, significant progress has been achieved. With this progress have come new, challenging questions and a wealth of knowledge on the disc's characteristics. Related research may begin to merge with TMJ disc engineering due to the increased knowledge of TMJ disc design criteria. Tissue engineered TMJ constructs may now be validated with the increased fund of information on the tissue's native characteristics. With these tools at hand, TMJ research will continue to rapidly progress to, hopefully, a viable tissue engineering implant.

Figures

Figure 1

Early Stage — Slight anterior displacement

Early/Intermediate Stage — Slight thickening of posterior edge

Intermediate Stage — Anterior displacement with prolapse of the disc

Intermediate/Late Stage — Increased severity of intermediate stage with early to moderate hard tissue remodeling

Late Stage — Disc perforation, gross deformity of disc and hard tissues, essentially arthritic changes

Figure 1: The stages of TMJ internal derangement as described by Wilkes. Schematics describe the progression of TMJ internal derangement; these schematics were created based upon radiologic findings described by Wilkes.[8] In early stages, clinical symptoms are limited (no significant pain or mechanical symptoms); however, a slight anterior displacement of the disc can be observed. As the derangement progresses towards the intermediate stage, a few episodes of pain along with occasional joint tenderness, headaches, and mechanical problems are reported. Here, the disc displacement is slightly more forwards and the posterior edge thickens. At the intermediate stage, pain intensifies along with other clinical symptoms; anterior displacement of the disc is significant and coupled with disc prolapse. As the disorder progresses toward late stages, chronic pain develops; disc displacements are severe and hard tissue remodeling ensues. In late stages, joint scraping and difficulty in function are evident. The disc may be out of position, degenerated, or perforated. Hard tissue remodeling is severe; the joint is essentially arthritic.

Figure 2
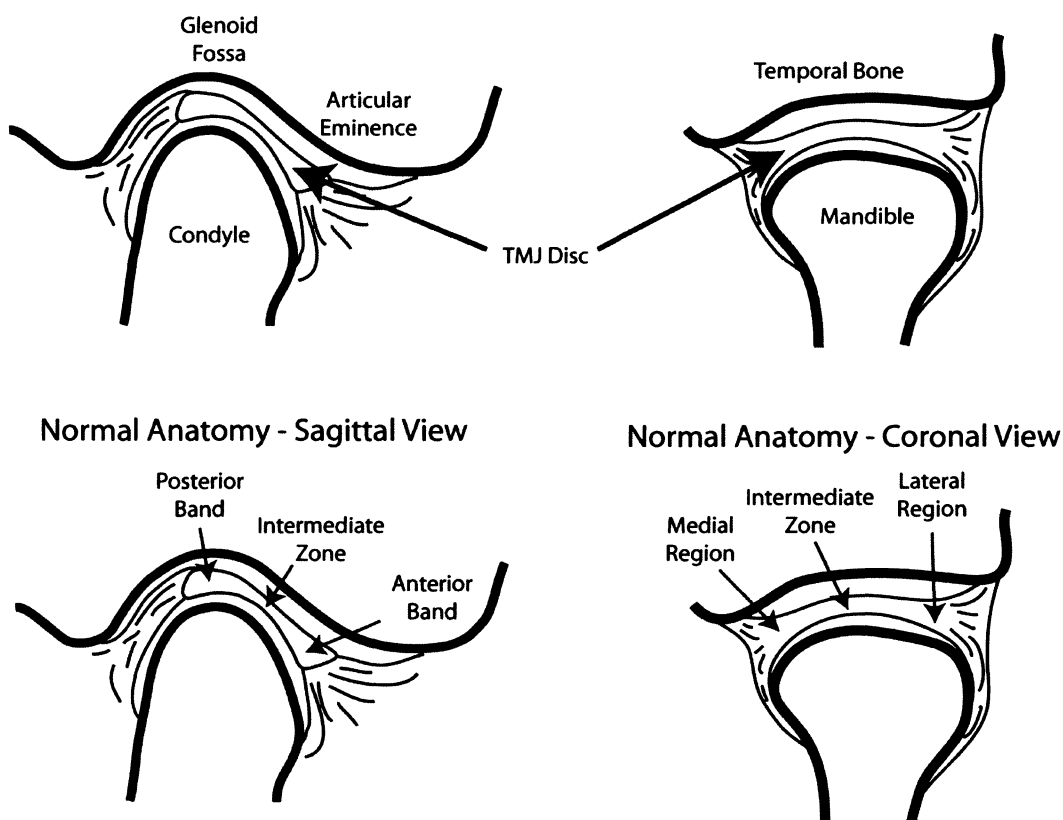
Figure 2: **Joint anatomy and disc regions**. The TMJ disc is located between the mandibular condyle and fossa-eminence of the temporal bone. The disc is fibrocartilaginous and has a biconcave shape in both sagittal and coronal views. Thickness variations are evident in the sagittal view, where the thick posterior and anterior bands differ significantly from the intermediate zone. In the coronal view, thickness variations are less pronounced; however, the medial and lateral extents of the disc are slightly thicker than the intermediate zone.

Figure 3

Cell Source
Tissue Engineering
TMJ Disc: Thomas (1991)
    Springer (2001)
    Almarza (2004b, 2005, 2005a, 2005b)
    Detamore (2004, 2005a)
    Bean (2005)
Shoulder Cartilage: Puelacher (1994)
Mandibular Condyle: Girdler (1998)
Fossa-Eminence: Springer (2001)

Related Studies
Dermal Fibroblasts: French (2004)
Articular Cartilage: Darling (2005)
TMJ Disc Cells: Allen (Submitted)
Stem Cells: Many

CELLS   SCAFFOLDS

SIGNALS

Scaffolds
Collagen I: Thomas (1991)
    Poshusta (2001)
PGA: Puelacher (1994)
    Almarza (2004)
PLLA: Puelacher (1994)
Alginate: Almarza (2004)
Polyamide: Springer (2001)
ePTFE: Springer (2001)
Bone Blocks: Springer (2001)

Biochemical Signals
TGF-β1: Landesberg (1996)
    Detamore (2005b)
    Almarza (2005b)
PGE₂: Landesberg (1996)
PDGF: Detamore (2004)
IGF-1: Detamore (2004, 2005 b)
    Almarza (2005b)
bFGF: Detamore (2004, 2005b)
    Almarza (2005b)
Ascorbic Acid: Bean (2005)
Cell-to-Cell Contact: Almarza (2005a)

Biomechanical Signals
TMJ Disc
Low Shear Fluid: Detamore (2005a)
Hydrostatic Pressure: Almarza (2005)

Relative Tissues
Tension: Deschner (2005)
Direct Compression/Tension: AufderHeide (2005)
Perfusion: Davisson (2002)

Figure 3: A tissue engineering paradigm: history of TMJ disc engineering.
Tissue engineering, generally, is conducted by combining cells and signals on an appropriate scaffolding material. This approach has been the standard thus far in TMJ disc engineering. References to significant studies of scaffolding, signals, and cell source for the TMJ disc are placed within the classic paradigm figure. Clearly, TMJ disc engineering is very young; however, it is apparent that the field is rapidly expanding.

Figure 4

Articular Chondrocytes

Articular chondrocyte expression changes
due to passage (Darling, 2005); this expression
profile becomes more fibroblastic with passage.

Fibrochondrocytes

Dermal fibroblasts have demonstrated chondrocytic potential
when seeded over proteins (French, 2004); thus, cell phenotype
may be recovered with proper techniques

TMJ disc cells also lose chondrocytic expression
with passage (Allen, submitted); however, these
cells also lose expression ofcollagen type I.

Limited Expression

Dermal Fibroblasts

Figure 4: From chondrocyte to fibroblast
In our laboratory, we have investigated the relationship between chondrocytes, fibrochondrocytes, and dermal fibroblasts. First, chondrocytes progressively dedifferentiate as a function of monolayer culture [1]. As these cells are passaged, they become more fibroblastic in nature, characterized by a loss of chondrocytic ECM gene expression and a gain in fibroblastic expression. Fibrochondrocytes follow a similar loss in gene expression; however, fibroblastic gene expression is also lost as a function of passage [2]. However, it may be possible to regain these losses by seeding passaged cells over proteins; dermal fibroblasts have demonstrated a chondrocytic response when seeded over specific extracellular matrix proteins [3].

Chapter 2: An Interspecies Comparison of the Temporomandibular Joint Disc

Abstract

The temporomandibular joint (TMJ) disc plays a critical role in normal function of the joint, and many disorders of the TMJ are a result of disc dysfunction. Previous quantitative TMJ characterization studies examined either the human or a specific animal model, but no single study has compared different species in the belief that differences in joint morphology, function, and diet would be reflected in the material properties of the disc. In this study, we examined topographical biochemical (collagen, glycosaminoglycan and DNA content) and biomechanical (tensile and compressive) properties of the human TMJ disc, and also discs from the cow, goat, pig, and rabbit. Regional and interspecies variations were identified in all parameters measured, and certain disc characteristics were observed across all species, such as a weak intermediate zone under mediolateral tension. While human discs possessed properties distinct from the other species, pig discs were most similar to the human, suggesting that the pig may be a suitable animal model for TMJ bioengineering efforts.

Introduction

The temporomandibular joint (TMJ) disc has several important functions, most notably the dissipation and distribution of masticatory loads.[74] Disorders of the TMJ are widespread, likely afflicting between 5% and 15% of the adult population[75], and approximately 70% of these are associated with displacement of the disc.[7] In its normal relationship, the disc is positioned between the mandibular condyle and glenoid fossa of the temporal bone. However, displacement leading to internal derangement can occur, resulting in uncoordinated movements of the disc relative to the joint surfaces.[76] Previous attempts to replace the disc with alloplastic devices have failed, resulting in further joint degradation.[77, 78] Therefore, studies aimed at tissue engineering the TMJ, and especially the disc, are warranted.[79, 80]

To establish design criteria for tissue engineering efforts, thorough characterization of native TMJ disc tissue is necessary. A general characterization of the biochemical makeup of the disc can be elucidated from previous examinations. Collagen constitutes approximately 30% of the wet weight[22], of which the majority is collagen type I. Total collagen concentration of the porcine disc is highest in the center relative to the lateral region.[81] The total concentration of glycosaminoglycans (GAGs) in the TMJ disc is between 0.6 to 10% of the dry weight[82]. Studies of pig and cow discs indicate that the greatest GAG content is located in the center relative to the periphery[31, 81], but the opposite trend has been seen in primate discs.[26] The cells of the TMJ disc reflect a heterogeneous fibrochondrocyte cell population consisting of both fibroblast

and chondrocyte-like cells. Regionally, the greatest DNA concentration and cell number have been seen in the medial portion of the pig disc[81], and the anterior and posterior bands of primate discs.[26]

Previous biomechanical examinations have highlighted anisotropic and heterogeneous properties. Tensile strength and stiffness correlate with local collagen orientation, with greater values present in the central region when tested in the anteroposterior direction relative to the mediolateral direction.[33, 34, 83] Compressive properties vary topographically; the relaxation modulus of the medial region is highest while the posterior and anterior bands appear to support the highest instantaneous loads.[38, 39, 84, 85] Overall, the disc is 10-1000 times softer under compression than it is under tension.[74]

While these studies have increased the collective knowledge of TMJ disc physiology, no single study has compared biomechanical and biochemical characteristics of the human disc to an animal model. Furthermore, there are no studies examining topographical variations or orientation-dependent characteristics. The porcine disc has been identified as the model most appropriate for comparison to the human based on similarities such as disc size and shape, joint anatomy, masticatory patterns, and omnivorous diet.[43, 86-88] Other species examined include cows[89, 90], dogs[83, 91], goats[92], rabbits[93, 94], rats[95], and sheep[96]. In an effort to better understand the quantitative similarities and differences between some of these models, this study compares the regional biochemical and biomechanical properties of the human, cow, goat, pig and rabbit discs.

Materials and Methods

Specimen Procurement

Tissue specimens were procured from skeletally mature sources over one month. Goat (8 months old (m.o.), half male, half female), pig (12 m.o., all female), rabbit (12 m.o., half male, half female), and cow (24 m.o., all female) heads with intact joint capsules were obtained from local abattoirs within hours of slaughter. Human TMJ discs were dissected from seven dentate female cadaver donors of age 63-84 years, mean age 73. All tissues were fresh or fresh frozen (human) and were never fixed. TMJ discs were carefully dissected from their attachments and verified to be grossly normal. Discs were washed in phosphate-buffered saline (PBS), then wrapped in gauze soaked with PBS containing protease inhibitors (10 mM N-ethylmaleimide and 1 mM phenylmethylsulfonyl fluoride, Sigma, St. Louis, MO) and frozen at -20°C until testing.

Biochemical Analysis

For quantitative biochemistry six (rabbit, goat, pig), five (cow), or four (human) left discs were thawed in PBS and then sectioned into five pieces as depicted in Fig. 1A. All specimens were blotted dry, weighed to obtain a wet weight, and then lyophilized for 48 h. Samples were digested in 1.5 mL of 125 mg/mL papain (Sigma) solution overnight at 60°C. The DNA content of the samples was measured by reaction of DNA with Picrogreen reagent (Invitrogen, Carlsbad, CA). The total amount of sulfated GAG was measured using a dimethylmethylene blue colorimetric assay kit (Biocolor, Newtownabbey, UK).

The total collagen content was determined using a hydroxyproline assay, as described previously.[81]

Histology

For topographical histology, a right disc from each species was divided into five regions as shown in Fig. 1A. Disc samples were snap frozen in freezing medium (Triangle Biomedical, Durham, NC) and cryo-sectioned at 12 µm in the anteroposterior direction. Qualitative analysis of sulfated GAG was conducted using safranin-O/fast green staining.

Tensile Sample Preparation and Testing Procedure

Discs from each species were thawed and cut into three regions in either an anteroposterior or mediolateral direction as described in Fig. 1B. Regions were sectioned in a cryotome to a uniform thickness between 300 and 600 µm, with a width of 1 mm. These sections were taken from the middle zone after removing the superior surface. Tests were conducted on a materials testing machine (Instron 5565, Canton, MA) in an isotonic saline bath at room temperature. A 0.02 N tare load was applied to the samples followed by preconditioning with 15 cycles of 5% strain at a rate of 10 mm/min. After preconditioning, step strains were applied at 5% increments beginning with 10% and up to 40%, with 10 min between steps for stress relaxation. Data were retained only from samples that failed away from the grips. Peak and relaxed

moduli were obtained by constructing stress vs. strain plots through points of peak and relaxed stresses at each step strain.[34]

Compression Sample Preparation and Testing Procedure

Cylindrical tissue plugs were taken from five regions of each disc as shown in Fig. 1A, and sectioned such that the superior and inferior surfaces were parallel using a cryotome. The final sample thicknesses ranged from 0.8 – 4 mm. Unconfined compression testing was performed on the Instron in a saline bath at room temperature. A 0.02 N tare load was applied to the sample, followed by preconditioning with 5% strain for 15 cycles. During the test, 10% step strains were applied from 10% up to 30% strain, with 10 min intervals between steps for stress relaxation. Values for instantaneous modulus, relaxation modulus, and coefficient of viscosity were obtained by fitting data to a viscoelastic solution for a Kelvin solid.[39]

Results

Gross Morphology

Gross morphology and measured dimensions of discs from all five species are presented in Fig. 1C – D. The pig was the only species that was not significantly different from the human in both mediolateral and anteroposterior dimensions.

Biochemical Analysis

Quantitative biochemical results and two-factor ANOVA analysis is shown in Fig. 2. Numerical data along with one-factor ANOVA analysis within each species can be found in Supplemental Table 3. The mean collagen content normalized to wet weight (ww) was found to vary between 16.5% and 30.1% for all species and regions tested. TMJ discs from the cow showed significantly greater collagen/ww than all other species except the pig (Fig. 2A). Human discs were not statistically different from either the pig or rabbit discs. The PBC displayed significantly greater collagen/ww than IZL, but there were no other statistical differences among the disc regions.

The mean DNA/ww varied between 0.0055% and 0.0358%, showing stark differences in both region and species. Human discs contained significantly less DNA/ww than all of the other species, but there were no other interspecies variations (Fig. 2B). Regionally, ABC and PBC contained significantly more DNA than all three regions of the intermediate zone. DNA content was the only biochemical parameter that showed a consistent trend in regional variation within the species (Supplemental Table 3).

The mean sulfated GAG/ww content was found to vary between 0.273% and 0.936% for all samples tested. Cow discs contained significantly more GAG/ww than all species except the goat (Fig. 2C). The GAG concentration of the human TMJ discs was significantly different from all other species, falling in-between the rabbit and pig discs. While all three regions of the intermediate zone possessed significantly more GAG than the anterior band, only IZM contained more GAG than the posterior band.

Histology

Histological staining supported the quantitative biochemical results. Positive safranin-O staining for sulfated GAGs is clearly visible in all samples except the anterior band of the human disc and all regions of the pig disc (Fig. 2D). Haematoxylin staining indicates fewer cells in human samples relative to the other four species, and fewer cells in the intermediate zone compared to the bands for the rabbit, goat, and pig specimens.

Tension

Peak and relaxed Young's moduli under tension are presented in Fig. 3. Raw data for tensile properties with one-way and two-way ANOVA analysis are shown in Supplemental Table 1. Analysis of intraspecies topographical variation demonstrated significance for all parameters. Topographically, the ML C samples exhibited weaker and softer behavior than all other groups, though no other regional variation was found (Fig. 3A and B). With regard to interspecies variation, human tissue was significantly stiffer and stronger than all other species, while rabbit tissue was softer than all other groups. Strength values ranged from 0.2 MPa for bovine ML C to 13.8 MPa for the human AP C tissue. The human AP C group also displayed the highest peak and relaxed moduli of 51.7 MPa and 34.4 MPa, compared with the bovine ML C values of 0.2 MPa and 0.1 MPa, respectively.

Compression

Instantaneous and equilibrium compressive moduli at 20% strain are shown in Fig. 4. Raw data for compressive assessments with one-way and two-way ANOVA analysis are shown in Supplemental Table 2. All parameters increased with increasing strain. The interspecies analysis showed that the bovine, leporine, and caprine tissue had the highest relaxation and instantaneous moduli (Fig. 4A and B). Porcine tissue had the lowest moduli overall, and was similar to human tissue at 20% and 30% strain for both moduli. Topographically, the bands yielded higher instantaneous and relaxed moduli relative to the intermediate zone samples, with the exception of the relaxation modulus of the IZC region. The highest relaxed modulus of 199 kPa was obtained from the bovine PBC samples, while the highest instantaneous modulus of 6.55 MPa was noted from the goat ABC group. The softest tissue was from the lateral region of the pig disc. The band regions of the goat and cow displayed the highest viscosity coefficients, with values between 35 and 40 MPa · s at 30% strain.

Discussion

While previous studies of the TMJ disc investigated regional variation in biochemical and biomechanical properties, this study is the first to examine these properties across species. Furthermore, this is the first study to quantify both biochemical and biomechanical properties concurrently. The advantage of this study's approach is that animal models could be compared to the human disc using the same testing methods in a consistent environment, mitigating variability associated with comparisons made across different studies. Due to the

contradictory nature of prior studies, the results of this investigation do not agree with all prior work, but they are consistent with previous studies performed in our group using the pig model.[25, 34, 39, 81, 85] The interspecies characterization data collected here will provide valuable design parameters for tissue engineers seeking to recapitulate the properties of the disc *in vitro*, and for those looking to study functional replacements *in vivo*.

Prior studies have indicated that structure function relationships exist within the porcine TMJ disc[82], but now a comprehensive comparison can be made, not only within a single species, but also across species. Sulfated GAG content is frequently related to compressive stiffness, and indeed in this study, the species with the greatest GAG/ww (cow) also had the highest compressive moduli. In contrast, regional variations in GAG content showed no relationship with compressive properties. Instead, the region with the highest total collagen/ww (PBC) also possessed the highest compressive properties, as seen previously for the pig disc.[85] Although collagen is generally thought to mediate tensile properties, no correlations with total collagen content were observed in this study. As seen previously, tensile properties of the disc depend more on the orientation of collagen rather than total content.[34] These data emphasize that tissue engineering studies will have to account not only for biochemical content, but also organization to produce heterogeneous mechanical properties similar to native tissue.

Collecting a significant amount of interspecies data within a single study allows correlation of disc properties to the greater functional requirements of

each animal. It is apparent that some properties of the disc vary with the specific anatomy or diet of each species. For example, the herbivores (cow, goat, and rabbit), whose joint motion is primarily translatory[97], had greater GAG content and compressive properties across all disc regions compared to the omnivores (human and pig), whose motion is both rotatory and translatory. On the other hand, some regional variations were constant among species, indicating that certain portions of the disc may have similar functional requirements within all species. For example, the intermediate zone under mediolateral tension was always weaker than other regions. While it is clear that the disc from each species is unique, it does appear that some properties of the disc transcend species.

While this study provides a significant reference for interspecies variations in the TMJ disc, there are a few limitations to the work. Although the human specimens appeared grossly normal, they were derived from cadavers of advanced age, whose lack of TMJ dysfunction could not be verified with medical records. These factors could have affected the measured discal properties. Aging of the TMJ disc has been shown to result in stiffer tissues[90] with lower cellularity[20], which matches well with the human data in this study. While this study did examine regional variations, it did not examine every region of the disc and it only measured properties *in vitro*. Future studies should build on this work by investigating interspecies variations in other important discal properties, such as cellular populations, as well as imaging of the intact joints. This imaging would

allow both correlation of the measured properties to native movement of the disc and verification that there is no disease present.

A major goal of this study was to quantify the differences and similarities among animal models, and specifically, how these relate to their appropriateness as analogs of the human TMJ disc. Taking into account all of the parameters tested in this study, it can be argued that the pig disc is most similar to the human. This is based on the pig disc demonstrating the most statistical similarities to the human disc, including dimensions, collagen and GAG content, and compressive properties. Therefore, the results of this study point to the pig as the most appropriate animal model and support prior anatomical studies.

Tables and Figures

Supplemental Table 1. Tensile values and assessment of statistical variation. A) Values for peak modulus, relaxed modulus, and strength under unilateral tension accompanied by analysis of intraspecies topographic variation. Data are represented as mean ± S.D. Statistically significant intraspecies topographic variation, as determined using a one-way ANOVA and Tukey's HSD *post-hoc* test with α = 0.05, is represented by superscript letters where applicable. B) Interspecies and topographic variation of tensile properties analyzed using a two-way ANOVA and Tukey's HSD *post-hoc* test with α = 0.05. Values not connected by same letter are significantly different. Between four and six samples were examined for each topographical location in each species.

A)

Species	Sample	Strength (MPa)	Peak modulus (MPa)	Relaxed modulus (MPa)
Human	AP C	^{A}13.8 ± 2.8	^{A}51.7 ± 7.7	^{A}34.4 ± 12.2
	AP M	^{AB}12.8 ± 3.3	^{AB}37.2 ± 4.1	^{A}30.0 ± 3.8
	ML A	^{BC}6.7 ± 4.3	^{BC}25.5 ± 13.2	^{AB}18.5 ± 10.0
	ML C	^{C}4.2 ± 1.5	^{C}9.5 ± 1.7	^{B}6.1 ± 1.9
	ML P	^{BC}6.7 ± 3.9	^{B}21.2 ± 12.1	^{AB}17.0 ± 9.6
Pig	AP L	^{A}5.1 ± 1.7	^{A}24.0 ± 6.9	^{A}18.5 ± 5.9
	AP C	^{A}4.3 ± 2.0	^{A}23.0 ± 10.0	^{A}17.9 ± 7.5
	AP M	^{A}5.8 ± 1.7	^{A}23.9 ± 8.7	^{A}18.7 ± 7.9
	ML A	^{AB}3.2 ± 1.2	^{AB}15.5 ± 8.2	^{AB}11.4 ± 6.3
	ML C	^{B}0.5 ± 0.3	$^{B.0}$2.0 ± 1.4	^{B}1.6 ± 1.1
	ML P	^{A}5.0 ± 1.5	^{A}28.5 ± 8.2	^{A}19.6 ± 6.3
Cow	AP L	^{AB}5.1 ± 1.1	^{A}13.0 ± 4.9	^{AB}8.9 ± 2.7
	AP C	^{BC}3.0 ± 1.3	^{A}14.9 ± 6.7	^{A}11.0 ± 4.7
	AP M	^{A}6.8 ± 1.8	^{A}19.4 ± 5.1	^{A}15.8 ± 4.6
	ML A	^{A}6.1 ± 2.2	^{A}17.6 ± 3.7	^{A}14.0 ± 2.8
	ML C	^{C}0.2 ± 0.1	^{B}0.2 ± 0.0	^{B}0.1 ± 0.0
	ML P	^{AB}4.6 ± 1.3	^{A}18.2 ± 7.9	^{A}14.6 ± 6.6
Goat	AP L	^{AB}3.6 ± 1.2	^{AB}12.6 ± 2.0	^{AB}10.3 ± 1.9
	AP C	^{B}3.4 ± 0.6	^{AB}14.9 ± 3.3	^{AB}10.4 ± 2.6
	AP M	^{AB}4.1 ± 1.9	^{AB}16.7 ± 5.9	^{AB}12.7 ± 3.6
	ML A	^{A}8.9 ± 3.1	^{A}24.1 ± 5.8	^{A}20.4 ± 6.1
	ML C	^{B}2.2 ± 0.9	^{B}6.1 ± 2.0	^{B}5.0 ± 2.3
	ML P	^{AB}6.7 ± 3.9	^{A}21.2 ± 12.1	^{A}17.0 ± 9.6
Rabbit	AP L	^{AB}2.9 ± 1.2	^{A}11.5 ± 6.2	^{AB}6.8 ± 3.8
	AP C	^{BC}1.9 ± 0.8	^{AB}7.0 ± 2.4	^{AB}4.5 ± 1.8
	AP M	^{A}3.6 ± 0.3	^{A}11.7 ± 2.7	^{A}8.6 ± 2.9
	ML A	^{BC}1.6 ± 0.6	^{AB}6.6 ± 1.5	^{AB}4.4 ± 1.0
	ML C	^{C}0.8 ± 0.4	^{B}2.1 ± 2.0	^{B}1.4 ± 1.3
	ML P	^{A}4.3 ± 0.5	^{AB}7.3 ± 3.4	^{AB}5.4 ± 2.7

B)

Species	Strength	Peak	Relaxed
Human	A	A	A
Pig	BC	B	B
Goat	B	B	B
Cow	BC	B	B
Rabbit	C	C	C

Region	Strength	Peak	Relaxed
AP L	A	A	A
AP C	A	A	A
AP M	A	A	A
ML A	A	A	A
ML C	B	B	B
ML P	A	A	A

Supplemental Table 2. Compressive values and assessment of statistical variation. A) Values for relaxation modulus, instantaneous modulus, and coefficient of viscosity for stress relaxation tests under unconfined compression. Data are represented as mean ± S.D. Statistically significant intraspecies topographic variation, as determined using a one-way ANOVA and Tukey's HSD *post-hoc* test with $\alpha = 0.05$, is represented by superscript letters where applicable. B) Interspecies and topographic variation of compressive properties analyzed using a two-way ANOVA and Tukey's HSD *post-hoc* test with $\alpha = 0.05$ where applicable. Values not connected by same letter are significantly different. Between four and six samples were tested for each topographical location and species.

A)

Species	Region	Relaxation modulus (kPa) Strain			Instantaneous modulus (kPa) Strain			Coefficient of viscosity (MPa s) Strain		
		10%	20%	30%	10%	20%	30%	10%	20%	30%
Human	PBC	60.9 ± 28.1	71.9 ± 44.9	102.3 ± 72.1	^{A}991 ± 673	2823 ± 2157	4800 ± 3597	1.5 ± 0.1	^{A}20.0 ± 11.8	35.1 ± 19.3
	ABC	31.4 ± 15.8	43.4 ± 23.7	60.7 ± 34.6	^{AB}266 ± 192	1783 ± 768	3086 ± 1903	0.4 ± 0.2	^{B}2.9 ± 2.5	15.6 ± 7.7
	IZM	32.6 ± 19.5	17.8 ± 7.8	27.9 ± 10.9	^{B}216 ± 114	908 ± 666	2402 ± 1368	1.2 ± 0.8	^{AB}11.1 ± 6.8	25.9 ± 13.9
	IZC	24.3 ± 11.0	34.8 ± 14.4	54.4 ± 17.2	^{B}226 ± 170	774 ± 527	2085 ± 662	0.4 ± 0.1	^{AB}7.1 ± 3.6	23.3 ± 10.9
	IZL	15.8 ± 16.3	19.0 ± 22.2	30.5 ± 36.9	^{B}57 ± 17	287 ± 78	1116 ± 153	1.0 ± 1.3	^{AB}6.1 ± 8.4	16.3 ± 22.1
Pig	PBC	^{A}24.3 ± 7.4	^{A}57.0 ± 19.1	^{A}112.5 ± 31.4	^{A}121 ± 66	^{A}2287 ± 1307	3310 ± 1551	0.7 ± 0.4	4.6 ± 4.0	14.6 ± 6.1
	ABC	^{AB}17.1 ± 1.9	^{B}30.4 ± 5.8	^{B}54.3 ± 14.7	^{AB}84 ± 68	^{AB}1852 ± 627	4039 ± 1283	1.1 ± 0.8	2.5 ± 1.0	11.6 ± 6.4
	IZM	^{AB}14.3 ± 5.9	^{B}23.2 ± 13.4	^{B}42.3 ± 24.3	^{B}32 ± 37	^{BC}557 ± 576	1957 ± 1331	1.2 ± 0.3	2.1 ± 0.8	12.9 ± 8.7
	IZC	^{AB}15.0 ± 3.1	^{B}26.4 ± 6.4	^{B}52.0 ± 16.5	^{B}20 ± 2	^{BC}453 ± 155	2079 ± 581	1.8 ± 0.3	3.6 ± 1.8	13.4 ± 7.8
	IZL	^{B}12.4 ± 4.4	^{B}21.6 ± 10.9	^{B}38.8 ± 17.3	^{B}16 ± 6	^{C}522 ± 412	2140 ± 858	1.7 ± 0.4	2.4 ± 0.7	9.1 ± 6.6
Goat	PBC	^{A}61.5 ± 22.5	^{A}91.1 ± 29.4	^{A}126.3 ± 28.5	^{A}937 ± 704	^{A}3492 ± 1150	^{A}5953 ± 941	1.5 ± 1.1	^{A}12.0 ± 5.6	^{A}38.3 ± 17.4
	ABC	^{AB}44.5 ± 10.1	^{AB}83.8 ± 7.2	^{A}117.6 ± 13.1	^{A}896 ± 236	^{A}4003 ± 417	^{A}6554 ± 541	0.7 ± 0.3	^{A}10.4 ± 1.2	^{A}35.5 ± 1.6
	IZM	^{B}22.2 ± 9.0	^{C}42.7 ± 15.2	^{BC}67.9 ± 20.0	^{AB}353 ± 249	^{AB}2400 ± 913	^{AB}4512 ± 1159	0.3 ± 0.1	^{B}4.1 ± 2.9	^{AB}21.5 ± 9.7
	IZC	^{B}34.3 ± 4.7	^{BC}53.8 ± 7.8	^{AB}93.0 ± 6.9	^{B}171 ± 130	^{BC}1140 ± 579	^{B}3480 ± 749	1.1 ± 0.6	^{B}3.4 ± 1.4	^{AB}23.8 ± 6.4
	IZL	^{B}23.7 ± 1.8	^{C}33.2 ± 5.7	^{C}52.0 ± 9.1	^{B}64 ± 52	^{C}736 ± 661	^{B}2603 ± 1656	0.5 ± 0.3	^{B}3.8 ± 1.4	^{B}11.1 ± 3.1
Cow	PBC	^{A}70.2 ± 18.1	^{A}119.5 ± 23.7	198.6 ± 35.6	^{A}616 ± 422	3269 ± 1301	6245 ± 1578	1.4 ± 0.8	10.6 ± 5.2	35.6 ± 15.9
	ABC	^{AB}67.2 ± 18.3	^{AB}113.4 ± 51.8	166.5 ± 97.3	^{AB}304 ± 198	2121 ± 1041	4479 ± 1057	2.7 ± 0.3	11.5 ± 3.7	39.0 ± 19.8
	IZM	^{B}30.8 ± 19.3	^{B}45.3 ± 32.5	80.3 ± 51.6	^{AB}226 ± 187	2529 ± 1808	4621 ± 3166	0.7 ± 0.6	4.7 ± 1.9	14.7 ± 9.0
	IZC	^{B}38.6 ± 17.9	^{AB}56.5 ± 24.4	88.2 ± 33.8	^{B}83 ± 42	683 ± 248	2173 ± 416	2.7 ± 2.3	8.6 ± 3.4	23.9 ± 8.9
	IZL	^{B}32.4 ± 7.6	^{AB}53.0 ± 17.5	85.7 ± 32.5	^{B}75 ± 61	1086 ± 1027	3487 ± 2175	1.1 ± 0.4	3.5 ± 1.9	13.5 ± 10.2
Rabbit	PBC	64.7 ± 30.2	^{A}105.2 ± 34.6	^{A}165.2 ± 41.5	^{AB}379 ± 182	^{AB}2509 ± 320	^{AB}5193 ± 625	2.3 ± 1.6	8.1 ± 6.1	27.2 ± 12.7
	ABC	49.6 ± 10.3	^{AB}64.7 ± 13.9	^{AB}104.9 ± 23.2	^{A}683 ± 483	^{A}3000 ± 1404	^{A}5874 ± 1222	1.1 ± 0.1	3.3 ± 1.3	11.7 ± 4.7
	IZM	28.8 ± 15.5	^{B}33.8 ± 28.8	^{B}70.6 ± 45.5	^{B}156 ± 148	^{C}721 ± 413	^{ABC}3111 ± 1286	0.8 ± 0.4	4.7 ± 4.3	8.7 ± 8.2
	IZC	51.6 ± 26.6	^{AB}73.9 ± 46.4	^{AB}93.9 ± 62.9	^{AB}331 ± 187	^{ABC}1772 ± 884	^{BC}2667 ± 1686	1.6 ± 1.1	4.6 ± 4.3	15.2 ± 11.2
	IZL	24.0 ± 17.2	^{B}37.2 ± 22.8	^{B}53.9 ± 32.3	^{B}138 ± 168	^{BC}996 ± 1310	^{C}2078 ± 2068	1.3 ± 0.4	2.3 ± 1.1	8.0 ± 5.4

B)

Species	Relaxation modulus 10%	20%	30%	Instantaneous modulus 10%	20%	30%	Coefficient of viscosity 10%	20%	30%
Human	B	B	C	A	B	B	B	A	AB
Pig	C	B	C	B	B	B	AB	C	C
Goat	AB	A	B	A	A	A	B	ABC	A
Cow	A	A	A	AB	AB	A	A	AB	A
Rabbit	AB	A	AB	A	AB	AB	AB	BC	BC

Region	Relaxation modulus 10%	20%	30%	Instantaneous modulus 10%	20%	30%	Coefficient of viscosity 10%	20%	30%
PBC	A	A	A	A	A	A	.	A	A
ABC	AB	B	B	A	A	A	.	B	AB
IZM	C	C	C	B	B	B	.	B	BC
IZC	BC	BC	BC	B	B	B	.	B	BC
IZL	C	C	C	B	B	B	.	B	C

Supplemental Table 3. Numerical data from all biochemical assays and intraspecies statistical analysis. Total collagen, total DNA, and total sulfated GAG content have been normalized to the wet weight of the samples and are presented as mean ± S.D. Regional variations within each species were investigated using a one-way ANOVA and Tukey's HSD *post-hoc* test with α = 0.05. Groups not connected by the same letter are statistically different from each other. DNA content was the only parameter that showed a consistent trend in regional variation across a majority of the species.

Species	Region	Collagen/Wet Weight (%)	DNA/Wet Weight (%)	GAG/Wet Weight (%)
Rabbit	PBC	20.9 ± 0.830	0.0293 ± 0.00678 (A)	0.545 ± 0.0632
	ABC	20.3 ± 1.40	0.0333 ± 0.0134 (A)	0.579 ± 0.100
	IZM	23.1 ± 1.03	0.00555 ± 0.00183 (B)	0.739 ± 0.228
	IZC	21.1 ± 1.79	0.00849 ± 0.00378 (B)	0.773 ± 0.222
	IZL	21.6 ± 3.59	0.00734 ± 0.00233 (B)	0.746 ± 0.231
Goat	PBC	21.4 ± 1.53 (A)	0.0331 ± 0.0106 (A)	0.656 ± 0.0962 (B)
	ABC	18.0 ± 1.87 (B)	0.0358 ± 0.0110 (A)	0.630 ± 0.193 (B)
	IZM	17.4 ± 2.02 (B)	0.0153 ± 0.00490 (B)	0.821 ± 0.166 (AB)
	IZC	19.6 ± 1.97 (AB)	0.0112 ± .00301 (B)	0.732 ± 0.186 (AB)
	IZL	16.5 ± 2.01 (B)	0.00985 ± 0.00412 (B)	0.930 ± 0.0971 (A)
Human	PBC	21.7 ± 0.573	0.00866 ± 0.00155 (AB)	0.554 ± 0.203 (AB)
	ABC	22.8 ± 1.46	0.00978 ± 0.000814 (A)	0.273 ± 0.0536 (B)
	IZM	22.2 ± 2.08	0.00638 ± 0.000877 (B)	0.634 ± 0.180 (A)
	IZC	24.3 ± 1.45	0.00779 ± 0.00137 (AB)	0.576 ± 0.126 (AB)
	IZL	23.1 ± 3.20	0.00653 ± 0.000927 (B)	0.589 ± 0.124 (AB)
Pig	PBC	28.1 ± 3.11 (A)	0.0355 ± 0.0123 (A)	0.310 ± 0.0955
	ABC	22.2 ± 2.62 (C)	0.0308 ± 0.0147 (AB)	0.377 ± 0.115
	IZM	24.3 ± 3.18 (ABC)	0.0113 ± 0.00245 (C)	0.324 ± 0.0838
	IZC	27.6 ± 4.41 (AB)	0.0190 ± 0.00760 (BC)	0.380 ± 0.0754
	IZL	22.3 ± 2.05 (BC)	0.0162 ± 0.00436 (BC)	0.434 ± 0.0489
Cow	PBC	28.5 ± 3.14	0.0217 ± 0.00731	0.864 ± 0.0868
	ABC	30.0 ± 2.92	0.0191 ± 0.00471	0.764 ± 0.167
	IZM	25.2 ± 4.65	0.0162 ± 0.00828	0.871 ± 0.235
	IZC	24.1 ± 3.94	0.0112 ± 0.00374	0.936 ± 0.176
	IZL	23.1 ± 6.88	0.0127 ± 0.00490	0.841 ± 0.227
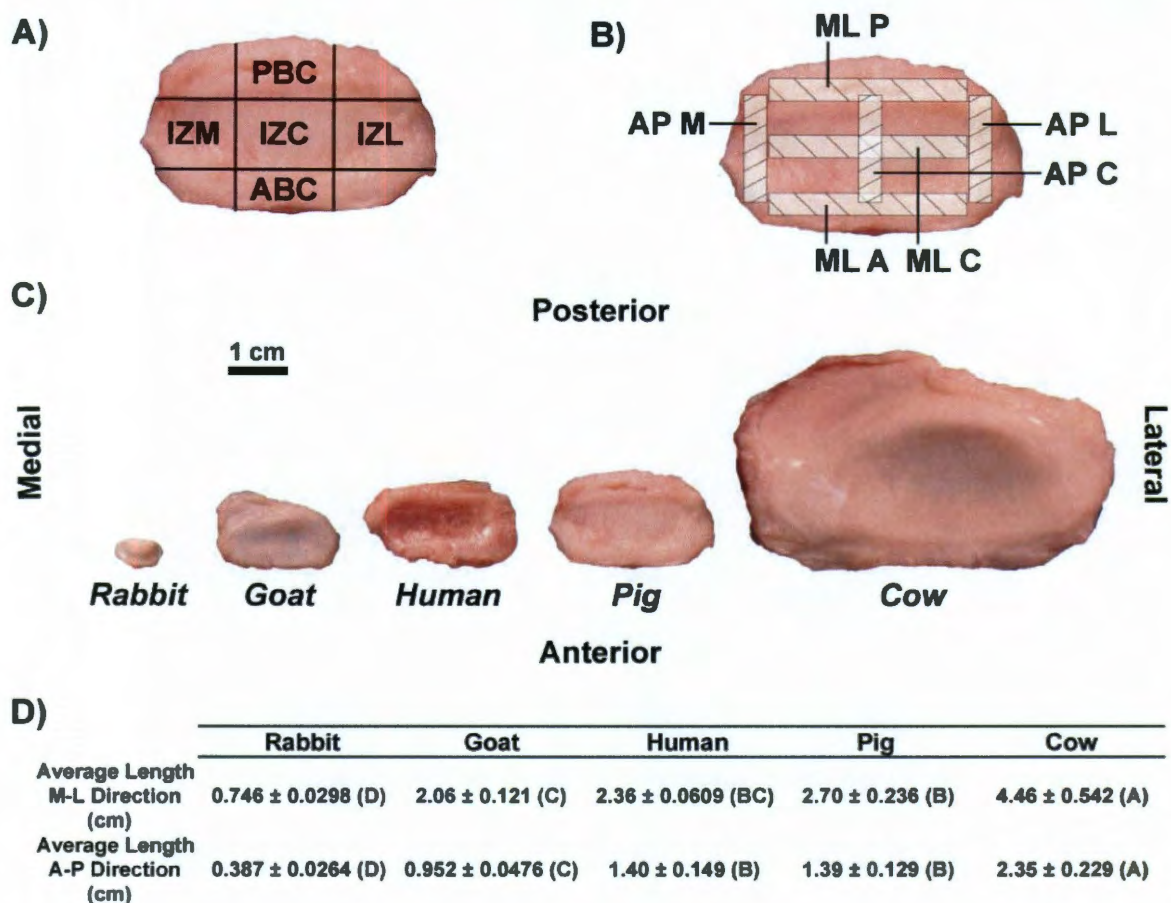
Figure 1. Description of the TMJ disc regions tested in this investigation and gross morphology of the collected discs. A) Regions of the TMJ disc used for biochemical, histological, and compression testing: posterior band central (PBC), intermediate zone (IZ) medial (IZM), IZ central (IZC), IZ lateral (IZL), and anterior band central (ABC). B) Regions of the TMJ disc used for tensile testing: mediolateral (ML) posterior (ML P), ML central (ML C), ML anterior (ML A), anteroposterior (AP) medial (AP M), AP central (AP C), AP lateral (AP L). C) Scaled figure showing the gross morphology of TMJ discs collected from the five different species tested. D) Dimensions of discs collected from each species measured in the mediolateral (M-L) and anteroposterior (A-P) direction. Data are presented as mean ± S.D. A one-way ANOVA was conducted on the data from each direction and animals not connected by the same letter are statistically different from one another. The pig was the only animal with dimensions not significantly different from the human in both the A-P and M-L directions.
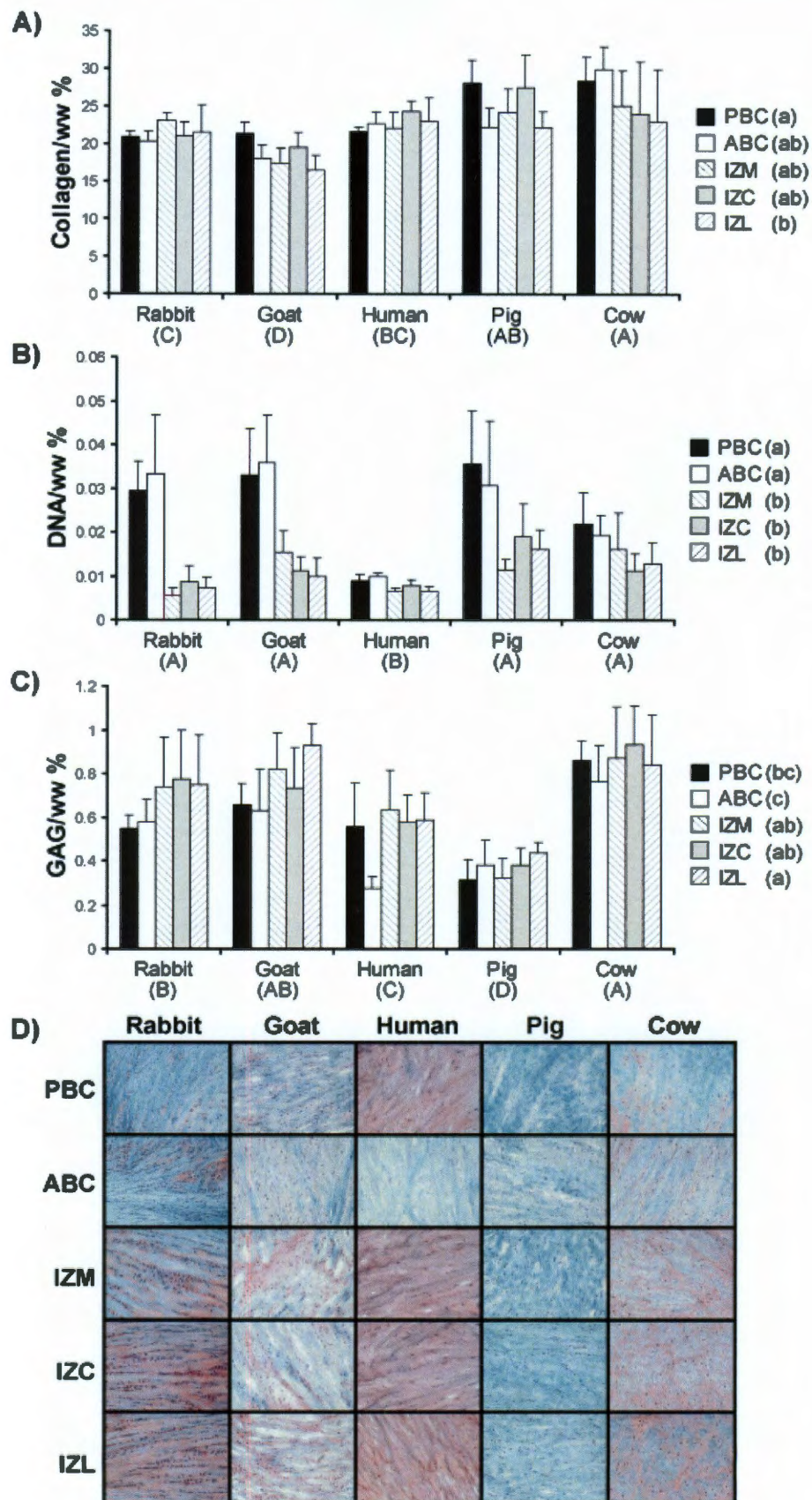
Figure 2. Biochemical and histological analysis. A - C) show an interspecies comparison of the quantitative biochemical content of the TMJ disc. Data were normalized to wet weight and are presented as mean ± S.D. A two-way ANOVA is presented with the factors of species and region. Samples not connected by the same letter are statistically different from each other. A) Total collagen content of human samples was not statistically different from pig or rabbit discs. B) Human discs contained significantly less DNA content than the other species, likely due to age. C) Sulfated GAG content of human samples fell in between the pig and rabbit samples. D) Safranin-O/fast green staining of sections from the TMJ disc. Positive Safranin-O staining (red to purple color) is clear in all samples except human ABC and all regions of the pig disc. Images were taken on a Nikon E600 microscope with a 20X objective. (Note: the complete tensile data set is presented online in Supplemental Table 3.)
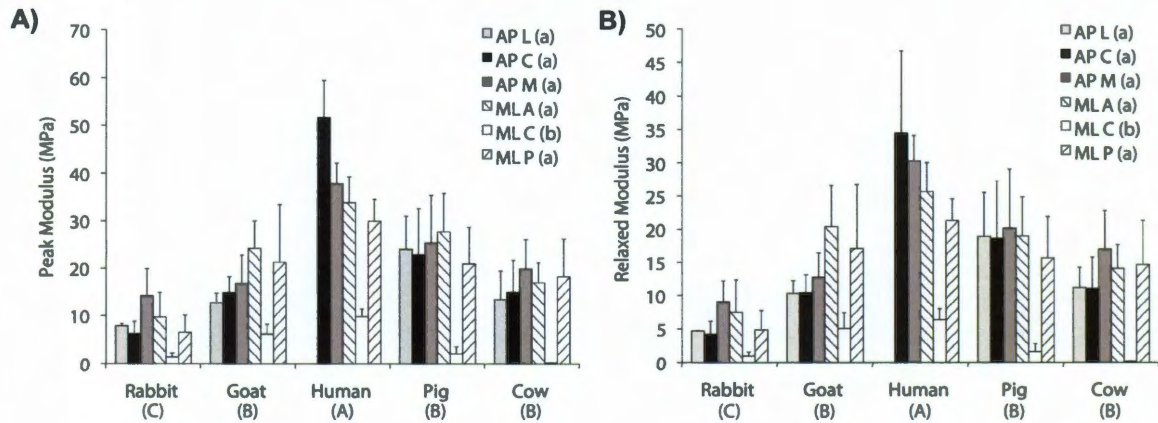
Figure 3. Biomechanical properties under tension. Data are presented as mean ± S.D. Data were analyzed using a two-way ANOVA with Tukey's HSD test *post hoc* where appropriate, and groups not connected by the same letter are significantly different ($p < 0.05$). Peak (A) and relaxed (B) Young's moduli under tensile loading. Human tissue was the stiffest among the species, and the central region under mediolateral strain was the most compliant among the regions under both loading conditions. (Note: the complete tensile data set is presented online in Supplemental Table 1.)
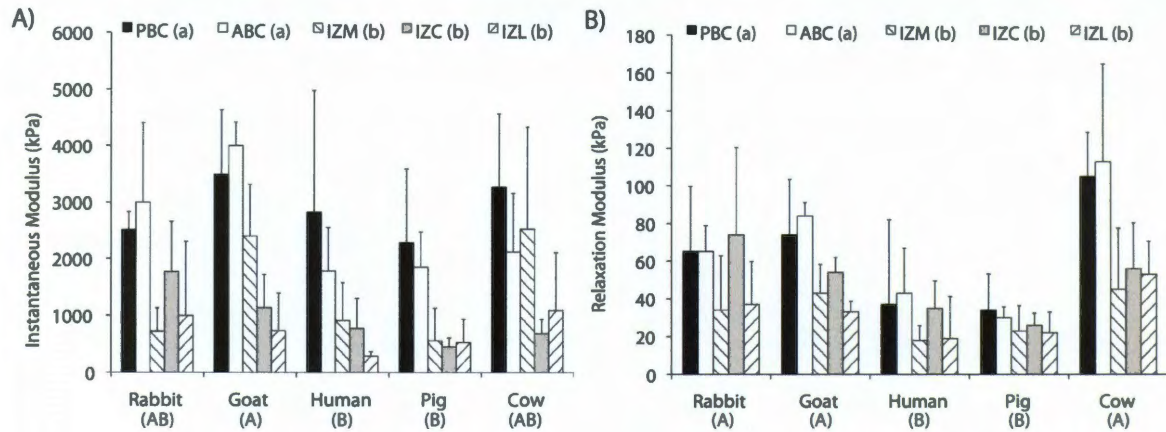
Figure 4. Biomechanical properties under compression at 20% strain. Data are presented as mean ± S.D. Data were analyzed using a two-way ANOVA with Tukey's HSD test *post hoc* where appropriate, and groups not connected by the same letter are significantly different ($p < 0.05$). A) Compressive moduli under instantaneous loading. The porcine, leporine, and bovine tissue yielded statistically similar values to the human, while the caprine tissue was stiffer than the human tissue. B) Compressive moduli at equilibrium. Human and pig discs were significantly more compliant than rabbit, goat, and cow discs. The band regions were significantly stiffer than the intermediate zone regions under both instantaneous and relaxed conditions. (Note: the complete compressive data set is presented online in Supplemental Table 2.)

Chapter 3: Characterization of the Attachments of the Temporomandibular Joint Disc

Abstract

Objective: The complex movement of the temporomandibular joint (TMJ) disc during mastication is controlled in large part by the disc's attachments to the surrounding tissues. Unfortunately, the properties of these discal attachments have not been studied. In an effort to identify critical design standards and understand the function of the TMJ disc-attachment complex, this study characterizes key biochemical, morphological, and histological properties of these structures.

Design: TMJ disc-attachment complexes from a porcine model were carefully dissected into six discal attachments and five TMJ disc regions. The disc and its attachments were assayed biochemically for total collagen, glycosaminoglycan (GAG), DNA, and water content. Additionally, histology was performed on the whole joint to investigate the anatomy of the disc-attachment complex, and to verify the regional distribution of cells, glycosaminoglycans, collagen, and elastin.

Results: Quantitative biochemical assays showed that overall water content was fairly constant in all disc and attachment regions. Disc regions

generally showed higher sulfated GAG and collagen content than the attachments. In contrast, the attachments contained greater DNA content than the disc. Histological staining supported the quantitative results and also indicated more elastic fibers and vascularity to be present in the attachments than the disc.

Conclusions: Although macroscopically the TMJ disc and its attachments form a seamless complex within the joint, a closer look at regional biochemical constituents reveals that these two components are distinct. While the disc and attachments both contain the same major constituents (water, collagen, GAG, elastin, cells), their relative amounts vary based on the functional requirements of the tissue. With this specific knowledge of regional variation in biochemical content, tissue engineering efforts to address TMJ pathologies can progress toward the ultimate goal of producing a fully functional disc-attachment complex.

Introduction

The temporomandibular joint (TMJ) is a hinge joint that allows for normal opening and closing of the mandible, and is essential in everyday functioning of the mouth such as chewing and speaking. It is comprised of the superior (glenoid fossa) and inferior (mandibular condyle) articulating surfaces, and a fibrocartilaginous disc suspended between them which helps align and reduce friction in the joint.[74] However, this joint is prone to a variety of pathologies that inhibit normal jaw function through pain, tissue degeneration, and displacement of the TMJ disc. Collectively, temporomandibular joint disorders (TMDs) cause

loss of jaw function and affect millions of people in the United States.[82] Unfortunately, the causes of TMD are ill-understood and current clinical therapies are limited to managing the painful symptoms of the disease.[76] In extreme cases tissue resection is performed to alleviate discomfort, but this course of action is not optimal as it is often followed by further joint degeneration.[98]

Tissue engineering efforts to recapitulate the complex biochemistry and biomechanics of the TMJ disc are currently underway, and may provide a possible clinical alternative to tissue resection in cases such as these where the TMJ disc is damaged. However, if a suitable disc replacement is engineered how it will be attached within the joint will need to be carefully considered. In the native joint, the attachments of the TMJ disc with the surrounding tissues are extremely important for the coordinated movements of the TMJ.[99] Anteriorly, the disc attaches inferiorly to the anterior condyle and superiorly to the eminence by bending with the joint capsule (Fig 1A). Posteriorly, it attaches to the bilaminar zone, which is in turn attached superiorly to the temporal bone and inferiorly to the posterior condyle. Laterally and medially, the disc attachments blend into the joint capsule near its attachment to the condylar head (Fig 1B). To properly produce an engineered replacement for the TMJ disc and its attachments, their properties, including their biochemical content, need to be fully understood.

With regards to the TMJ disc, its biochemical content and distribution has been described quite extensively. The disc is composed primary of collagen comprising approximately 30% of the wet weight,[22] or 83-96% of the dry weight.[17, 81] This collagen is primary type I, although collagens type II, III, VI, IX,

and XII can also be found in trace amounts.[23] Collagen concentration is highest in the bands of the disc relative to lateral region.[81] Reports about the total amount of glycosaminoglycans (GAGs) in the TMJ disc have varied widely, but the general consensus is around 1% of the dry weight.[82] The major constituent of this GAG is chondrotin sulfate, which comprises about 74% of the total GAG content.[25, 100] Studies indicate that the greatest GAG content is located in the center of the disc relative to the bands.[25, 81] Histological studies of the pig disc indicate that approximately 70% of the cells in the disc are fibroblastic in morphology, with the remainder displaying a round chondrocyte morphology.[16] Cellular density is highest in the anterior and posterior bands.[81]

Although the discal attachments are vital for proper movement and health of the TMJ disc, currently little is known about the quantitative properties of these tissues. Histological studies have indicated that collagen and elastin are present throughout the attachments,[101-103] there is a general lack of chondroitin sulfate proteoglycans,[26, 104] and the cells possess a fibroblastic morphology.[105] Polarized light microscopy and scanning electron microscopy (SEM) have shown that collagen fibrils extend from the disc into the attachments and are particularly dense in the posterior attachment.[101, 103] While these studies provide a starting point for understanding the attachments, they are clearly not enough to engineer the attachments or understand structure-function relationships in this tissue.

Although the disc attachments are an integral part of the TMJ, little is still known about the exact biochemistry of these tissues and how they compare to the TMJ disc itself. Therefore, this study seeks to characterize the

anteroposterior and mediolateral disc-attachment complex biochemically and histologically. It is hypothesized that the attachments of the disc will show biochemical similarity to the disc itself, but that regional variations in biochemical content will be observed. The major findings of this study will help to inform TMJ tissue engineering strategies by providing anatomical references for engineering a disc-attachment complex and where the attachments should eventually be integrated in the joint.

Materials and Methods

Specimen Procurement

Pig heads from female animals 6-9 months of age were obtained from a local abattoir (Yosemite Meat Co., Modesto, CA). A porcine model was used based on prior work.[88, 106] The entire TMJ and its surrounding bony structures (e.g., condylar process, temporal bone and zygomatic arch) were removed *en bloc* using an osteotome and mallet. Carful dissection of the disc attachment was performed utilizing Carl Zeiss surgical loupes at 3.5 magnification. A number 15 scalpel blade was used initially to sever the attachments at the insertion points of the medio-posterior aspect of the zygomatic arch and the lateral aspect of the temporal bone from the anterior to the posterior direction on both medial and lateral aspects of the joint. The superior attachment at the glenoid fossa (mandibular fossa) and articular eminence and inferior attachments at the mandibular condylar process were dissected out utilizing the same technique. Then a 24G periosteal elevator was used to elevate the soft tissue attachments

en toto. Adson forceps were used to apply traction during the procedure and to finally deliver the entire TMJ disc and its attachments. During the procedure a periodic irrigation with PBS solution was used to avoid drying the specimen. All the muscular and adipose tissues were carefully trimmed using straight scissors. All specimens were removed without penetration of the superior or inferior joint compartments. Following isolation, all soft tissues were assessed grossly, and no signs of degeneration were seen.

Biochemical Analysis

After isolation, TMJ discs were dissected into five regions and discal attachments were dissected into six regions as shown in Fig. 1B. The five regions of the disc tested were: posterior band (PB), anterior band (AB), intermediate zone medial (IZM), intermediate zone central (IZC), and intermediate zone lateral (IZL). The six discal attachments examined were: posterior attachment superior (PAS), posterior attachment inferior (PAI), anterior attachment superior (AAS), anterior attachment inferior (AAI), medial attachment (MA), and lateral attachment (LA). Following dissection, samples were blotted dry and wet weights were measured. Samples were frozen for 24 hrs and lyophilized for 48 hrs before dry weights were taken. Samples were digested in 125 mg/mL papain (Sigma, St. Louis, MO) solution overnight at 60°C. At the end of digestion, no residual tissue remained. DNA content was measured with the Quant-iT Picrogreen dsDNA Assay Kit (Invitrogen, Carlsbad, CA). Following hydrolysis with 4 N NaOH for 20 min at 110°C, collagen content of the samples was

quantified with a modified chloramine-T hydroxyproline assay.[81] Finally, sulfated GAG content was quantified using Blyscan Glycosaminoglycan Assay Kit (Accurate Chemical and Scientific Corp., Westbury, NY). Six samples per group were used for all biochemical analysis.

Histology

Two left joints *en bloc* were trimmed and fixed in 10% neutral buffered formalin for one wk. Joints were decalcified using 10% formic acid and cut into regional sections using a band saw. Each joint was cut into three pieces: 1) sagittal through the center of the entire joint, 2) coronal through the medial side of the joint, 3) coronal through the lateral side of the joint. Samples were embedded in paraffin wax and sectioned at 5 μm. Cellular distribution and general matrix compositions were investigated with hematoxylin and eosin staining. Alcian blue staining at pH 2.5 was used to examine the distribution of sulfated GAGs. Collagen and elastin were examined with Verhoeff's Van Gieson staining.

Statistical Analysis

All quantitative results were compared using a one-way analysis of variance (ANOVA). A Tukey's HSD *post hoc* test was used where appropriate. A significance level of $p < 0.05$ was used for all statistical analysis.

Results

Biochemical Analysis

Biochemical results for the TMJ disc and its attachments are shown pictorially in Fig. 2 and the raw data can be found in Table 1. The biochemical content for the disc was similar to that measured in prior studies.[25, 81, 106]

Water Content

Overall, the water content was quite similar among all tissues examined with most groups having a mean water content of ~73%. Water content did not vary among the five regions of the TMJ disc measured. The discal attachments did show significant differences, with MA containing the most water at 82.2% and LA containing the least water at 68.5%. Water content of AAS was also high at 80.4%.

Distribution of Collagen

Similar to the water content, there were not many statistical differences among the disc and attachment regions. Overall, the disc had greater mean collagen content at 80.6%, compared to the attachments which had a mean of 71.2%. Statistically, PB contained the most collagen per dry weight at 87.3%, but the other band of the disc, AB, was also very high at 84.2%. AAS contained the least collagen content overall at 67.7%. The attachment with the most collagen per dry weight was PAI with a mean of 78.9%.

Distribution of Glycosaminoglycans

Sulfated GAG per dry weight showed a larger regional variation among the tissues than the other biochemical parameters. Overall, the TMJ disc had a higher mean GAG content at 0.95%, compared to the attachments which had a mean of 0.63%. The one-way ANOVA indicated that IZM and IZL contained the most GAG per dry weight at 1.11% and 1.18%, respectively. The only region of the disc that did not contain a large amount of GAG was PB which had a mean of 0.59%. Statistically, the tissue with the least GAG was PAS at 0.40%, although AAI and LA were also low. The three attachments with the most GAG were PAI, AAS, and MA with contents of 0.76%, 0.82% and 0.88% respectively.

Distribution of DNA

DNA content normalized to dry weight also showed a distinct regional variation, although the variation was more prominent in the attachments. Overall, the attachments had a higher mean DNA content at 0.19%, compared to the disc which had a mean of 0.16%. Statistically, AAS and MA contained the most DNA per dry weight at 0.21% and 0.20% respectively. The attachment with the least DNA was PAS at 0.16%. The one-way ANOVA indicated that the tissue with the least DNA was IZC at 0.14%. IZL was the only disc region with a high DNA content (0.18%).

Histological Analysis

Whole Joint Histology

Whole joint histological staining was used to examine the anatomy of the discal attachments. In Fig. 3A, a sagittal view of the disc and its attachments shows that the anterior attachment is markedly smaller than the posterior attachment. The matrix of the posterior attachment appears to be a similar density as the TMJ disc itself, while the anterior attachment shows more diffuse fibers that run superiorly and inferiorly in the joint. The medial and lateral attachments (Fig. 3B and C) are similar to the anterior attachment in appearance, but these attachments join mainly with the inferior mandibular condyle. The medial attachment connects at the top of the condylar head, while the lateral attachment connects very low on the condyle.

Regional Histology

Assessment of the different regions of the disc and attachments showed some differences in matrix components (Fig. 4). As seen in the whole joint histology (Fig. 3), regional hematoxylin and eosin staining of the disc-attachment complex indicate that the posterior band has a similar matrix density to the disc, and the anterior, medial, and lateral attachments have more diffuse matrices. Alcian blue staining for regional GAG content showed that overall GAG content was more apparent in the disc than in the attachments, though the attachments were not devoid of this component. Elastic fibers were also apparent throughout the disc and attachments, but this component was more apparent in the attachments, especially the AAI and MA, than in the disc itself. Elastin staining also stained blood vessels in the attachments, but was most prevalent in AAI.

Discussion

As the field of tissue engineering embarks on producing a replacement for the TMJ disc, it is clear that little information is known about the attachments that anchor the disc within the joint. Based on the quantitative biochemical evaluation carried out in this study, the discal attachments show many key similarities with the TMJ disc itself. They both contain the same basic components (collagen, GAG, cells, and elastin) and much of the matrix is continuous between the tissues since they blend seamlessly together. Although vast differences were not found, the disc and attachments were found to be regionally distinct, and these distinctions are likely related to the functional requirements of each region.

Overall, DNA content was lower and GAG and collagen content were higher in the disc compared to the attachments. These distinctions appear to be related to the disc being characterized as a fibrocartilage, while the attachments are seen as ligamentous tissues.[101] The most basic difference between these tissues is that fibrocartilage has more GAG and the presence of collagen type II. Higher cellular density in the attachments may be attributed to two factors: 1) cellular density is typically higher in ligamentous tissues compared to cartilages,[107] and 2) greater vascular innervation was seen in the attachments. Although the sulfated GAG content of the disc and attachments are both quite low (≤1.2%), the fibrocartilaginous disc was found to contain more GAG overall. This is particularly true in the intermediate zone of the disc where higher GAG content is accompanied by more chondrocyte-like cells and collagen type II content.[16, 25] The higher collagen content observed in the disc is not necessarily a

trait of cartilaginous tissues, but is likely related to the higher density of the ECM seen in histology. Additionally, the greater elastic fiber staining and vasculature seen in the attachments probably reduces their relative collagen content. Although they are not vast, the biochemical distinctions between the disc and its attachments relate well to their tissue classifications, and also likely relate to functional properties. Based on these results, it is prudent that future mechanical characterization of the attachments be performed so that these relationships can be conclusively drawn.

Regional variation in the discal attachments was present and was most obvious in their sulfated GAG content. In the anteroposterior direction, AAS and PAI had high mean GAG contents, while AAI and PAS had little GAG. Since sulfated GAG content is generally related to compressive requirements of the tissue, this variation can be logically described in terms of mastication. As the disc translates forward during jaw opening, AAI is under tension at the front of the condyle, while AAS gets compressed between the disc and fossa.[108-110] In the posterior of the joint, the opposite is true. PAS becomes stretched with disc translation, while PAI becomes compressed beneath PB.[108-110] A similar argument may be made for the increased GAG content of MA versus LA. MA attaches high on the condylar head (Fig. 3B) and is clearly within the articulating surface. As a result, it likely experiences more compressive loading than LA, which attaches low on the side of the condylar head (Fig. 3C). Water content is generally correlated with sulfated GAG content because the negative charges draw in water molecules.[111] This trend was accurately seen within the

attachments. Collagen content did not vary greatly among the attachments, although PAI had the highest mean content. This is consistent with a prior report which indicated that the PAI attachment contained the largest diameter collagen fibers.[101]

Understanding the salient characteristics of the attachments is essential not only in terms of elucidating structure-function relationships in the TMJ *in vivo*, but also toward establishing approaches for implanting TMJ grafts or tissue engineered constructs. Future tissue engineering efforts are likely to benefit from the fact that the biochemical components of both disc and attachments are similar. It appears that the main distinction between these tissues is that the disc is a fibrocartilage, while the attachments are generally fibrous tissues. Although these tissues are distinct, they are similar enough that it is possible to start with the same cell population. Literature on tendon tissue engineering has demonstrated that starting with a fibroblast cell population, it is possible to produce both fibrous and fibrocartilaginous tissues by varying the local mechanical environment that the cells experience. Specifically, if the fibroblasts seeded in a scaffold experience only tension then they form a purely fibrous tissue, but if they experience both tension and compression then they form fibrocartilage.[112-114] It may also be possible to go the other direction, as chondrocytes exposed to cyclic tension take on a fibroblastic phenotype.[115] Construction of a tension-compression bioreactor for recapitulating the regional variation of the disc-attachment complex would be difficult, but may provide the best functional results. Furthermore, knowledge about the attachments is

expected to guide how grafts of tissue engineered constructs need to be attached or secured *in situ*.

Knowledge of the similarities and differences between the TMJ disc and its attachments is crucial for understanding TMD pathologies as well as providing tissue engineered replacements. Plenty of additional mechanical characterization is needed to fully understand the structure-function relationships within the disc and attachments, but the quantitative biochemical parameters presented here are a crucial first step. This work provides important design parameters for engineering a functional disc-attachment complex.

Figures
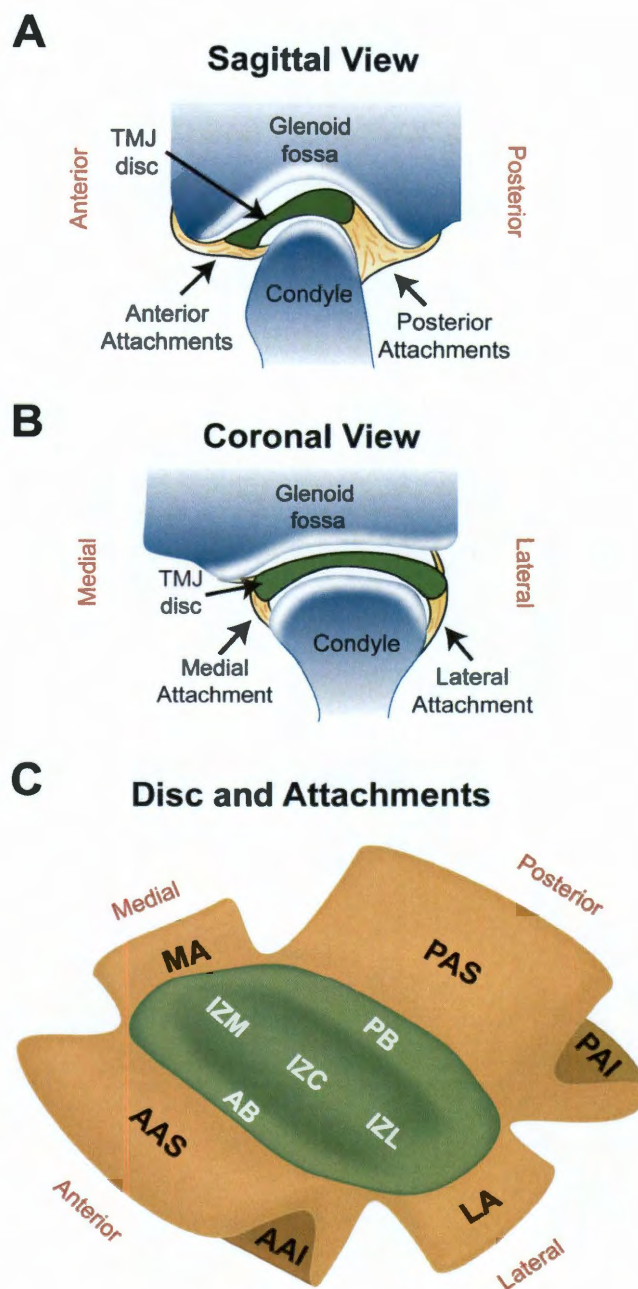
Figure 1: Anatomy and regions of the TMJ disc and its attachments. **(A)** Sagittal view of the TMJ showing the anterior and posterior discal attachments which both bifurcate into superior and anterior attachments. **(B)** Coronal view of the TMJ detailing the medial and lateral attachments which both blend into the joint capsule near its attachment to the condyle. **(C)** Depiction of the 5 disc regions and 6 discal attachments analyzed in this study which span the joint in the anteroposterior and mediolateral directions.
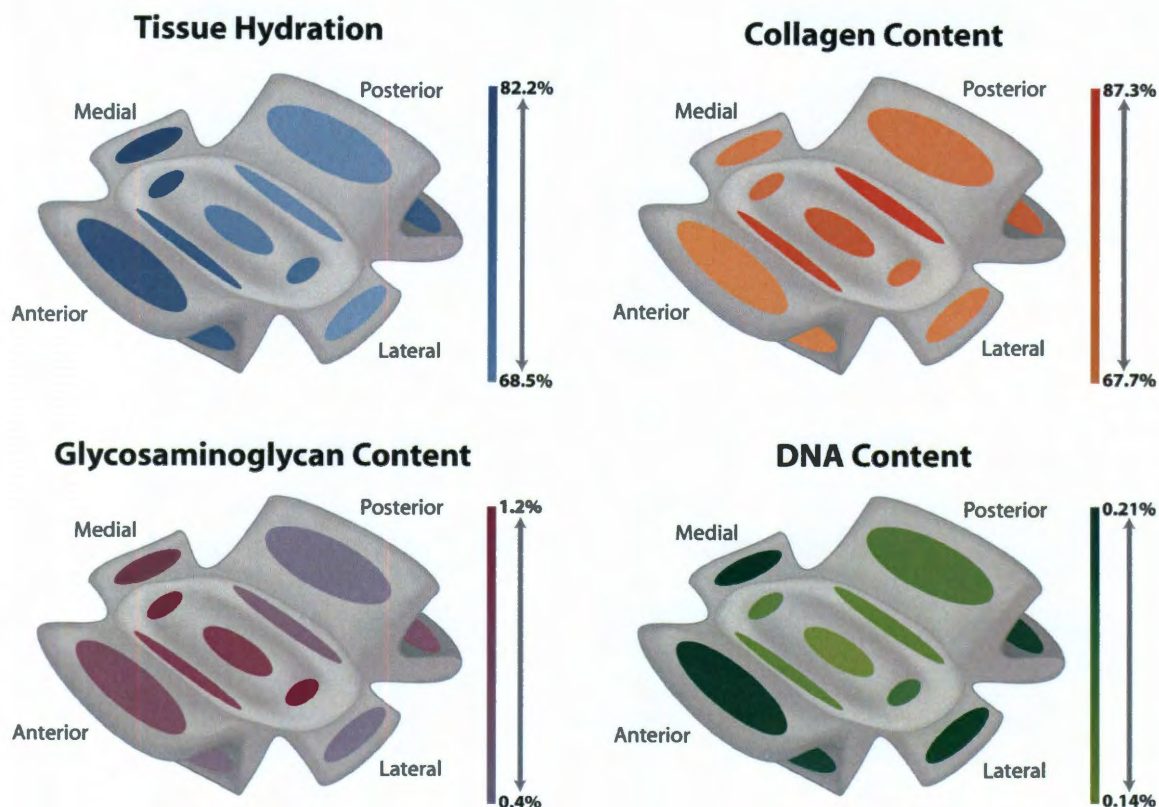
Figure 2: Heat maps of biochemical content throughout the TMJ disc and its attachments. Mean content normalized to dry weight for each region is presented as color intensity in the scale to the right of each picture. The top and bottom of the scale represent the highest and lowest mean value for each parameter. Water content was highest in anterior and medial attachments with few large variations. Collagen content was highest in the disc compared to the attachments, particularly in the bands of the disc. Overall, the disc contained more sulfated GAG than the attachments, although the medial attachment and the superior portion of the anterior attachment did contain a significant amount of GAG. DNA per dry weight was generally higher in the attachments than the disc, except in the superior portion of the posterior band.

Table 1: Quantitative results for the biochemical content of the TMJ disc and its attachments. Data is presented at mean ± SD. ANOVA results presented are from a one-way with a Tukey's HSD *post hoc* test. Groups not connected by the same letter are statically different from each other. Water content did not vary greatly, but was highest in MA and lowest in LA. PB contained the highest collagen per dry weight, while AAS contained the least. Sulfated GAG content was statically higher in IZM and IZL, while PAS had statically less. DNA per dry weight was greatest in AAS and MA, whereas it was the least in IZC.

Tissue	Region	Water Content (%)		Collagen/Dry Weight (%)		sGAG/Dry Weight (%)		DNA/Dry Weight (%)	
		Mean ± SD	ANOVA	Mean ± SD	ANOVA	Mean ± SD	ANOVA	Mean ± SD	ANOVA
Attachment	PAS	68.81 ± 2.86	BC	71.75 ± 7.08	AB	0.4 ± 0.11	D	0.16 ± 0.03	BCD
	PAI	73.76 ± 1.78	BC	78.9 ± 10.08	AB	0.76 ± 0.18	ABCD	0.19 ± 0.01	AB
	AAS	80.35 ± 2.39	AB	67.72 ± 13.96	B	0.82 ± 0.2	ABC	0.21 ± 0	A
	AAI	73.2 ± 4.06	BC	68.45 ± 8.1	AB	0.5 ± 0.14	CD	0.2 ± 0.01	AB
	MA	82.15 ± 1.19	A	71.16 ± 9.26	AB	0.88 ± 0.16	ABC	0.2 ± 0.01	A
	LA	68.49 ± 4.44	C	69.27 ± 12.38	AB	0.4 ± 0.28	CD	0.19 ± 0.03	ABC
Disc	PB	69.09 ± 1.51	BC	87.3 ± 7	A	0.59 ± 0.07	BCD	0.15 ± 0.01	CD
	AB	73.81 ± 4.95	BC	84.2 ± 12.13	AB	0.94 ± 0.23	AB	0.15 ± 0.03	CD
	IZM	73.22 ± 1.75	BC	76.36 ± 9.4	AB	1.11 ± 0.25	A	0.16 ± 0.01	BCD
	IZC	70.26 ± 1.87	BC	80.46 ± 7.15	AB	0.93 ± 0.13	AB	0.14 ± 0.02	D
	IZL	72.02 ± 3.94	BC	74.71 ± 4.79	AB	1.18 ± 0.36	A	0.18 ± 0.02	ABCD
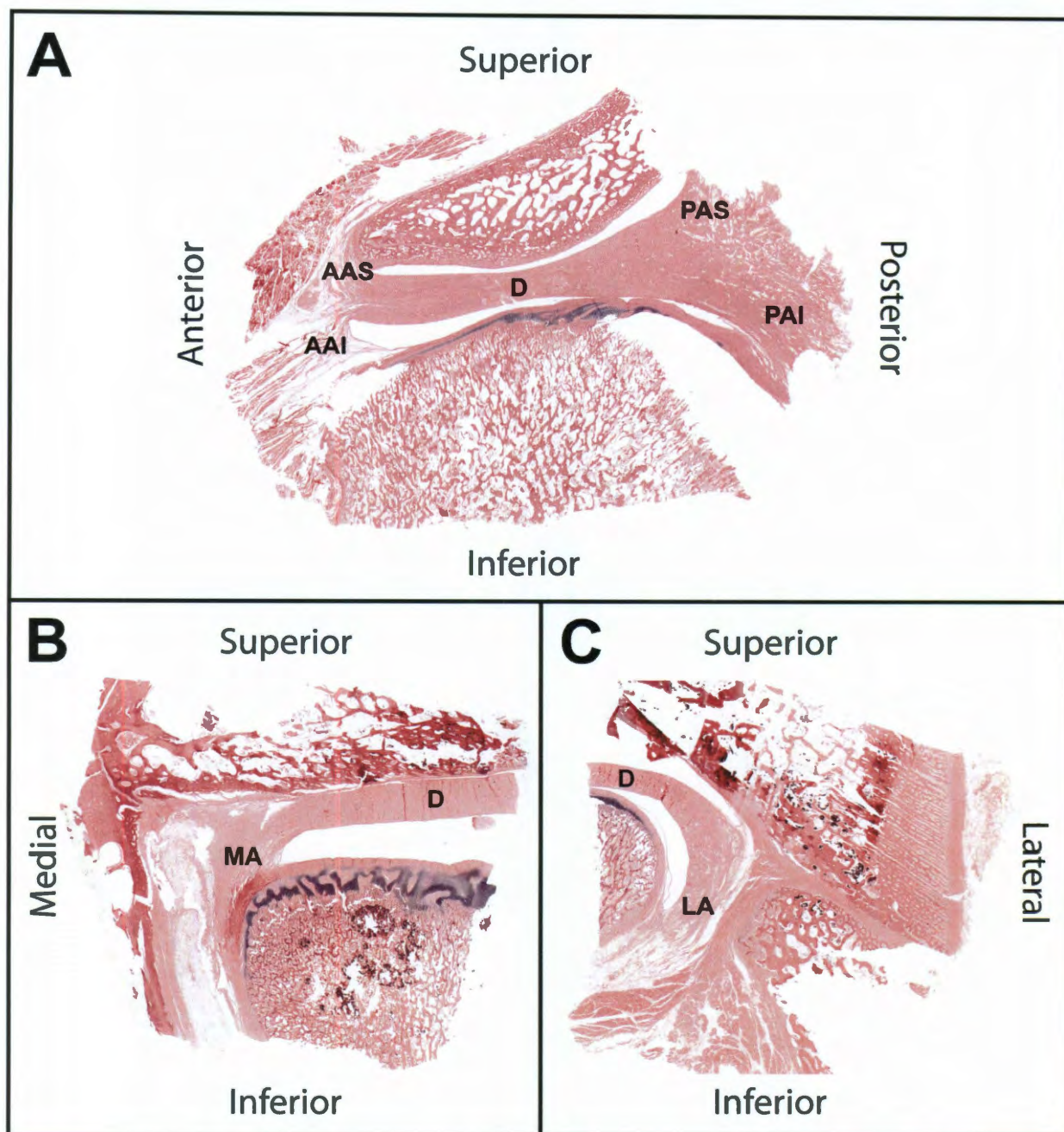
Figure 3: Whole joint histology of the TMJ. Sections were cut at 5 µm and stained with hematoxylin and eosin. **(A)** Anteriorly and posteriorly the disc blends into the attachments which both bifurcate into superior and anterior boney connections. The disc has a denser matrix than the attachments. **(B)** In the medial portion of the TMJ, the disc blends into the medial attachment high in the joint and the attachment to the condyle is at the top of the condylar head. **(C)** On the medial side of the joint, the disc wraps around the side of the condylar head and the lateral discal attachment attaches to the condyle near its base.
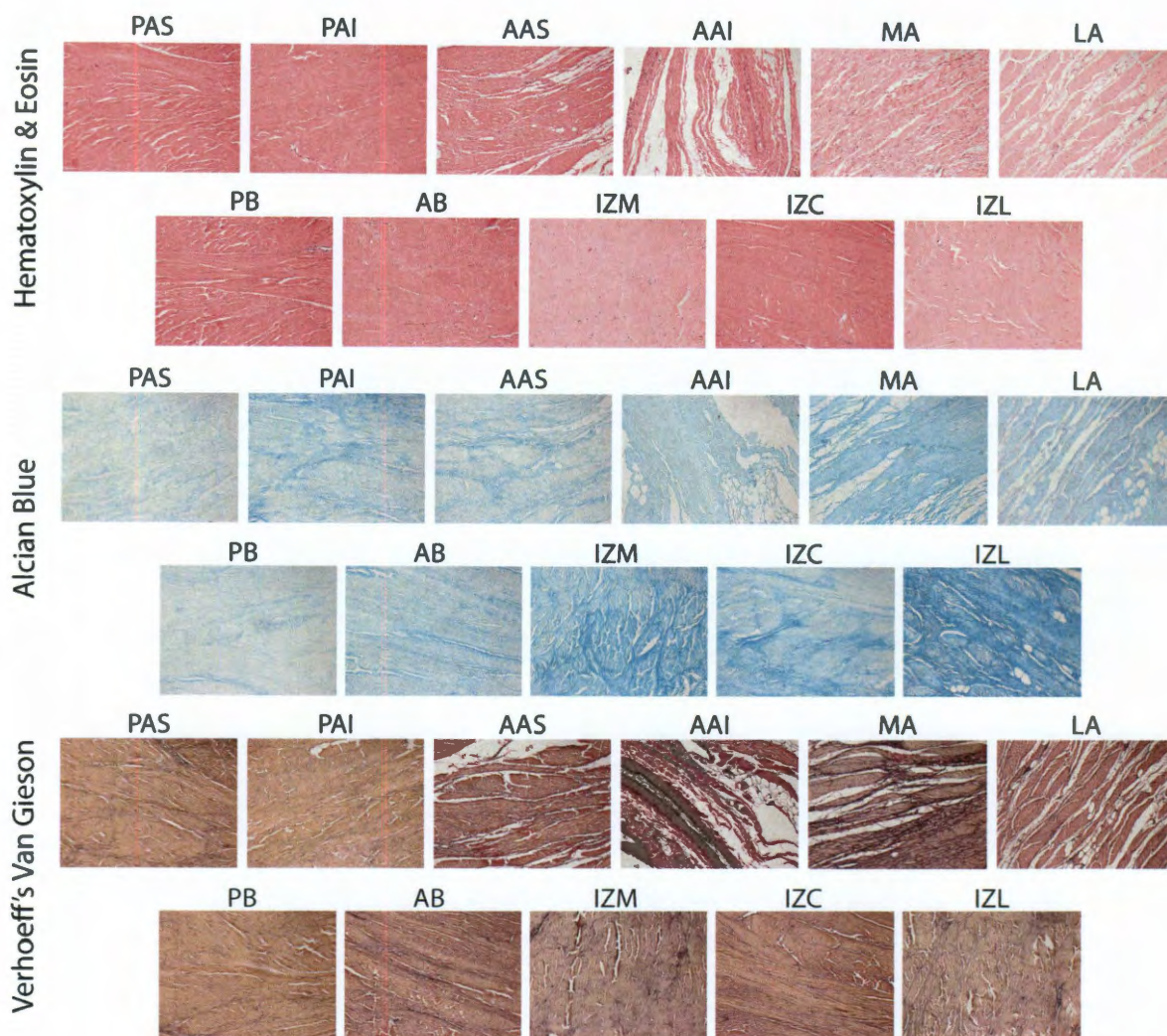
Figure 4: Regional histological staining of the TMJ disc and its attachments. In general, all histological staining verified quantitative results. Hematoxylin and eosin illustrate that cellular density is higher in the attachments, while the disc contains a denser ECM than all of the attachments expect PAS and PAI. Alcian blue staining clearly shows the higher sulfated GAG content of the TMJ disc in comparison to the attachments. IZM and IZL have the most GAG overall, while MA was the attachment with the most staining. Verhoeff's Van Gieson staining clearly shows collagen (red-brown) and elastic (black) fibers throughout the TMJ. PAS and PAI appeared to have similar content to the disc, but the other attachments show more elastin staining.

...

Chapter 4: The Effects of Glycosaminoglycan Depletion on the Compressive Properties of the Temporomandibular Joint Disc

Abstract

Sulfated glycosaminoglycans (GAGs) are known to play a major role in maintaining compressive integrity in GAG-rich tissues such as articular cartilage, but less is known about their mechanical role in fibrocartilaginous tissues in which GAGs are much less abundant. This study investigates the effects of GAG removal on the viscoelastic compressive properties in different regions of the temporomandibular joint (TMJ) disc. Chondroitinase ABC (C-ABC) was used to deplete GAGs in five different disc regions and treated specimens were assayed using an unconfined compression stress-relaxation test. Compared to untreated controls, the only regions affected by GAG removal in terms of biomechanical properties were in the intermediate zone, the most GAG-rich portion of the disc. Without GAGs, all intermediate zone regions showed a decrease in tissue viscosity, and the intermediate zone lateral region also showed a 12.5% decrease in modulus of relaxation. However, in the anterior and posterior band regions none of the compressive properties changed following GAG depletion,

but overall these regions showed the highest compressive properties. These results show that even though GAGs are not the major extracellular matrix molecule of the TMJ disc, they are responsible for some of the viscoelastic compressive properties of the tissue. Furthermore, the mechanical role of sulfated GAGs in the TMJ disc varies regionally in the tissue, and GAG abundance does not always correlate with higher compressive properties. Overall, this study found that sulfated GAGs are important to TMJ disc mechanics, especially in the intermediate zone, and this information can be used to set design characteristics for future tissue engineering efforts.

Introduction

The fibrocartilaginous temporomandibular joint (TMJ) disc resides between the mandibular condyle and temporal bone, aiding in the complex rotational and translational motions of the jaw. The disc's most important roles during mastication include shock absorption and load distribution.[116] However, as much as 25% of individuals in the United States (about 80% of whom are young women) have temporomandibular disorders (TMDs).[4, 8] The severity of TMDs vary from discomforting to debilitating and are commonly manifested through inhibited range of jaw motion, anterior disc displacement, and degeneration of the TMJ disc itself.[7] As the causes of TMD are unknown, current clinical therapy focuses mainly on pain reduction and tissue resection. It is clear, however, that the TMJ disc plays an important role in the temporomandibular joint, and its resection eventually leads to degeneration of the joint as a whole.[98] Tissue

engineering efforts may address the need for replacement discs in cases where total discectomy is necessary, but before a functional TMJ disc can be engineered the tissue's structure-function relationships must be better understood.

Currently, TMJ disc structure-function relationships are described only in terms of its most abundant biochemical element, collagen. At ~80-90% of the dry weight,[17, 81] collagen is the major structural component of the disc, and its anisotropy and contributions to the tensile properties of the tissue have been thoroughly investigated. Collagen fibers form a ring-like alignment around the periphery of the TMJ disc, with a strong anteroposterior alignment through the intermediate zone.[25, 83, 94] Correspondingly, the tensile strength and stiffness of specimens tested in the anteroposterior direction are an order of magnitude greater than those in the mediolateral direction.[33-35] The compressive stiffness of the disc is at least an order of magnitude less than the tensile stiffness,[85] but is still related to collagen. The posterior band of the disc possesses both the highest collagen content, and also the greatest compressive moduli.[106]

While the contribution of collagen to the mechanical integrity of the disc is readily measured due to its abundance, the contributions of other biochemical components of the disc to its functional properties are not as clear. Approximately 1% of the dry weight of the disc is attributed to sulfated glycosaminoglycans (GAGs), with dermatan and chondroitin sulfates being the most prevalent GAGs.[25, 100] Regionally, GAGs are found in the greatest quantities in the lateral region of the intermediate zone.[31, 81, 100] In other cartilages, such as

hyaline cartilage, GAGs are highly abundant and are mainly associated with the tissue's compressive properties.[117] Despite having the most GAG, however, the lateral region of the disc does not correspond to the highest compressive or tensile moduli.[34, 85, 106] It is unclear, therefore, how sulfated GAGs contribute to the viscoelastic properties of the disc.

To better understand the mechanical contributions of sulfated GAGs to TMJ disc properties, this study tests the viscoelastic compressive properties of the tissue with and without sulfated GAGs. GAG removal is achieved through the application of chondroitinase ABC (C-ABC) which is a GAG-cleaving enzyme that selectively cleaves chondroitin and dermatan sulfate side chains, as well as hyaluronic acid.[118] As the GAGs within the TMJ disc are overwhelmingly chondroitin and dermatan sulfate,[25] this is an optimal enzyme for testing GAG depletion. C-ABC has been used extensively to investigate the contribution of sulfated GAGs to the compressive properties of musculoskeletal tissues including articular cartilage[117, 119, 120] (abundant GAG) and ligament[121] (scarce GAG). In articular cartilage, sulfated GAG removal resulted in a marked decrease in the tissue's aggregate modulus,[119] whereas similar treatment on ligaments increased tissue permeability but did not affect the modulus.[121] Given these findings, it was hypothesized that GAG depletion in the TMJ disc would have minimal impact on the tissue's compressive moduli, similar to ligament. Furthermore, as GAG content varies amongst disc regions, it was hypothesized that the GAG contribution will vary regionally within the disc.

Materials and Methods

Specimen Procurement

Pig heads were obtained from a local abattoir (Yosemite Meat Company, Modesto, CA). TMJ discs were harvested from the left joint of seven female pigs of age 6-9 months. TMJ discs were carefully excised free from attachments and washed in 0.01 M phosphate-buffered saline (PBS). Hyaline articular cartilage served as a benchmark control for this investigation. Full-thickness cartilage was harvested from the tibial plateau of five 1-week-old male calves (Research 87, Boston, MA) and washed in PBS. After washing all specimens were wrapped in gauze soaked with PBS containing protease inhibitors (2mM EDTA, 150 mM sodium chloride, 5 mM benzamidine hydrochloride, 10 mM N-ethylmaleimide, and 1 mM phenylmethylsulfonyl fluoride) and then frozen at -20°C until testing.

Glycosaminoglycan Depletion

TMJ discs and hyaline cartilage samples were thawed in PBS at 4°C. A 3 mm dermal punch (Miltex, York, PA) was used to remove samples from 5 regions of the TMJ disc, spanning both the mediolateral and anteroposterior directions (Fig. 1A). Specifically, the five regions of the disc tested were: posterior band (PB), anterior band (AB), intermediate zone medial (IZM), intermediate zone central (IZC), and intermediate zone lateral (IZL). For the hyaline cartilage benchmark samples, 3 mm punches were taken from the center of the tibial plateau as shown in Fig. 1B. Depletion of sulfated GAGs was carried out with C-ABC at 1 U/mL in Tris-buffered saline (TBS) containing 300 mM sodium acetate

and 0.05% bovine serum albumin (all from Sigma, St. Louis, Missouri). Treatment was carried out at 37°C for 3 hrs on an orbital shaker. A 3 hr incubation was chosen because it produced >90% removal of sulfated GAGs from TMJ disc samples. Treatment controls were incubated in exactly the same manner, except the buffer contained no C-ABC.

Biochemical Analysis

Samples were frozen overnight at -20°C and then lyophilized for 48 hrs. Dry weights were recorded and then the samples were digested in papain, 125 µg/mL papain (Sigma) in 50 mmol phosphate buffer (pH 6.5) containing 2 mmol N-acetyl cysteine, for 18 hrs at 60°C. After digestion, sulfated GAG content was measured using the Blyscan Sulfated GAG Assay kit, a 1,9-dimethyl-methylene blue colorimetric assay (Accurate Chemical and Scientific Corp., Westbury, NY). Total collagen content of the samples was measured using a hydroxyproline colorimetric assay.[81] 5 samples per group were used for all biochemical analysis.

Histology

Control and C-ABC treated samples were cryoembedded in histoprep (Fisher Scientific, Pittsburgh, PA) and cryosectioned at 12 µm. To examine sulfated GAG distribution in the samples, sections were fixed with 10% phosphate buffered formalin and stained with Safranin-O. 2 samples per group were used for histological analysis.

Stress-Relaxation Compressive Testing

Prior to sulfated GAG depletion, the superior and inferior surfaces of compression samples were delicately cut with cryotome blades until the surfaces were parallel. The final sample thicknesses ranged from 0.8 – 1.6 mm. Following C-ABC treatment, the final dimensions of the each sample was measured using digital calipers. The stress-relaxation compressive testing procedure for this investigation was similar to that used in previous studies.[39, 85] Compression testing was performed in an unconfined compression chamber fitted onto a materials testing machine (Instron 5565, Canton, MA). Specimens were placed on the lower platen of a PBS-filled bath, and a rigid upper platen with a 19 mm diameter was used to apply unconfined compression. A 0.02 N tare load was applied to the sample and the platen-to-platen separation was taken as the initial specimen height from which strains were based. Samples were preconditioned with 5% strain for 15 cycles, and then 20% stain was applied. 10 min were allowed for stress relaxation. For TMJ disc samples, 7 samples per group were used for compressive testing, while 5 hyaline cartilage samples were used for testing.

Viscoelastic compressive properties were calculated by fitting equation 1 below, based on a Kelvin solid model, to the stress-relaxation curves.[85]

$$\sigma(t) = \sum_{i=1}^{n}\left[\frac{3}{2}\frac{E_r(u_i - u_{i-1})}{z}\left\{1 + \left(\frac{\tau_\sigma}{\tau_\varepsilon} - 1\right)e^{\left(\frac{-(t - t_i)}{\tau_\varepsilon}\right)}\right\}\right] \quad (1)$$

Specimen height (z) and time of strain event (ti) were determined *a priori*. Deformation (u), time (t), and stress (σ) were recorded during testing. Relaxation

modulus (E_r), relaxation time constant (τ_ε), and creep time constant (τ_σ) could be approximated from model fits, then converted into relaxation modulus, instantaneous modulus, and coefficient of viscosity equivalents.[85]

Statistical Analysis

TMJ disc samples were analyzed with two separate statistical methods. First, a 2-way analysis of variance (ANOVA) was used to compare the two overall factors of disc region and C-ABC treatment. A Tukey's HSD *post hoc* test was used where necessary. Second, the treated and untreated samples within a single region of the disc were compared directly using a paired student's t-test. Treated and untreated hyaline cartilage samples were also compared with a student's t-test. A significance level of $\alpha = 0.05$ was used for all statistical analysis.

Results

Biochemical Content

C-ABC treatment at 1 U/mL for 3 hrs was able to provide nearly complete GAG depletion in TMJ disc samples. In all regions of the disc, C-ABC treatment was able to remove ≥ 96 % of the sulfated GAG content (Fig. 2A). For example, the GAG content of IZL decreased from 0.93 % to 0.032 %. Regional GAG variation in TMJ disc samples showed that the IZL and IZM groups contained more GAG per dry weight than the PB, which is consistent with previous reports.[81, 106] The same C-ABC treatment when applied to hyaline cartilage did not produce the same magnitude of GAG depletion. Treatment reduced the

sulfated GAG / dry weight by ~50 % in cartilage samples from 19.2 % to 10.5 % (Fig. 2B). Comparing the treatment control samples, the native TMJ disc has approximately 20 times less sulfated GAG per dry weight than hyaline cartilage.

Since it is the major structural component in the TMJ disc, the collagen content of all samples was also measured. C-ABC treatment of the disc had no effect on the collagen per dry weight (Fig. 2C). Regionally, the PB contained the greatest collagen content at 88.3 %, in agreement with prior work.[81, 106] In contrast to the disc, C-ABC treatment of hyaline cartilage did alter the collagen per dry weight, increasing it by approximately 10%, from 60.9 % to 70.3 % (Fig. 2D). This increase in collagen content is due to the fact that ~10% of the previous dry weight of the tissue had been removed due to GAG depletion. Overall, the native TMJ disc contained approximately 20 % more collagen per dry weight than hyaline cartilage.

Histology

Safranin-O staining of the TMJ disc clearly demonstrates the low levels of sulfated in this tissue (Fig. 3). In the control samples, positive red-orange staining can only be seen localized directly around some of the cells, with little to no staining in the bulk matrix. Decreased staining in C-ABC treated samples is visible in most regions, although difficult to detect. Inter-regional variations on the other hand are not detectible due to the low overall staining intensity. In contrast to the disc, hyaline cartilage clearly demonstrates positive Safranin-O staining throughout the entire matrix, with enhanced staining localized to the lacunae surrounding the cells. C-ABC treatment of cartilage samples produced a clear

depletion of sulfated GAG starting at the edge and proceeding toward the center of the tissue. Additionally, there is a decrease in staining surrounding the cells in the center of the treated cartilage.

Compressive Properties

The Kelvin solid viscoelastic model was able to fit all stress-relaxation curves with a high degree of accuracy ($R^2 > 0.90$). Regional variations in all compressive properties of the TMJ disc were consistent with prior reports.[39, 85, 106]

Instantaneous Modulus

While C-ABC treatment was able to deplete sulfated GAGs from the TMJ disc, it had no effect on the instantaneous modulus of the tissue (Fig. 4A). Regionally, the bands of the disc, PB and AB, were stiffer than the intermediate zone with moduli of 1.49 and 0.93 MPa respectfully. Similar to the TMJ disc, C-ABC treatment of hyaline cartilage also produced no statistically significant difference in instantaneous modulus, although it did appear to trend lower with treatment (Fig. 4B). The instantaneous modulus of hyaline cartilage was at least twice that of all regions of the disc, with a mean value of 3.60 MPa.

Relaxation Modulus

An overall comparison using a 2-way ANOVA showed no significant effect of C-ABC treatment across all regions of the disc. On the other hand, a t-test comparing only treated and untreated samples within a region indicated that GAG depletion did produce a statistically significant decrease in IZL. The overall

decrease in relaxation modulus of IZL was ~12.5% from 24.1 to 21.1 kPa. Regional variations were also seen, with PB possessing the highest relaxation modulus at 30.2 kPa. In contrast to the disc, C-ABC treatment of hyaline cartilage produced a more dramatic decrease in relaxation modulus (Fig. 5B). Treatment resulted in a 50% drop in modulus from 347 to 174 kPa, mirroring the drop in sulfated GAG content of the tissue. Overall, the relaxation modulus of the TMJ disc was ~10 times less than hyaline cartilage.

Coefficient of Viscosity

Compared to the moduli, C-ABC treatment produced considerably more change in the coefficient of viscosity. A 2-way ANOVA indicated an overall decrease in viscosity across the TMJ disc due to GAG depletion (Fig. 6A). Specifically, C-ABC treatment produced a drop in viscosity across the entire intermediate zone (IZM, IZC, IZL) by ~30%. Viscosity of the AB and PB were not affected by treatment, although PB did possess the overall highest coefficient of viscosity at 4.84 MPa s. Similar to the relaxation modulus, C-ABC treatment of hyaline cartilage produced a ~50% drop in its coefficient of viscosity from 8.23 to 3.84 MPa s (Fig. 6B). Again, this 50% drop in magnitude mirrors the 50% drop in sulfated GAG content of the tissue. The coefficient of viscosity for hyaline cartilage was found to be at least twice that of the TMJ disc.

Discussion

It is fairly clear that the mechanical properties of the TMJ disc are likely more dependent on its abundant collagen fibers than its proteoglycans, but the true structure-function relationships within the disc have not been fully investigated. To our knowledge, this study is the first to understand the contributions of sulfated GAGs in the TMJ disc to the tissue's compressive properties. Although GAGs only make up about 1% of the total dry weight of the TMJ disc, the present results indicate that they are still able to impart tissue viscosity and compressive properties in the intermediate zone. Other disc regions, however, did not show an appreciable change in compressive properties following GAG depletion. This variation in contributions to compressive properties, shown to be directly related to regional GAG density, and compressive properties are shown not to be related to GAG content topographically, highlight complex relationships TMJ disc GAGs have with the tissue's mechanics.

The regional variation in GAG contribution to compressive properties of the disc highlighted the highly heterogeneous nature of this tissue. Overall, there was an inverse relationship between GAG content and compressive stiffness with the bands having the highest compressive moduli. At the same time, as the GAG content of the regions increased, so did the contribution of that GAG to the tissue's compressive properties. For example, in the intermediate zone of the disc where GAGs are most abundant (0.76%-0.93% per dry weight), C-ABC treatment resulted in a marked decrease in tissue viscosity. Additionally, GAG removal in the most GAG-rich region of the intermediate zone, the IZL (0.93%

per dry weight), also resulted in a decreased modulus of relaxation. Due to the range of proteoglycan concentrations in the TMJ disc, this study was able to measure the effects of GAG abundance on compressive mechanics. Below a certain range (<0.69% concentration) GAG removal had no effect on viscoelastic compressive properties, but as GAG abundance increased (>0.74%), so did its contribution to tissue viscosity. This regional variation in sulfated GAG content as well as GAG contribution to compressive properties will be an important but challenging consideration for future tissue engineering efforts.

A macroscopic view of the results presented here reveals that GAGs contribute very differently to the compressive properties of the disc than they to hyaline articular cartilage. Prior reports show that removal of sulfated GAGs from articular cartilage decreased compressive aggregate moduli and increased permeability due to less inhibition to water leaving the tissue.[117, 119, 120] Similarly in this study, removal of ~50% of sulfated GAGs from tibial cartilage resulted in a matched decrease of ~50% in relaxation modulus and coefficient of viscosity. This proportional change in compressive properties due to GAG depletion was not seen in the TMJ disc. The stiffest regions of the disc under compressive loading, PB and AB, showed no change in viscoelastic compressive properties due to GAG depletion. Even in the regions of the intermediate zone which showed a response to the C-ABC treatment, the magnitudes of the changes were far lower than for hyaline cartilage. A 97% reduction in sulfated GAG content of IZL only resulted in a 12.5% decrease in relaxation modulus and a 30% reduction in viscosity. Clearly removal of sulfated GAGs from the TMJ disc

does not produce an equivalent change in viscoelastic compressive properties as it does in hyaline cartilage.

Although the hyaline cartilage control generally responded to C-ABC treatment as expected, it produced one unanticipated finding. While the modulus of relaxation and the coefficient of viscosity decreased in an equivalent manner to the GAG depletion, the instantaneous modulus of the tissue did not decrease. Prior studies reporting a drop in compressive modulus after GAG depletion of cartilage have all reported their findings in terms of an aggregate modulus (H_A),[119-121] which is similar to the relaxation modulus used in this investigation. Henninger et al.[121] measured reduced peak stresses following GAG depletion of femoral cartilage, but their strain rate (0.01%/s) was significantly slower than that used in this study (10%/s). Clearly sulfated GAGs play a vital role in the modulus of the tissue at equilibrium, but it appears that they may play less of a role under instantaneous loading. Instead of the GAGs dictating the instantaneous modulus, it may instead be the inertia of the pressurized interstitial fluid that is the key contributor.

There are potentially several reasons why the GAGs of the TMJ disc provide a different contribution to the tissue compressive properties than the GAGs of articular cartilage. First, the sulfated GAG content of hyaline cartilage is ~20 times greater on a per dry weight basis. When tibial cartilage loses 50% of its GAGs there is a much more dramatic change in tissue composition than when the disc loses an equivalent percentage of GAGs. In addition to the quantity of GAGs, there are also important differences in the proteoglycans with which the

GAGs are associated. In articular cartilage, the GAGs are primarily associated with the proteoglycan aggrecan which has around one hundred GAG side chains. The multitude of GAG chains provide the large negative charge that prevents water movement from the tissue.[111] In contrast, the proteoglycans in the TMJ disc are mainly decorin and biglycan,[100] which only contain one or two GAG chains. Though the side chains of decorin and biglycan do not contribute a large negative charge, they alter the matrix by controlling collagen fibril diameter and organization.[122-124] Therefore the low overall GAG content of the TMJ disc may be providing more of an indirect contribution to compressive properties by shepherding collagen molecules to form a highly organized matrix able to withstand physiologic forces. This is likely to be particularly important for the posterior band of the disc which has higher collagen content and fewer GAGs than the intermediate zone, but still retains greater compressive stiffness.

This investigation provides an important insight into the role of sulfated GAGs in providing mechanical integrity to the TMJ disc, and indicates that this contribution is highly region-specific. In the outer bands of the disc, GAGs do not provide a direct contribution to compressive stiffness, but in the intermediate zone they do play a direct role in the tissue's viscoelastic compressive properties. More investigations are needed to understand how the interactions between collagen and GAGs contribute to structure-function relationships in the disc. These results are, however, a promising first step toward understanding the role of GAGs in the disc and provide valuable design parameters for tissue engineering of a disc replacement.

Figures

A) TMJ Disc   B) Tibial Plateau
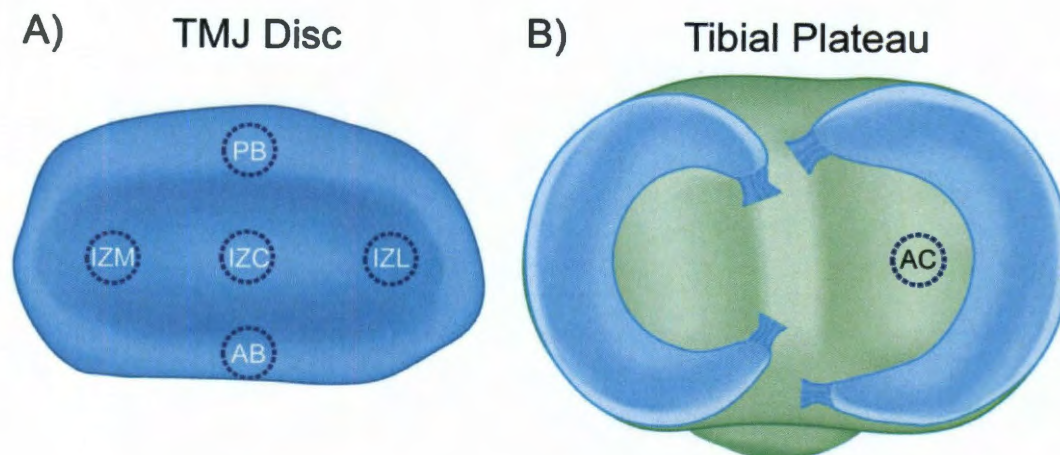
Figure 1: Regions of the TMJ disc and tibial cartilage used in this investigation. Because of the heterogeneous nature of the TMJ disc, the contribution of GAGs to the compressive properties of the tissue was tested regionally. **(A)** 3 mm discs were harvested from five regions of the disc: posterior band (PB), anterior band (AB), intermediate zone medial (IZM), intermediate zone central (IZC), and intermediate zone lateral (IZL). Hyaline articular cartilage (AC) from the tibial plateau was as a benchmark control in this investigation. **(B)** A 3 mm disc has harvested from the center of the tibial plateau on the medial side of the joint (B). (Not drawn to scale)
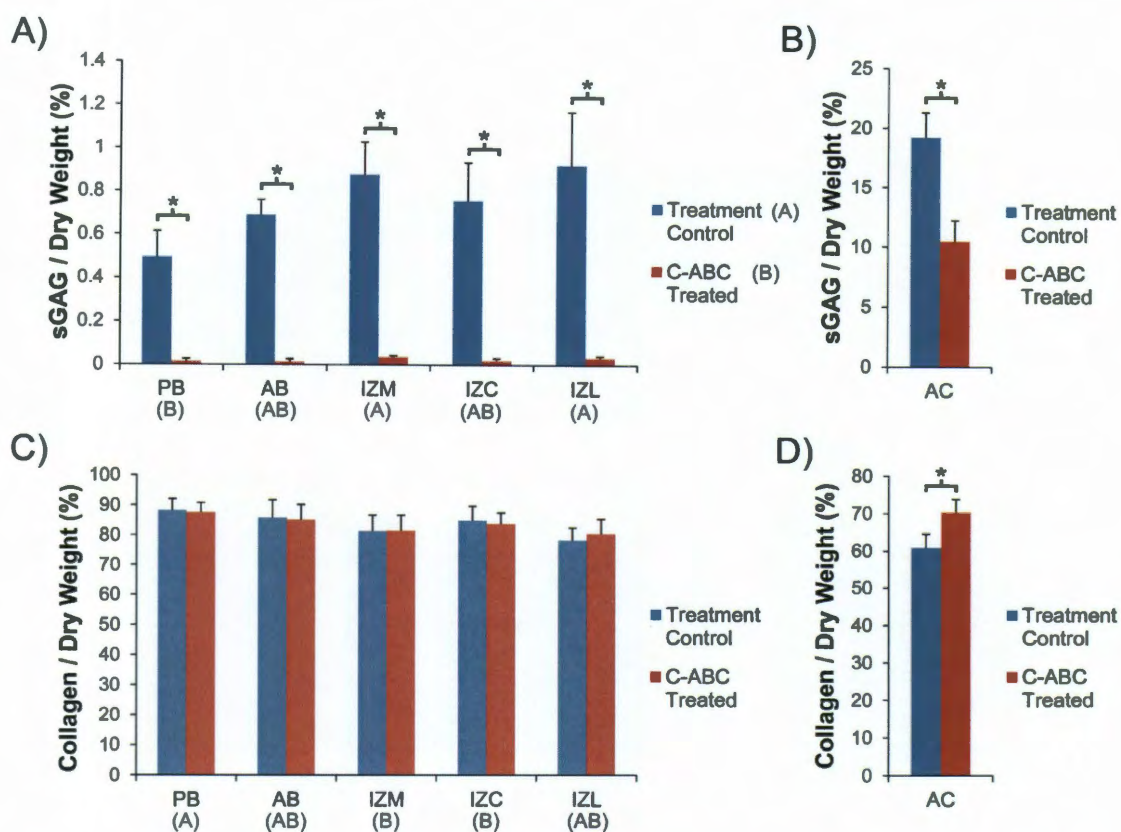
Figure 2: Sulfated GAG and collagen content of C-ABC treated samples. (A)
C-ABC treatment produced extensive GAG depletion (≥96%) in all regions of the
TMJ disc. (B) Using the same treatment, GAG depletion in tibial cartilage was
~50%. (C) C-ABC treatment produced no change in collagen per dry weight
within the TMJ disc, although there were regional differences in collagen content,
with PB containing the most. (D) Treatment of hyaline cartilage with C-ABC did
increase the collagen per dry weight (~10%), because 10% of the original dry
weight left during GAG depletion. All data was normalized to dry weight of the
specimens and is presented as mean ± SD. Two distinct statistical tests are
presented. Letters in brackets represent the results of a 2-way ANOVA with the
factors of disc region and C-ABC treatment. Groups not connected by the same
letter are statistically different. Asterisks indicate statistical significance measured
with a paired t-test.
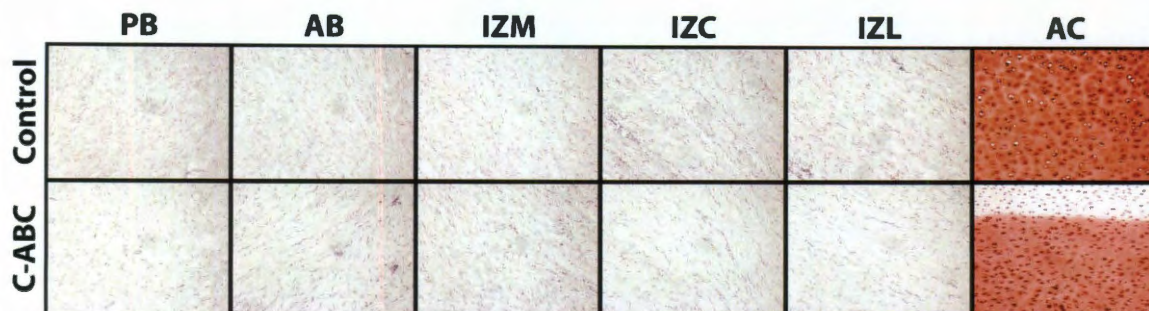
Figure 3: Safranin-O staining of C-ABC treated specimens to look at distribution of sulfated GAGs. Some positive staining (red color) can be seen in TMJ disc samples located immediately surrounding some cells, but there is very low staining overall, and no staining in the matrix. In contrast, intense positive staining can be seen throughout the matrix of articular cartilage. C-ABC treatment produced a small but visible difference in TMJ disc samples. Treatment of hyaline cartage produced a very obvious depletion of GAGs starting at the edge of the tissue and proceeding toward the center.
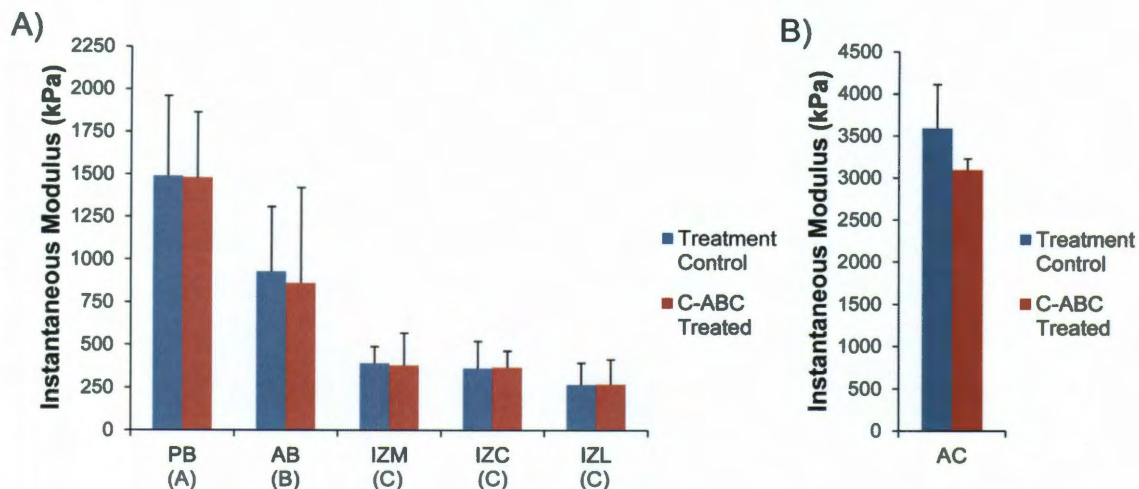
Figure 4: Instantaneous compressive modulus of tested samples. **(A)** GAG depletion with C-ABC did not produce a significant difference in instantaneous modulus in any region of the TMJ disc. **(B)** C-ABC treatment also had no effect on the instantaneous modulus of the tibial cartilage, although it did trend lower. Data is presented as mean ± SD. Letters in brackets represent the results of a 2-way ANOVA with the factors disc region and C-ABC treatment. Groups not connected by the same letter are statistically different.
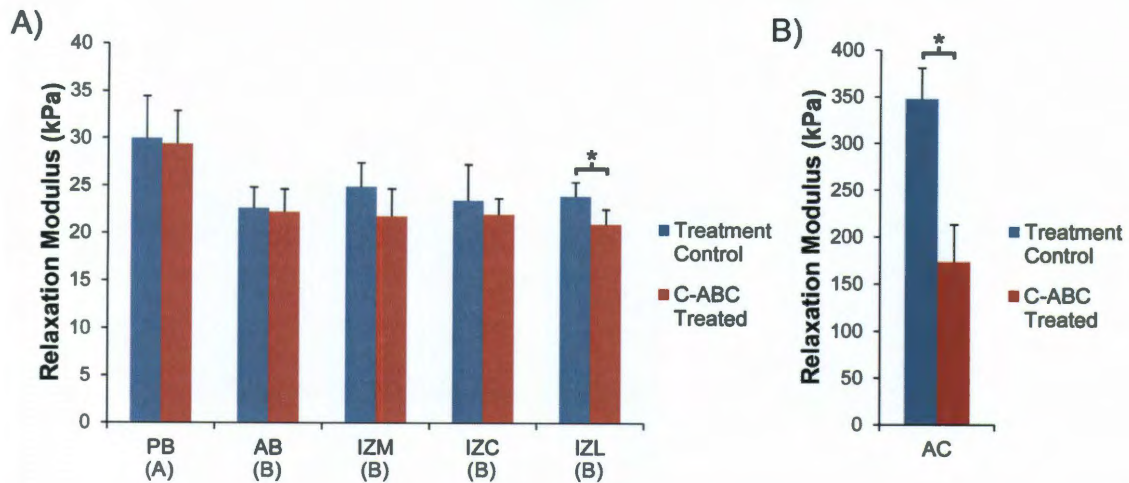
Figure 5: Relaxation compressive modulus of tested samples. **(A)** Overall, C-ABC treatment did not produce a change in the relaxation modulus of TMJ disc samples, but just within IZL, there was a statically significant drop in modulus. **(B)** GAG depletion in articular cartilage produced a ~50% decrease in relaxation modulus, which mirrored the 50% drop in GAG content. Data is presented as mean ± SD. Two distinct statistical tests are presented. Letters in brackets represent the results of a 2-way ANOVA with the factors of disc region and C-ABC treatment. Groups not connected by the same letter are statistically different. Asterisks indicate statistical significance measured with a paired t-test.
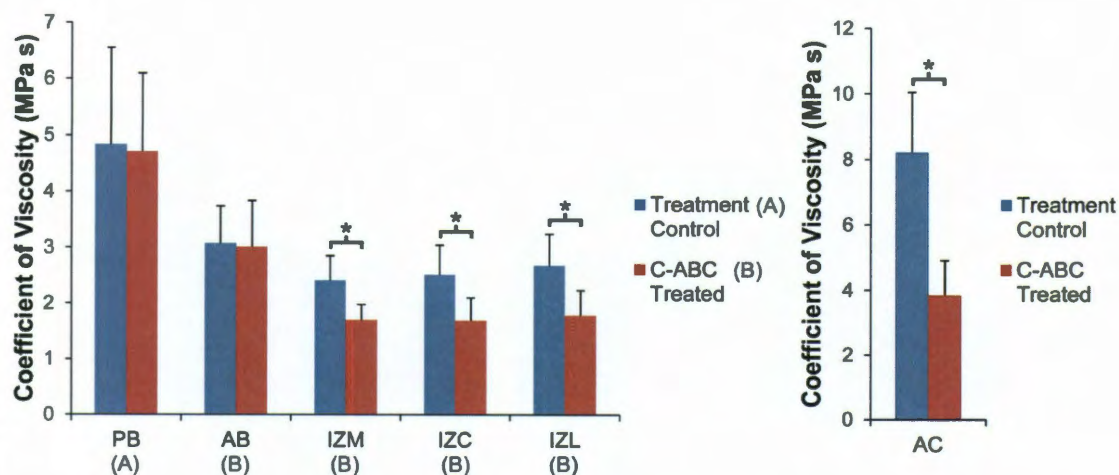
Figure 6: Coefficient of viscosity for tested samples. **(A)** GAG depletion produced and overall decrease in the coefficient of viscosity for TMJ disc samples. All regions of the intermediate zone (IZM, IZC, IZL) displayed a ~30% decrease in viscosity, although the bands of the disc (PB, AB) showed no effect. **(B)** C-ABC treatment of hyaline cartilage let to a ~50% decrease in the coefficient of viscosity, mirroring the drop in sulfated GAG content. Data is presented as mean ± SD. Two distinct statistical tests are presented. Letters in brackets represent the results of a 2-way ANOVA with the factors of disc region and C-ABC treatment. Groups not connected by the same letter are statistically different. Asterisks indicate statistical significance measured with a paired t-test.

Chapter 5: Tissue Engineering of the Temporomandibular Joint

Abstract

Temporomandibular joint (TMJ) morbidities effect around a quarter of the US population, yet there are no consistently successful treatment solutions. The TMJ is comprised of the articulating tissues between the mandibular condyle and the temporal fossa. Its fibrocartilaginous components form the articulating surfaces, with the biconcave TMJ disc allowing for smooth movement between the condyle and fossa during normal mastication. Each tissue within the joint displays unique cellular, biochemical, and biomechanical characteristics. These characteristics are important for the tissue engineer to understand, given the joint's limited ability for self-repair following injury. The TMJ is susceptible to pathologies such as osteoarthritis and internal derangement of the disc, which are extremely painful and often require clinical intervention. Current therapies include anti-inflammatory measures, occlusal splints, and in extreme cases total joint replacement. These therapies, however, are only semi-permanent and fail to restore full functionality to the joint. Tissue engineering may provide functional biological replacements for TMJ tissues, resulting in a long term solution to TMJ

pathologies. Research using alternate cell sources, scaffolds, bioactive factors, and mechanical stimulation has shown promise, but more research must be done to determine optimal combinations of these factors.

Introduction

Tissue engineering of the temporomandibular joint (TMJ), or jaw joint, is still in its early development. While a large body of knowledge exists for the characterization and tissue engineering of other synovial joints, only recently has the TMJ received significant attention. Tissue engineering functional TMJ tissues is a promising technology for the treatment of TMJ disorders (TMDs), potentially improving the lives of millions of people. Because of the complex loading patterns that engineered tissues will experience in the TMJ, complete design parameters from native tissue are critical. Unfortunately, neither the normal or diseased states of the TMJ are fully understood at present, hindering tissue engineering efforts. Within the TMJ, the fibrocartilaginous disc has received the most attention thus far, but efforts are underway to engineer the mandibular condyle cartilage and bone as well. Implantation of engineered tissues may help to alleviate pain, restore range of motion, and return the patient to normal jaw function. The potential impact of a biological TMJ replacement is even greater considering the significant lack of long term treatment options for TMD patients. This chapter provides a survey of the literature related to the rapidly expanding field of TMJ tissue engineering.

Gross Anatomy and Physiology of the TMJ

The anatomy and physiology of the TMJ have been reviewed in detail in the literature.[99, 125-127] This section provides a summary of the pertinent anatomy and physiology for engineers. The TMJ is composed of the condyle of the mandible articulating against the glenoid fossa and articular eminence of the temporal bone with an interposed disc (Figure 1). The mandibular condyle is the moving component of the articulation, while the fossa-eminence remains stationary relative to the cranium. Both of the articulating surfaces of the TMJ are covered by fibrocartilage, unlike the knee, where the articulating surfaces are covered by hyaline cartilage. Positioned between the condyle and fossa-eminence is a fibrocartilaginous disc that is attached to the periphery of the joint, and is free to move over both the superior and inferior articulating surfaces. The TMJ disc serves to increase congruity between these surfaces, distribute load, and aid in joint lubrication.[128] The TMJ is surrounded by a capsule, which encloses the intra-articular environment and attaches to the disc near the condylar head.

Movement of the TMJ is unique because it includes both rotation relative to the transcranial axis, as well as translation forward relative to the skull base. During normal mastication, the joint movement is mainly rotational, allowing vertical opening and closing of the mouth. It is only during wide mouth opening (to around 40 mm) that translation becomes a major component of the movement.[126] Under normal rotational movements, a complex pattern of compression and shear loading occurs between the anterior side of the condyle

and posterior slope of the eminence.[129] A healthy TMJ disc and synovial fluid act to dissipate these loads across the joint. If the disc becomes displaced the lack of force dissipation results in abnormal loading patterns and can cause degradation of the joint.

The attachments of the TMJ disc with the surrounding tissues are extremely important for the coordinated movements of the TMJ. Anteriorly, the disc attaches inferiorly to the anterior condyle and superiorly to the eminence by bending with the joint capsule. Posteriorly, it attaches to the bilaminar zone, which is in turn attached superiorly to the temporal bone and inferiorly to the posterior condyle. Laterally and medially, the disc attachments blend into the joint capsule near its attachment to the condylar head. This complex attachment pattern allows the condyle to rotate relative to the disc but still allows the disc and condyle to translate as a single unit during wide mouth opening.[99] Additionally the disc and its attachments separate the joint space into distinct inferior and superior regions. It has been proposed that the TMJ is mainly a translatory joint in the superior space and primarily a rotational joint in the inferior space.[130] This means that the loading patterns experienced by the two surfaces of the disc during normal motion are considerably different.

Like other diarthrodial joints, the TMJ is surrounded by a capsule. The inner surface of which is lined by synovium, a layer of cells that specialize in the production of synovial fluid. Synovial fluid serves two main functions within the TMJ. First it acts as a lubricating fluid with a coefficient of friction of approximately 0.001.[131] Secondly, synovial fluid acts as a transmission medium

for nutrients to the fibrocartilages within the joint and also serves to remove waste products. The volumes of synovial fluid in the inferior and superior joint spaces of the TMJ are about 0.5 and 1.0 mL, respectively.[125] Since it nourishes all the tissues of the joint, the importance of a healthy synovium should not be overlooked by tissue engineers.

Characterization of TMJ Tissues

TMJ tissue engineering requires finely tuned design criteria in order for constructs to effectively handle the complex loading environment of the TMJ. These design criteria are determined through characterization of the tissue in three major categories: cells contained in the tissue, its biochemical makeup, and its biomechanical properties. Understanding these components of TMJ tissues is critical for the development of mechanically functional engineered constructs, though the number of characterization studies of TMJ tissues remains relatively small in comparison to other synovial joints, such as the knee. Fortunately, recent characterization studies, particularly for the TMJ disc, have significantly increased our understanding of these complex tissues. Reviewing this information can greatly improve tissue engineering efforts by illuminating the TMJ's structure-function relationships and providing gold standard specifications.

TMJ Disc

The TMJ disc is a biconcave fibrocartilaginous tissue that sits atop the mandibular condyle and articulates against the glenoid fossa of the temporal

bone. It allows for smooth jaw movement during normal daily activities such as eating and talking. Due to its unique shape, the disc is commonly thought of consisting of three regions in the anteroposterior direction: the anterior band, intermediate zone, and posterior band (Figure 2). The intermediate zone also exhibits mediolateral variation and it is thus divided into the medial, central, and lateral regions. Finally, the two surfaces of the TMJ disc have varying properties, so the disc can also be classified into inferior and superior regions. The cellular, biochemical, and biomechanical properties that accompany this unique architecture provide the appropriate lubricating and cushioning functions for the joint. This section provides a summary of the salient TMJ disc properties for tissue engineers. Further information about the cellular, biochemical, and biomechanical properties of the disc have been reviewed in the literature.[15, 79, 82, 130, 132]

Cells

Similar to other fibrocartilages such as the knee meniscus, the TMJ disc contains a heterogeneous population of cells. These cells possess characteristics of both fibroblasts and chondrocytes and are therefore termed fibrochondrocytes.[23] The overall cellularity of the disc is reported to be between 20-50 million cells/g of tissue.[23, 81] Although the TMJ disc contains multiple cell types, the overall population appears to be more fibroblastic than chondrocytic. Histological investigations have shown that approximately 70% of the disc cells are fibroblast-like, with the remaining 30% being chondrocyte-like.[16] The

chondrocyte-like cells lack a pericellular matrix found around hyaline chondrocytes, and are mostly located in the intermediate zone.[16, 18, 26] Regional variations in cell number appear to vary with species. The anterior band was seen to contain the smallest number of cells in the porcine disc,[16, 81] while the intermediate zone was found to have the fewest cells in primate discs.[26] Regardless of distribution, the heterogeneous fibrochondrocyte cell population has been seen in all species and difficulty involved with recreating this cellular environment should be appreciated by tissue engineers.

Collagen

The main extracellular matrix (ECM) component of the TMJ disc is collagen, which largely controls the functional properties of the tissue. Collagen makes up about 37% of the wet weight[22], 50% of the wet volume[133], or 69-85% of the dry weight.[17, 81] Regional distribution of total collagen has been seen to vary depending on the animal model tested. The anterior and posterior bands were seen to contain the most collagen in the rat[26], while the intermediate zone was reported to contain more collagen in the porcine disc.[81] Although there are several types of collagen in the TMJ disc, collagen type I is by far the most prevalent.[23, 26] Collagen type II, the primary component in hyaline cartilage, can be found in small amounts in the intermediate zone, surrounding chondrocyte-like cells.[23, 25, 26] Trace amounts of other fibrillar (type III) and non-fibrillar (types VI, IX, XII) collagens have also been found in the TMJ disc.[19, 20, 134] Collagen type

I is by far the most prevalent component of the TMJ disc's ECM and will need to be recreated in a tissue replacement.

The orientation of collagen fibers in the TMJ disc is anisotropic, but there is a basic symmetry. Collagen fibers near the periphery of the disc align in a ring-like structure, while the collagen fibers in the intermediate zone run predominately in an anteroposterior direction.[24, 25, 94] In the center of the disc, transition regions are observed where the anteroposterior directed fibers of the intermediate zone meet the mediolateral directed fibers of the anterior and posterior bands.[24] It has been speculated that the outer ring of fibers serves to maintain the disc shape under both tensile and compressive loads.[135] The average collagen fiber diameter in the disc is 18±9 µm.[25] Finally, collagen fibers in the disc exhibit a wavy or crimped appearance throughout the full thickness of the tissue.[136] The unique ring-like collagen fiber orientation of the TMJ disc has important ramifications for the mechanical properties of the tissue, as described below.

Glycosaminoglycans and proteoglycans

Together glycosaminoglycans (GAGs) and proteoglycans can contribute to the compressive and tensile properties of a tissue. GAGs are long repeating disaccharide chains with without branching that possess at least one negatively charged side group. Proteoglycans are composed of a central protein core with one or many GAG side chains. There is little agreement in the literature about the

total quantity and regional variation of GAGs in the TMJ disc. The total sulfated GAG content has been reported between 1 and 10% of the dry weight.[28, 30] This is a large range, but most studies indicate that disc GAG content is below 5%.[17, 25, 28, 31, 81] Regionally, studies of the porcine TMJ disc have indicated that the posterior band has the least sulfated GAG.[25, 81] Similar results have been seen in the bovine disc, where the bands were shown to have less GAG content than the intermediate zone.[31] The exact opposite distribution of GAGs has been seen in the primate disc, with the anterior and posterior bands having the highest content.[26] Regardless of conflicting results, it is clear that the GAG content of the disc is much lower than hyaline cartilage.[15]

The main proteoglycans in the TMJ disc are chondroitin sulfate (CS) and dermatan sulfate (DS). The GAG chains associated with these two proteoglycans make up 75-93% of the total GAG content of the disc.[17, 25, 31] Other proteoglycans including keratan sulfate and heparin sulfate have been found in trace amounts.[17, 25, 28, 31] Similar to GAGs, there are conflicting reports about the regional proteoglycan distribution in the TMJ disc. In the rat disc, the highest concentrations of CS proteoglycans were found in the bands and the greatest concentration of DS proteoglycans was found in the intermediate zone.[100] The exact opposite trends in CS and DS proteoglycan distributions were seen in the porcine disc.[25] Unfortunately, the studies that have investigated regional distribution of proteoglycans and GAGs have all used different assays. As a result, it is difficult to determine if the regional disparities seen are a result of interspecies variations, or a byproduct of the different assays used.

Tissue mechanics

It is important to understand the mechanical properties of the TMJ since engineered constructs will need to support the same loads imparted on the native tissue. The compressive properties of the disc have been studies fairly extensively, but the measured mechanical properties have varied widely between studies. Under unconfined compression, the porcine disc displays an instantaneous and relaxed moduli of 500 and 30 kPa, respectively.[39, 85] These results match well with other porcine and human disc studies.[38, 137] The canine and bovine discs demonstrate a much larger compressive resistance, with instantaneous moduli of 31 and 15 MPa under unconfined compression and stress relaxation, respectively.[35, 84] It is unclear whether these drastic differences are due to interspecies variations or the different testing modalities used. Regionally, the greatest instantaneous moduli have been seen in the anterior and medial portions of the disc from porcine and bovine samples.[39, 84, 85] Additionally, a large instantaneous modulus has been observed in the posterior band of the porcine disc, but this was not observed in bovine samples. The central portion of the disc is reported to have a modulus equal to or less than the anterior and posterior bands.[38, 39, 84, 85] This is an interesting finding, since the center of the disc is generally reported to have more sulfated GAGs, which often correlates to compressive stiffness.[82] From these data, it appears that compressive properties are more closely related to total collagen content than GAG, probably due to the exceedingly low GAG content in the TMJ disc.

Tensile testing of the TMJ disc has also resulted in large variations in reported mechanical properties. Reported tensile moduli for the TMJ disc range from 0.5 to 100 MPa.[33-35, 83] This large range of recorded properties is related to dramatic variations in regional tensile properties, which are fairly consistent across studies. The tensile modulus of the porcine disc is higher in the anteroposterior direction than the mediolateral direction.[33, 34] Regionally in the mediolateral direction, the relaxation moduli of the posterior band, anterior band and intermediate zone in the porcine disc are 23.4 MPa, 9.5 MPa, and 0.58 MPa, respectively.[34] Similar results have been seen in the canine disc.[83] The dramatic two-fold decrease in tensile modulus between the posterior band and intermediate zone is interesting because it does not correspond to a dramatic difference in biochemical content. Instead, it is due to the fact that the collagen fibers in the intermediate zone are aligned in the anteroposterior direction, perpendicular to loading.[34] Tensile variation in the anteroposterior direction is not as substantial, but the central region is the stiffest followed by the medial, and then lateral sections.[34, 35] It is clear that collagen alignment is important for the tensile properties of the tissue and should be considered in all engineering efforts.

Condylar and Fossa Cartilages

While characterization of the TMJ disc is not fully complete, it is far more comprehensive than the current characterization of condylar cartilage. This cartilage lines the articulating surface of the mandibular condyle and moves

against the inferior surface of the TMJ disc. Like the disc, condylar cartilage is a fibrocartilaginous tissue with noted amounts of collagen types I and II. This tissue exhibits a zonal architecture, and is commonly divided into four zones in a superior to inferior fashion: fibrous, proliferative, mature, and hypertrophic (Figure 3). The articulating fibrous zone is a fibrocartilaginous region that sits on top of a highly cellular proliferative zone. The mature and hypertrophic zones, which border the subchondral bone, are considered to be like hyaline cartilage. This section provides an overview of the salient properties of condylar and fossa cartilages. It should be noted however that scant information exists on fossa cartilage. More detailed reviews of structure and composition can be found in the literature.[132, 138, 139]

Cells

Similar to other fibrocartilages, the cells of condylar cartilage are a heterogeneous fibrochondrocyte population, but unlike the TMJ disc, true chondrocytes can be found in some regions. The articulating surface of mandibular cartilage contains flat fibroblast-like cells, which is indicative of this region being called the fibrous zone.[140, 141] The proliferative zone is a highly cellular region that appears to play a role as a cell reservoir for the other zones. It produces cells for the overlying fibrous zone,[142, 143] as well as chondrocyte precursors for the underlying mature zone.[144-146] Terminally differentiated chondrocytes are the main cell type in the mature and hypertrophic zones, although hypertrophic chondrocytes can be found near the junction with the

subchondral bone.[147] The fact that the proliferative zone produces cells for all of the other zones should be noted by tissue engineers. If this layer can be purified, the cells it contains may be a potent cell source for engineering condylar cartilage.

Extracellular matrix

Although collagen appears to be the main constituent in condylar cartilage, there is little known about the exact quantity of collagen present. A value of 165 nmol of hydroxyproline/mg of dry weight has been reported,[148] as well as 2.2 µg/mg of wet weight.[132] In contrast, the types of collagen present in condylar cartilage have been studied quite thoroughly using immunohistochemistry. Collagen type I can be found throughout the cartilage, but is primarily located in the fibrous and proliferative zones.[18, 149, 150] Collagen type II is the primary collagen of the mature and hypertrophic zones,[18, 150] although type X can also be found in these regions.[151] The fibrous zone contains collagen type III in addition to type I, which is representative of its fibrous nature.[149] More studies need to be completed on the quantitative distribution of collagens in condylar cartilage.

Collagen orientation in condylar cartilage has also been seen to have zonal heterogeneity. Microscopic investigations of the fibrous zone have indicated a transversely isotropic collagen fiber alignment, with sheets of fibers stacked on top of each other.[147, 152, 153] More recently, a macroscopic study of the fibrous zone showed anisotropic fiber orientation.[154] The proliferative zone is

mostly cellular and contains few collagen fibrils.[155] The mature and hypertrophic zones exhibit randomly oriented collagen fiber bundles, indicating that there is an isotropic arrangement of collagen in these zones.[152, 155] Overall, collagen organization results indicate the presence of a bi-layered fiber structure with an anisotropic layer near the articular surface and an isotropic layer near the underlying bone.[139]

The total GAG content in mandibular cartilage is reported to be 6.4 μg/mg wet weight in the rat,[149] or about 0.19 mg in the rabbit.[148] Keratin and chondroitin sulfates are the only GAGs that have been studied in mandibular cartilage, and there is contradictory evidence about their distribution. A primate study found these GAGs only in the mature and hypertrophic regions,[18] while they were found in the fibrous and proliferative zones of porcine and rat cartilage.[156, 157] Regionally, cartilage from the anterior and posterosuperior portions of the condyle have been found to contain more chondroitin sulfate than the superior region.[158] There is a zonal distribution of proteoglycans as well, with aggrecan located primarily in the mature and hypertrophic zones.[156, 157] Decorin on the other hand, is distributed fairly evenly throughout the cartilage.[159] Even though condylar cartilage contains chondrocytes, its GAG and proteoglycan content are significantly different from articular cartilage.

Tissue mechanics

Tensile testing of condylar cartilage has revealed a dramatic anisotropy in tensile stiffness, which matches the collagen fiber organization discussed earlier.

The Young's modulus of condylar cartilage in the anteroposterior and mediolateral directions has been reported to be 9.0 and 6.6 MPa respectively when the cartilage is connected to subchondral bone.[160] When the cartilage is tested independent of bone, the modulus ranges from 8.0 to 11.0 MPa in the M-L direction, and 22 to 29 MPa in the A-P direction.[154] This anisotropy has also been seen under dynamic shear testing, where the storage moduli of condylar cartilage were found to range from 1.50 to 2.03 MPa in the anteroposterior direction and 0.33 to 0.55 MPa in the mediolateral direction.[161, 162] Overall, condylar cartilage is stiffer under tension and shear in the anteroposterior direction, which is also true for the TMJ disc.

Compressive testing of condylar cartilage has been conducted using numerous methodologies, but unfortunately there is no consensus about the anteroposterior variation in compressive properties. Studies using nanoindentation and dynamic compression have found that cartilage from the anterior region of the condyle was stiffer than the posterior region.[163, 164] In contrast, studies using creep indentation and unconfined compression reported that the posterior cartilage was the stiffest.[165, 166] In regards to mediolateral variation, multiple studies have agreed that cartilage from the medial region of the condyle is the stiffest.[164, 166] In general, the aggregate modulus of condylar cartilage has been reported in the range of 45 to 75 kPa.[166] Unfortunately, there is no consensus about the regional variation in compressive properties of condylar cartilage, and more data are required to provide exact design requirements for tissue engineering.

Although little characterization of the fossa cartilage has occurred, the compressive properties have been tested using creep indentation. The average aggregate modulus of fossa cartilage was reported to around 36 kPa, with cartilage from the posterior fossa being the stiffest and anterior fossa cartilage being the most compliant.[38] Overall the fossa cartilage was found to be 57% thinner and 50% stiffer than the TMJ disc. Although this study provides a start for fossa characterization, a significant amount of further research is needed.

Mandibular Condyle and Temporal Fossa

The mandibular condyle, covered by a thin layer of fibrocartilage, is the major moving structure in the TMJ. It articulates against the glenoid fossa, also called mandibular fossa, which is a part of the upper temporal bone.[132] Looking at the structural organization of bones, they are typically composed of two microarchitectures: woven and lamellar bone, which are organized into dense cortical bone (compact bone) and porous cancellous bone (spongy or trabecular bone), as reviewed.[167] For example, underneath the condylar cartilage, a compact bone plate covers cancellous bone in the mandibular condyle.[138] From the viewpoint of chemical composition, bone is a well-organized composite matrix that is composed of a protein based soft hydrogel template (e.g., collagens, noncollagenous proteins and water) and hard inorganic components (such as hydroxyapatite), as reviewed.[168] Specifically, a large amount of nanocrystalline hydroxyapatite, typically 20-80 nm long and 2-5 nm thick, is found in the bone matrix.[167] Additionally, 90% of the organic phase in bone is made of type I

collagen, which contributes to the elastic properties of bone. Other noncollagenous proteins including various adhesive proteins (such as laminin, fibronectin and vitronectin), bone-inductive proteins (such as osteopontin, osteonectin and osteocalcin), growth factors and cytokines are found in the bone matrix to mediate cell-bone functions.[167, 169] Unlike cartilage, bone has strong self-repairing potential. Various bone cells including osteoblasts (bone forming cells), osteoclasts (bone resorbing cells), and osteocytes (mature osteoblasts) are actively involved in normal bone functions including extracellular matrix (ECM) mineralization and new bone synthesis.

Clearly, the mandibular condyle's unique structure and composition must support a variety of mechanical loads during daily activities. To date there have been several studies investigating the mechanical properties (such as stiffness and strength) of the cortical or cancellous bones in the TMJ.[170-174] For instance, it was reported that the cancellous bone of human mandibular condyle has anisotropic mechanical properties: the compressive elastic modulus and ultimate stress of axial specimens in mandibular condylar bones were 431 MPa and 4.5 MPa when compared to 127 MPa and 1.6 MPa of respective transverse specimens.[171] Cortical bone throughout the human mandibular condyle has been shown to posses significantly more stiffness than cancellous bone, exhibiting elastic moduli roughly 12.2-26.6 GPa varying with different axes and locations.[172] It was also observed that the cortical plate on the lateral side was much thicker than the medial side. These anisotropic properties should be kept in mind when

trying to engineer condylar bone. Unlike mandibular bone, little information exists about the bone of the glenoid fossa and further characterization is needed.

Pathology of the TMJ

Disorders of the TMJ (TMDs) include a wide variety of conditions for which the etiology is not fully understood. Signs and symptoms of TMDs include limited mouth opening, deviation of the jaw during opening, dislocation, clicking, locking, and muscle pain during jaw movements.[175] Epidemiological studies report that about a quarter of the population has symptoms of TMD,[4] but after reviewing patient records it appears that only 3 to 4% of the population seek treatment.[5] Three common pathologies of the TMJ which end up requiring clinical treatment are internal derangement, degenerative joint disease, and ankylosis. The first two mainly affect the soft tissues of the joint and the third affects the bony structures.

Internal derangement of the TMJ is defined as an abnormal relationship of the articular disc to the mandibular condyle and articular eminence.[125] It is believed to be the result of multiple pathological processes, including softening of the tissues, perforation of the disc, alterations in synovial fluid lubrication, and overactive musculature.[126] Disc displacement typically occurs on the anterior medial side of the condyle. The result of TMJ disc derangement depends largely on the extent and duration of the displacement. Long term internal derangement typically results in altered loading patterns in the joint, reduced mobility, and increasing degradation of the soft tissues.[126] These long term degenerative effects are thought to be caused by a direct mechanical injury and/or a hypoxia-

reperfusion injury.[176] A progression of five stages of internal derangement has been described involving increasing joint degradation over time.[8] Most TMD patients with intermediate stage internal derangement progress into the later stages. Understanding internal derangement is particularly important because a prior study has indicated that 70% of patients with TMD have disc displacement.[7]

Degenerative joint disease involves a catabolic loss of articular tissue and is a common form of degeneration in synovial joints. The main form of degenerative joint disease in the TMJ is osteoarthritis caused by excessive loading, but rheumatoid arthritis caused by auto-immune responses can also occur. Osteoarthritis of the TMJ is characterized by degradation and abrasion of the articular cartilage surfaces, which is accompanied by secondary inflammation.[177] The exact etiology of osteoarthritis in the TMJ is unknown, but it likely involves trauma to the joint, excessive loading, immobility, and increasing age.[178] During TMJ osteoarthritis, expression of matrix metalloproteinases (MMPs) and vascular endothelial growth factor (VEGF) in the joint are elevated resulting in increased inflammation and degradation of the soft tissues.[179] The result is abnormal remodeling and breakdown of the TMJ cartilages. TMJ degenerative joint disease can result from internal defragment, or it can develop on independently.

The next TMJ pathology differs from the preceding conditions, because it involves a disorder of bone metabolism, rather than soft tissue. TMJ ankylosis involves hypertrophic bone formation in the condyle or temporal bones. This excessive bone growth reshapes the articulating surfaces, and if given time to

grow, can completely bridge the joint space. This results in immobilization of the mandible and a complete lack of joint function. Trauma to the joint cavity in young children, or repetitive trauma from surgeries is connected to the development of ankylosis.[180] Removing the hypertrophic bone is typically not a long term solution for ankylosis, as the bone will commonly regenerate.

Engineers must appreciate the complex pathologies of the TMJ. Without understanding the factors responsible for destruction of the native joint, it will not be possible to produce a permanent biological replacement. For example, if the joint degradation is initially caused by a displaced disc, not only must the disc be repositioned or replaced, but the catabolic and inflammatory environment of the joint must also be addressed. Because of the joint disease, the synovial fluid will be saturated with inflammatory factors that, if left unchecked, will likely lead to destruction of the newly implanted disc. Understanding TMJ pathology will significantly increase the likelihood of success for future tissue engineered TMJ replacements.

Current Therapies

As TMJ pathology progresses, an increase in symptoms often causes patients to seek clinical care. The most common reason for TMD patients to request medical care is pain.[128] Current clinical treatment options can be broken down into four categories: non-invasive, minimally invasive, invasive, and alloplastic replacement. As detailed elsewhere,[98] the goals for treatment of TMD patients should include: 1) decreased joint pain, swelling and reflex masticatory

pain; 2) increased joint function; 3) prevention of further damage; and 4) prevention of disability and disease-related morbidity. This section provides an overview of common clinical treatments for TMD. More detailed information can be found in the literature.[98, 126]

The first stage of clinical treatments for TMD is non-invasive and generally includes, occlusal splints, physical, myofunctional and behavioral therapy as well as medications. Occlusal splints provide physical separation of the teeth. The goal of occlusal splints is to eliminate occlusal factors which trigger para-functional habits and masticatory muscle hyperactivity thereby reducing the involuntary overloading of the joint. Mandibular repositioning splints are used in order to achieve a repositioning of a dislocated TMJ disc. Due to the multifactorial nature of TMDs and the numerous types and concepts for occlusal splints, there are mixed reports on the effectiveness of this treatment.[181] Physical therapy, including active and passive joint movement and myofunctional therapy, is another important component of non-invasive therapy which has been seen to reduce pain in TMD patients.[182] Occlusal splints and physical therapy are commonly combined with behavioral therapy such as biofeedback and techniques for stress management, which has emerged as an extremely important component of TMD therapy. Non-steroidal anti-inflammatory agents, such as ibuprofen, are the most common medications given for TMJ pain.

Following or in conjunction with non-invasive treatments, minimally invasive therapies include injections, arthrocentesis, and arthroscopy. Corticosteroid injections are used occasionally for severe inflammation, but

repeated injections can lead to cartilage destruction.[183] Intra-articular injections of hyaluronic acid to increase lubricity of the joint have been suggested,[184] but are not yet approved for clinical practice. During arthrocentesis, a needle is used to flush and drain the joint space, with the goal of removing inflammatory mediators and enhancing lubrication. Arthroscopy of the TMJ is mainly used for diagnosis of early stage arthritis,[185] although some manipulation can be done such as removing fibrotic tissue.

Even though a majority of TMD patients can be managed with minimally invasive treatment, there is a subset of patients (~20%), which will require surgical intervention.[186] TMJ arthroplasty is a relatively common surgical procedure that requires replacement of the disc with, for example, an autogenic material. Typically the local temporalis muscle flap is used for disc replacement,[187] although a tissue engineered disc would be of great utility in this situation. Hemi-arthroplasty, reshaping the fossa or replacing it with an alloplastic implant became popular in the 1960s, but is rarely used today because of concerns about degradation of the remaining joint tissues.[126] Although orthognathic surgery is an option for TMD patients, it is not frequently used since the outcomes are poor for patients with pre-existing TMJ degradation.[188] Instead, orthognathic surgery is now used in conjunction with total joint replacement to enhance facial symmetry.

When advanced degenerative disease is present in the TMJ, currently the only clinical option is an alloplastic total joint replacement. Replacing all or part of the TMJ with an alloplastic material will always come under intense scrutiny

based on the poor history of these procedures. In the late 1980s a Teflon-Proplast implant was approved for TMJ disc replacement by the Food and Drug Administration (FDA). These implants ended up fragmenting under normal loading conditions, leading to a large foreign body giant cell inflammatory response and causing immense resorption of the condyle and fossa.[189] In spite of this failure, alloplastic total joint replacements for the TMJ have been researched intensely for the last 20 years. Currently, there are three total joint replacement systems approved by the FDA, manufactured by Christensen, Biomet, and TMJ Concepts. TMJ total joint replacements generally consist of a chromium-cobalt-molybdenum condylar head articulating against an ultra-high molecular weight polyethylene (UHMWPE) fossa. The total alloplastic TMJ reconstruction is considered an appropriate treatment of advanced-stage degenerative TMJ disease, although the lifetime of the device and the long term implications for the surrounding tissues are not yet known.[98] Tissue engineering may provide a functional and permanent biological replacement for the TMJ, eliminating the need for alloplastic regeneration.

Tissue Engineering

While many tissues in the body when injured have an innate capacity to self-repair, there are some tissues that have little to no self-repairing capacity. The tissues of the TMJ fall into the latter category. Additionally, due to the complex interplay of tissues within the joint, a deficiency in one area can detrimentally affect the surrounding tissues, causing pathology of the joint as a

whole. Widespread injury of the TMJ, combined with its limited reparative capacity necessitates some form of clinical intervention in order to maintain normal function and eliminate pain for the patient. Presently, clinical therapies fall short of addressing the full spectrum of issues and are only semi-permanent. Tissue engineering may address these deficits by providing permanent, biomimetic, replacement tissue systems for the TMJ. To achieve this, scientists use the tissue engineering paradigm (Figure 4). In this paradigm, native tissue is first characterized to create design parameters for tissue engineering. These design parameters are then used to inform the selection of an appropriate cell source, bioactive factors, biomechanical stimulation, and/or scaffold for the creation of an implantable biomimetic tissue. In this section, current tissue engineering efforts for the disc, condylar cartilage and condyle will be reviewed.

TMJ Disc

Characterization data for the TMJ disc have determined certain specifications that should be considered when tissue engineering a suitable replacement. It is known that this tissue houses a distinct cell population and has unique geometry and mechanical properties, brought on by the anisotropic behavior of its biochemical components. Tissue engineering of the disc, therefore, must recapitulate these characteristics of the disc in order to preserve its function within the joint. Unlike other tissues of the TMJ, a considerable number of studies have investigated engineering of the disc. Although the first report of TMJ disc tissue engineering appeared in 1994, a majority of the tissue

engineering efforts have been conducted recently. This section reviews important advances in cell and scaffold selection, as well as the role of bioactive factors and mechanical stimulation used in the field of TMJ disc tissue engineering.

Cell sources

Selection of a cell source is likely the most important aspect of any tissue engineering strategy. These cells are responsible for ECM production and maintenance resulting in a functional replacement tissue. The most commonly used cells for engineering the TMJ disc have been primary disc cells.[41, 43, 45, 48, 51, 56, 190-194] Although primary TMJ disc cells have been studied extensively, there are two main problems with this cell source: 1) lack of donor cells, and 2) donor site morbidity. It is possible to passage cells in monolayer to increase cell numbers, but unfortunately TMJ disc cells dedifferentiate rapidly in culture and their phenotype is difficult to recover.[195-197] Due to concerns about donor site morbidity, costal chondrocytes have recently been investigated as an alternative cell source for TMJ disc engineering.[198-201] This research was prompted by the fact that oral surgeons already use costal rib grafts for replacement of the mandibular condyle and donor site morbidity is minimal.

To completely eliminate concerns about primary cell sources, progenitor cells will likely need to be used for future TMJ tissue engineering efforts. Recently, a series of self-renewing and highly potent human stem cells such as multipotent mesenchymal stem cells (MSCs), umbilical cord matrix stem cells and pluripotent embryonic stem cells (ESCs) have emerged and have shown

promise for TMJ tissue regeneration. These stem cells, as shown in Figure 5, have a large proliferation capacity enabling them to expand without losing their phenotype. Even after expansion, they are able to differentiate into cartilage, bone and tendon/ligament. Both adult and embryonic stem cells have been shown to be capable of differentiating into fibrochondrocytes that can be used for TMJ disc engineering.[202-205] Additionally, progenitor cells from the skin have been shown capable of differentiating down a chondrogenic linage in response to ECM molecules.[3, 206] Future studies will need to further investigate the differentiation of progenitor cells and their application in TMJ tissue engineering.

Scaffolds

Scaffolds are an important consideration in tissue engineering since they provide the constructs' initial mechanical integrity and allow for cell attachment. The first TMJ disc tissue engineering study used a porous collagen scaffold and produced constructs with appreciable size and ECM.[41] Similar success was seen with porous polyglycolic acid (PGA) and polylactic acid (PLA) scaffolds. Both materials were shown to support cell attachment and matrix production for up to 12 wks.[207] Another early study compared PGA, polyamide filaments, expanded polytetrafluoroethylene (ePTFE), and bone blocks for disc engineering.[43] While all scaffolding materials supported cell attachment, there was poor ECM production in all groups. The majority of more recent TMJ disc engineering efforts have used PGA non-woven mesh scaffolds.[45, 48, 51, 190-192] While PGA scaffolds do support cell attachment and biosynthesis, its fibers degrade too rapidly,

producing constructs of very small size. As a result, Allen and Athanasiou (2008) compared the use of PGA to poly-L-lactic acid (PLLA) non-woven meshes. PLLA scaffolds produced constructs with enhanced dimensions and mechanical integrity compared to PGA.[193] Additionally, encapsulation of TMJ disc cells in alginate hydrogels has been investigated, but cell viability and ECM production were quite low after 4 wks.[51] Overall, significantly better results have been observed when culturing TMJ disc cells on natural and synthetic mesh scaffolds than encapsulating the cells in hydrogels.

Although scaffolds are typically an integral part of tissue engineering, it is also possible to produce scaffold-less constructs. Recent efforts to engineer the TMJ disc using costal chondrocytes have produced large functional constructs using a scaffold-less "self-assembly" technique.[198-201] In this procedure, cells are seeded at very high density into a non-adherent well, which forces the cells to bind to each other.[208] The cells then secrete their own ECM scaffolding over time. Ultimately, both scaffold-less and scaffold based approaches have seen beneficial results for tissue engineering the TMJ disc and both techniques should be further investigated.

Bioactive agents

Growth factors are commonly used in tissue engineering because of their ability to enhance cellular proliferation and/or biosynthesis. So far five different growth factors have been investigated for TMJ disc tissue engineering: platelet-derived growth factor (PDGF); basic fibroblast growth factor (bFGF); transforming

growth factor-β 1 (TGF-β1); transforming growth factor-β 3 (TGF-β3); and insulin-like growth factor-I (IGF-I). In monolayer culture, TGF-β1, IGF-I, and bFGF have all been shown to increase TMJ disc cell proliferation and biosynthesis.[23, 47] It was noted that higher concentration of growth factors favored cell proliferation, while low concentrations of growth factors favored biosynthesis.[47] In three-dimensional culture, the effects of growth factors in TMJ disc tissue engineering have been investigated with both PGA and PLLA mesh scaffolds. On PGA scaffolds, both IGF-I and TGF-β1 were shown increase collagen synthesis of porcine TMJ disc cells.[48] In contrast, with PLLA constructs, only TGF-β1 showed a significant increase in biochemical and biomechanical properties.[193] This differential effect may be related to the fact that PGA degrades much faster than PLLA. Growth factors have also been used to enhance TMJ disc tissue engineering using costal chondrocytes. IGF-I enhanced the cellular and biochemical properties of scaffold-less costal chondrocyte constructs.[199]

Although growth factors have received the most attention, other bioactive agents can have a significant impact on TMJ disc tissue engineering as well. TMJ disc cells cultured in media with 25 μg/mL of ascorbic acid produced constructs with higher collagen content than cells cultured under concentrations of 0 or 50 μg/mL.[192] Molecules such as ascorbic acid are important to ECM protein synthesis and should be considered when choosing a media for tissue engineering. Recent evidence from articular cartilage engineering suggests that using catabolic agents can improve construct properties. Natoli et al. (2009) recently demonstrated that applying chondroitinase-ABC (C-ABC, a GAG

removing enzyme) during the midpoint of culture can improve the tensile properties of engineered cartilage. The GAGs that were depleted by C-ABC return by the end of culture and there is no loss in compressive properties.[209] Non-traditional bioactive agents such as this deserve future investigation for TMJ disc tissue engineering.

Mechanical stimulation

The native TMJ disc experiences significant loading which encompasses compression, tension, and shear components.[54] Since the disc is such a mechanically important tissue, it makes sense that mechanical stimuli may be required to produce an optimal tissue engineering construct. The first study to investigate mechanical cues on TMJ tissue engineering used a rotating wall bioreactor to create a low-shear fluid environment. Constructs grown in the rotating wall bioreactor ended up being statistically the same as culture controls and no benefit of the low-shear environment was observed.[56] Continuous hydrostatic pressure of 10 MPa has been shown to increase ECM synthesis of TMJ disc cells both in monolayer and in PGA scaffolds.[191] In contrast, intermittent hydrostatic pressure of 10 MPa applied at 1 Hz was seen to be detrimental to TMJ disc cell biosynthesis. In two-dimensional culture, TMJ disc cells exposed to dynamic tensile strain significantly reduced production of MMPs in response to the pro-inflammatory cytokine interleukin-1 β (IL1-β).[210] While it is clear that mechanical cues have an impact on TMJ disc tissue engineering, more research

is needed to determine if other stimuli used in articular cartilage engineering, such as compression and shear, are beneficial.

Condylar Cartilage

Of the three TMJ tissues for which tissue engineering has been attempted, condylar cartilage has received the least amount of attention. The first report of three-dimensional condylar cartilage engineering did not appear in the literature until 2007. Similar to the disc, condylar cartilage has limited repair capabilities and is an excellent candidate for tissue engineering. To this point, disc and condylar cartilage engineering have been conducted independent of each other, although tissue engineering results from one tissue will likely benefit the other. Since engineering of condylar cartilage is a new field, efforts thus far have focused on the issues of cell source and application of bioactive agents.

Cell sources

The majority of condylar cartilage tissue engineering efforts thus far have used primary cells from the tissue.[211-216] Currently two methods have been used for harvesting primary condylar chondrocytes. The first uses collagenase to digest the cartilage,[211] and the second allows the cells to migrate out of tissue explants.[212] The collagenase method isolates cells from all four cartilage zones, whereas the tissue explant method isolates only cells from the fibrous zone. While condylar chondrocytes do grow in culture and respond to growth factors, they show relatively low ECM production *in vitro*.[138] Due to the low matrix

production, chondrocytes from other parts of the body have been used for condylar cartilage engineering. Articular chondrocytes from the ankle have been compared to condylar chondrocytes during both monolayer and three-dimensional culture. In monolayer, condylar chondrocytes showed greater proliferation but ankle chondrocytes produced tremendously more matrix.[217] On PGA scaffolds ankle chondrocytes again produced an order of magnitude more ECM than condylar chondrocytes.[218] Future studies using primary cells will likely use a chondrocyte source from somewhere other than the condyle.

Due to the standard concerns about primary cell sources (insufficient cell number and donor site morbidity), progenitor cells have begun to be investigated for condylar cartilage engineering. Recently human umbilical cord mesenchymal stromal cells (hUCMSCs) have been identified as an attractive cell source for condylar engineering. hUCMSCs are multipotent stem cells that develop from the extraembryonic mesoderm of the umbilical cord. When hUCMSCs were compared to condylar chondrocytes for tissue engineering, hUCMSCs were seen to proliferate more rapidly and produce significantly more matrix.[214] External stimuli have been shown to increase the matrix production of hUCMSCs even further.[204, 205] Capitalizing on the deficiencies of primary cells, multipotent stem cells appear to have a bright future in condylar cartilage engineering.

Scaffolds

While there are many potential scaffolds for condylar cartilage engineering, at this point only two scaffolding materials have been used. The

most common scaffold choice has been a PGA mesh.[204, 205, 214, 218] The choice of PGA has likely been influenced by TMJ disc engineering where it had previously been used. As mentioned earlier PGA supports good cell attachment and matrix production, but degrades too rapidly in culture. Other than PGA, one study has investigated encapsulation of condylar chondrocytes in alginate gel beads.[219] After 4 wks the cells maintained a chondrogenic phenotype based on immunostaining. As the field of condylar cartilage expands it is clear that attention will need to be paid to scaffold choice.

Bioactive agents

To date the use of bioactive agents in condylar cartilage engineering has focused on the application of growth factors to condylar chondrocytes and hUCMSCs. The growth factors investigated are similar to those used for TMJ disc engineering, including bFGF, IGF-I, TGF-β1, and epidermal growth factor (EGF). A high concentration of bFGF appears to have the greatest effect on condylar chondrocyte proliferation, although it may inhibit ECM biosynthesis of the cells.[213, 215, 216] IGF-I has been shown to be a potent promoter of both cell proliferation and matrix synthesis, particularly GAG production.[216, 220, 221] Condylar chondrocyte biosynthesis has also been shown to increase with TGF-β1 application, but it is unclear whether it exhibits positive effects on cell proliferation.[216] Cells from the fibrous zone of condylar cartilage have been show to be stimulated by EGF, but the remaining zones have not been investigated.[212] Finally, IGF-I has also been shown to enhance the fibrochondrogenesis and

matrix synthesis of hUCMSCs.[205, 217] These results provide basis for further investigations into using external stimuli to enhance condylar cartilage engineering.

Mandibular Condyle

Unlike tissue engineering the TMJ disc which began in the early 1990s, condylar engineering did not appear in the literature until 2000. Fortunately, bone tissue engineering in general has been studied extensively. Although still lagging behind the TMJ disc, there has been more effort to engineer the mandibular condyle than the condylar cartilage. The current field of mandibular condylar tissue engineering combines a variety of cell types (i.e., osteoblasts, chondrocytes), mandibular condyle shaped scaffolds (i.e., polymers, ceramics), and bioactive factors (i.e., TGF-β, IGF-I, bFGF), to restore the functionality of damaged tissues. A majority of the efforts thus far have been focused on creating a condyle-shaped scaffold since this is a non-trivial shape.

Cell sources

Mature osteoblasts and chondrocytes are the most commonly used cell types to regenerate new bone and cartilage tissues. Specifically, osteoblasts have been investigated as one of the main cell sources for subchondral bone repair.[222] They can actively interact with proteins and minerals to adhere, proliferate, and develop a mineralized ECM and differentiate into mature bone. Weng et al. (2001) created a tissue-engineered mandibular condylar construct

via a combination of osteoblasts, chondrocytes and scaffolds. They seeded osteoblasts into a PGA/PLA scaffold and then painted chondrocytes onto the surface of the scaffold.[223] This study showed that the formation of a bone/cartilage composite *in vivo* is promising for future mandibular condylar reconstructions.

The lack of clinical translatability for primary cells has also been recognized in mandibular condyle engineering. A recent push has been made to investigate the used of stem cells in condylar engineering. Many studies have revealed promising results of bone marrow derived MSCs for repairing condylar defects.[224-227] Alhadlaq and colleagues (2003) once encapsulated the chondrogenically and osteogenically differentiated bone marrow MSCs into biphasic poly(ethylene glycol)-based hydrogels in order to create a human-shaped mandibular condyle. After 8 weeks of *in vivo* implantation, it was demonstrated histologically that cartilaginous and osseous phenotypes were present in two stratified layers.[224] In summary, stem cells are emerging as a promising cell source for mandibular condyle tissue regeneration, though they require more investigations to fully explore their medical potentials.

Scaffolds

Scaffolds play an important role in mandibular condylar tissue engineering through providing structural and mechanical supports for cell growth and tissue formation. Due to the ease of fabrication, good biocompatibility, suitable mechanical properties and controllable biodegradability, natural or synthetic

polymers have been extensively used as bone, and osteochondral tissue engineering scaffolds. Popular polymers for tissue engineering the mandibular condyle have been poly(ethylene glycol) (PEG), polycaprolactone (PCL), PLA, PGA, and poly-lactic-co-glycolic acid (PLGA). Ueki et al. (2003) implanted poly-lactic acid/poly-glycolic acid/gelatin sponges (PGS) with or without recombinant human bone morphogenic protein-2 (BMP-2) into condylar defects of rabbit TMJs. After 4 weeks, it was observed that the PGS scaffolds with or without BMP-2 induced new bone and cartilage-like tissues in the TMJ.[228] In another study, a tissue engineered bone construct with a mandibular condyle shape was obtained by combining osteogenically differentiated mesenchymal stem cells and PLGA scaffolds.[229]

Calcium phosphate ceramics such as hydroxyapatite (HA) and tricalcium phosphate (α- or β-crystalline TCP) share a similar crystal structure and chemical composition to natural bone. As a result, they have good osteoconductive and osteoinductive properties and have been considered as popular bone substitutes, filler materials, and bone tissue engineering scaffolds.[168] For mandibular condylar tissue engineering, calcium phosphates are usually fabricated with polymers into a composite. The Hollister group has generated various load bearing tissue engineered scaffolds with appropriate bulk geometry and microarchitecture through image-based design and solid free-form fabrication methods from polymers (PLA, PGA, PLGA, PPF, etc.), ceramics (HA or TCP) or their composites (PLA/HA, PPF/TCP, HA/TCP).[230-234] For instance, a biphasic PLA/HA composite scaffold was made and fibroblasts with BMP-7 and chondrocytes were

separately seeded into the HA and PLA phases.[230] The results showed simultaneous growth of bone, cartilage, and a mineralized interface tissue in the tissue engineered scaffold. Thus this technology holds potential for repairing osteochondral defects in the TMJ.

Natural tissues or organs have numerous nano features and cells directly interacting with nanostructured ECM. Therefore, biomimetic nanomaterials, which have basic structural units, grains, particles fibers or other constituent components smaller than 100 nm in at least one dimension, have been investigated for TMJ implants, bone, and cartilage regenerations.[168, 235] For example, by using chemical vapor deposition technology, a nanostructured diamond film with high hardness and enhanced toughness was deposited on articulating surfaces of TMJ implants and exhibited excellent biocompatibility and mechanical properties.[236] In addition, some *in vitro* studies showed that nanophase HA significantly enhanced osteoblast adhesion and inhibited undesirable fibroblast adhesion compared to conventional HA[167]. Venugopal and colleagues (2008) demonstrated that osteoblast proliferation, alkaline phosphatase activity, and mineralization were significantly improved on the electrospun fibrous PCL/HA/gelatin nanocomposite when compared to PCL alone. It was also reported that the electrospun PCL nanofibrous scaffolds effectively induced chondrogenic differentiation of MSCs *in vitro*,[64] and bone formation *in vivo*.[237] Even though few results of nanostructured scaffolds for mandibular condylar tissue engineering are available, it is a promising research

field due to its use of biomimetic surface topography, increased wettability, and better mechanical properties.

Bioactive agents

Even though condylar engineering is a new field, one recent study has investigated the effects of growth factors on tissue development. Srouji et al. (2005) evaluated *in vivo* mandibular defect repair by hydrogel scaffolds with IGF-I and TGF-β1. After 6 weeks, significant bone formation was observed in the mandibular defects implanted with TGF-β1, IGF-I, and TGF-β1 + IGF-I incorporated hydrogels.[238] Although this study provides a preliminary insight, more research needs to be performed to determine the full potential of bioactive agents for condylar engineering.

Future Directions for TMJ Tissue Engineering

TMJ tissue engineering has progressed quite dramatically over the last ten years. There are now investigators actively working on biological replacements for the disc as well as the cartilage and bone of the condyle. The current literature provides a reference point for tissue engineering challenges such as cell source and scaffold selection, although the amount of prior work varies between tissues. There is still a significant amount of work that needs to be completed to produce functional replacements for TMJ tissues. Clear directions for the future of TMJ tissue engineering include progenitor cells, enhanced external stimulation, and engineering of the remaining TMJ tissues.

Progenitor Cells

Previous work using primary TMJ cells has allowed the characterization of these cells *in vitro*, but a clinically relevant tissue engineered construct will likely not contain these cells. Problems with primary cells have been discussed above and include a lack of donor tissue and high donor site morbidity. A practical cell source for TMJ engineering should originate from healthy tissues which, when removed, should not result in significant morbidity.[132] The likely choice is progenitor cells whether adult or embryonic. Direct comparison has shown that multipotent progenitor cells outperform TMJ cells.[214] Both mesenchymal stem cells and embryonic stem cells have shown the ability to differentiate down fibrocartilaginous and osteogenic lineages.[203, 204, 224, 239] Although stem cells have been used for TMJ tissue engineering, different cell types have been used for each tissue in an investigator dependent manner. Additionally, the differentiation of these progenitor cells into TMJ-like cells is not fully understood. In the future there should be coordinated efforts to determine the appropriate progenitor cells for all TMJ tissues, as a total biological joint replacement must be the ultimate goal.

Mechanical Stimuli

Even though a significant number of TMJ tissue engineering studies have been completed, only three have investigated the effects of external mechanical stimuli. Since the TMJ is a frequently loaded joint it makes sense that mechanical

stimulation would enhance TMJ engineering. Biomechanical stimuli have been used extensively in articular cartilage engineering with great success.[240] Stimuli that may be beneficial for TMJ tissue engineering include: compression, tension, shear, and hydrostatic pressure. All of these mechanical loads are present in the TMJ.[132] Hydrostatic pressure[191] and tensile loading[210] have both shown promise for disc engineering and should now be carried forward toward tissue engineering of other TMJ tissues. Compression and shear have not yet been evaluated for TMJ engineering, but should certainly be incorporated into future studies.

Other TMJ Tissues

While current tissue engineering efforts have focused on engineering the disc and condyle, other tissues of the joint, including the fossa cartilage, disc attachments, and capsule, should also be considered. Each of these tissues plays an important role in the joint, and need to be considered toward engineering a total biological TMJ replacement. Although the fossa-eminence is not well characterized, fossa cartilage and bone engineering are likely to benefit directly from condylar cartilage and bone engineering studies. The disc attachments and joint capsule on the other hand are distinct tissues that will require independent characterization and tissue engineering efforts.

Disc attachments

Although significant attention has been paid to characterization and engineering of the disc, very little focus has been placed on the disc attachments. These attachments connect the disc to the capsule and bony structures of the joint. The discal attachments are important for keeping the position of the disc in the joint relative to the condyle and fossa.[99] Maintaining disc position is critical for preserving normal loading patterns and a breakdown in the discal attachments will result in joint degradation. Characterization of the native disc attachments will provide important information about how a tissue engineered disc should be implanted in the joint. It is possible to anchor an engineered disc directly to the condylar head, but this will prevent movement of the disc relative to the condyle and alter the loading pattern in the joint. A more likely solution would be to engineer a disc with its attachments so that the attachments could be anchored to the condyle and sutured to the capsule. This would allow a natural movement of the disc within the joint. Future studies will need to investigate the properties and the tissue engineering potential of the disc attachments.

Joint capsule

Like the discal attachments, the capsule is a critically important by poorly understood component of the TMJ. Globally, the capsule provides a barrier which isolates the intra-articular joint spaces. Unlike the fibrocartilages of the joint, the TMJ capsule is innervated with various groups of nerve endings including Pacinian corpuscles.[126] Inclusion of these nerve endings may be necessary for a physiologically normal joint replacement. Additionally, the capsule is lined with

synovium, which produces the lubricating and nourishing synovial fluid for the joint. Lubrication is critically important for maintaining normal TMJ loading and must be incorporated into an engineered replacement. The exact difficulties involved in recreating the TMJ capsule will need to be investigated in the future. Ultimately all of the TMJ tissues including the fossa, disc attachments, and capsule will need to be tissue engineered to produce a total biological replacement for the TMJ.

Conclusions

Although it has only recently received attention, the field of TMJ tissue engineering is growing rapidly. The pathology of the TMJ is complex, but it is important to address these diseases for the millions of people suffering from TMD. Even though characterization of native TMJ tissues is not yet complete, the available literature has provided a rough set of design and validation criteria on which tissue engineering efforts can be based. Current tissue engineering efforts provide a basis for selecting a cell source, scaffold, and external stimuli, although technological advancements provide new options regularly. The rapid increase in TMJ disc characterization and engineering studies over the last ten years provides optimism for the remaining TMJ tissues that are not as well studied. It is clear that significant effort must be put forth before the ultimate goal of creating a functional biological replacement for the TMJ can be reached, but the future looks bright for this technology.

Figures
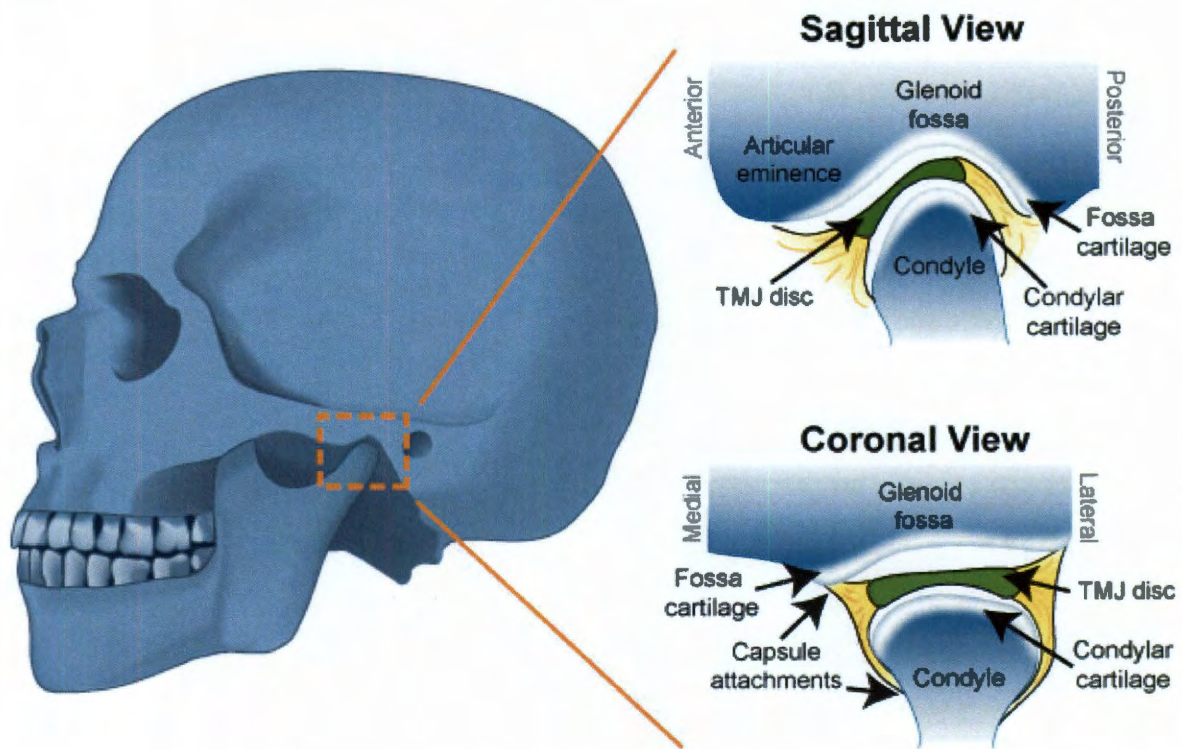
Figure 1: Anatomy of the TMJ

Figure 1: Location and anatomy of the TMJ in the sagittal and coronal planes. The TMJ is capable of both rotational and translational movement and is composed of three articulating structures: the mandibular condyle, TMJ disc, and the glenoid fossa. The mandibular condyle and glenoid fossa are both covered by fibrocartilage and the TMJ disc is positioned between these two structures.
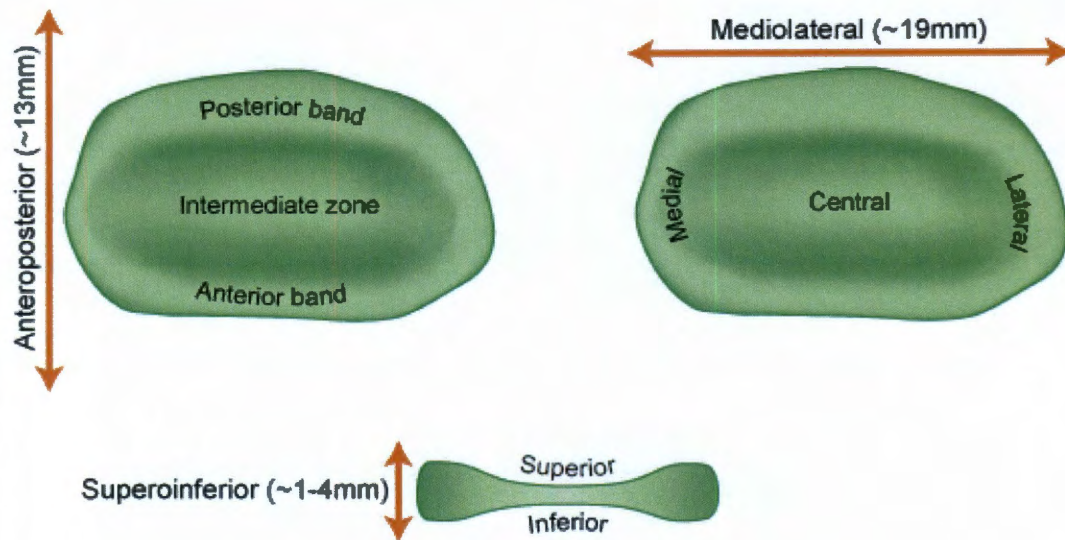
Figure 2: Regions of the disc

Figure 2: Regional variations and approximate dimensions of the TMJ disc. The TMJ disc is commonly classified into the posterior band, intermediate zone and anterior band in the anteroposterior direction. In the mediolateral direction the disc is can be separated into the medial, central, and lateral regions. The disc exhibits a biconcave shape in the superoinferior direction with each surface having distinct properties.
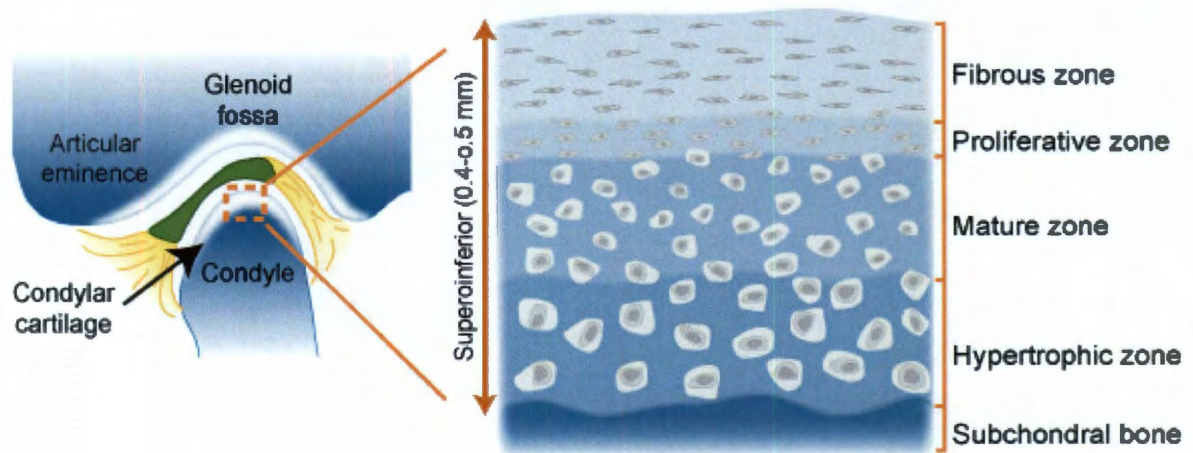
Figure 3: Condylar cartilage zones

Figure 3: Zonal architecture and approximate dimensions of condylar cartilage. Condylar cartilage is commonly divided into four zones in the superoinferior direction: fibrous, proliferative, mature, and hypertrophic.

Native tissue

Biomechanics   Biochemistry   Cells

Scaffold   Bioactive factors   Mechanical stimulation   Cell source

Implantable tissue engineered construct
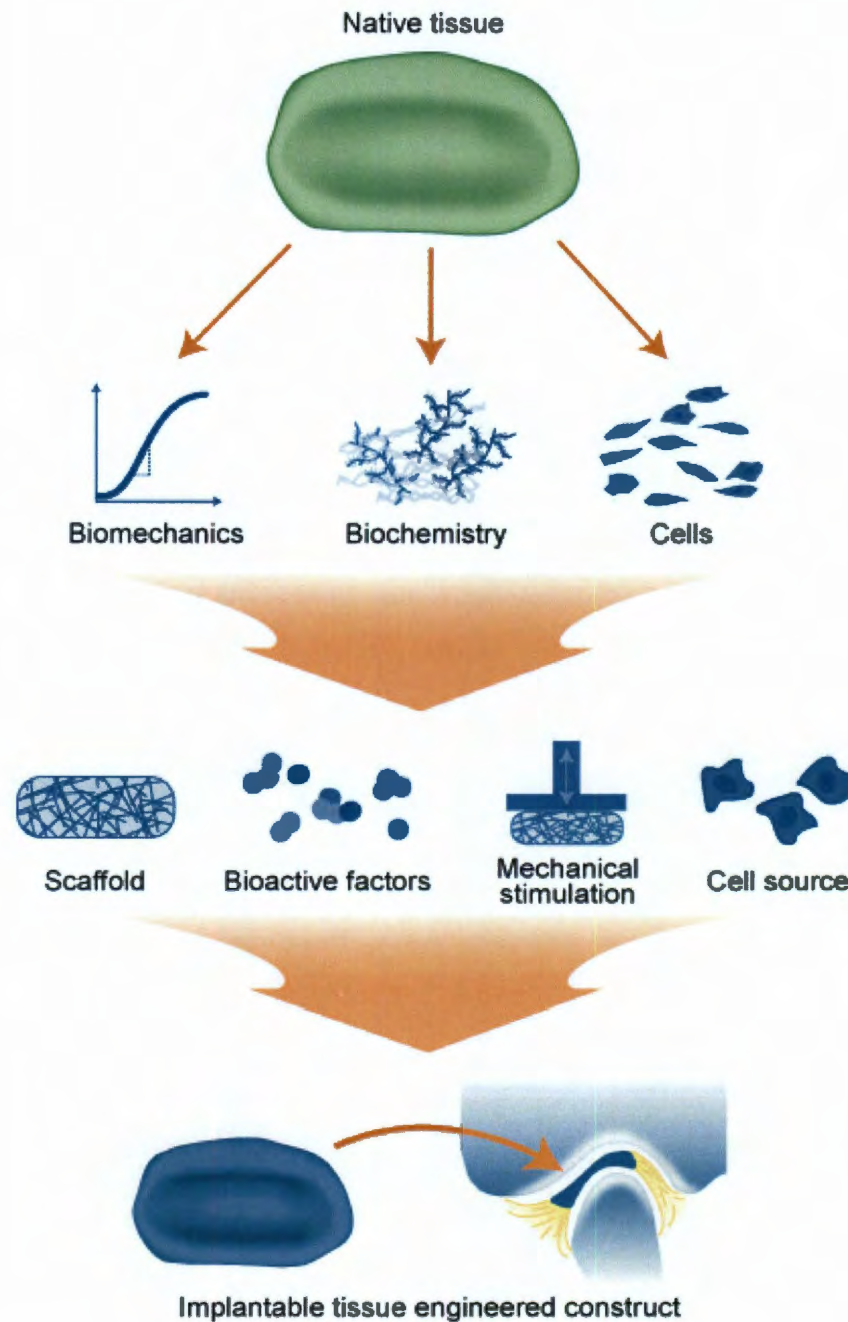
Figure 4: Tissue engineering paradigm

Figure 4: Tissue engineering paradigm for engineering TMJ tissues. The tissue engineering process is initiated by characterizing the biomechanical, biochemical and cellular properties of the native tissue to created design parameters for tissue engineering. Next, cells are combined with scaffolds, bioactive agents and mechanical stimuli to produce a tissue engineered TMJ tissue that can be implanted *in vivo*.
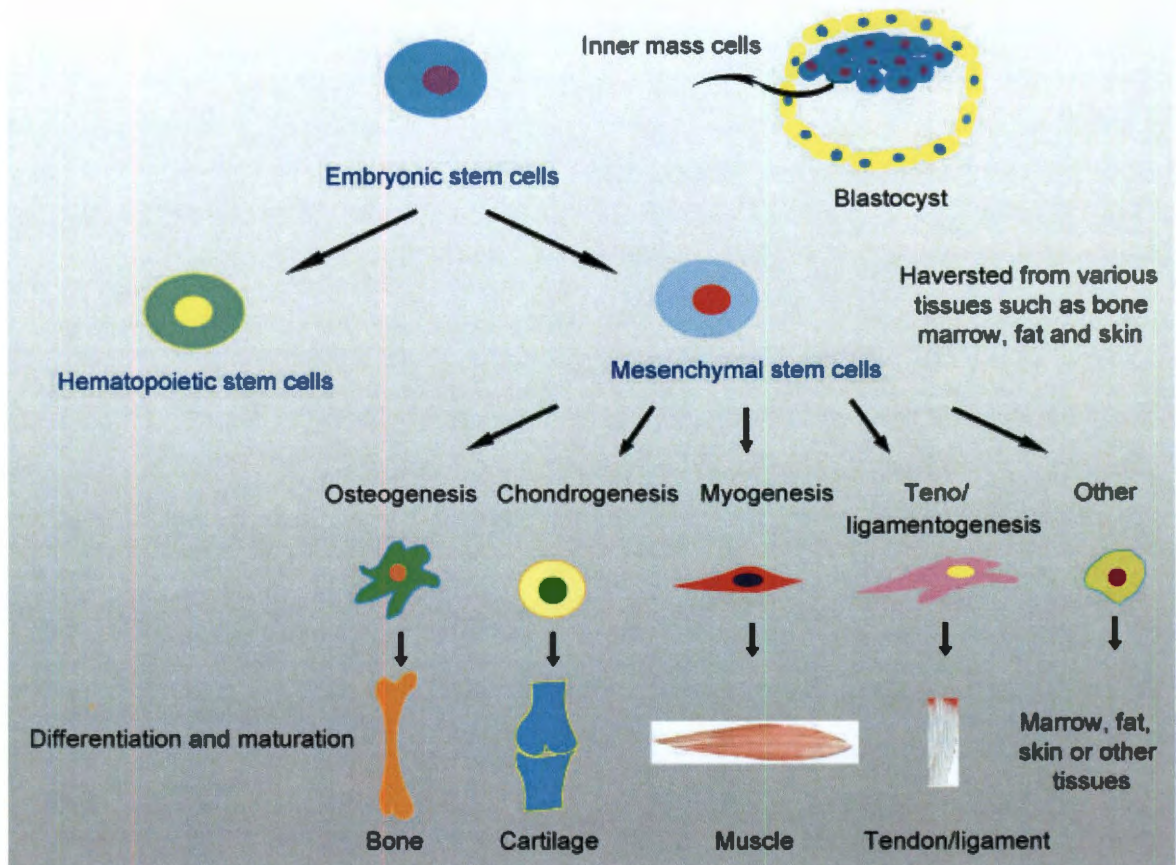
Figure 5: Differentiation lineage of human stem cells

Figure 5: The hierarchal structure of human embryonic and mesenchymal stem cells. Embryonic stem cells are derived from the inner cell mass of the blastocyst and can differentiate down any of the three germ lineages. Mesenchymal stem cells are multipotent and can differentiate into any mesenchymal tissue including cartilage and bone.

Chapter 6: Fibrochondrogenesis of hESCs: Growth factor combinations and co-cultures

Abstract

The successful differentiation of human embryonic stem cells (hESCs) to fibrochondrocyte-like cells and characterization of these differentiated cells is a critical step toward tissue engineering of musculoskeletal fibrocartilages (e.g., knee meniscus, temporomandibular joint disc, intervertebral disc). In this study growth factors and primary-cell co-cultures were applied to hESC embryoid bodies (EBs) for three weeks and evaluated for their effect on the synthesis of critical fibrocartilage matrix components: glycosaminoglycans (GAG) and collagens (types I, II, and VI). Changes in surface markers (CD105, CD44, SSEA, PDGFRα) after the differentiation treatments were also analyzed. The study was conducted in three phases: 1) examination of growth factors (TGF-β3, BMP-2, BMP-4, BMP-6, PDGF-BB, sonic hedgehog protein); 2) comparison of two co-cultures (primary chondrocytes or fibrochondrocytes); and 3) the combination of the most effective growth factor and co-culture regimen. TGF-β3 with BMP-4 yielded EBs positive for collagens I, II, and VI, with 3-6 fold and 2-5 fold increases in GAG and collagen, respectively. Analysis of cell surface markers showed a significant increase in CD44 with the TGF-β3 + BMP-4 treatment compared to the controls. Co-cultures with fibrochondrocytes resulted

---

in up to 6 fold increases in collagen II production. The combination of the growth factors BMP-4 + TGF-β3 with the fibrochondrocyte co-culture led to an increase in cell proliferation and GAG production compared to either treatment alone. This study determined two powerful treatments for inducing fibrocartilaginous differentiation of hESCs and provides a foundation for using flow cytometry to purify these differentiated cells.

Introduction

Human embryonic stem cells (hESCs) are an emerging cell source for fibrocartilage tissue engineering.[241] These cells are exciting for tissue engineering applications as they have unlimited proliferative capacity and are multipotent.[242, 243] Moreover, in the future there is great potential for using these cells in patient-specific therapies, whether through hESC banks or somatic cell nuclear transfer.[244, 245] Creating functional fibrocartilages, such as the temporomandibular joint disc, intervertebral disc, and the knee meniscus, requires that these multipotent cells be differentiated down a fibrocartilaginous lineage. Determining efficient and efficacious methodologies for differentiation is a critical goal for the field.

One way to recreate the cues needed for differentiation is through modifying the growth medium, and such cues can be taken from fibrocartilage, as well as cartilage-related literature. Differentiation down a cartilaginous lineage, as well as other lineages, can occur spontaneously through culture without specific

differentiation treatments.[246] To make this differentiation more efficient and enhance cartilaginous matrix production, many groups are employing a 'chondrogenic' base medium consisting of ITS+ (insulin, transferrin, selenium, and bovine serum albumin), dexamethasone, ascorbic acid, and pyruvate.[63, 247-249] Using the immense research with adult progenitor cells and primary cells as a guide, recent work has largely focused on supplementing this chondrogenic medium with growth factors from the TGF-β superfamily. Levenberg and associates[250] used TGF-β1 to create cartilaginous matrix in hESC-seeded scaffolds and Toh and associates[251] found that supplementation with BMP-2 increased GAG and collagen II staining in hESC embryoid body outgrowths. In contrast, one study showed that chondrogenic medium alone outperformed two different differentiation regimens using sequential dosing of TGF-β3, TGF-β1, IGF-I, and BMP-2.[252] Studies of hESC-derived cells and human embryonic germ cells have shown benefits with TGF-β growth factors (β1 or β3), while combinations with BMP-2 were not beneficial.[253, 254] A larger variety of growth factors has been tried with mouse embryonic stem cells (mESCs), but the results have been mixed in regards to the most effective combination and dosing of TGF-βs and BMPs.[255-258] Other growth factor combinations including TGF-β3 + PDGF-BB and TGF-β1 + BMP-4 have also shown promise in mESC studies toward enhanced collagen II and GAG production.[259] Additional growth factors that have shown significant capacity to differentiate adult progenitors include BMP-6 and sonic hedgehog (SHH) protein.[260-264] As can be seen from the array

of data, there is, as of yet, no gold standard for differentiation of embryonic stem cells with growth factor combinations.

Another methodology for recapitulating the microenvironment milieu of development is co-culture with primary cells. One study examined hESCs grown on inserts over 'feeder layers' of first passage nasal chondrocytes.[265] The cells were co-cultured for 4 weeks prior to implantation in a nude mouse in PDLLA foam scaffolds. The co-cultured implants were found to have increased GAG and collagen, as well as a greater collagen II/I ratio over controls. Similar co-cultures with varying degrees of contact between primary cells (intervertebral disc) and adult progenitor cells have also been used toward fibrocartilage applications.[266, 267] One challenge with this approach is that it requires appropriate primary cells. However, the advantage is that the primary cells are more capable of recreating the complex biochemical signaling environment that may be needed for differentiation.

In this study, a wide range of differentiation conditions are studied with the objective of differentiating hESCs to cells that produce fibrocartilaginous extracellular matrix (ECM). Differentiation to 'fibrochondrocytes' *per se* is not reasonable because specific markers have yet to be identified for a fibrochondrocyte. However, a functional definition of fibrocartilaginous differentiation can be applicable for tissue engineering purposes where the goal is functional restoration. Fibrocartilage is composed of varying ECM based on the region of the tissue. For example, the inner third of the meniscus contains collagen II while the outer portion is predominantly collagen I, with smaller

amounts of type VI.[268-271] To engineer such a complex and heterogeneous tissue it will be necessary to differentiate hESCs to cells capable of producing these types of matrix in varying ratios. This is a three-phase study examining differentiation through the use of 1) growth factors, 2) co-culture conditions, and 3) the combination of the most effective growth factor and co-culture regimens. In the first phase, we initially compare control chondrogenic medium to medium supplemented with TGF-β3, chosen over TGF- β1 due to its enhanced potency,[272] to determine whether TGF-β3 treatment is beneficial compared to chondrogenic medium alone. Next, TGF-β3 treatment is combined with varying concentrations of PDGF-BB, SHH, BMP-2, BMP-4, and BMP-6 to further increase fibrocartilaginous matrix production. Specific hypotheses include the following: 1) TGF-β3 enhances fibrocartilaginous matrix production, 2) the performance of TGF-β3 is enhanced by combinations with other factors, including BMPs, PDGF-BB, and SHH, 3) combinations with BMPs specifically increase GAG production and 4) combination specifically with BMP-4 additionally increases collagen production. In the second phase of the study we compare hESC co-cultures with primary articular chondrocytes and meniscal fibrochondrocytes. We hypothesize that co-cultures lead to increased specific collagen production. Finally, the most beneficial growth factor and co-culture methodology, as determined by fibrocartilaginous protein production, are studied in combination. In this final phase the hypothesis is that the combination outperforms either treatment alone.

'Spin embryoid bodies'[273, 274] of H9 hESCs are utilized to allow for uniform differentiation and analysis at the protein level to determine differentiation toward a fibrocartilaginous lineage. Looking toward future work with the differentiated cells we also analyze an array of cell surface markers to identify markers predictive of protein production. Specifically, 1) CD44, the hyaluronan receptor and an important mesodermal marker, 2) CD105, the TGF-β3 receptor, 3) platelet-derived growth factor α (PDGFRα), a mesodermal marker, and 4) SSEA-4, marker of undifferentiation in hESCs.[243, 259, 275-277]

Materials and Methods

hESC culture

H9 hESCs (abbreviated 'H9,' Wicell, Madison, WI) were cultured according to the manufacturer's instructions on irradiated CF-1 mouse embryonic fibroblasts (MEFs) (Charles River Laboratory, Wilmington, MA). Colonies were passaged using 0.1% type IV collagenase (Invitrogen, Carlsbad, CA) every 4-6 days. Colonies were passaged onto Matrigel (BD Biosciences, San Jose, CA) coated plates for the final passage prior to embryoid body (EB) formation. While on Matrigel, the colonies were given MEF-conditioned medium supplemented with bFGF (Invitrogen).

Spin EB formation

Spin embryoid bodies (EBs)[273, 274] were prepared by lifting cells off the Matrigel with 4 minutes of 0.05% trypsin with EDTA (Invitrogen) application.

Trypsin was stopped with hESC medium, the cells were counted and seeded at 1×10^5 cells/100 µl of bFGF-supplemented conditioned medium into low-adherence V-bottom 96 well plates (Sarstedt, Newton, NC). The plates were centrifuged for 5 minutes at 950 x g. The plates were then allowed to incubate for 48 hours. Spin EBs were lifted out of the wells with gentle pipetting and resuspended in appropriate medium for differentiation in six well plates, at approximately 20-30 EBs/well. Culture plates were coated in 2% agarose to prevent EBs from adhering to the well bottom.

Differentiation treatments

The base chondrogenic medium contained 1% fetal bovine serum (FBS) (Gemini, West Sacramento, CA), DMEM with 4.5 g/L-glucose and L-glutamine (Invitrogen), 1% non-essential amino acids, 0.4 mM proline, 50 µg/ml L-ascorbate-2 phosphate (Sigma, St. Louis, MO), 100 µg/ml Na pyruvate (Sigma), 1% ITS+ (BD Biosciences), and 100 nM dexamethasone. Growth factor treatments included: TGF-β3 (Peprotech, Rocky Hill, NJ), PDGF-BB (Peprotech), rhSHH-N (R&D Systems, Minneapolis, MN), BMP-4 (Peprotech), BMP-2 (Peprotech), and BMP-6 (Promokine, Heidelberg, Germany). Low (L) and high (H) concentrations for each growth factor and the applied combinations are described in Table I. All growth factors were diluted per manufacturer's instructions.

The primary cells for feeder layers, meniscal fibrochondrocytes and articular chondrocytes, were harvested from the inner two-thirds of the medial

meniscus and the distal femora, respectively, of approximately 1-wk old male calves (Research 87, Boston, MA) less than 36 hours after slaughter. Tissue was minced and digested overnight with 0.2% collagenase II (Worthington, Lakewood, NJ) in 10% FBS culture medium. The FBS culture medium is DMEM with 4.5 g/L-glucose and L-glutamine (Gibco, Grand Island, NY), 10% FBS (Gemini), 1% fungizone, 1% Penicillin/Streptomycin, 1% non-essential amino acids, 0.4 mM proline, 10 mM HEPES, and 50 μg/ml L-ascorbic acid (Sigma). To obtain sufficient cells for the experiment, cells from three animals were frozen at -80°C and later pooled to create a mixed primary cell population. Co-cultures were prepared by thawing cells into a T-75 tissue culture treated plastic flask (BD Biosciences) for 48 hours; cells were then collected by trypsinization and irradiated with 6000 rads. Cells were seeded at 5×10^5 cells per well of a 6 well plate. To separate EBs from the feeder layers, nylon mesh cell strainers were coated along the bottom and sides with 2% agarose (Sigma). EBs were then placed within the strainers. The agarose coating created a barrier between the EBs and the feeder layer while allowing diffusion of media and proteins (Figure 1). Control treatment EBs were grown on agarose coated wells or agarose coated cell strainers.

For all treatments, half medium changes were made every three days. New feeder layers were prepared each week. EBs were cultured a total of 3 weeks prior to analysis.

Immunohistochemistry and histology

Samples were frozen and sectioned at 12 μm. Immunohistochemical analysis was performed by fixing sections in chilled acetone, rehydrating, treating with 3% H_2O_2 in methanol, and blocking with horse serum. The following primary antibodies were diluted in PBS and applied for 1 hour: 1:100 rabbit anti-human collagen VI pAb (US Biological, Swampscott, MA), 1:750 rabbit anti-human collagen II pAB (Cedarlane, Burlington, NC), and 1:650 mouse anti-human collagen I (Chondrex, Redmond, WA). Visualization using a secondary biotinylated antibody, the ABC reagent, and DAB was performed using the Vectastain kit (Vector Laboratories, Burlingame, CA), and counterstaining was done with Harris's Hematoxylin. Sections of articular cartilage and meniscal fibrocartilage were run as positive controls, while samples were stained without application of the primary antibody as negative controls. To determine if undesired differentiation had occurred, Von Kossa and oil red-O stains were performed for evidence of calcification and adipose tissue, respectively. Addtionally, both Alcian Blue and Safranin-O were employed as qualitative methods of demonstrating chondrogenesis.

Quantitative biochemistry

Samples were lyophilized for 48 hours and digested in 125 μg/ml papain (Sigma) for 18 hours at 60°C. Cell number was determined using Picogreen Cell Proliferation Assay Kit (Molecular Probes, Eugene, OR). A hydroxyproline assay was performed to gauge total collagen using bovine collagen standards (Biocolor, Newtonabbey, Northern Ireland). After finding positive Alcian Blue and

Safranin-O staining, we then proceeded to quantify the GAG and other matrix production through a sulfated GAG assay using the Blyscan GAG Assay Kit (Biocolor). For each assay, 5-10 samples were analyzed. Data are reported as total matrix produced normalized to that produced by control or TGF- β3, as well as total matrix divided by the number of cells in the EB to give marix production per cell.

Samples for enzyme linked immunosorbent assay (ELISA) were digested in papain at 4°C for 4 days and then a 1/10 volume of elastase (Sigma) solution in 10x TBS buffer was added to achieve a concentration of 0.1 mg/ml elastase. Samples were allowed to digest an additional 48 hours. Between each incubation step in the ELISA, plates were washed using PBS with 0.05% Tween-20. For the collagen I ELISA, plates were incubated overnight at 4°C with 1:400 mouse anti-human capture mAb (US Biological), blocked with 2% bovine serum albumin (BSA), samples and standards were added, then exposed to rabbit anti-human pAb (US Biological). Finally, goat anti-rabbit pAb was added, and the color developed in TMB as a liquid peroxidase substrate. The collagen II ELISA was performed using the Chondrex (Redmond, Washington) capture mAb, the Chondrex biotinylated mAb, and streptavidin peroxidase was used with TMB to develop the color. Absorbance was read at 450 nm in a Genios plate reader (Tecan, San Jose, CA). For the ELISAs, 4-8 samples were analyzed.

Flow cytometry

The best performing differentiation treatments from each phase were selected for flow cytometry analysis. EBs were analyzed 48 hours after formation ('undifferentiated') and after 3 weeks of differentiation treatment. Three samples were prepared per treatment per primary antibody. EBs were digested to obtain a single cell suspension, by applying trypsin for 1 hour, followed by 0.2% type II collagenase (Worthington). The collagenase digestion was terminated when undigested material was no longer visible (1-1.25 hours). Cells were blocked with goat serum, and the following primary antibodies were applied at 10 μg/ml for 30 minutes: mouse IgG isotype control (Invitrogen), mouse anti-human PDGFRα (R&D Systems), mouse anti-human CD44 (Sigma), or mouse anti-human CD105 (Invitrogen). Additionally, mouse anti-human SSEA-4 (Developmental Studies Hybridoma Bank) was applied at 0.6 μg/ml. Cells were washed in PBS, and then the Alexa Fluor 488 goat anti-mouse FITC (Molecular Probes, Carlsbad, CA) was applied for 30 minutes. Samples were fixed in 0.5% paraformaldehyde, and stored at 4°C until analysis. Samples were run on a FACSCalibur flow cytometer (BD Biosciences). Data were analyzed for forward scatter and the percentage of cells labeled at a fluorescence level exceeding a 95% threshold on the isotype control.

Statistics

All data were compiled as mean ± standard deviation and a one-factor ANOVA was used to examine means from the quantitative biochemistry and flow cytometry data. If analysis showed a significant difference, a Tukey's *post hoc* or

Student's-t test analysis was performed. A significance level of $p<0.05$ was used in all statistical tests performed. The R^2 values were calculated using linear regression of the data sets under evaluation [278].

Results

Growth factor differentiation

TGF-β3 treatment resulted in a significant 60% increase in GAG production over control (Figure 2). There was no significant difference between the control and the TGF-β3 treated group in total collagen or collagen II quantity. Immunohistochemistry indicated very faint and non-uniform staining for collagen I, although no collagen I was detected by ELISA. As TGF-β3 showed benefit toward fibrocartilaginous differentiation, combinations of this growth factor were tested with varying concentrations of 1) PDGF or SHH and 2) BMP-2, BMP-4, or BMP-6. In the first experiment, high and low concentrations of PDGF-BB or SHH were combined with TGF-β3, and all results were normalized to the TGF-β3 treated group. Immunohistochemistry showed the presence of collagen VI in all groups and collagen II was present in those treated with SHH. Quantitative biochemistry showed there was no significant change in cell number per EB or collagen II production for either combination with PDGF or SHH (Figure 3A). In contrast, SHH treatment actually decreased GAG production compared to TGF-β3 alone. PH showed a 115% increase in total collagen production, and SHH showed a trend toward increasing collagen production. When normalized per cell, PH did not show improvement in collagen or GAG over TGF-β3 alone; only

SH showed an increase in collagen per cell compared to TGF-β3. A comparison of BMPs combined with TGF-β3 netted greater improvements in matrix production. Immunohistochemistry demonstrated positive staining for collagen II and VI in all BMP-treated groups; however, collagen I was only present in 4H, 6L, and 6H (Figure 4). Only 4H showed an increase in cell number over TGF-β3 (Figure 3B). Both 2H and 4H showed increased GAG production, 6.1 and 6.7 fold increases respectively. Only 4H showed a significant 4.8 fold increase in collagen over TGF-β3 alone. There was no increase in collagen II with any treatment. Normalization per cell showed similar trends to the per sample data, with the exception of 6L showing significantly greater collagen per cell compared to TGF-β3 alone. No collagen I was detectable by ELISA for these experiments, however, immunohistochemistry showed intense staining in the 4H group, and pale staining in the 6H group (Figure 4). Von Kossa and oil red-O staining for extraneous differentiation were negative (data not shown).

Co-culture mediated differentiation

In a preliminary study it was found that a primary cell feeder layer density of 5.0×10^5 cells/ well showed more effect on matrix production than 2.5×10^5 cells/ well (data not shown), so the greater feeder density was utilized in the follow-up experiment. Culture of EBs in an agarose coated cell strainer in the absence of a feeder was also compared to EBs grown in agarose coated wells; no significant differences were found between the groups for matrix production or cell proliferation (data not shown). Use of articular cartilage and meniscal

fibrocartilage-derived feeder layers only significantly increased specific collagen production (Figure 5). While collagen I was undetectable in all groups either through ELISA or immunohistochemistry, collagen type II content was 4.5 and 6 fold that of the control in the chondrocyte and fibrochondrocyte co-cultures, respectively. These changes were similar when normalized to cell number. Von Kossa and oil red-O staining for extraneous differentiation were negative (data not shown).

Combination of growth factor and co-culture conditions

The combination treatment of BMP-4 + TGF-β3 and fibrochondrocyte co-culture resulted in GAG and collagen content 7 and 2 fold, respectively, that of the control, as well as enhanced cell proliferation over control (Figure 6A). However, there was no significant difference compared to the BMP-4 + TGF-β3 treatment alone. Collagen I, II and VI were present as shown by immunohistochemistry (Figure 6B). When normalized to the cell content, no significant differences were found. Von Kossa and oil red-O staining for extraneous differentiation were negative (data not shown).

Flow cytometry

Undifferentiated EBs and EBs treated with control medium, BMP-4 + TGF-β3, and a fibrochondrocyte co-culture were analyzed for the presence of four cell surface markers (Figure 7). The selected differentiation treatments were the highest protein producers determined in each phase. Only the growth factor

combination significantly increased CD44, 32.2±1.9% positive. Both undifferentiated cells and growth factor combination-treated cells showed increased CD105, at 14.3±3.2% and 17.9±1.0% positive, respectively. All of the treatment groups showed significant drops in SSEA-4 compared to undifferentiated cells. The forward scatter, given as dimensionless measures of mean fluorescence intensity, offer a gauge of cell size (from largest to smallest): for the BMP-4+TGF-β3 groups it was 693±39, 578±2 for the undifferentiated cells, 490±14 for fibrochondrocyte co-cultured cells, and 466±17 for control treated cells (Supplemental Figure 8). The combination treatment produced cells with similar levels of surface markers and size distribution to those resulting from the BMP-4 + TGF-β3 treatment (data not shown).

Discussion

Fibrocartilage tissue engineering with hESCs is in its infancy; this study is the first to examine a large variety of growth factor combinations and co-cultures specifically toward fibrocartilage differentiation. Prior work has identified an appropriate hESC line and differentiation time[241] and in this study a three phase approach was taken to refine the differentiation process. First growth factor treatments were compared and TGF-β3 was found to enhance GAG synthesis, while its combination with BMP-4 was found to increase GAG, total collagen, and collagen type I production. In the second phase, this study found that co-culture with fibrochondrocytes successfully induced greater collagen II production over control or articular chondrocyte co-cultures. Combinations of TGF-β3 with PDGF-

BB or SHH were found to be less fruitful. In the third phase, combining the best performing growth factor combination with the co-culture resulted in a trend of increased GAG and collagen synthesis over either treatment alone. Flow cytometry analysis showed that the treatments differentially affected the cell surface geography and cell size, demonstrating a powerful link between protein production and cell size and surface markers. Overall, we have identified a treatment, BMP-4 + TGF- β3, that results in enhanced synthesis of important fibrocartilaginous proteins, while using a co-culture with fibrochondrocytes markedly increases collagen II production. Moreover, increased CD44, maintenance of CD105 levels, as well as marked differences in cell size indicate that future work purifying these cells may be possible.

The utility of TGF-β3 in enhancing GAG synthesis correlates well to several previous studies of hESCs, mESCs, and other similar cell lines.[250, 254, 255, 259, 279] The lack of enhanced collagen II production or GAG synthesis when TGF-β3 was combined with PDGF-BB or SHH was surprising, given evidence with mesenchymal stem cells (MSCs) and mESCs to support these combinations.[259, 260] SHH acts upstream of TGF-β signaling and is known to increase expression of TGF-β isoforms.[280, 281] One hypothesis for the lack of response is that the TGF-β3 concentration used here was already at a saturation level. Future work may study whether SHH could be more effective in the presence of BMPs, as downstream expression of BMP receptors has been shown.[282]

Three different BMPs were examined in this study since each has shown utility in different systems; for example, BMP-2 combined with TGF-β3

outperformed similar combinations with BMP-4 and BMP-6 in a study of mesenchymal stem cells,[283] BMP-6 appears to be particularly effective with adipose-derived progenitor cells compared to BMP-2, 4, and 7,[262, 263] while BMP-4 has outperformed BMP-2 in mESC chondrogenesis.[259] The large increases in fibrocartilaginous matrix synthesis seen in this study with BMP-2 or BMP-4 combined with TGF-β3 contrasts with recent work with hESC derived cells[254, 255] but are supported by work with mESCs.[257, 259] Additional studies with adult progenitors, both bone marrow and adipose derived, also show positive and even synergistic results in combining a TGF-β growth factor with a BMP.[262-264, 284] The increases in GAG and collagen seen in this study may have been due to direct effects of the BMPs, BMP-induced increases in TGF-β receptors,[263] or a combination of these two effects. Overall, combinations of TGF-β3 and BMP-4 merits greater study as the increases in matrix, 6.7 fold in GAG and 4.8 fold in collagen compared to TGF-β3 alone, were significant. Although this study examined a dose range covering most previously studied concentrations of BMPs, 20-100 ng/ml, a dose-response was still observed, thus a saturation concentration may still need to be identified.

An alternative to growth factor mediated differentiation is the use of co-cultures to provide the biochemical stimuli for differentiation. In using primary cells, there are the added challenges of an appropriate source and varying potency of the primary cells. Despite these considerations, co-cultures may provide a powerful stimulus, one that may even be responsive to the signals given off by the differentiating cells; i.e., there is opportunity for cross-talk

between the two cell populations. It was hypothesized in this study that the co-cultures would differentially regulate specific collagen production as the cells themselves have very different collagen synthesis profiles, and, interestingly, both cell types appeared to increase collagen II production with little effect on collagen I. The 7-10 fold increase in collagen II production is an important advance in fibrocartilaginous differentiation. Prior work with nasal chondrocytes co-cultured with the hESC H1 line showed large increases in GAG production and collagen II staining.[265] Future work will further examine appropriate 'dosing' of the co-culture, including issues such as cell density, how often new feeder layers should be prepared, and whether feeder layers should be treated with growth factors or other stimuli. Additionally, recent studies using chondrocyte-conditioned medium to differentiate MSCs[267, 285] or the mixing of MSCs and primary cells[267, 286, 287] also show promise. Future work comparing conditioned medium, direct mixing of the cells, and the set-up used in this study in which the two cell populations were separated by a protein-permeable barrier will help further elucidate the role of cross-talk between the progenitor cells and primary cells. Moreover, in this study, a cross-species co-culture was utilized due to convenience in cell procurement; future studies must look toward comparing different sources of primary cells for co-cultures in terms of their practicality and especially the elimination of source-to-source variation in the level of stimulus provided.

One of the prominent challenges in using a co-culture is that there may be variation in the differentiating capacity of the primary cells used in the co-

cultures, especially if taken from different donors. This variation may explain the results of the combination growth factor- co-culture study (phase 3) versus the co-culture alone study (phase 2). Although co-culture cells were pooled from multiple animals for each phase, there may have been variation in the differentiating capacity of these two pooled populations of cells. This variation was evidenced by the large increases in collagen II measured in phase 2 while these increases in collagen II quantity were not reproduced in phase 3. In contrast, the increases in collagen and GAG, expected with the use of the growth factors, were observed in both phases. The co-culture clearly played a role in terms of mitogenic stimulation, as the combination treatment resulted in a large increase in cell number. Future work utilizing cell lines may enhance the consistency of this differentiation tool. However, co-culture with patient-derived cells may be more appropriate for future therapeutic use. In such a case, examination and assessment of the differentiating capacity of co-cultures will be critical as co-cultures can clearly serve as powerful differentiation stimuli.

The flow cytometry component of this study was undertaken as a first evaluation of an important tool for later studies: purifying populations of differentiated cells. Flow cytometry analysis may also be a powerful tool to identify a marker indicative of fibrocartilaginous matrix production which could be used to screen large numbers of differentiation strategies rather than laborious and expensive protein-level analyses. First, we used SSEA-4 expression as a gauge of whether the cells had retained their multipotency. As expected there was a 70-80% drop in this marker during the differentiation period studied. We

then examined three other cell surface markers that have been linked to chondrogenesis: PDGFRα, CD44, and CD105. Although PDGFRα+ mESCs have shown significant increases in chondrogenesis,[259] none of the treatments markedly changed PDGFRα expression in this study. A particularly promising potential marker for cartilaginous differentiation is CD44; this marker appears early in chondrogenesis and is important in the formation of chondrocyte pericellular matrix.[288-290] This marker has also been correlated to increased chondrogenicity in adult chondrocyte populations.[277, 291] Of the markers examined, CD44 was the only one that significantly increased over the undifferentiated and control treatment populations. We can speculate that increased presence of this hyaluronan receptor correlates to the enhanced GAG production seen in the EBs created with the BMP-4 + TGF-β3 treatment (R^2= 0.78). Furthermore, since increased GAG was not seen with the fibrochondrocyte co-culture, it is consistent that CD44 was not increased. It was hypothesized that CD105 would increase with TGF-β3 treatment and be a positive indicator of fibrochondrogenesis. Comparisons between the BMP-4 + TGF-β3 group and the control/co-culture groups, which were not treated with TGF-β3, support this hypothesis. The lack of difference between the undifferentiated cells and the BMP4 + TGF-β3 group suggest that the treatment led to the maintenance of this cell surface maker, while in the other groups the marker was lost during culture. Thus, CD105 could be used as a differentiation indicator only after the cells have been purified of cells expressing undifferentiation markers. The presence of CD105 has been used prior to differentiation to isolate a chondrogenic

population; by maintaining the presence of this surface marker, the BMP4 + TGF-β3 treatment may have had increased efficacy in fibrocartilage differentiation.[276] These data lay a foundation for using flow cytometry to purify particularly promising populations for chondrogenesis. For example, treated cells could first be purified to remove all SSEA-4+ cells, and then sorted to obtain a CD44+ and CD105+ population. As this study cannot show to what degree these populations overlap, such an examination will be important to more concretely establish these markers for chondrogenesis.

This work shows significant gains in fibrocartilage matrix synthesis in hESC embryoid bodies comparing 15 differentiation strategies. The combination of BMP-4 + TGF-β3 was effective in stimulating production of collagens I, II, and VI, and markedly increasing total collagen and GAG production. It was also demonstrated that BMP-4 + TGF-β3 differentiated hESCs posses a greater forward scatter (gauge of cell size) and the highest CD44 presence compared to the other groups; both of these changes may serve as important markers for purifying these cells. These refined methods for differentiation can now be applied in a tissue engineering strategy to create hESC-derived fibrocartilage.

Tables and Figures

Differentiation Treatments

Control	chondrogenic base medium
T3	10 ng/ml TGF-β3
PL	T3 + 20 ng/ml PDGF-BB
PH	T3 + 100 ng/ml PDGF-BB
SL	T3 + 200 ng/ml SHH
SH	T3 + 1000 ng/ml SHH
2L	T3 + 20 ng/ml BMP-2
2H	T3 + 100 ng/ml BMP-2
4L	T3 + 20 ng/ml BMP-4
4H	T3 + 100 ng/ml BMP-4
6L	T3 + 20 ng/ml BMP-6
6H	T3 + 100 ng/ml BMP-6
A	articular chondrocyte co-culture
M	meniscal fibrochondrocyte co-culture
4HM	4H + M

Table I: Differentiation conditions. This study examined 16 conditions to elicit differentiation of hESCs to fibrochondrocyte-like cells. Growth factor treatments and primary cell co-cultures have been studied extensively in the past with mESCs and adult stem cells for chondrogenic differentiation. We approached the study of differentiation treatments in three phases: 1) examination of growth factors (TGF-β3, BMP-2, BMP-4, BMP-6, PDGF-BB, sonic hedgehog protein); 2) comparison of two co-cultures (hESCs with primary chondrocytes or fibrochondrocytes in the presence of TGF-β3); and 3) combination of the most effective growth factor and co-culture regimen selected from phases 1 and 2, respectively.
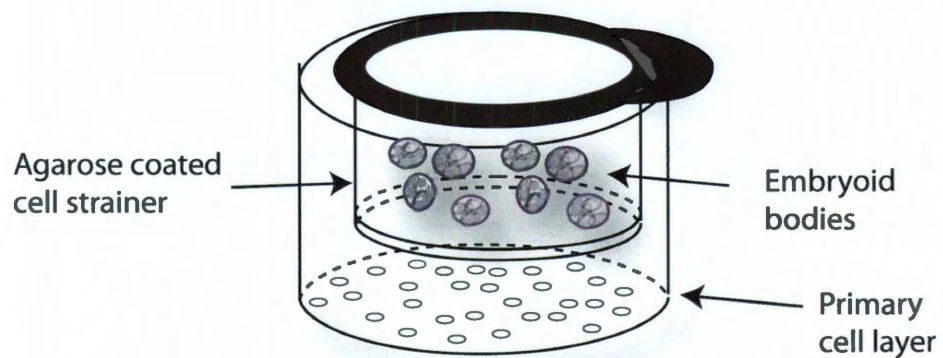
Figure 1: Co-culture set-up. Nylon cell strainers were coated with 2% agarose and placed in wells seeded with irradiated primary cells. EBs were placed within the agarose-coated strainer. This set-up creates a cell-cell barrier between the EBs and the irradiated primary cells while allowing the diffusion of media and proteins.
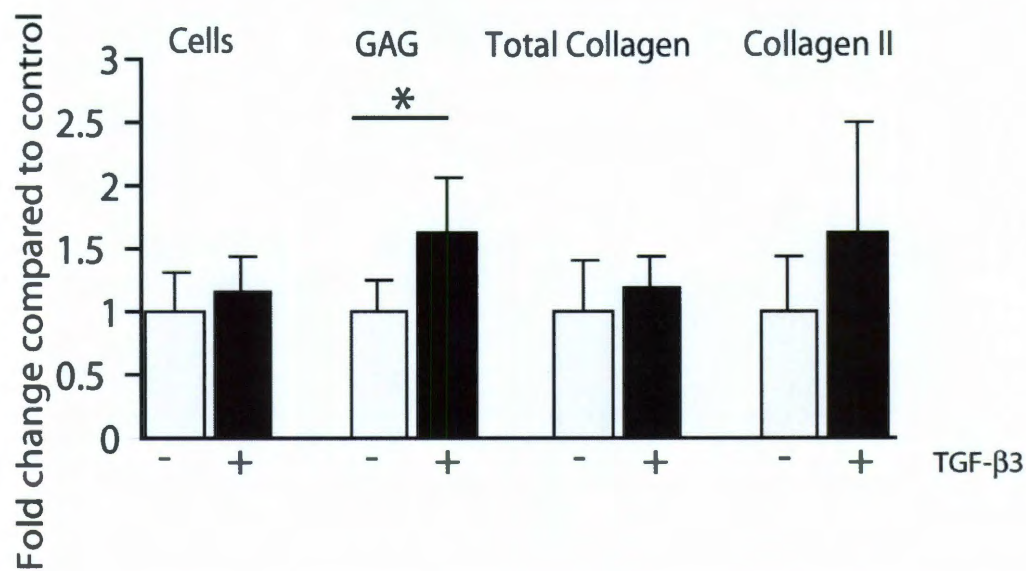
Figure 2: Biochemical content, Phase 1. TGF-β3 treatment resulted in increased GAG synthesis over control (chondrogenic medium with no growth factor addition), while collagen II content trended higher. Taking an optimization approach, follow-up studies examined combinations with TGF-β3. * indicates p<0.05.
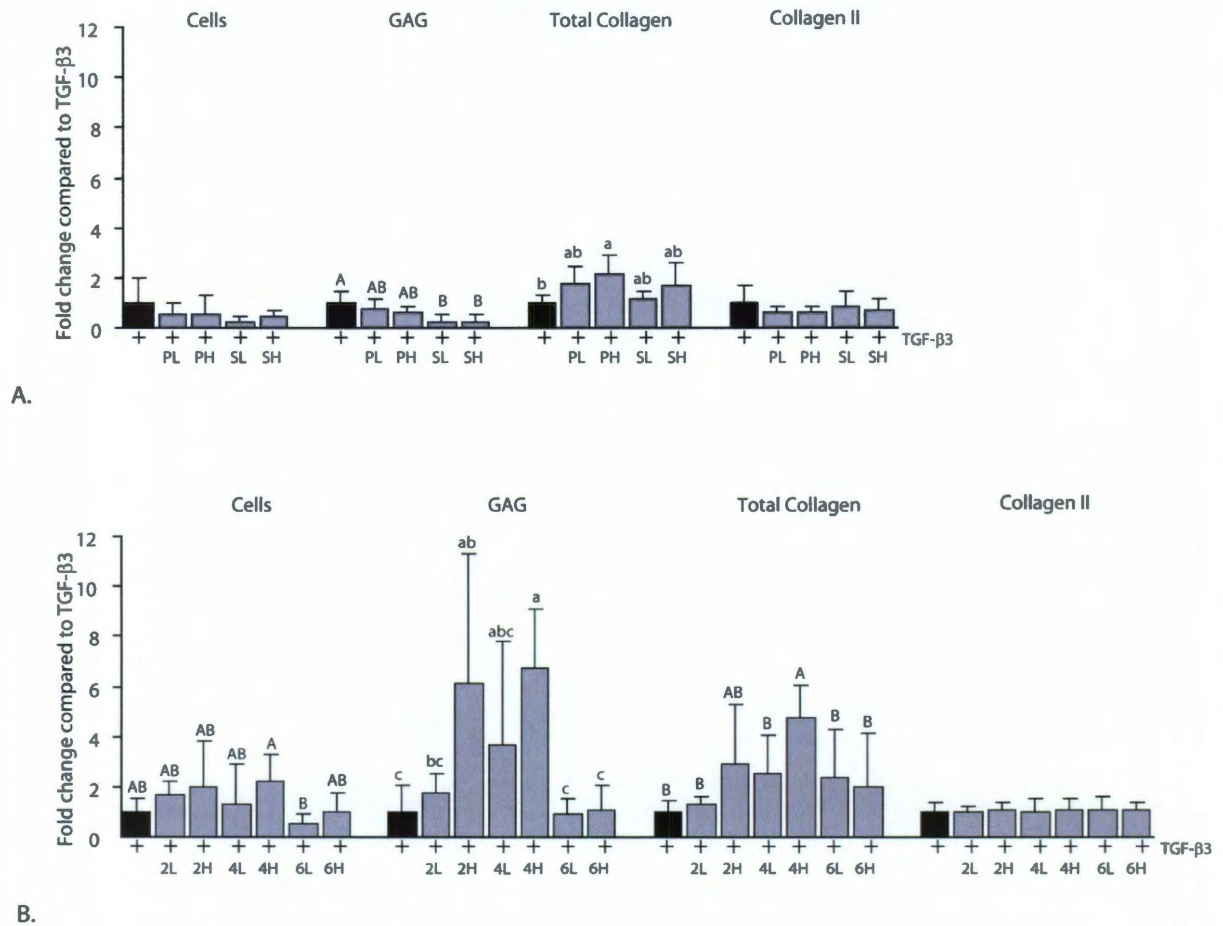
Figure 3: Biochemical content, Phase 2. A. Combinations of PDGF with TGF-β3 at the high dose showed increased total collagen, but showed no other benefits over TGF-β3 alone. SHH was shown to decrease GAG synthesis. B. Combinations of TGF-β3 with BMP-2 or BMP-4 proved to be powerful stimuli, as both collagen and GAG synthesis were increased over TGF-β3 alone. Experimental groups not connected by the same letter, within each type of analysis (cells, GAG, total collagen, collagen II) are statistically different (p<0.05).

| | Control | TGF-β3 | 4H | M |
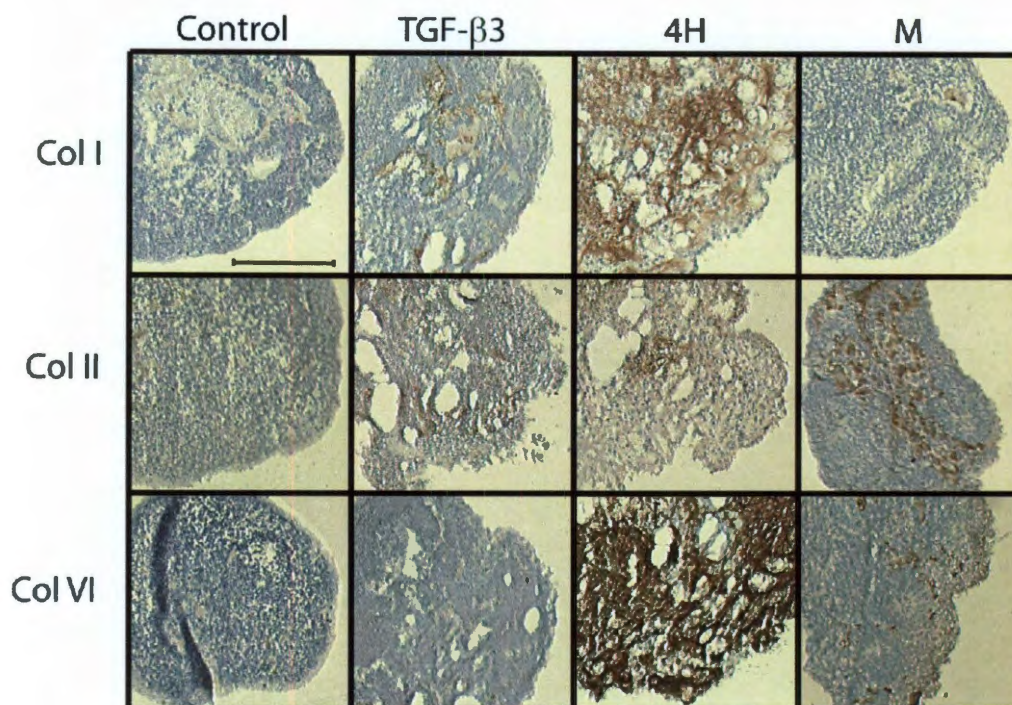
Figure 4: Immunohistochemistry. Immunohistochemistry for collagens I, II and VI, where rust-color indicates positive staining. BMP-4 + TGF-β3 showed collagens I, II, and VI, while the control only showed minimal staining. The meniscal fibrochondrocyte co-cultures showed intense collagen II staining. Scale bar is 200 μM.
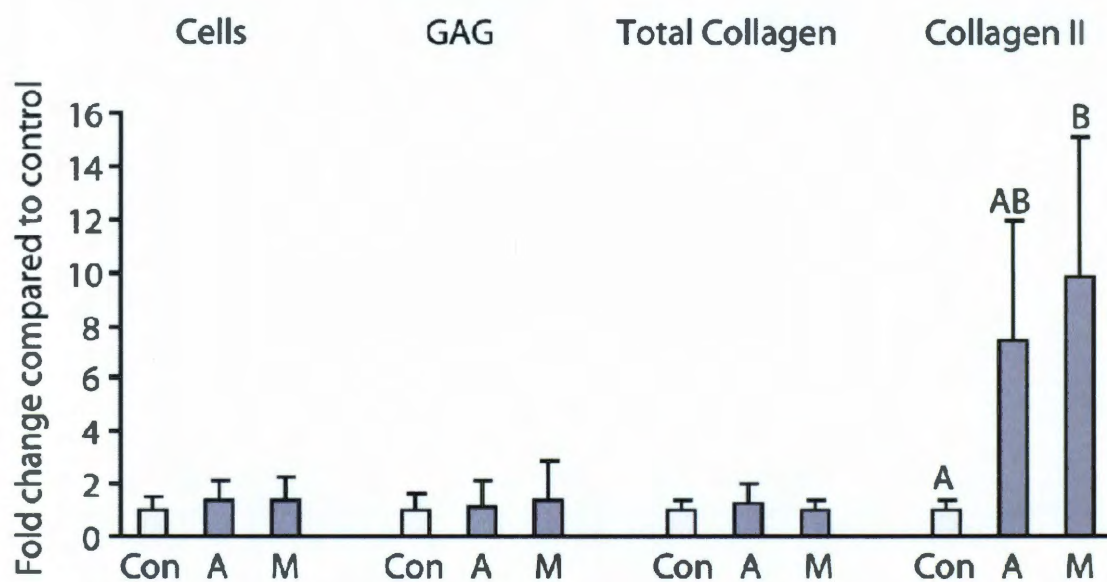
Figure 5: Biochemical content, Phase 3. Co-culturing hESCs with either chondrocytes or fibrochondrocytes resulted in dramatic changes in collagen II content compared to chondrogenic medium alone (control). Groups not connected by the same letter are statistically different (p<0.05).
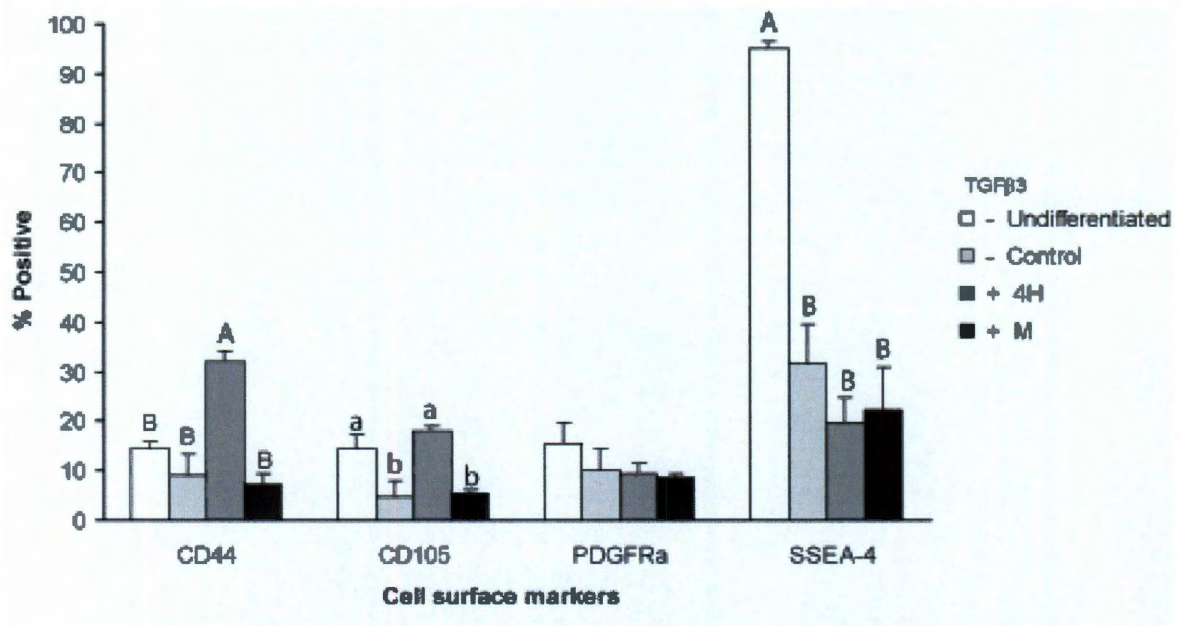
Figure 6: Flow cytometry for cell surface markers. All treatments significantly decreased SSEA-4, a sensitive marker for undifferentiation. Only BMP-4 + TGF-β3 led to increased CD44 and CD105. These markers may be used in future studies to isolate differentiated cells. Experimental groups not connected by the same letter, within each marker analysis are statistically different (p<0.05).
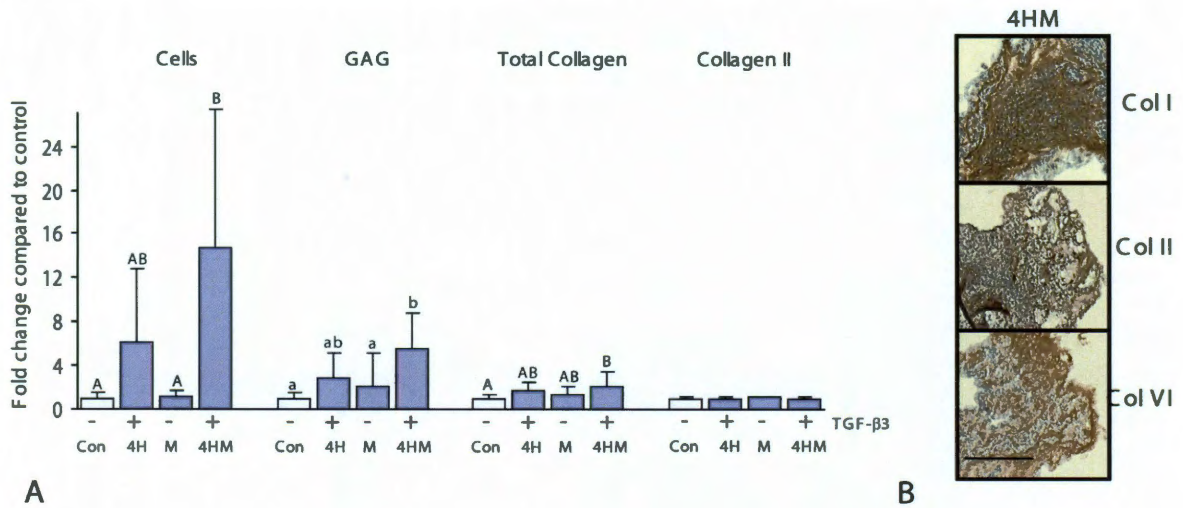
Figure 7: Biochemical content, Phase 4. A. Combination of BMP-4 + TGF-β3 and the meniscal fibrochondrocyte co-culture resulted in significant increases in cell number, GAG, and total collagen compared to control. Groups not connected by the same letter are statistically different (p<0.05). B. Immunohistochemistry for collagen I, II and VI (rust-color indicates positive staining). The combination treatment showed all three fibrocartilaginous collagens. Scale bar is 200 μM.
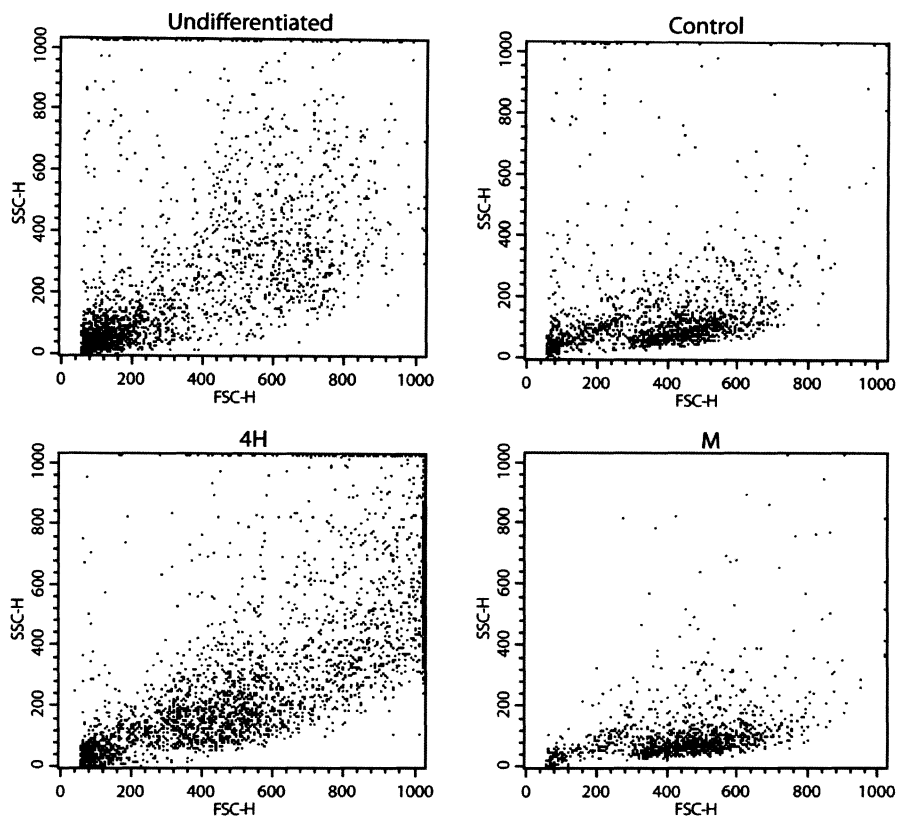
Supplemental Figure 8: Flow cytometry. The forward scatter, given as dimensionless measures of mean fluorescence intensity, shows the relative size of the cell populations obtained in this study. The control treatment cells were the smallest, while the largest cells were obtained by treatment with BMP-4+TGF-β3.

Chapter 7: Mechanical Characterization of Differentiated Human Embryonic Stem Cells

Abstract

Background: Human embryonic stem cells (hESCs) possess an immense potential in a variety of regenerative applications. A firm understanding of hESC mechanics, on the single cell level, may provide great insight into the role of biophysical forces in the maintenance of cellular phenotype and elucidate mechanical cues promoting differentiation along various mesenchymal lineages. Moreover, cellular biomechanics can provide an additional tool for characterizing stem cells as they follow certain differentiation lineages, and thus may aid in identifying differentiated hESCs which are most suitable for tissue engineering.

Method of Approach: This study examined the viscoelastic properties of single undifferentiated hESCs, chondrogenically differentiated hESC subpopulations, mesenchymal stem cells (MSCs), and articular chondrocytes (ACs). hESC chondrogenesis was induced using either Transforming Growth Factor-β1 (TGF-β1) or Knock Out Serum Replacer (KOSR) as differentiation agents and the resulting cell populations were separated based on density. All cell groups were mechanically tested using unconfined creep cytocompression.

Results: Analyses of subpopulations from all differentiation regimens

resulted in a spectrum of mechanical and morphological properties spanning the range of hESCs to MSCs to ACs. Density separation was further successful in isolating cellular subpopulations with distinct mechanical properties. The instantaneous and relaxed moduli of subpopulations from TGF-β1 differentiation regimen were statistically greater than those of undifferentiated hESCs. In addition, two subpopulations from the TGF-β1 group were identified which were not statistically different from native articular chondrocytes in their instantaneous and relaxed moduli, as well as their apparent viscosity.

Conclusion: Identification of a differentiated hESC subpopulation with similar mechanical properties as native chondrocytes may provide an excellent cell source for tissue engineering applications. These cells will need to withstand any mechanical stimulation regimen employed to augment the mechanical and biochemical characteristics of the neotissue. Density separation was effective at purifying distinct populations of cells. A differentiated hESC subpopulation was identified with both similar mechanical and morphological characteristics as ACs. Future research may utilize this cell source in cartilage regeneration efforts.

Introduction

The biomechanical properties of single cells may significantly influence tissue development and homeostasis. The physical characteristics of individual cells play a vital role in the generation of local stress-strain fields within the cellular microenvironment[292] and the forces in turn experienced by the nucleus.[293] It has recently been observed that cellular mechanical properties may

be indicative of phenotypic alterations within mesenchymal lineages.[294, 295] Hence, cell biomechanical techniques have emerged as potential tools for the characterization and identification of cell populations during various developmental or differentiation processes. The most common of these biomechanics methodologies are atomic force microscopy,[296] micropipette aspiration,[297] cytoindentation,[298] and unconfined cytocompression,[299] which can yield the elastic or viscoelastic material properties of single cells given the assumptions of isotropy, incompressibility, and homogeneity.

Examining the mechanical properties of single human embryonic stem cells (hESCs) is of particular interest due to the pluripotent nature of these cells and their clear potential in an array of regenerative medicine applications. The prospect for using an abundant alternative cell source, such as hESCs, in tissue engineering is particularly appealing since this would obviate the common concerns of donor tissue scarcity or of dedifferentiation during autologous cell expansion.[1] Despite their potential, an examination of the mechanical properties of naïve and differentiated hESCs has yet to be undertaken. An understanding of the mechanical characteristics of undifferentiated stem cells can greatly aid research investigating the forces necessary to promote differentiation into various cell lineages.[300-304]

Embryonic stem cells have recently been utilized in cartilage tissue engineering efforts.[202, 305] Studying the mechanical properties of chondro-induced hESCs may identify certain differentiated cell subpopulations that are most similar to native chondrocytes. It is believed that these cell subpopulations will be

most suited for use in a tissue engineering approach for articular cartilage since they would be able to sustain similar *in vivo* mechanical loads. In addition, through an understanding of the mechanical properties of these differentiated cell groups, loading regimens can be determined which elicit favorable biochemical[306, 307] or behavioral responses,[308] and thus promote neotissue growth.

Several differentiation strategies have been previously investigated to chondrogenically induce hESCs within embryoid body (EB) cultures.[250, 251, 254, 305] Biochemical agents, such as transforming growth factor-β (TGF-β),[255] or media supplements, such as Invitrogen's Knock Out Serum Replacer (KOSR) (unpublished data, E.J. Koay, K.A. Athanasiou), have been employed to promote the chondrogenic phenotype. However, a prevailing concern among the various approaches is the production of non-uniform cell populations post differentiation.[309] Thus, cell purification techniques are necessary to ensure that tissue engineered constructs are formed with homogeneous, chondrogenically differentiated hESCs. One such methodology, a Percoll gradient system, is capable of separating articular chondrocytes (ACs) based primarily on cell density, resulting in populations that differ in cell morphology, nucleus size, and protein synthesis.[310, 311] Moreover, cell fractions originating from embryonic cells have shown significant differences in chondrogenic potential, both in monolayer and micromass cultures.[312] Therefore, it is of interest to examine potential differences in various chondro-induced hESC subpopulations, separated based on cell density.

The objectives of this study were to characterize the viscoelastic material properties of single hESCs and to identify mechanical differences between hESCs and their chondrogenically differentiated counterparts. Chondrogenesis was induced using two differentiation agents (TGF-β1 and KOSR), and the resulting cell populations were fractionated based on density. Mechanical properties of the undifferentiated hESCs and differentiated hESC cell subpopulations were measured using unconfined creep cytocompression.[299] We hypothesized that density separation of differentiated hESCs would yield subpopulations with different mechanical characteristics. We further hypothesized that a chondrogenically differentiated hESC subpopulation can be identified with stiffness properties and morphologies similar to those of native mesenchymal stem cells (MSCs) or ACs.

Materials and Methods

Chondrogenic differentiation of human embryonic stem cells

The NIH-approved H9 hESC line (Wicell, Madison, WI) was cultured at passage 39 according to Wicell's instructions on irradiated CF-1 mouse embryonic fibroblasts (MEFs, Charles River Laboratory, Wilmington, MA). Colonies were passaged using 0.1% type IV collagenase (Invitrogen, Carlsbad, CA) every 4-6 days. For the final passage prior to EB formation, colonies were passaged onto Matrigel (BD Biosciences, San Jose, CA) coated plates to reduce contamination of hESC colonies with feeder cells. While on Matrigel, the colonies were given MEF-conditioned medium. Once the hESC colonies on Matrigel

reached 70-80% confluence, dispase (0.1% w/v in DMEM/F-12) was applied for 10–15 min to lift the hESC colonies from the culture dish. This left MEFs behind to form EBs from the hESC colonies.[313] After two washes with DMEM/F-12, the EBs were suspended in a chondrogenic medium containing either 1 ng/ml TGF-β1 (Peprotech, Rocky Hill, NJ) or 5% KOSR (Invitrogen, Carlsbad, CA). The base chondrogenic medium consisted of high-glucose DMEM (Invitrogen, Carlsbad, CA), 10^{-7} M dexamethasone, ITS+ Premix (6.25 ng/ml insulin, 6.25 mg transferrin, 6.25 ng/ml selenious acid, 1.25 mg/ml bovine serum albumin, and 5.35 mg/ml linoleic acid; Collaborative Biomedical, San Jose, CA), 40 µg/ml L-proline, 50 µg/ml ascorbic acid, and 100 µg/ml sodium pyruvate. The EBs were then distributed into Petri dishes (Fisher, Hampton, NH) containing 15 ml of medium per dish. EBs were cultured for 3 wks with media changes every 48 h.

EB digestion and density separation

After 21 days of differentiation, EBs were digested in 0.05% trypsin-EDTA (Invitrogen, Carlsbad, CA) for 1 h followed by up to 1 h of 0.15% collagenase II (Worthington Biochemical Corp., Lakewood, NJ) digestion until a suspension of single cells was created. Cells were counted with a hemocytometer, washed with DMEM containing 1% FBS, centrifuged at 200 x g, and resuspended in 2 ml of DMEM.

Density separation of differentiated hESCs was performed as described previously for chondrocytes[311] and heart mast cells[314]. Isotonic Percoll (Sigma, St. Louis, MO) was mixed with sterile PBS (HyClone, Logan UT) to produce a

60% stock solution. The stock was further diluted with PBS to produce Percoll solutions of 10, 20, 30, 40, 50, and 60%. A pre-formed density gradient was created by sequentially layering 2 ml of each Percoll solution, starting with 60%, into a 15 ml conical bottom tube (VWR, Bridgeport, NJ). Two ml of DMEM containing the differentiated hESCs was carefully layered on top of the gradient, and the tube was centrifuged at 400 x g for 20 min. After centrifugation, the cells collect at the interface between Percoll layers, which relates to their cellular density. The interface between each density layer was then isolated along with 1 ml of Percoll above and below each interface, using a sterile pipette. The Percoll was diluted with 8 ml of DMEM, centrifuged at 200 x g, and the cell pellet was resuspended in 2 ml DMEM. Cells from each interface were counted with a hemocytometer.

MSC culture and articular cartilage isolation

Human MSCs from the bone marrow of one donor, age 35, were obtained from the Tulane Center for Gene Therapy (New Orleans, LA). Cells were seeded at 60 cells/cm^2 in T75 flasks (BD Biosciences, San Jose, CA) and cultured in α-MEM (Invitrogen, Carlsbad, CA) containing 16.5% Fetal Bovine Serum ('FBS', Atlanta Biologicals, Lawrenceville, GA), 4 mM L-glutamine, and 100 units/ml penicillin/streptomycin (Invitrogen, Carlsbad, CA). Cells were passaged every 7-10 days using 0.05% trypsin-EDTA (Invitrogen, Carlsbad, CA) and replated into T75 flasks. Undifferentiated MSCs were used for the experiment at passage 4.

Human ACs were isolated from healthy cartilage of one donor, age 25, excised as part of a surgery at M.D. Anderson Cancer Center (Houston, TX) to remove an osteosarcoma (Rice University IRB approval #08-115X). Articular cartilage tissue was digested overnight using 0.2% collagenase type II (w/v) (Worthington Biochemical Lakewood, NJ) in supplemented DMEM (0.1 mM NEAA, 100U/ml penicillin/streptomycin, 0.25 µg/ml fungizone) at 37°C and 10% CO_2.

Cell seeding

Isolated cells from each density layer were resuspended in their appropriate differentiation medium (TGF-β1 or KOSR) and seeded within a silicone isolator (PGC Scientifics, Gaithersburg, MD) onto a tissue culture dish to yield an approximate density of 3.8 x 10^4 cells/cm^2. Culture plates were incubated for 3 – 5 h at 37°C and 10% CO_2 to allow for proper cell attachment prior to cytocompression testing. Previous studies in our laboratory have shown that seeding time after a minimum of 3 h does not affect the viscoelastic properties of single cells.[315, 316] The same seeding method was employed for undifferentiated hESC, human AC, and human MSC controls.

Creep cytocompression

Unconfined creep cytocompression experiments were performed on each experimental group (n > 10 cells / group) using the same medium as the seeding phase, supplemented with HEPES buffer (Fisher Scientific, Pittsburgh, PA) to

prevent pH changes while the culture dish was exposed to ambient conditions. A previously validated creep cytoindentation apparatus[298, 299] was used to apply controlled stresses onto single adherent cells via a 50.8 μm diameter tungsten probe. Cells were positioned directly below the probe, as confirmed through visualization on an inverted microscope. The compressing tip was driven toward the cell by vertical control over the far end of the probe using a piezoelectric actuator. A laser displacement meter simultaneously tracked the true position of the probe tip (Fig. 1). Before each trial, the system was calibrated by comparing known piezoelectric displacements with recorded measurements from the laser micrometer. During cytocompression, the deflection of the probe (δ) was calculated based on the differences in piezoelectric movement and laser displacement measurements. Cantilever beam theory was then used to calculate the reaction force by the cell, based on known physical parameters of the tungsten probe and the measured deflection distances. Finally, a closed-loop algorithm was employed to maintain a constant force level of 100 nN onto each cell for 30 s by appropriately moving the piezoelectric actuator. Cell diameter was measured with a reticle in the microscope objective. Applied stress was defined as the force divided by the maximum cell diameter. Cell height was determined by measuring the contact distance between the probe and the culture dish after each test, and comparing it to the contact distance of the cell.

Viscoelastic properties

The unconfined compression creep behavior of single cells was fitted to a standard linear viscoelastic solid model. Previous work has shown that the viscoelastic model accurately depicts the initial creep behavior of single chondrocytes.[299] Briefly, this model considers the cell to be an isotropic, homogeneous, and incompressible viscoelastic solid undergoing small deformations. It yields three unique material properties: instantaneous modulus (E_o), relaxed modulus (E_∞), and apparent viscosity (μ). The experimental deformation behavior of single cells over time was analyzed using the following equations:

$$u(t) = \frac{2\sigma h_o}{3E_\infty}\left[1 + \left(\frac{\tau_\varepsilon}{\tau_\sigma} - 1\right)e^{\frac{-t}{\tau_\sigma}}\right]H(t) \tag{1}$$

$$E_o = \frac{\tau_\sigma}{\tau_\varepsilon}E_\infty \tag{2}$$

$$\mu = \tau_\varepsilon\left(E_o - E_\infty\right) \tag{3}$$

where $u(t)$ is the cell deformation over time, σ is the applied constant stress, h_o is the initial cell height, $H(t)$ is the step function, and τ_σ and τ_ε are the stress and creep relaxation time constants, respectively. Creep curves were fitted to this viscoelastic model using Matlab 6.5 (The MathWorks, Natick, MA), via the non-linear Levenburg-Marquardt method.

Histology and immunohistochemistry

To confirm cartilaginous differentiation of the hESCs, representative EBs from the TGF-β1 and KOSR groups were frozen in cryoembedding medium and

sectioned at 12 μm thicknesses. Safranin-O and fast green staining was used to examine the presence of sulfated glycosaminoglycans (s-GAG).[317] Additional slides were processed with immunohistochemistry (IHC) analyses to visualize collagen types I and II. Briefly, these slides were fixed in chilled acetone, quenched of exogenous peroxidase activity with 3% H_2O_2 in methanol, blocked with serum (Vectastain ABC kit, Burlingame, CA), and incubated with either mouse anti-collagen type I antibody (Axell, Westbury, N.Y.) or rabbit anti-collagen type II antibody (Cederlane, Burlington, NC). The appropriate mouse or rabbit secondary antibody (Vectastain ABC kit) was applied, followed by the avidin-biotinylated enzyme complex (Vectastain ABC kit), DAB reagent (Vector Labs), and hematoxylin counterstain to visualize nuclei. Native tendon and articular cartilage served as positive and negative controls. To assess if the hESCs had differentiated along other mesenchymal lineages, additional slides were processed with Von Kossa and oil red O stains for mineralization and adipose tissue, respectively.

Data analysis

Analysis of variance was used to discern differences in mechanical properties among all differentiated hESC and control groups, with a Tukey's post-hoc test when warranted. Significance was defined as $p < 0.05$ throughout the study.

Results

hESC differentiation and density separation

Positive staining was observed for s-GAGs, and collagen types I and II in EBs from both TGF-β1 and KOSR differentiation regimens (Fig. 2), suggesting a cartilaginous differentiation. Staining with Von Kossa and oil red O was negative (data not shown), indicating the absence of undesired differentiation. Subpopulations of chondrogenically differentiated hESCs were isolated based on cell density (Fig. 3). The percentage of cells isolated at each Percoll density interface for both differentiation regimens is given in Table 1. Due to the low cell yield in the TGF 10-20, KOSR 10-20, KOSR 40-50, TGF 50-60, and KOSR 50-60 groups, mechanical testing of these subpopulations was not possible.

Viscoelastic properties and cell morphologies

The deformation behavior of single cells in response to a 100 nN step load was fitted to a viscoelastic model (eqs. 1 – 3) to yield an instantaneous modulus, relaxed modulus, and apparent viscosity. Representative creep curves for undifferentiated and differentiated hESCs and native ACs are shown in Fig. 4. Creep cytocompression testing of cell subpopulations from both differentiation regimens resulted in a spectrum of mechanical properties ranging from undifferentiated hESCs to MSCs to ACs (Fig. 5).

The instantaneous moduli values were 0.53 ± 0.33 kPa, 1.03 ± 0.33 kPa, 1.71 ± 0.63 kPa, 1.83 ± 0.75 kPa, 0.85 ± 0.25 kPa, 0.52 ± 0.11 kPa, 1.16 ± 0.53 kPa, 1.33 ± 0.37 kPa, for hESC, TGF 20-30, TGF 30-40, TGF 40-50, KOSR 20-30, KOSR 30-40, MSC, and AC groups respectively. Differences in E_o were

observed between differentiation regimens, among the TGF-β1 subpopulations, and between hESC and all TGF-β1 groups. Moreover, both the TGF 30-40 and 40-50 groups were not different in E_o from the AC group.

The relaxed moduli values were 0.37 ± 0.20 kPa, 0.71 ± 0.26 kPa, 1.04 ± 0.40 kPa, 1.09 ± 0.44 kPa, 0.63 ± 0.20 kPa, 0.44 ± 0.07 kPa, 0.73 ± 0.43 kPa, 1.14 ± 0.31 kPa, for hESC, TGF 20-30, TGF 30-40, TGF 40-50, KOSR 20-30, KOSR 30-40, MSC, and AC groups respectively. Differences in E_∞ were observed between differentiation regimens, among the TGF-β1 subpopulations, and between hESC and all TGF-β1 groups and the KOSR 20-30 group. In addition, the TGF 30-40 and 40-50 groups were not different in E_∞ from MSC and AC groups. Notably, the E_∞ of ACs was also greater than MSCs.

The apparent viscosity values were 0.43 ± 0.44 kPa-s, 0.53 ± 0.38 kPa-s, 1.66 ± 1.63 kPa-s, 1.58 ± 1.48 kPa-s, 0.54 ± 0.49 kPa-s, 0.58 ± 0.48 kPa-s, 1.20 ± 0.93 kPa-s, and 0.99 ± 1.05 kPa-s, for hESC, TGF 20-30, TGF 30-40, TGF 40-50, KOSR 20-30, KOSR 30-40, MSC, and AC groups respectively. Differences in apparent viscosity were observed between hESC and TGF 30-40 and TGF 40-50 groups. In addition, the TGF 30-40 and TGF 40-50 groups were not different from the MSC and AC groups.

The creep time constant values were 2.32 ± 1.92 s, 2.50 ± 1.47 s, 6.03 ± 2.44 s, 5.97 ± 2.17 s, 2.75 ± 1.82 s, 3.84 ± 1.96 s, 5.13 ± 3.79 s, and 3.69 ± 2.95 s, for hESC, TGF 20-30, TGF 30-40, TGF 40-50, KOSR 20-30, KOSR 30-40, MSC, and AC groups respectively. The time constant values of the TGF 30-40, TGF 40-50, and MSC groups were found to be greater than the hESC group,

suggestive of a longer time to reach equilibrium deformation under compression. In addition, only the TGF 30-40 group was different from the AC group.

The morphological characteristics of the hESCs, as described by the ratio of cell height to width, changed as a result of the differentiation process and fell within the range of MSCs to ACs (Fig. 6). The cell height : width values were 0.34 ± 0.14, 0.63 ± 0.25, 0.63 ± 0.18, 0.72 ± 0.31, 0.63 ± 0.17, 0.65 ± 0.18, 0.44 ± 0.11, 0.82 ± 0.18, for hESC, TGF 20-30, TGF 30-40, TGF 40-50, KOSR 20-30, KOSR 30-40, MSC, and AC groups respectively. Moreover, the TGF 40-50 and KOSR 30-40 groups were not different from ACs. For comparison, cell height values were 7.30 ± 2.59, 8.89 ± 3.31, 8.12 ± 1.30, 8.73 ± 3.56, 8.23 ± 3.51, 10.3 ± 2.56, 6.92 ± 1.34, 9.41 ± 2.07, for hESC, TGF 20-30, TGF 30-40, TGF 40-50, KOSR 20-30, KOSR 30-40, MSC, and AC groups respectively.

Discussion

The use of hESCs in regenerative medicine is an exciting approach with direct applications to tissue engineering. This study was designed to examine the mechanical properties of hESCs and chondrogenically differentiated hESC subpopulations, using MSCs and ACs as controls. Two differentiation regimens (TGF-β1 or KOSR) were utilized, and the resulting subpopulations were separated based on cell density. Confirming our hypotheses, this study presents several notable findings relating to cellular mechanics and chondrogenic differentiation. First, the mechanical characteristics of single hESCs were investigated and directly compared to native human MSCs and ACs. Second, the

density gradient technique was successfully employed to separate cell subpopulations with distinct mechanical properties. Finally, a subpopulation of differentiated hESCs was identified with similar mechanical and morphological properties as native chondrocytes.

To our knowledge, this is the first study to examine the mechanical properties of single hESCs, a necessary step toward understanding the role of mechanical factors in cellular homeostasis and differentiation. It is well established that hESCs are mechanosensitive cells and respond differentially to applied forces or their three-dimensional mechanical environment.[300, 302] For instance, previous research has employed dynamic compression[303] and hydrostatic pressure[318] as successful differentiation agents for hESC chondrogenesis. In addition, changes in substrate rigidity and scaffold porosity, which are intimately linked with the transduction of forces on to single cells, can promote a desired embryonic stem cell differentiation[319]. Therefore, an understanding of the mechanical properties of hESCs may greatly aid research toward identifying an appropriate loading regimen and mechanical environment which induce a favorable cellular differentiation. In the future, this information can be coupled with traditional biochemical differentiation agents, such as growth factors, to optimize hESC differentiation approaches in the laboratory.

The reported hESC characteristics were directly compared to MSCs and native ACs to yield the 'mechanical range' of single cells along the chondrogenic lineage. Phenotypic changes during chondrogenesis are manifested by changes in cytoskeletal structure and cellular morphology,[320-323] which in turn contribute

substantially to altered cellular mechanics.[316, 324] Examining mechanical changes during cartilage development on the single cell level sheds light on the role of biomechanical factors in healthy tissue formation and maintenance of the cellular microenvironment.[301] In this experiment, cells became more rounded with differentiation to suggest continued rearrangement of the cytoskeleton. Moreover, parallels between the progression of cellular phenotype and mechanics can be drawn. It was found that the instantaneous modulus of hESCs was approximately 45% and 40% that of MSCs and ACs, respectively. In terms of the relaxed modulus, increases were observed from hESCs to MSCs (~2-fold) and from MSCs to ACs (~1.5-fold). Thus, cellular stiffening appears to coincide with chondrodifferentiation. Moreover, the observed differences in stiffness properties between hESCs, MSCs, and ACs may be indicative of the types of forces each of the cells typically is exposed to *in vivo*. For instance, mature native ACs must withstand high compressive loading in articular cartilage [325] and therefore need to be stiffer, while hESCs or MSCs experience primarily non-deformational hydrostatic forces, although at different levels, in the developing embryo or limb bud.[301]

Density separation was successfully utilized to isolate cell subpopulations with different mechanical properties. It is of great interest to identify an effective methodology to purify nonhomogeneous cell populations for use in tissue engineering. Both differentiation methods yielded subpopulations with properties distributed along the 'mechanical range' from hESCs to ACs. For example, the instantaneous modulus of TGF 20-30 cells was akin to that of MSCs, while the

TGF 40-50 subpopulation was similar only to ACs. Interestingly, no differences in cell morphology (e.g., cell height and diameter) were observed among the separated hESC subpopulations, suggesting that the mechanical differences were related to cytoskeletal and organelle densities. In light of this counterintuitive finding, mechanics may be a finer tool to detect differences among cell populations. Thus, it is particularly exciting to observe, for the first time, that the density separation can be utilized to isolate cells with unique mechanical properties. Therefore, future studies should compare this separation technique to more traditional cell sorting methodologies, such as Fluorescence-Activated Cell Sorting (FACS) and Magnetic-Activated Cell Separation (MACS).[326, 327]

Unconfined cytocompression was then employed to identify a subpopulation of differentiated hESCs potentially suitable for articular cartilage tissue engineering. While all of the differentiated hESC subpopulations were more rounded than undifferentiated hESCs, only the TGF 40-50 and KOSR 30-40 groups were not morphologically different from ACs. Of these two groups, only the TGF 40-50 subpopulation was similar to ACs with regards to all viscoelastic material parameters. Moreover, TGF 40-50 cells were 4-fold higher in apparent viscosity than undifferentiated hESCs, which is suggestive of a transformation from elastic to viscoelastic mechanical behavior.[299] This coincides with previous research demonstrating the important role of vimentin intermediate filaments, minimally present in hESCs, in maintaining the chondrocyte phenotype[320] and a viscoelastic response to an applied load.[324] Identification of a

differentiated hESC subpopulation with similar mechanical properties as native chondrocytes may provide utility in tissue engineering. These cells will need to withstand any mechanical stimulation regimen employed to augment the functional characteristics of engineered tissue,[328] as well as the highly mechanical environment in the native joint.[325] If the cells are too soft, they may experience non-physiologically high strain levels during normal loading activity. It has been shown that mechanical behavior of chondrocytes is strain-dependent and that beyond a critical point cells can no longer recover from the applied strain, suggestive of a breakdown in the cytoskeleton or other pathogenic changes.[308] Conversely, if the differentiated hESCs are too stiff, the necessary levels of mechanical stimulation may not be reached to maintain chondrocyte homeostasis.[329] Thus, the TGF 40-50 subpopulation may prove to be a valuable cell source for cartilage regeneration.

Creep cytocompression is a powerful methodology to infer changes in cell physiology, as long as the results are taken within the appropriate context. The behavior of individual cells seeded on a Petri dish can potentially be quite different to that of cells distributed within extracellular matrix. For instance, the microenvironment of chondrocytes has been shown to significantly influence the transmission of forces around individual cells.[330] Moreover, testing single cells does not consider the role of cell communication and the transmission of signaling molecules in the response of cells to an applied force.[331] An additional limitation is in regards to the assumptions necessary to yield viscoelastic properties to describe the cell. In this study, cells were considered to be

homogeneous, isotropic, and incompressible materials. While all cell types are unquestionably complex arrangements of organelles, cytoskeletal structures, and nuclear components, the previous assumptions in material behavior facilitate ease in data analysis and allow for consistent comparisons across all experimental groups. Despite the aforementioned caveats, approaches in single cell mechanics have been successfully utilized to distinguish cells based on zonal arrangement within a tissue,[296, 315] pathogenic state,[332] and phenotype.[295] Thus, mechanical differences between single cell populations may be retained after isolation *in vitro* and may not be entirely dependent on the cellular microenvironment and biochemical factors. Moreover, the creep curves generated for all groups in this study fit well to the theoretical viscoelastic model employed. Taking these considerations in tandem, single cell mechanical testing may be a suitable method to identify changes indicative of hESC chondrogenesis.

This study identifies cellular mechanics as an important marker for phenotypic changes. We have elucidated mechanical and morphological differences between hESCs, MSCs, and ACs, which may be indicative of changes in intracellular structures or the cellular mechanical environment during chondrogenesis. Using a density separation technique, we were able to distinctly isolate subpopulations with unique mechanical characteristics. Furthermore, from these subpopulations, we identified one group of differentiated hESCs with similar mechanical properties as native ACs, which may be useful in future cartilage tissue engineering efforts. An understanding of the mechanical

characteristics of undifferentiated and differentiated hESCs may have implications toward elucidating the role of physical forces in promoting specific cellular phenotypes.

Tables and Figures

Table 1: Distribution of cells based on density separation. Distribution of cells isolated at each Percoll gradient interface for cells differentiated using either TGF-β1 or KOSR. Values are given as a percentage of the total cells collected from the entire gradient.

Percoll Interface	TGF	KOSR
Top (0-10%)	0.57	0.38
10-20%	2.82	6.54
20-30%	22.6	52.69
30-40%	50.28	27.31
40-50%	16.95	9.23
50-60%	4.52	3.08
Bottom (60%)	2.26	0.77
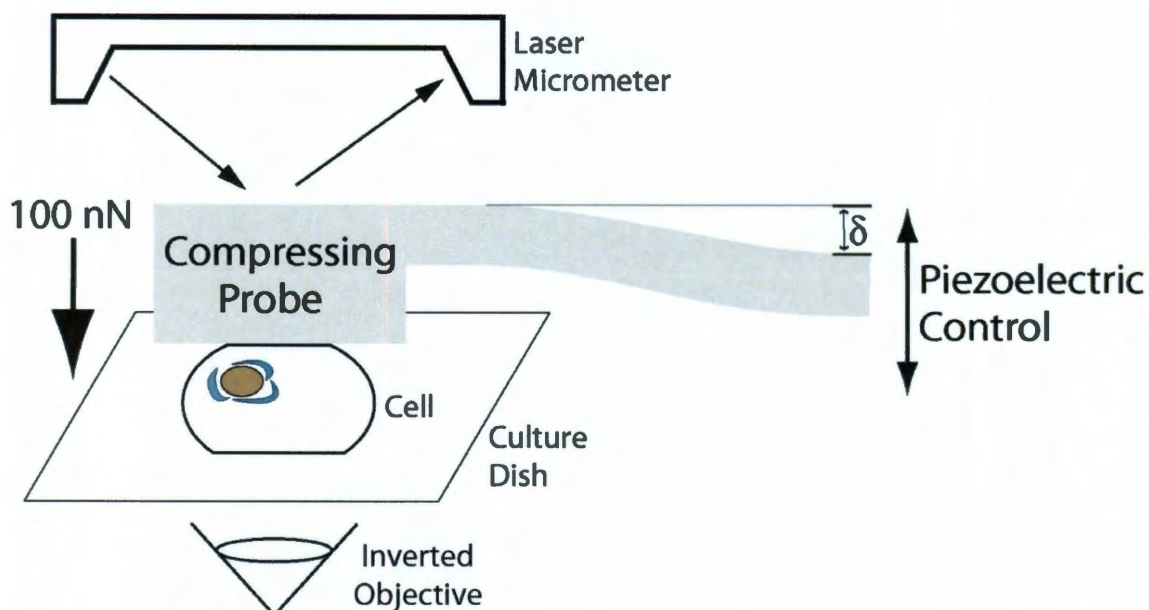
Figure 1: Experimental setup. Illustration of the creep cytocompression apparatus. A piezoelectric actuator drives a 50.8 µm tungsten probe axially toward cells seeded onto a culture dish and the free end of the probe is simultaneously tracked by a laser micrometer. The difference in recorded displacement by the laser micrometer and piezoelectric motor results in a probe deflection (δ), which is correlated to a reaction force using cantilever beam theory. Through a negative feedback algorithm, the position of the probe is continuously altered to hold a step load of 100 nN onto the single cells. An inverted objective located below the stage is used to position the probe and the cell, as well as measure cell diameters.
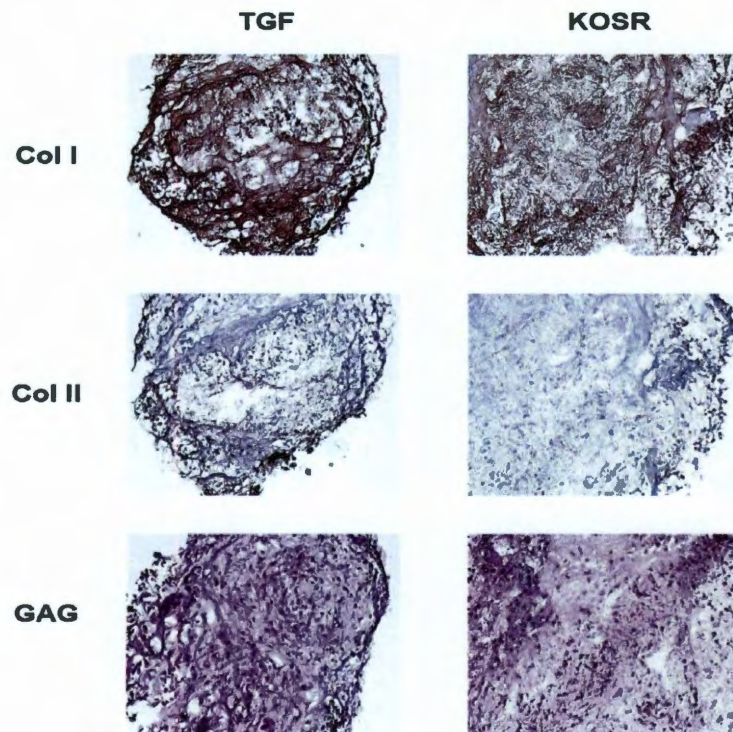
Figure 2: Histology. Histological sections of EBs differentiated with TGF-β1 (column 1) and KOSR (column 2). Original magnification, 40X. Collagen type I, collagen type II, and s-GAGs well all present, indicating a cartilaginous differentiation of the hESCs.
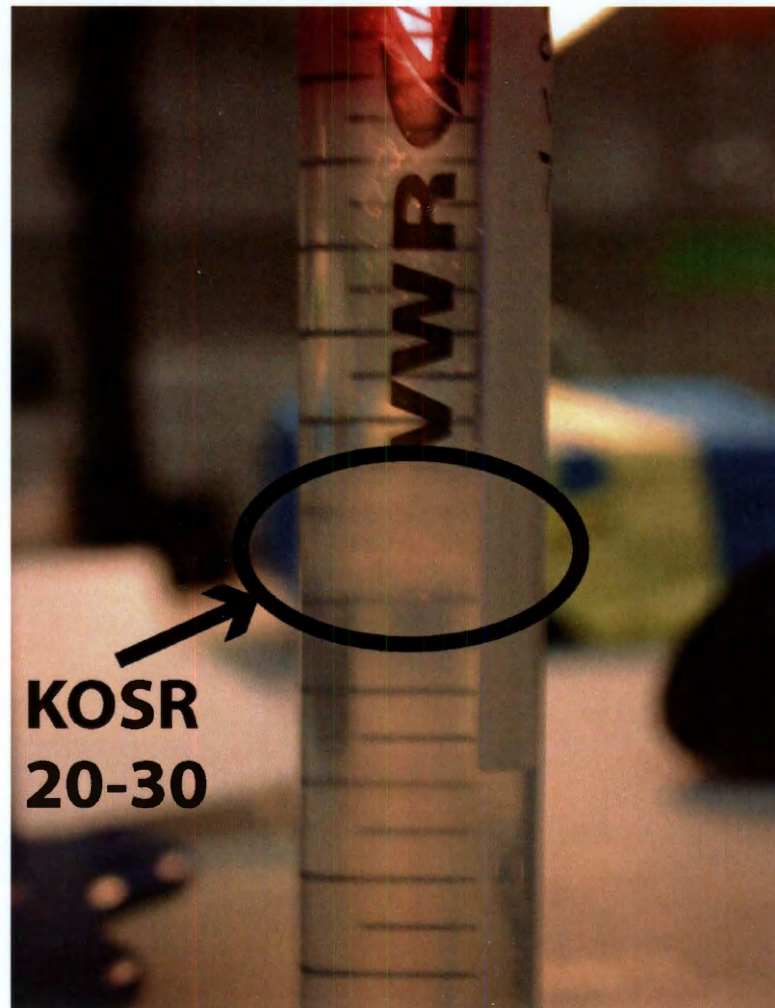
Figure 3: Density separation. Density separation of differentiated hESC subpopulations with the Percoll gradient technique. For this figure, chondro-induction was achieved with KOSR. Differentiated hESCs were centrifuged through Percoll solutions ranging from 10 to 60% and the cell interface between each density layer was counted and seeded for cytocompression testing. The majority of the KOSR cells (52.7%) fell within the 20-30% density interfaces.
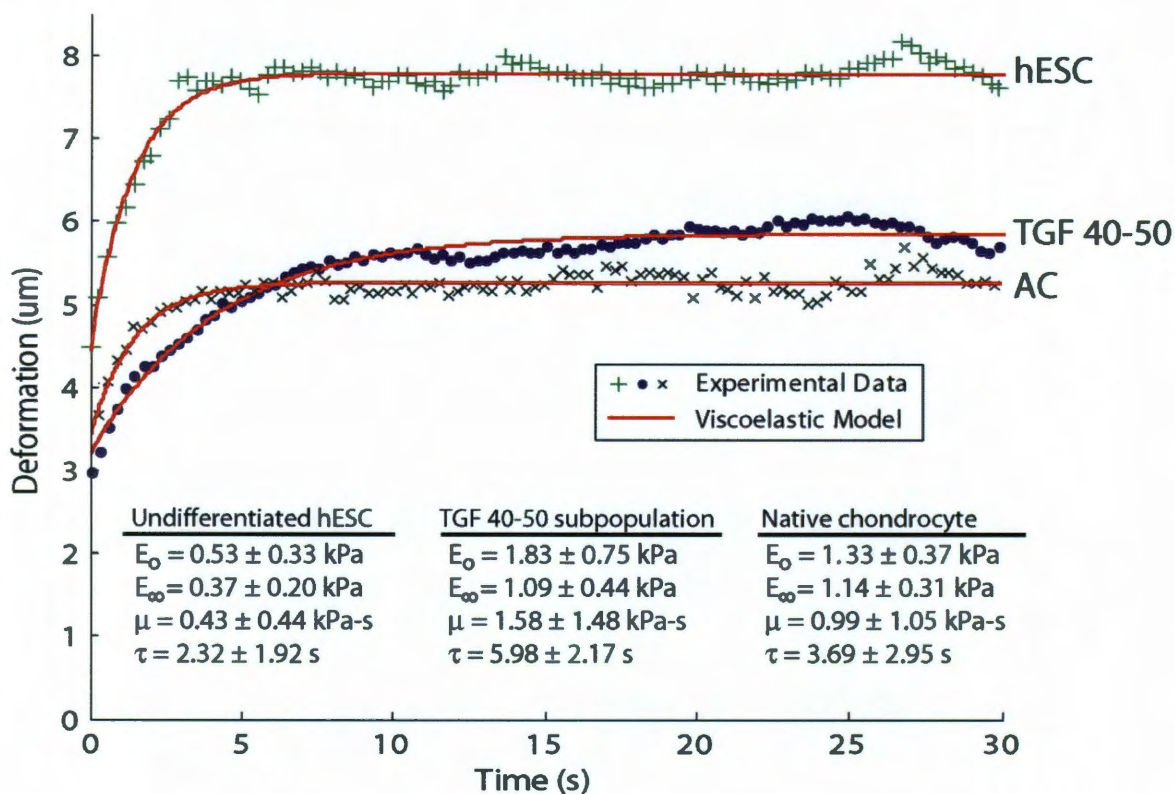
Figure 4: Creep compression curves. Representative creep curves of single cells. The experimental data points were fitted to a viscoelastic model to yield an instantaneous modulus, relaxed modulus, apparent viscosity, and a creep time constant. Undifferentiated hESCs typically exhibited a greater deformation, suggestive of a lower stiffness, and a faster time to equilibrium, suggestive of a lower apparent viscosity and time constant, than differentiated hESCs (example shown from TGF 40-50 group) in response to the same applied load. In addition, the equilibrium deformation of single cells from the TGF 40-50 subpopulation was akin to that of native chondrocytes, indicative of their similar stiffness values. For clarity, only one out of every 1000 experimental data points is shown for each curve. Representative cells were of 12 μm height.
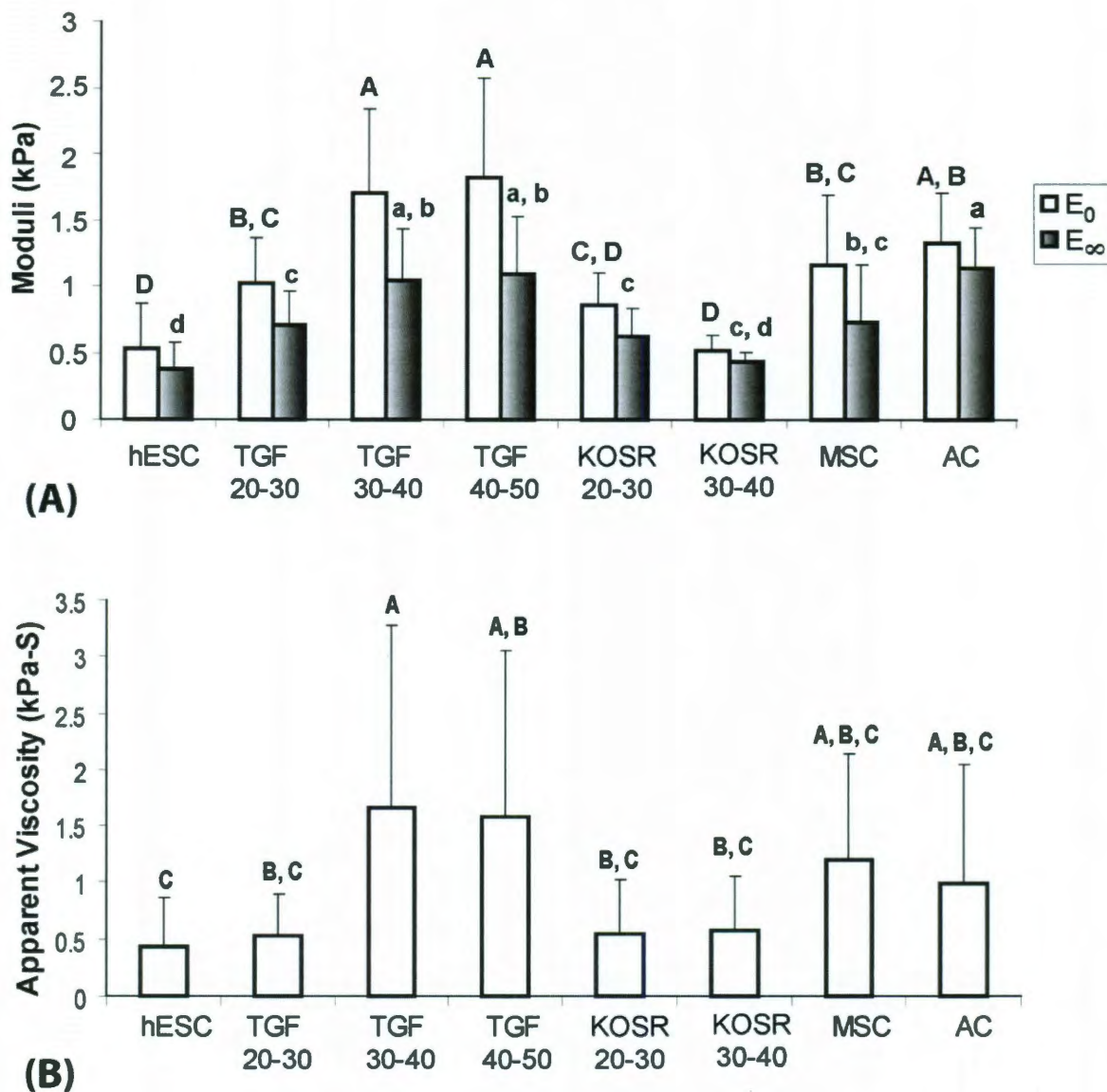
Figure 5: Viscoelastic cellular properties. Viscoelastic material properties of undifferentiated and differentiated single hESCs, as well as mesenchymal stem cell and articular chondrocyte controls. Differences in instantaneous and relaxed moduli were observed between density interfaces (TGF 20-30 vs TGF 30-40 or TGF 40-50), differentiation regimens (TGF-β1 vs. KOSR), and differentiation state (hESC vs. MSC vs. TGF 40-50) (A). Moreover, differentiated cell subpopulations (TGF 30-40 and TGF 40-50) were identified which were not different than native ACs. In addition, the apparent viscosities of the TGF 30-40 and TGF 40-50 groups were greater than that of undifferentiated hESCs (B). Data presented as mean ± standard deviations.
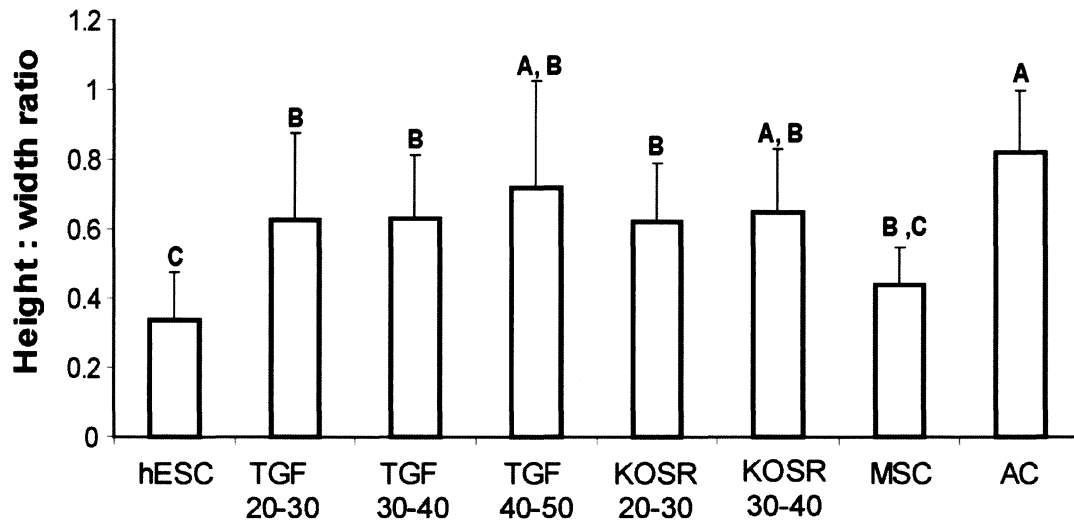
Figure 6: Morphology. Morphological properties of undifferentiated and differentiated single hESCs, as well as mesenchymal stem cell and articular chondrocyte controls. The cell height-to-width ratios of all differentiated cell subpopulations were greater than that of undifferentiated hESCs and approaching 1.0, which is indicative of a more rounded cell morphology. The values for differentiated hESCs all fell between the range of MSCs to ACs. Moreover, there was no difference between the cell height-to-width ratio of the TGF 40-50 and KOSR 30-40 cells and native ACs. Data presented as mean ± standard deviations.

Chapter 8: Producing a Spectrum of Cartilages from Human Embryonic Stem Cells by Employing a Chondrogenic Tuning Process

Abstract

Cartilages such as the knee meniscus, hyaline cartilage, and the temporomandibular joint (TMJ) disc are prone to debilitating pathologies and have an inherent inability to self-repair. As these tissues display distinct biochemical and biomechanical properties, the most useful cartilage engineering technologies must be able to produce a variety of cartilaginous tissues. Harnessing the pluripotent nature of human embryonic stem cells (hESCs) may provide a possible solution. This study sought to investigate the use of chondrogenic tuning to expand cells from chondrogenically differentiated H9 embryoid bodies (EBs) toward the production of a spectrum of cartilages. Following EB differentiation, cells were dissociated and self-assembled into constructs (P0 cells), or were chondrogenically tuned by passaging up to 5 times (P1-P5 cells) in a chondrocyte specific medium containing 1% serum and 4 ng/mL bFGF. Cells from each chondrogenic tuning passage were then allowed to self-assemble into constructs and cultured for 4 weeks. Flow cytometry and qRT-

PCR of cells prior to self-assembly both revealed an overall increase in mesenchymal phenotype with chondrogenic tuning passage. Self-assembled constructs from each passage showed differing amounts of cartilage-specific matrix components, indicating that cells from different passages can be used to make a variety of cartilages. In particular, P1 cells formed constructs with matrix similar to the TMJ disc, and P3 and P4 constructs produced large amounts of sulfated glycosaminoglycans and collagen type II, similar to the matrix of the inner meniscus. This study demonstrated the utility of chondrogenic tuning and self-assembly in producing a variety of cartilages from differentiated hESCs. Because of its simplicity and ability to efficiently yield a large number of cartilage-producing cells, this method can help realize the potential of hESC-based cartilage technologies to provide functional replacements for damaged tissue.

Introduction

Hyaline cartilages and fibrocartilages are essential for lubrication, stabilization, and load distribution in joints such as the knee and temporomandibular joint (TMJ). Based on the type and geometry of the joint in which they reside, these cartilages have developed highly specialized structure-function relationships to aid in normal joint movement. Though all classified as cartilages, hyaline articular cartilage, the knee meniscus, and the TMJ disc are distinct in many ways including ratios of collagen type, amount of sulfated glycosaminoglycans (GAGs), and extracellular matrix (ECM) organization.[15] In fact, a closer look at articulating cartilages reveals a veritable spectrum of tissues

ranging from those with high concentrations of collagen type II and GAGs to those with high collagen type I content and tensile properties. It follows, therefore, that the most useful technologies for reconstructing articulating cartilages should be able to produce a variety of cartilages with different biochemical and biomechanical properties.

Injury and disease of musculoskeletal cartilages frequently leads to irreversible damage due to the lack of vascularity and intrinsic healing capacity of these tissues.[333] Issues with current cartilage replacement technologies include a lack of starting material, donor site morbidity, and the production of tissue with suboptimal functional properties. Tissue engineering strategies are therefore investigating the production of cartilages using a variety of alternative cell sources from adult and embryonic stem cells.[334] Human embryonic stem cells (hESCs) have emerged as an attractive alternate cell source for cartilage engineering due to their unlimited proliferative capacity, pluripotency, and potential as an allogeneic cell source.[335] The flexibility provided by these cells is especially useful in cartilage engineering, where a variety of engineered tissues are needed to recapitulate the spectrum of cartilages that may need replacement.

The traditional method for inducing chondrogenesis in hESCs is via three-dimensional embryoid body (EB) culture. EB culture is effective at differentiating hESCs, but unfortunately it is ineffective at differentiating all of the cells in the same manner. Because the EB mimics gastrulation during embryogenesis, it results in multiple cell phenotypes at the end of differentiation.[309] Despite this

concern, EB derived chondrogenic cells have been used extensively in both scaffold-free[202, 251, 305, 336, 337] and scaffold based[254, 255, 338-340] tissue engineering. While EB derived cells have been used to produce engineered cartilage, the matrix composition and functional properties of these constructs leave room for improvement. It is possible that if a more consistent population of chondroprogenitors could be derived from hESCs, the resulting cartilage would also be improved. Because traditional cell purification techniques (e.g. fluorescence active cell sorting) are expensive and time consuming, two-dimensional (2-D) differentiation of is now being investigated as a way to improve homogeneity of the cell population. There are three reports of 2-D chondrogenesis in the literature,[341-343] but currently their complexity limits them to small scale cell culture and the use of large amount of animal serum. While 2-D differentiation shows promise, it cannot currently produce the large number of cells needed for cartilage tissue engineering.

This investigation attempted to produce a spectrum of engineered cartilages by combining EB differentiation with a 2-D chondrogenic tuning process. Our group has recently used chondrogenic tuning on adult chondrocytes with excellent results. Specifically, expanding the cells in chondrocyte specific medium resulted in the cells producing better engineered cartilage than non-tuned cells.[344] Here, chondrogenic tuning was employed following EB differentiation, to address the issues of cell number and homogeneity while priming the cells for tissue engineering. An overview of this approach is shown in Figure 1. It was hypothesized that the phenotype of EB

derived chondroprogenitors would be modified during the course of the chondrogenic tuning process, resulting in a variety of tissue engineered cartilages.

Experimental Procedures

hESC Culture

H9 human embryonic stem cells (H9) (WiCell Research Institute, Madison, WI) were cultured according to WiCell's protocols on gamma-irradiated CF-1 (Charles River Laboratories, Wilmington, MA) mouse embryonic fibroblasts (MEFs). Colonies were passaged every 4-6 days using the StemPro passaging tool (Invitrogen, Carlsbad, CA). For the final passage before EB formation, hESCs were cultured under feeder-free conditions on Matrigel (BD Biosciences, San Jose, CA) using MEF-conditioned media. H9s were used for this investigation at passage 38 (P38) and 39.

Embryoid Body Differentiation

When hESCs on matrigel reached 70% confluence, the cells were incubated in 0.1% (w/v) dispase solution for 10 to 15 min until the colonies lifted off the plate. After two washes with DMEM (Invitrogen), the cells were suspended in chondrogenic media and distributed into 100 mm low adherence petri dishes (Corning, Lowell, MA). For this investigation, chondrogenic media consisted of DMEM supplemented with 10^{-7} M dexamethasone, ITS+ premix (6.25 ng/mL insulin, 6.25 mg transferrin, 6.25 ng/mL selenious acid, 1.25 mg/mL bovine

serum albumin, and 5.35 mg/mL linoleic acid; BD Biosciences), 40 µg/mL L-proline, 50 µg/mL ascorbic acid, and 100 µg/mL sodium pyruvate. EB differentiation was conducted for 3 wks in chondrogenic media supplemented with 1% fetal bovine serum (FBS, Atlanta Biologics, Atlanta, GA) and 10 ng/mL TGF-β1 (Peprotech, Rocky Hill, NJ). Media was changed every 48 hrs.

Chondrogenic Tuning

After 3 wks, EBs were dissociated into single cells by first incubating the EBs in 0.05% Trypsin-EDTA (Invitrogen) for 45 min with shaking. EBs were washed once in DMEM and then incubated in 0.2% collagenase type II (Worthington Biochemical, Lakewood, NJ) for up to 1.5 hrs until all matrix had been removed. Resulting cells were washed once in DMEM and then counted with a hemacytometer. Differentiated cells were used directly for cellular analysis and cartilage constructs (P0), or they were chondrogenically tuned. Chondrogenic tuning involved 2-D expansion of the cells in a low-serum cartilage specific media. Cells were plated at 8000 cells/cm^2 in cell culture flasks (BD Bioscience) in chondrogenic media containing 10% FBS. After 24 hrs of seeding, cells were washed with PBS and media was replaced with chondrogenic media supplemented with 1% FBS and 4 ng/mL bFGF (Peprotech). When the cells reached 90% confluence, they were passaged using 0.05% trypsin. In total five passaged were conducted during the chondrogenic tuning process (P1-P5). At each passage, cells were analyzed with RT-PCR and flow cytometry, or they were used to form self-assembled cartilage constructs.

Self-Assembly of Chondrogenically Differentiated hESCs

Scaffold-free self-assembled cartilage constructs were formed as previously described.[202, 208, 336, 337] A single cell suspension of 6 x 10^5 cells in 30 μL of chondrogenic media was seeded into a 3 mm cylindrical well made of 2% agarose. The cells were allowed to assemble for 3 hrs after which 2 mL of chondrogenic media was gently added to the top of the wells. Cartilage constructs were cultured for 4 wks with daily feeding. After 4 wks, constructs were collected for morphological, biochemical, and histological assessment.

Quantitative Reverse-Transcriptase PCR

Total RNA was isolated from cells using the RNAqueous micro kit (Ambion, Austin, TX). One microgram of total RNA per 20 μL reaction volume was reverse-transcribed into cDNA using SuperScript III First-Strand Synthesis System (Invitrogen). Real Time-PCR reactions were performed using SYBR Green PCR Mastermix (Qiagen, Valencia, CA) with a Roto-gene 3000 (Qiagen) real-time amplification system. cDNA samples (2 μL in total volume of 25 μl per reaction) were analyzed for the gene of interest and for the reference gene beta-2 microglobulin (B2M). QuantiTect primer assays for each of the genes of interest (Oct-4, Sox9, collagen I, collagen II, aggrecan) were purchase from Qiagen. The fold change for each target gene was calculated as $-2^{\Delta\Delta Ct}$. Four biological replicates were used per group.

Flow Cytometry

Cells were blocked in 5% goat serum for 30 min, followed by 30 min staining with a primary antibody: immunoglobulin (Ig)G_1 isotype control, IgG_3 isotype control, mouse anti-human CD44, mouse anti-human CD29, or mouse anti-human SSEA-4 (all from BD Biosciences except SSEA-4 from Developmental Studies Hybridoma Bank). Cells were washed with PBS and then a Alexa Fluor 488 goat anti-mouse (Invitrogen) secondary antibody for 30 min. Samples were fixed in 0.5% paraformaldehyde in PBS and stored at 4°C for 24 hrs until analysis. Flow cytometry analysis was conducted on a BD FACScan system and data was analyzed for the percentage of cells with a fluorescence level exceeding a 95% threshold on the isotype control. Three biological replicates were used per group.

Biochemical Analysis

Samples were lyophilized for 48 hours and digested in 125 μg/ml papain (Sigma, St.Louis, MO) for 18 hours at 60°C. Cell number was determined using Picogreen® Cell Proliferation Assay Kit (Molecular Probes, Carlsbad, CA). A hydroxyproline assay was performed to gauge total collagen using bovine collagen standards (Sircol, Newtonabbey, Northern Ireland). Sulfated GAG was measured with the Blyscan GAG Assay Kit (Biocolor, Belfast, Ireland). For biochemical analysis, six to eight samples were used per experimental group. ELISAs for collagens type I and II were performed as described previously.[203]

Histology and Immunohistochemistry

Samples were cryoembedded and sectioned at 12 µm. Safranin-O staining with hematoxylin counter staining was used to examine glycosaminoglycan (GAG) distribution. To determine whether undesired differentiation had occurred, Von Kossa and oil red O stains were performed for evidence of calcification and adipose tissue, respectively. Immunohistochemical analysis was performed by fixing sections in chilled acetone, rehydrating, treating with 3% H2O2 in methanol, and blocking with horse serum. The following primary antibodies were diluted in PBS and applied for 1 hour: 1:300 rabbit anti-human collagen VI pAb (US Biologicals, Swampscott, MA), 1:500 rabbit anti-human collagen II pAB (Cedarlane, Burlington, NC), and 1:750 mouse anti-human collagen I (Chondrex, Redmond, WA). Visualization using a secondary biotinylated antibody, the ABC reagent, and DAB was performed using the Vectastain kit (Vector Laboratories, Burlingame, CA), and counterstaining was done with Harris's Hematoxylin. Sections of articular cartilage, meniscal fibrocartilage, bone, and skin tissue were run as positive controls.

Statistical Analysis

All quantitative data were compared using a one-way analysis of variance (ANOVA) with a Tukey's HSD *post hoc* test where necessary. A significance level of $p < 0.05$ was used in all statistical tests.

Results

Chondrogenic Tuning

Following chondrogenic differentiation in EBs (P0 cells), cells were chondrogenically tuned from passage 1 to 5. Chondrogenic tuning resulted in a 16-fold increase in differentiated cell number. At each passage level the morphology and phenotype of the cells were analyzed.

Cell Morphology

Changes were observed in overall cell morphology with passage during chondrogenic tuning (Fig. 2A). At P0 cells appear rounded with few cell processes. At P1, cells appear more spread, and begin to exhibit more cell processes. From P2 to P5, cells were observed to take on a more spindle-shape but remained small and looked like low passage number mesenchymal stem cells.

Flow Cytometry

Flow cytometric analysis was performed to detect pluripotency cell surface marker SSEA-4, and mesenchymal cell surface markers CD44 and CD29. SSEA-4 was found on all cell types, but higher levels of this marker were observed in P3 and P4 cells, followed by P2 and P5 cells (Fig. 2B). P1 cells showed the lowest expression of SSEA-4. Cells from P1 through P4 showed statistically higher amounts of CD44 than P0 and P5 cells, with P2 cells showing the highest overall amount. The percentage of CD29 positive cells was

statistically higher in P4 cells compared with P0, P1, P2, and P5 cells, but was not statistically different from P3 cells.

qRT-PCR

Quantitative real-time RT-PCR was performed on all cells (P0-P5) prior to self-assembly, and resultant data was normalized to P0. In general, Oct-4 mRNA decreased with chondrogenic tuning (P1-P5). Sox-9 mRNA levels also decreased with respect to P0 cells, but P2 cells showed the lowest expression, and expression levels of P1, P3, P4, and P5 cells were not statistically different from each other. Collagen type I expression levels did not change more than 2-fold in any of the tuned cells compared with P0 control cells. Collagen type II and aggrecan expression, however, did show a dramatic decrease with passaging during chondrogenic tuning.

Gross Morphology

Self-assembled constructs were made from P0 cells (straight from EBs) or P1-P5 chondrogenically tuned cells and cultured for 4 weeks in chondrogenic media. Following 4 weeks in culture, gross morphological differences were observed (Fig. 4A). P0 constructs were largest in diameter (3.52 ± 0.18 mm) and smallest in thickness (0.89 ± 0.05 mm) (Fig. 4B). P1 through P5 constructs were thicker (~1.42-1.96 mm) than P0 constructs, but also had smaller diameters (~2-2.75 mm). Of all of the passaged constructs, P4 constructs showed the largest overall diameter and thickness, 2.75 ± 0.08 mm and 1.96 ± 0.07 mm,

respectively. P0 (3.86 ± 0.28 mg) and P4 (3.57 ± 0.23 mg) constructs also showed significantly higher wet weights than other groups. A similar trend was seen in dry weight comparisons of the constructs, with P0 and P4 constructs higher than the rest.

Biochemistry

Quantitative biochemical analysis of all cartilage constructs is shown in Figure 5. Interestingly, sulfated GAG content did not show a positive correlation with chondrogenic tuning. P0, P1, P2, and P5 constructs all had measureable amounts of GAG (~2%/dry weight), but GAG content was significantly higher in P3 and P4 constructs (>2 times P0). Total collagen content, however, was highest in P5 constructs, but P3, P4, and P5 constructs all showed statistically higher collagen contents than P0 and P1 constructs. In general, there was a trend toward higher total collagen content with passage. Total cellularity of the constructs was relatively constant, but P0 constructs showed statistically higher cellularity than P5 constructs. The ratio of collagen type II to collagen type I content (measured via ELISA) followed a trend similar to the sulfated GAG content. The ratio was highest in P3 and P4 constructs, being 8 and 14 fold higher than P0, respectively.

Histology and Immunohistochemistry

Histological analysis of constructs made from primary (P0), and chondrogenically tuned (P1-P5) cells is shown in Figure 6. All histological results

mirrored the quantitative biochemical results. Positive Safranin-O staining (indicating sulfated GAG content) was present in all groups to some degree, but was abundant only in constructs made from P3 and P4 chondrogenically tuned cells. Interestingly, though P3 and P4 constructs showed abundant GAG content, P5 constructs showed only slight GAG staining, similar to P0, P1, and P2 constructs. Immunohistochemical analysis was also performed to detect collagen types I, II, and VI. Collagen type I was observed throughout the tissue in all groups, with the most intense staining observed in P0 constructs. All groups also stained positively for collagen type VI and collagen type II, but intense staining for collagen type II was observed only in P3 and P4 constructs.

Discussion

Human embryonic stem cells present an attractive alternate cell source for use in cartilage tissue engineering. However, to produce enough chondrogenically differentiated cells for functional cartilage engineering, methods must be identified that can reduce the inhomogeneous differentiation of EBs and enhance cell yield following differentiation. In an effort to address these needs, this study employed chondrogenic tuning following EB differentiation. This method was able to modify cell phenotype and produce a spectrum of cartilaginous tissues with varying composition. Chondrogenic tuning also increased the number of differentiated cells by 16-fold, providing abundant cells for cartilage engineering efforts.

The scaffold-free self-assembly method was used to create cartilage constructs from P0 and chondrogenically tuned cells, resulting in a variety of cartilaginous tissues. P0 constructs, which did not receive any stimuli associated with chondrogenic tuning, were consistent with prior studies containing similar levels of GAG and collagen, and producing a highly hydrated tissue with minimal contraction.[202, 305, 336, 337] Interestingly, cells at each chondrogenically tuned passage produced different levels of cartilage-specific matrix components. P1 constructs were on the fibrous end of the fibrocartilages, with low GAG content and abundant collagen type I. P3 and P4 constructs were by far the most cartilaginous with 2-fold more GAG and 8- to 14-fold more collagen type II than other constructs. Notably, constructs made from cells chondrogenically tuned for 5 passages (P5 constructs) made similar matrix to P2 constructs containing abundant total collagen but low collagen type II and GAG. Overall, constructs made from P0 cells were less dense than any of the constructs made from chondrogenically-tuned cells. The chondrogenically-tuned cells cultured in monolayer took on an increasingly MSC-like morphology with passage. This phenotypic change resulted in the production of denser ECM. In the future, the contraction observed in these constructs may be harnessed to produce matrix anisotropy typically observed in fibrocartilaginous tissues.[345, 346]

P1, P2, and P5 constructs displayed biochemical matrix properties similar to those of the outer meniscus and TMJ disc with high collagen type I content and few GAGs. P4 constructs, however, were most similar to the inner meniscus containing a collagen type II to collagen type I ratio of around 1.2 and GAG

content of around 5% per dry weight. P3 constructs were similar to P4 construct but had a higher collagen type I content, showing similarities to the ECM content of the middle meniscus. This method of chondrogenic tuning, therefore, is able to produce a spectrum of cartilages similar in biochemical composition to the TMJ disc and knee meniscus. To our knowledge, this is the first study to demonstrate the production of a variety of cartilage types from human embryonic stem cells using monolayer expansion conditions. Chondrogenic tuning, therefore, is a simple and highly flexible technology that can be used to produce abundant cells and many types of cartilage from hESCs.

The mechanism that allows chondrogenic tuning to produce distinct populations of differentiated hESCs is not well understood. This study showed that surface marker presentation and gene expression levels are both affected under chondrogenic tuning conditions. Flow cytometric analyses performed in this study provide valuable insights into the specific phenotypic changes that occur with each passage. Compared with P0 cells, phenotypic changes at P1 include increased CD44 and CD29 surface marker presentation and decreased SSEA-4 presentation. Changes in P3 and P4 cells include enhanced cell morphological homogeneity and increased SSEA-4 and CD29 presentation. In P5 cells, however, all of the cell surface markers assayed decreased with respect to P3 and P4. As EB differentiation is known to produce a heterogeneous cell population that may still contain undifferentiated cells, the initial drop in SSEA-4 expression between P0 and P1 is likely due to differentiation of the remaining embryonic cells as they are cultured in monolayer. Interestingly, SSEA-4

expression increased with passage from P2 to P4. This result is not unexpected as SSEA-4 expression is found on MSCs from a variety of tissue sources and is associated with a high degree of plasticity.[347, 348] Increased SSEA-4 content was shown to parallel increases in CD44 and CD29 expression, and, as SSEA-4 is known to exist on MSCs, may indicate that chondrogenic tuning enhances the mesenchymal phenotype of these cells. CD29 is found on chondrocytes in vivo and is known to be an important factor in chondrocyte adhesion to collagen types II and VI.[349] High CD29 expression has also been implicated during re-differentiation of chondrocytes after expansion.[350] Thus, the high CD29 expression on P3 and P4 cells may explain the highly chondrogenic matrix produced by these cells.

Gene expression changes resulting from chondrogenic tuning can also be reasonably correlated to an increase in mesenchymal stem cell phenotype, with lower expression of collagen type II and aggrecan. However, gene expression profiles of cells at each passage did not predict biochemical content of constructs made from each population. In fact, P3 and P4 cells prior to self-assembly showed lower gene expression levels than P0 cells for collagen type II and aggrecan, yet produced significantly higher amounts of these proteins after 4 weeks in self-assembly. This difference in starting population phenotype and matrix production during construct culture indicates that the three-dimensional, non-adhesive environment of self-assembly may play a pivotal role in directing the cells toward a more chondrogenic phenotype following chondro-tuning.

The present work shows that chondrogenic tuning is a feasible method of priming a large number of differentiated hESCs to produce a variety of cartilage tissues. It is the first study to use the chondrogenic tuning method with embryonic stem cells, and produced similar results to those obtained with chondrogenically-tuned primary cartilage cells. Specifically, recent work using P3 and P4 chondrogenically-tuned adult leporine chondrocytes showed enhanced matrix production and compressive properties of constructs compared to those made from primary cells.[344] Chondrogenically-tuned cells also showed a statistically significant increase in Sox9 expression following self-assembly above that observed for primary cells. Although the present study did not measure Sox9 expression following self-assembly, the enhanced matrix production observed for self-assembled, chondrogenically-tuned hESCs suggest that enhanced Sox9 expression may also be occurring. Recent studies have shown that passaging MSCs with bFGF is beneficial for chondroinduction and proliferation and is an important redifferentiation factor for chondrocytes.[271, 351-355] It is likely, therefore, that a combination of biochemical and physical stimuli contribute to the phenotypic and gene expression changes observed with chondrogenic tuning of hESCs. While more investigations must be carried out to determine the specific gene expression changes caused by chondrogenic tuning and self-assembly, it is clear that this combination is beneficial for hESC chondrogenesis.

These data indicate that passaging hESCs under chondrogenic tuning conditions results in a variety of distinct cell populations, and that these populations can produce different cartilaginous matrices that match native tissue.

Chondrogenic tuning, therefore, provides a simple and effective method to achieve a high yield and more homogeneous phenotype of cells that can be used to tissue engineer the cartilage spectrum. Of particular importance is the finding that chondrogenically tuned and self-assembled P4 hESCs can produce matrix with the same GAG and collagen profiles as the inner meniscus and P1 hESCs can produce matrix resembling that of the TMJ disc. This is particularly useful given these tissues' inability to regenerate and the clinical need for autologous replacement therapies. More work should be done to elucidate the factors influencing phenotypic changes during chondrogenic tuning and self-assembly. Once a better understanding of the underlying principles is achieved, it is conceivable that this technology can be used to fabricate a replacement for any type of cartilage.

Figures
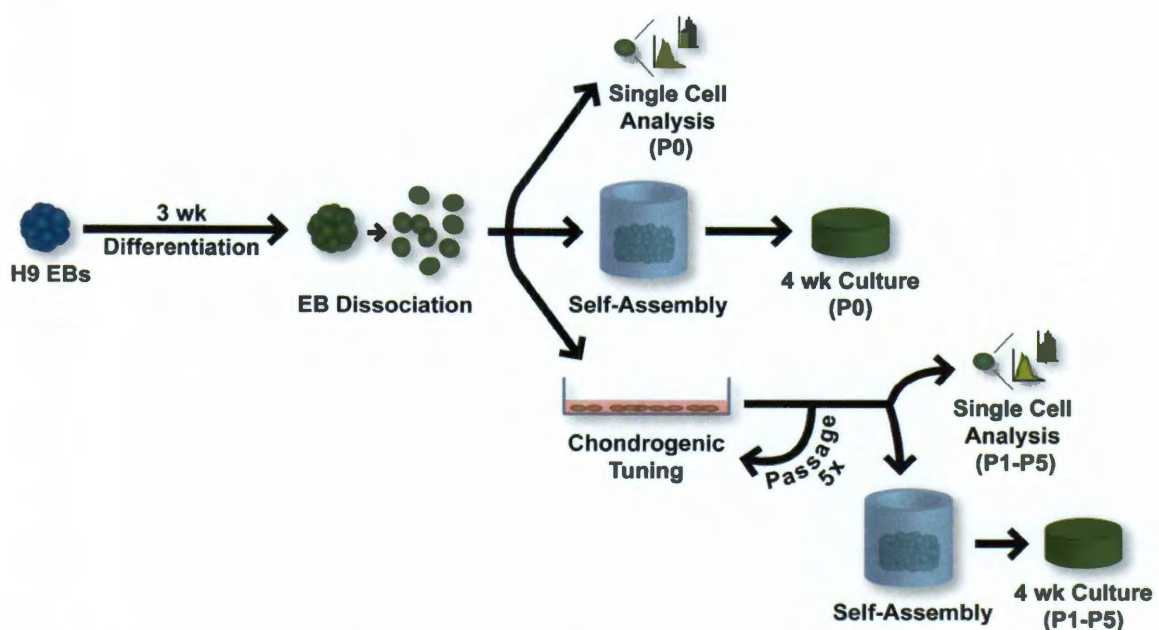
Figure 1: Overview of the approach taken in this investigation. H9 hESCs were differentiated for 3 wks in EBs using chondrogenic media. EBs were then enzymatically dissociated and the resulting cells (P0) were used i) for cellular analysis, ii) to form scaffold-less cartilage constructs, or iii) for chondrogenic tuning. Chondro-tuning was performed by expanding cells in monolayer with a chondrocyte specific medium. At each passage (P1-P5), cells were taken for RT-PCR and flow cytometry analysis or they were used to form self-assembled cartilage constructs.
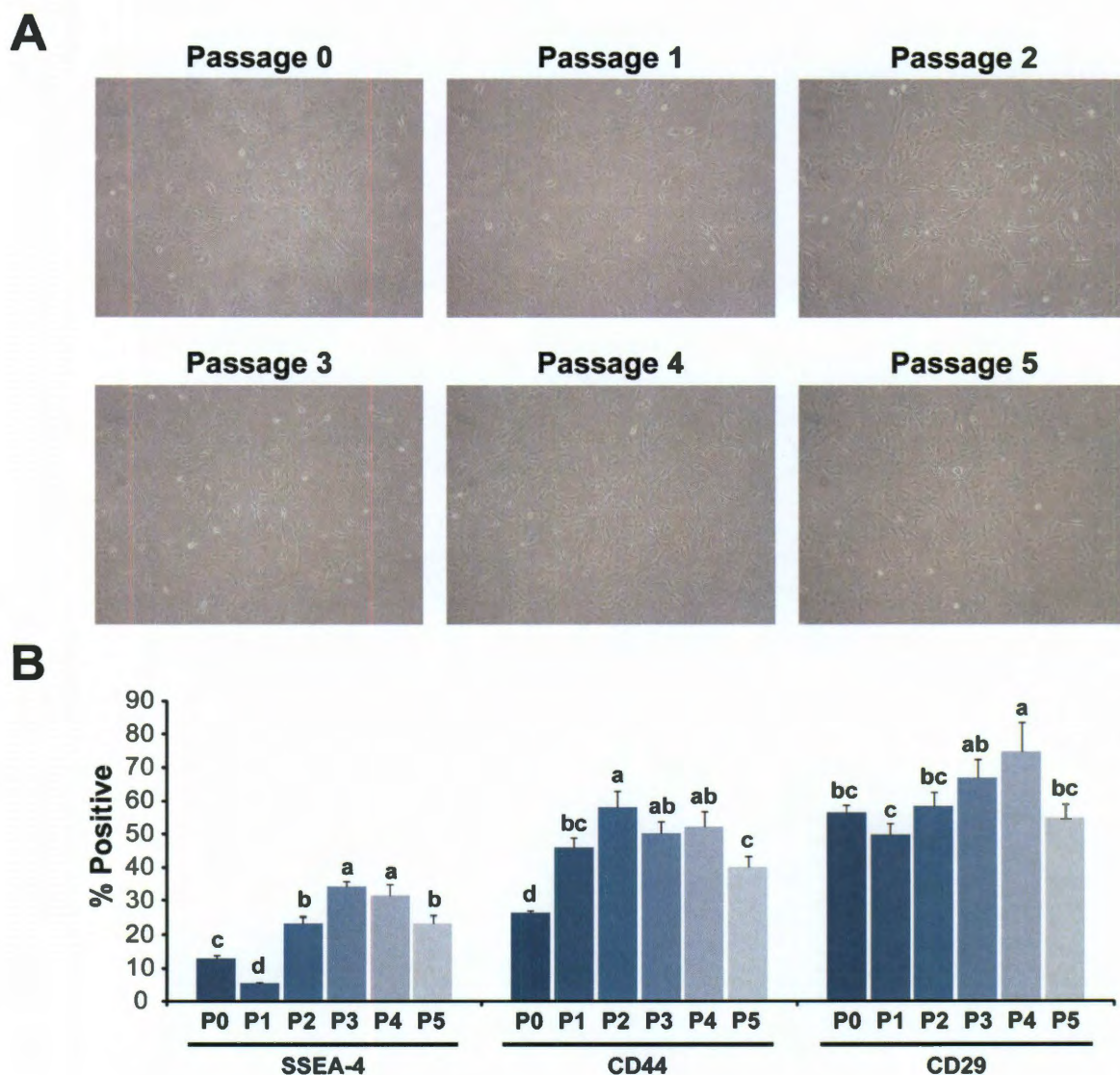
Figure 2: Cellular morphology and immunophenotype of chondrogenically tuned cells. (A) Cells fresh from the EBs (P0) were small and had a random morphology. During chondrogenic tuning (P1-P5) the consistency of cell morphology increased and the cells took on a spindle shape. **(B)** Expression of SSEA-4 and CD29 measured with flow cytometry both dropped at P1 and peaked at P3 and P4. The percentage of CD44 positive cells was highest at P2.
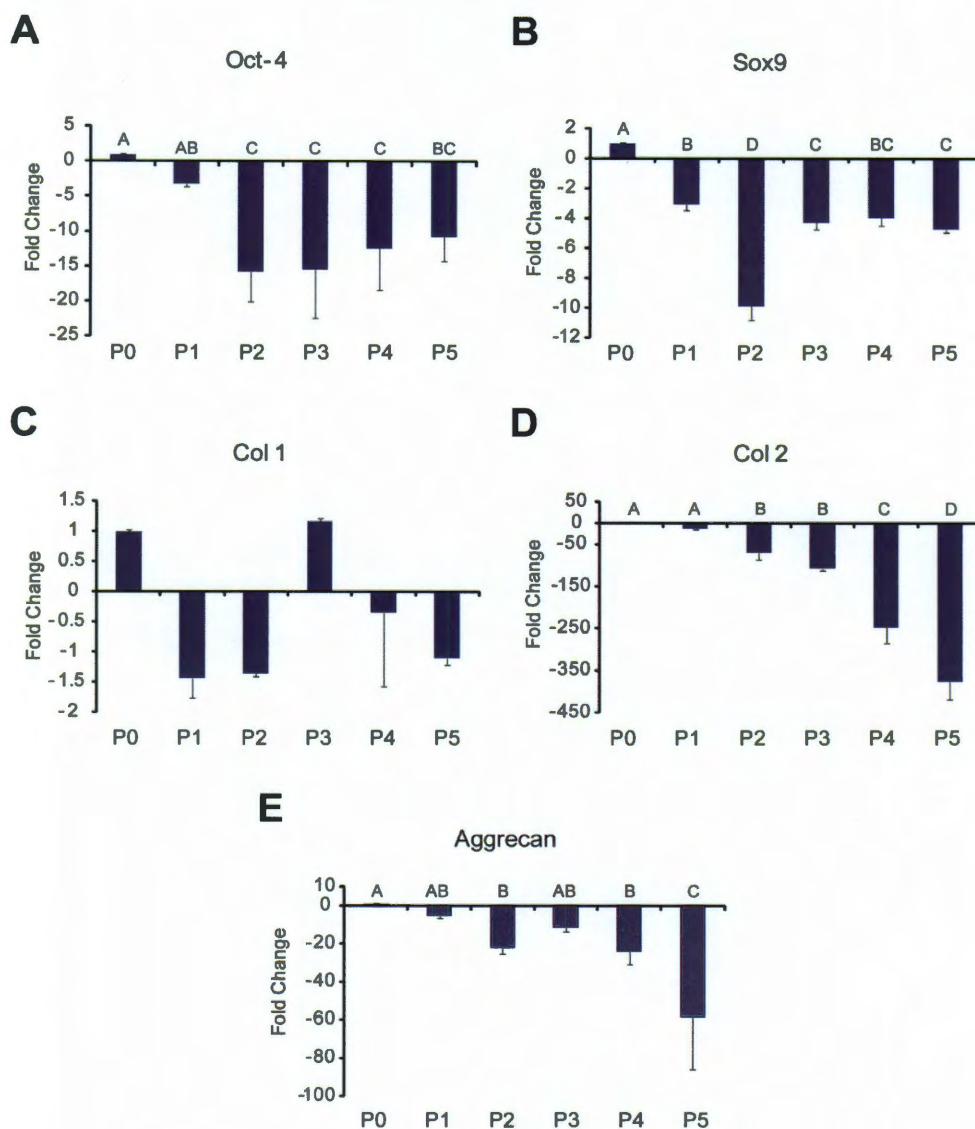
Figure 3: qRT-PCR analysis for pluripotency and chondrogenesis related genes during chondrogenic tuning. Data is calculated as a fold change relative to P0 and presented as mean ± SD. Letters represent the results of a one-way ANOVA and groups not connected by the same letter are statically different from each other. **(A)** Oct-4 expression dropped significantly by P2, but rose slightly higher at P5. **(B)** Similarly, Sox9 drop at P2, but then rose back higher for P3-P5. **(C)** There was no variation in collagen I expression. **(D)** There was a very dramatic decrease in collagen II gene expression with passage. **(E)** Aggrecan expression decreased with tuning but the effect was only dramatic at P5.
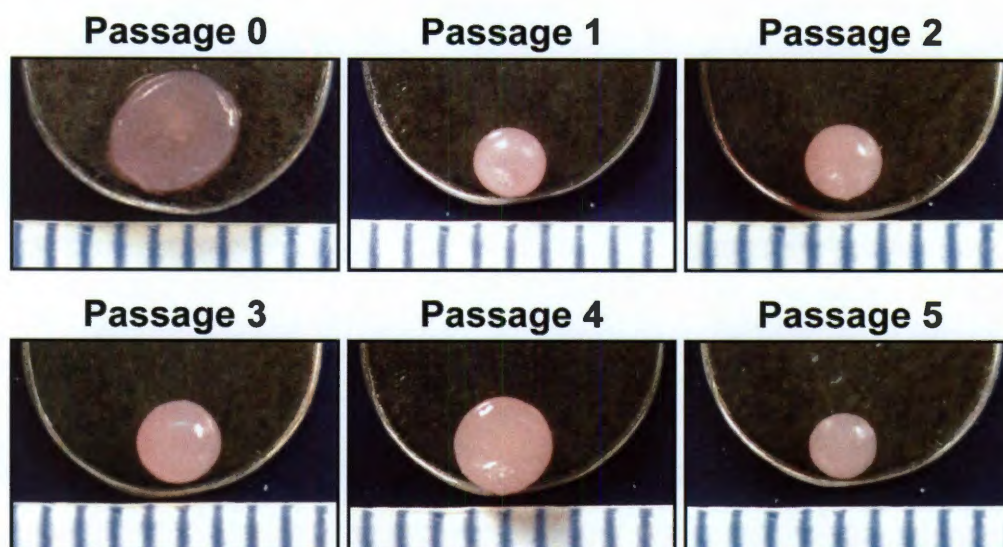
	Diameter (mm)	Thickness (mm)	Wet Weight (mg)	Dry Weight (mg)
P0	3.52 ± 0.18^A	0.89 ± 0.05^C	3.86 ± 0.28^A	0.42 ± 0.02^A
P1	2 ± 0.13^D	1.42 ± 0.17^B	1.56 ± 0.27^C	0.28 ± 0.03^B
P2	2.18 ± 0.13^{CD}	1.87 ± 0.22^A	1.81 ± 0.13^C	0.34 ± 0.04^B
P3	2.4 ± 0.21^C	1.86 ± 0.12^A	2.39 ± 0.2^B	0.33 ± 0.02^B
P4	2.75 ± 0.08^B	1.96 ± 0.07^A	3.57 ± 0.23^A	0.42 ± 0.04^A
P5	2 ± 0.15^D	1.77 ± 0.2^{AB}	1.75 ± 0.1^C	0.3 ± 0.02^B

Figure 4: Gross morphology and weights of cartilage constructs formed from chondrogenically tuned hESCs. P0 constructs possessed the largest diameter, but were also the thinnest. All chondrogenically tuned constructs (P1-P5) were contracted, with smaller diameters, but also were thicker than P0 constructs. P4 constructs were the largest tuned constructs with regards to both diameter and thickness. P0 and P4 constructs had the highest wet and dry weights, although the hydration of P0 constructs was greater. Data is presented as mean ± SD. Letters represent the results of a one-way ANOVA and groups not connected by the same letter are statically different from each other.
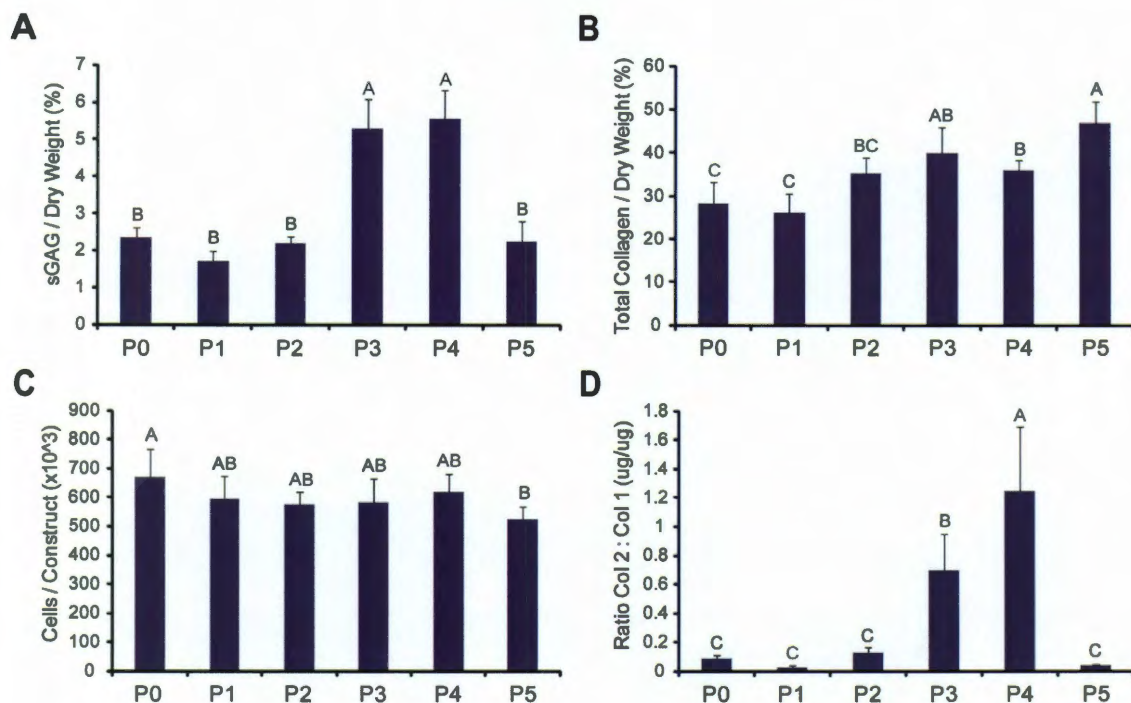
Figure 5: Biochemical content of constructs formed from chondrogenically tuned hESCs. Data is presented as mean ± SD. Letters represent the results of a one-way ANOVA and groups not connected by the same letter are statically different from each other. **(A)** sGAG content was only different in P3 and P4 constructs, being > 2-fold higher than all other groups. **(B)** Total collagen content generally increased with passage peaking at P5. **(C)** Cellular content of the constructs remained similar to the 6 x 10^5 cell seeding density. **(D)** Similar to the GAG content, the collagen II to collagen I ratio was 8 to 14-fold higher in the P3 and P4 constructs.
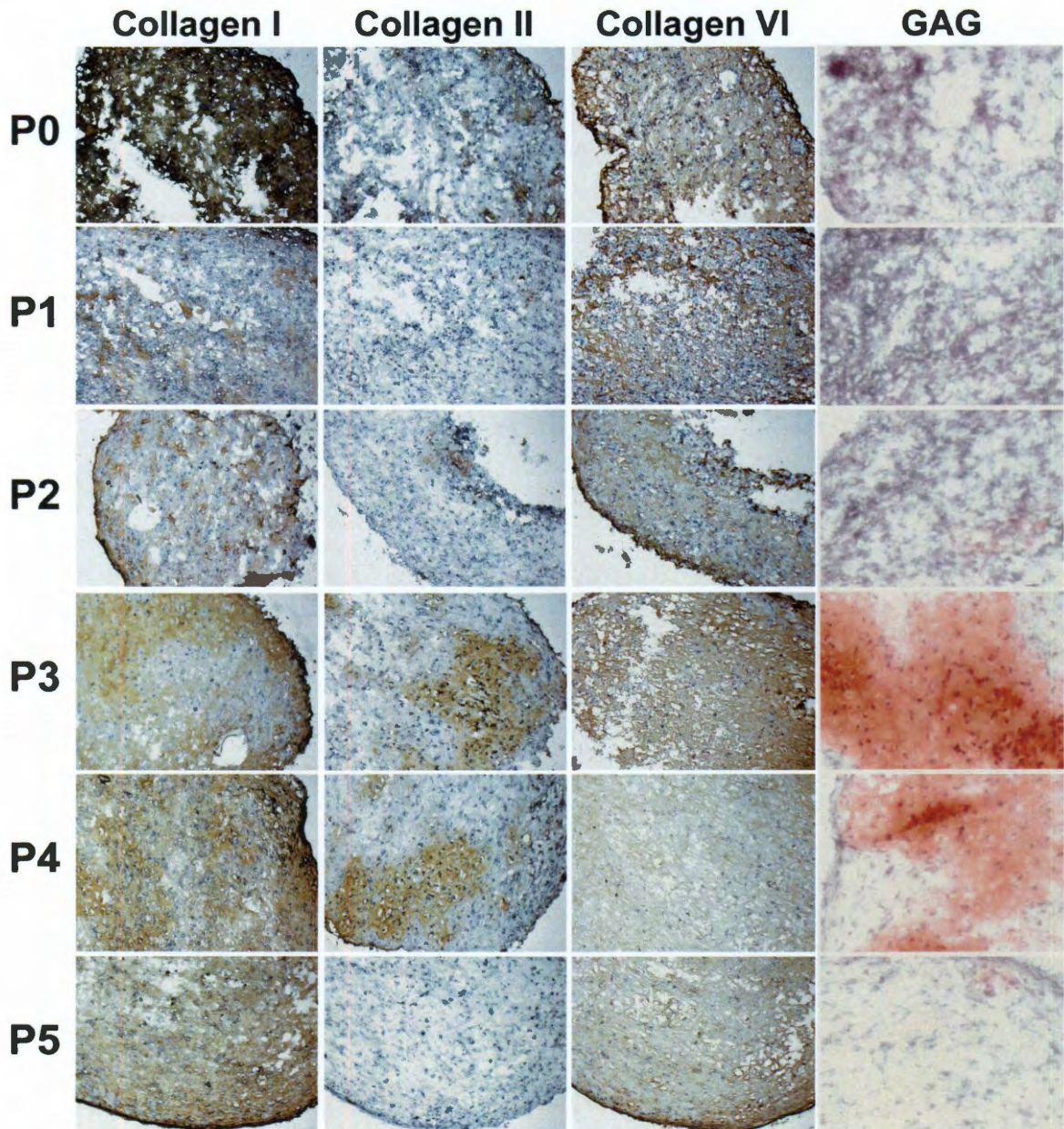
Figure 6: Immunohistochemistry and histology of chondrogenically tuned cartilage constructs. In general all staining mirrored quantitative biochemical results. All groups stained positively for collagens type I and VI. Only P3 and P4 constructs showed significant staining for collagen type II. Similarly, only P3 and P4 constructs stained significantly for sulfated GAG content via Safranin-O.

Conclusions

The potential impact of a tissue engineered TMJ disc is immense. Currently, patients suffering from TMJ dysfunction and/or degradation receive little benefit from clinical treatment.[98] This thesis investigated two components critical to the generation of a tissue engineered TMJ disc: 1) characterization of the native disc to identify a suitable animal model and create design parameters, and 2) development of approaches to use human embryonic stem cells (hESCs) in fibrocartilage tissue engineering. The work presented in this thesis identified the pig as a suitable animal model for TMJ disc engineering, furthered the understanding of TMJ disc structure-function relationships, and developed strategies for differentiation, expansion, and fibrocartilage tissue engineering using hESCs. This research was the first to elucidate the viscoelastic contribution of sulfated GAGs to TMJ disc compressive properties, measure mechanical properties of differentiated and undifferentiated hESCs, and use chondrogenic tuning with hESCs to produce a spectrum of cartilages. These findings provide key design parameters for TMJ tissue engineering and show that functional engineered TMJ replacements may truly be achieved using hESCs.

The first studies to examine the TMJ disc used a variety of animal sources.[26, 35, 92, 94] Of supreme importance for future characterization and engineering, was the definitive identification of a large animal model for the TMJ disc. Prior anatomical studies[86, 88] had indicated that the pig was the best model for the human, but no quantitative comparisons had ever been made. The interspecies characterization of the TMJ disc presented in this thesis (Chapter 2),

was the first study to concurrently examine regional biochemical and biomechanical properties across a variety of species. Regional and interspecies variations were identified in all parameters measured, and certain disc characteristics were observed across all species, such as a weak and soft intermediate zone under mediolateral tension. Ultimately, the pig was identified as the most suitable large animal model for human TMJ disc based on numerous biochemical, biomechanical, and morphological similarities. Additionally, the rabbit TMJ disc was also similar to the human in many aspects, indicating that if large animal studies are cost-prohibitive, rabbits may be used as a small animal model for TMJ tissue engineering.

In Chapter 3 more extensive characterization of the pig TMJ was carried out to begin to understand the TMJ disc attachments and their relationship to the disc. Discal attachments were known to be extremely important for the coordinated movements of the disc within the joint during mastication,[14, 110] but little was known about their composition. This chapter provided the first quantitative characterization of the TMJ disc attachments. Biochemical analysis of the attachments showed that while the biochemical constituents of the disc and attachments are similar, the ratios of each component vary regionally in both tissues. Overall, the attachments were found to have higher cellularity and lower total collagen and sulfated GAG content than the disc. Because of the biochemical similarities between disc and attachment, it is plausible that tissue engineering efforts could use one cell type to engineer the entire disc-attachment complex. These observations will help future tissue engineering efforts create

and attach a disc-attachment complex that may be able to replace damaged or diseased tissues.

The contribution of collagen to the mechanical properties of the TMJ disc has been well described,[25, 34, 83, 94] but little was known about the contribution of GAGs. Elucidating these structure-function relationships within the TMJ disc will identify the most important aspects to engineer into a replacement disc. To this end, Chapter 4 investigated the viscoelastic effects of removing sulfated GAGs from the disc. While it was known from the studies carried out in Chapters 2 and 3 that sulfated GAGs do not comprise a large fraction of the TMJ disc extracellular matrix, removing these molecules from the tissue still affected TMJ disc viscoelastic compressive properties. The relaxation modulus and viscosity were both shown to decrease in regions of the intermediate zone following GAG removal. However, the bands of the disc, which have the least native GAG content were found to be the stiffest under compression and were unaffected by GAG depletion. Because sulfated GAG chains are often associated with enhanced compressive properties in GAG-rich tissues such as hyaline cartilage, these results may seem counterintuitive. However, the highly organized, anisotropic nature of the collagen fraction in TMJ disc tissue may be responsible for this difference. These results, therefore, were the first to indicate that sulfated GAGs contribute substantially to the compressive properties of the TMJ disc, but only in certain regions. This is in stark contrast to other articulating cartilages such as hyaline cartilage, and highlights the unique structure-function relationships within the fibrocartilaginous TMJ disc.

The use of human embryonic stem cells in TMJ disc tissue engineering is an exciting prospect, given the unlimited proliferative capacity and pluripotency of these cells. Various methods to direct fibrochondrogenic differentiation, purify, and expand these cells were evaluated in Chapters 6, 7, and 8. The work completed in these chapters applies state-of-the-art technologies to achieve a high yield of homogeneous cells for use in TMJ tissue engineering, and gives convincing evidence that these cells are not only promising, but can produce tissues similar to the tissues characterized in chapters 2 through 4.

Prior work investigating the chondrogenesis of adult and embryonic stem cells had shown that both growth factors[258, 259, 262, 264] and co-cultures[265, 266] could be useful. Investigating use of growth factor combinations and co-cultures to fibrochondrogenically differentiate hESCs, Chapter 6 found both of these stimuli to be beneficial for increased cartilage-like ECM. In this study, the use of TGF-β and BMP-4 was found to be most effective at increasing total collagen and GAG synthesis by differentiating hESCs. In contrast, co-culturing the hESCs with primary fibrochondrocytes did not increase total matrix production, but did cause an increase in collagen II production relative to collagen type I. Growth factors and trophic factors from co-cultures were therefore found to be useful for fibrochondrogenesis using hESCs, though they produced distinct effects on differentiation.

Cell populations resulting from embryoid body (EB) differentiation as used in Chapter 6 are known to be heterogeneous.[309] Prior attempts to purify cells from EBs have used expensive and time consuming methods such as

fluorescence activated cell sorting and magnetic cell sorting.[326, 327] To improve the homogeneity of these differentiated cells, an inexpensive density gradient was evaluated in Chapter 7 to isolate the most chondrocyte-like cells. The mechanical properties of single cells from each density range were measured and compared to un-differentiated hESCs, mesenchymal stem cells, and chondrocytes. The results of this study showed mesenchymal stem cells were stiffer than hESCs, and chondrocytes were stiffer than MSCs. Additionally, two density ranges from hESCs differentiated with TGF-β showed mechanical similarities to chondrocytes. Therefore, phenotypic changes resulting from hESC differentiation were able to be correlated to cellular mechanical properties, and density separation was found to be a useful technique for purifying cells differentiated using EBs.

Tissue engineering efforts often require a large number of cells, and while the methods evaluated in Chapters 6 and 7 are useful for directing cellular differentiation and purification, they do not address the need for a high cell yield. In an effort to achieve high cell yield, as well as directed differentiation and homogeneity, Chapter 8 used a combination of EB differentiation and chondrogenic tuning. Chondrogenic tuning is a novel method of harnessing the simplicity of monolayer expansion to produce a cell population primed for chondrogenesis.[344] In the present work, chondrogenic tuning was able to produce a variety of cell populations, which, when self-assembled into tissue engineered constructs, created a spectrum of fibrocartilaginous tissues. Interestingly, chondrogenically-tuned cells from passages 3 and 4 produced

significantly more GAG and collagen type II than cells immediately following EB differentiation. This expansion method, therefore, was also able to modify the phenotype of these cells with each passage, creating populations suited for regenerating a variety of fibrocartilaginous tissues. This is an exciting result, as it indicates that expansion and phenotypic modification can be achieved simultaneously, eliminating the need for extra cell purification steps and enhancing the yield of usable cells. Using the methods developed in this chapter, researchers may be able to use a single population of differentiated hESCs to engineer the disc-attachment complex characterized in Chapter 3.

Overall, the work presented in this thesis provides a recommended animal model for *in vivo* studies and important design standards for TMJ tissue engineering, as well as methods for using hESCs to engineer replacement fibrocartilaginous tissue. Understanding the basic biochemical and biomechanical properties of the TMJ disc and attachments will undoubtedly advance the field of TMJ tissue engineering, ensuring that functional TMJ replacements can be realized. This thesis also provides guidance in terms of appropriate animal models to use, as evaluation of engineered prototypes will be another critical step toward clinical use. Finally, this work developed several useful methods to harness the differentiation potential of hESCs toward a fibrocartilaginous phenotype, and demonstrated their ability to produce tissues biochemically similar to the TMJ disc. These methods indicate that replacement of TMJ tissues with functional engineered tissues is feasible, and further development could yield a solution for those suffering from disorders of the TMJ.

References

1. Darling, E.M. and K.A. Athanasiou, *Rapid phenotypic changes in passaged articular chondrocyte subpopulations.* J Orthop Res, 2005. **23**(2): p. 425-32.

2. Allen, K.D. and K.A. Athanasiou, *Gene expression changes in passaged cells from TMJ fibrocartilage.* Submitted 2006.

3. French, M.M., et al., *Chondrogenic differentiation of adult dermal fibroblasts.* Ann Biomed Eng, 2004. **32**(1): p. 50-6.

4. Solberg, W.K., M.W. Woo, and J.B. Houston, *Prevalence of mandibular dysfunction in young adults.* J Am Dent Assoc, 1979. **98**(1): p. 25-34.

5. Gray, R.J.M., S.J. Davies, and A.A. Quayle, *Temporomandibular disorders: A clinical approach.* 1995, London: British Dental Association.

6. *TMJ Implants - A Consumer Information Update [FDA Report].* 1999, United States Food and Drug Administration.

7. Farrar, W.B. and W.L. McCarty, Jr., *The TMJ dilemma.* J Ala Dent Assoc, 1979. **63**(1): p. 19-26.

8. Wilkes, C.H., *Internal derangements of the temporomandibular joint. Pathological variations.* Arch Otolaryngol Head Neck Surg, 1989. **115**(4): p. 469-77.

9. LeResche, L., *Epidemiology of temporomandibular disorders: implications for the investigation of etiologic factors.* Crit Rev Oral Biol Med, 1997. **8**(3): p. 291-305.

10. Wong, M.E., K.D. Allen, and K.A. Athanasiou, *Tissue engineering of the temporomandibular joint*, in *Biomedical Engineering Handbook.* In Press, CRC Press.

11. Dimitroulis, G., *The role of surgery in the management of disorders of the temporomandibular joint: a critical review of the literature. Part 2.* Int J Oral Maxillofac Surg, 2005. **34**(3): p. 231-7.

12. Trumpy, I.G., B. Roald, and T. Lyberg, *Morphologic and immunohistochemical observation of explanted Proplast-Teflon temporomandibular joint interpositional implants.* J Oral Maxillofac Surg, 1996. **54**(1): p. 63-8; discussion 68-70.

13. Piette, E., *Anatomy of the human temporomandibular joint. An updated comprehensive review.* Acta Stomatol Belg, 1993. **90**(2): p. 103-27.

14. Rees, L.A., *The Structure and function of the mandibular joint.* Br Dent J, 1954. **96**: p. 125-33.

15. Almarza, A.J. and K.A. Athanasiou, *Design characteristics for the tissue engineering of cartilaginous tissues.* Ann Biomed Eng, 2004. **32**(1): p. 2-17.

16. Detamore, M.S., et al., *Cell type and distribution in the porcine temporomandibular joint disc.* J Oral Maxillofac Surg, 2006. **64**(2): p. 243-8.

17. Nakano, T. and P.G. Scott, *A quantitative chemical study of glycosaminoglycans in the articular disc of the bovine temporomandibular joint.* Arch Oral Biol, 1989. **34**(9): p. 749-57.

18. Milam, S.B., et al., *Characterization of the extracellular matrix of the primate temporomandibular joint.* J Oral Maxillofac Surg, 1991. **49**(4): p. 381-91.

19. Ali, A.M. and M.M. Sharawy, *An immunohistochemical study of collagen types III, VI and IX in rabbit craniomandibular joint tissues following surgical induction of anterior disk displacement.* J Oral Pathol Med, 1996. **25**(2): p. 78-85.

20. Minarelli, A.M. and E.A. Liberti, *A microscopic survey of the human temporomandibular joint disc.* J Oral Rehabil, 1997. **24**(11): p. 835-40.

21.   Gage, J.P., et al., *Presence of type III collagen in disc attachments of human temporomandibular joints.* Arch Oral Biol, 1990. **35**(4): p. 283-8.

22.   Gage, J.P., R.M. Shaw, and F.B. Moloney, *Collagen type in dysfunctional temporomandibular joint disks.* J Prosthet Dent, 1995. **74**(5): p. 517-20.

23.   Landesberg, R., E. Takeuchi, and J.E. Puzas, *Cellular, biochemical and molecular characterization of the bovine temporomandibular joint disc.* Arch Oral Biol, 1996. **41**(8-9): p. 761-7.

24.   Minarelli, A.M., M. Del Santo Junior, and E.A. Liberti, *The structure of the human temporomandibular joint disc: a scanning electron microscopy study.* J Orofac Pain, 1997. **11**(2): p. 95-100.

25.   Detamore, M.S., et al., *Quantitative analysis and comparative regional investigation of the extracellular matrix of the porcine temporomandibular joint disc.* Matrix Biol, 2005. **24**(1): p. 45-57.

26.   Mills, D.K., D.J. Fiandaca, and R.P. Scapino, *Morphologic, microscopic, and immunohistochemical investigations into the function of the primate TMJ disc.* J Orofac Pain, 1994. **8**(2): p. 136-54.

27.   O'Dell, N.L., et al., *Morphological and biochemical evidence for elastic fibres in the Syrian hamster temporomandibular joint disc.* Arch Oral Biol, 1990. **35**(10): p. 807-11.

28.   Axelsson, S., A. Holmlund, and A. Hjerpe, *Glycosaminoglycans in normal and osteoarthrotic human temporomandibular joint disks.* Acta Odontol Scand, 1992. **50**(2): p. 113-9.

29.   Kobayashi, J., *[Studies on matrix components relevant to structure and function of the temporomandibular joint].* Kokubyo Gakkai Zasshi, 1992. **59**(1): p. 105-23.

30.   Sindelar, B.J., et al., *Effects of intraoral splint wear on proteoglycans in the temporomandibular joint disc.* Arch Biochem Biophys, 2000. **379**(1): p. 64-70.

31.   Nakano, T. and P.G. Scott, *Changes in the chemical composition of the bovine temporomandibular joint disc with age.* Arch Oral Biol, 1996. **41**(8-9): p. 845-53.

32.   Scott, P.G., T. Nakano, and C.M. Dodd, *Small proteoglycans from different regions of the fibrocartilaginous temporomandibular joint disc.* Biochim Biophys Acta, 1995. **1244**(1): p. 121-8.

33.   Beatty, M.W., et al., *Strain rate dependent orthotropic properties of pristine and impulsively loaded porcine temporomandibular joint disk.* J Biomed Mater Res, 2001. **57**(1): p. 25-34.

34.   Detamore, M.S. and K.A. Athanasiou, *Tensile properties of the porcine temporomandibular joint disc.* J Biomech Eng, 2003. **125**(4): p. 558-65.

35.   Tanne, K., E. Tanaka, and M. Sakuda, *The elastic modulus of the temporomandibular joint disc from adult dogs.* J Dent Res, 1991. **70**(12): p. 1545-8.

36.   Chin, L.P., F.D. Aker, and K. Zarrinnia, *The viscoelastic properties of the human temporomandibular joint disc.* J Oral Maxillofac Surg, 1996. **54**(3): p. 315-8; discussion 318-9.

37.   Mow, V.C., et al., *Biphasic creep and stress relaxation of articular cartilage in compression? Theory and experiments.* J Biomech Eng, 1980. **102**(1): p. 73-84.

38.   Kim, K.W., et al., *Biomechanical tissue characterization of the superior joint space of the porcine temporomandibular joint.* Ann Biomed Eng, 2003. **31**(8): p. 924-30.

39.   Allen, K.D. and K.A. Athanasiou, *A surface-regional and freeze-thaw characterization of the porcine temporomandibular joint disc.* Ann Biomed Eng, 2005. **33**(7): p. 951-62.

40.   Tanaka, E., et al., *Shear properties of the temporomandibular joint disc in relation to compressive and shear strain.* J Dent Res, 2004. **83**(6): p. 476-9.

41. Thomas, M., D. Grande, and R.H. Haug, *Development of an in vitro temporomandibular joint cartilage analog.* J Oral Maxillofac Surg, 1991. **49**(8): p. 854-6; discussion 857.

42. Puelacher, W.C., et al., *Temporomandibular joint disc replacement made by tissue-engineered growth of cartilage.* J Oral Maxillofac Surg, 1994. **52**(11): p. 1172-7; discussion 1177-8.

43. Springer, I.N., et al., *Culture of cells gained from temporomandibular joint cartilage on non-absorbable scaffolds.* Biomaterials, 2001. **22**(18): p. 2569-77.

44. Almarza, A.J. and K.A. Athanasiou, *Effects of initial cell seeding density for the tissue engineering of the temporomandibular joint disc.* Ann Biomec Eng, 2005. **33**(7): p. 943-950.

45. Almarza, A.J. and K.A. Athanasiou, *Evaluation of three growth factors in combinations of two for temporomandibular joint disc tissue engineering.* Arch Oral Biol, 2006. **51**(3): p. 215-21.

46. Bean, A.C., A.J. Almarza, and K.A. Athanasiou, *Effects of ascorbic acid concentration for the tissue engineering of the temporomandibular joint disc.* J Eng Med, Accepted November 2005.

47. Detamore, M.S. and K.A. Athanasiou, *Effects of growth factors on temporomandibular joint disc cells.* Arch Oral Biol, 2004. **49**(7): p. 577-83.

48. Detamore, M.S. and K.A. Athanasiou, *Evaluation of three growth factors for TMJ disc tissue engineering.* Ann Biomed Eng, 2005. **33**(3): p. 383-90.

49. Allen, K.D. and K.A. Athanasiou. *Comparison of scaffolding biomaterials for TMJ disc tissue engineering.* in *Biomedical Engineering Society Annual Conference.* 2005. Baltimore, MD.

50. Poshusta, A.K. and K.S. Anseth, *Photopolymerized biomaterials for application in the temporomandibular joint.* Cells Tissues Organs, 2001. **169**(3): p. 272-8.

51.	Almarza, A.J. and K.A. Athanasiou, *Seeding techniques and scaffolding choice for tissue engineering of the temporomandibular joint disk.* Tissue Eng, 2004. **10**(11-12): p. 1787-95.

52.	Almarza, A.J. and K.A. Athanasiou, *Effects of hydrostatic pressure on TMJ disc cells.* Tissue Eng, Accepted August 2005.

53.	Girdler, N.M., *In vitro synthesis and characterization of a cartilaginous meniscus grown from isolated temporomandibular chondroprogenitor cells.* Scand J Rheumatol, 1998. **27**(6): p. 446-53.

54.	Tanaka, E., et al., *Dynamic shear properties of the temporomandibular joint disc.* J Dent Res, 2003. **82**(3): p. 228-31.

55.	Darling, E.M. and K.A. Athanasiou, *Biomechanical strategies for articular cartilage regeneration.* Ann Biomed Eng, 2003. **31**(9): p. 1114-24.

56.	Detamore, M.S. and K.A. Athanasiou, *Use of a rotating bioreactor toward tissue engineering the temporomandibular joint disc.* Tissue Eng, 2005. **11**(7-8): p. 1188-97.

57.	Deschner, J., B. Rath-Deschner, and S. Agarwal, *Regulation of matrix metalloproteinase expression by dynamic tensile strain in rat fibrochondrocytes.* Osteoarthritis Cartilage, 2005.

58.	Calve, S., et al., *Engineering of functional tendon.* Tissue Eng, 2004. **10**(5-6): p. 755-61.

59.	Hu, J.C. and K.A. Athanasiou, *A self-assembing process in articular cartilage tissue-engineering.* Tissue Eng, March 2006.

60.	Mauck, R.L., X. Yuan, and R.S. Tuan, *Chondrogenic differentiation and functional maturation of bovine mesenchymal stem cells in long-term agarose culture.* Osteoarthritis Cartilage, 2005.

61.	Wayne, J.S., et al., *In vivo response of polylactic acid-alginate scaffolds and bone marrow-derived cells for cartilage tissue engineering.* Tissue Eng, 2005. **11**(5-6): p. 953-63.

62.   Wang, Y., et al., *In vitro cartilage tissue engineering with 3D porous aqueous-derived silk scaffolds and mesenchymal stem cells.* Biomaterials, 2005. **26**(34): p. 7082-94.

63.   Tanaka, H., et al., *Chondrogenic differentiation of murine embryonic stem cells: effects of culture conditions and dexamethasone.* J Cell Biochem, 2004. **93**(3): p. 454-62.

64.   Li, W.J., et al., *A three-dimensional nanofibrous scaffold for cartilage tissue engineering using human mesenchymal stem cells.* Biomaterials, 2005. **26**(6): p. 599-609.

65.   Funakoshi, T., et al., *Application of tissue engineering techniques for rotator cuff regeneration using a chitosan-based hyaluronan hybrid fiber scaffold.* Am J Sports Med, 2005. **33**(8): p. 1193-201.

66.   Awad, H.A., et al., *Autologous mesenchymal stem cell-mediated repair of tendon.* Tissue Eng, 1999. **5**(3): p. 267-77.

67.   Juncosa-Melvin, N., et al., *Effects of cell-to-collagen ratio in mesenchymal stem cell-seeded implants on tendon repair biomechanics and histology.* Tissue Eng, 2005. **11**(3-4): p. 448-57.

68.   Moreau, J.E., et al., *Growth factor induced fibroblast differentiation from human bone marrow stromal cells in vitro.* J Orthop Res, 2005. **23**(1): p. 164-74.

69.   Altman, G.H., et al., *Cell differentiation by mechanical stress.* Faseb J, 2002. **16**(2): p. 270-2.

70.   Hankemeier, S., et al., *Modulation of proliferation and differentiation of human bone marrow stromal cells by fibroblast growth factor 2: potential implications for tissue engineering of tendons and ligaments.* Tissue Eng, 2005. **11**(1-2): p. 41-9.

71.   Mao, J.J. and H.D. Nah, *Growth and development: hereditary and mechanical modulations.* Am J Orthod Dentofacial Orthop, 2004. **125**(6): p. 676-89.

72. Aufderheide, A.C. and K.A. Athanasiou, *A direct compression stimulator for articular cartilage and meniscal explants.* Annals of Biomedical Engineering, Submitted 2005.

73. Davisson, T., R.L. Sah, and A. Ratcliffe, *Perfusion increases cell content and matrix synthesis in chondrocyte three-dimensional cultures.* Tissue Eng, 2002. **8**(5): p. 807-16.

74. Tanaka, E. and T. van Eijden, *Biomechanical behavior of the temporomandibular joint disc.* Crit Rev Oral Biol Med, 2003. **14**(2): p. 138-50.

75. Reston, J.T. and C.M. Turkelson, *Meta-analysis of surgical treatments for temporomandibular articular disorders.* J Oral Maxillofac Surg, 2003. **61**(1): p. 3-10; discussion 10-2.

76. Wong, M.E., K.D. Allen, and K.A. Athanasiou, *Tissue engineering of the temporomandibular joint.* , in *Biomedical engineering handbook.* 2006, CRC Press: Boca Raton. p. 52-1–52-22.

77. Estabrooks, L.N., et al., *A retrospective evaluation of 301 TMJ Proplast-Teflon implants.* Oral Surg Oral Med Oral Pathol, 1990. **70**(3): p. 381-6.

78. Henry, C.H. and L.M. Wolford, *Treatment outcomes for temporomandibular joint reconstruction after Proplast-Teflon implant failure.* J Oral Maxillofac Surg, 1993. **51**(4): p. 352-8; discussion 359-60.

79. Detamore, M.S. and K.A. Athanasiou, *Structure and function of the temporomandibular joint disc: implications for tissue engineering.* J Oral Maxillofac Surg, 2003. **61**(4): p. 494-506.

80. Detamore, M.S., K.A. Athanasiou, and J. Mao, *A call to action for bioengineers and dental professionals: directives for the future of TMJ bioengineering.* Ann Biomed Eng, 2007. **35**(8): p. 1301-11.

81. Almarza, A.J., et al., *Biochemical analysis of the porcine temporomandibular joint disc.* Br J Oral Maxillofac Surg, 2006. **44**(2): p. 124-8.

82.   Allen, K.D. and K.A. Athanasiou, *Tissue engineering of the TMJ disc: a review.* Tissue Eng, 2006. **12**(5): p. 1183-96.

83.   Shengyi, T. and Y. Xu, *Biomechanical properties and collagen fiber orientation of TMJ discs in dogs: Part 1. Gross anatomy and collagen fiber orientation of the discs.* J Craniomandib Disord, 1991. **5**(1): p. 28-34.

84.   del Pozo, R., et al., *The regional difference of viscoelastic property of bovine temporomandibular joint disc in compressive stress-relaxation.* Med Eng Phys, 2002. **24**(3): p. 165-71.

85.   Allen, K.D. and K.A. Athanasiou, *Viscoelastic characterization of the porcine temporomandibular joint disc under unconfined compression.* J Biomech, 2006. **39**(2): p. 312-22.

86.   Berg, R., *Contribution to the applied and topographical anatomy of the temporomandibular joint of some domestic mammals with particular reference to the partial resp. total resection of the articular disc.* Folia Morphol (Praha), 1973. **21**(2): p. 202-4.

87.   Strom, D., et al., *Gross anatomy of the mandibular joint and masticatory muscles in the domestic pig (Sus scrofa).* Arch Oral Biol, 1986. **31**(11): p. 763-8.

88.   Bermejo, A., O. Gonzalez, and J.M. Gonzalez, *The pig as an animal model for experimentation on the temporomandibular articular complex.* Oral Surg Oral Med Oral Pathol, 1993. **75**(1): p. 18-23.

89.   Hatton, M.N. and D.A. Swann, *Studies on bovine temporomandibular joint synovial fluid.* J Prosthet Dent, 1986. **56**(5): p. 635-8.

90.   Tanaka, E., et al., *Age-associated changes in viscoelastic properties of the bovine temporomandibular joint disc.* Eur J Oral Sci, 2006. **114**(1): p. 70-3.

91.   Tanaka, E., et al., *Viscoelastic properties of canine temporomandibular joint disc in compressive load-relaxation.* Arch Oral Biol, 1999. **44**(12): p. 1021-6.

92.   Bifano, C., G. Hubbard, and W. Ehler, *A comparison of the form and function of the human, monkey, and goat temporomandibular joint.* J Oral Maxillofac Surg, 1994. **52**(3): p. 272-5; discussion 276-7.

93.   Kurita, K., et al., *High condylar shave of the temporomandibular joint with preservation of the articular soft tissue cover: an experimental study on rabbits.* Oral Surg Oral Med Oral Pathol, 1990. **69**(1): p. 10-4.

94.   Scapino, R.P., et al., *The behaviour of collagen fibres in stress relaxation and stress distribution in the jaw-joint disc of rabbits.* Arch Oral Biol, 1996. **41**(11): p. 1039-52.

95.   Deschner, J., et al., *Regulatory effects of biophysical strain on rat TMJ discs.* Ann Anat, 2007. **189**(4): p. 326-8.

96.   Bosanquet, A.G. and A.N. Goss, *The sheep as a model for temporomandibular joint surgery.* Int J Oral Maxillofac Surg, 1987. **16**(5): p. 600-3.

97.   Herring, S.W., *TMJ anatomy and animal models.* J Musculoskelet Neuronal Interact, 2003. **3**(4): p. 391-4; discussion 406-7.

98.   Tanaka, E., M.S. Detamore, and L.G. Mercuri, *Degenerative disorders of the temporomandibular joint: etiology, diagnosis, and treatment.* J Dent Res, 2008. **87**(4): p. 296-307.

99.   Rees, L.A., *The structure and function of the mandibular joint.* Br Dent J, 1954. **96**(6): p. 125-33.

100.   Mizoguchi, I., et al., *An immunohistochemical study of the localization of biglycan, decorin and large chondroitin-sulphate proteoglycan in adult rat temporomandibular joint disc.* Arch Oral Biol, 1998. **43**(11): p. 889-98.

101.   Scapino, R.P., A. Obrez, and D. Greising, *Organization and function of the collagen fiber system in the human temporomandibular joint disk and its attachments.* Cells Tissues Organs, 2006. **182**(3-4): p. 201-25.

102. Clement, C., et al., *Quantitative analysis of the elastic fibres in the human temporomandibular articular disc and its attachments.* Int J Oral Maxillofac Surg, 2006. **35**(12): p. 1120-6.

103. Benigno, M.I., et al., *The structure of the bilaminar zone in the human temporomandibular joint: a light and scanning electron microscopy study in young and elderly subjects.* J Oral Rehabil, 2001. **28**(2): p. 113-9.

104. Kopp, S., *Topographical distribution of sulphated glycosaminoglycans in human temporomandibular joint disks. A histochemical study of an autopsy material.* J Oral Pathol, 1976. **5**(5): p. 265-76.

105. Paegle, D.I., A.B. Holmlund, and F.P. Reinholt, *Characterization of tissue components in the temporomandibular joint disc and posterior disc attachment region: internal derangement and control autopsy specimens compared by morphometry.* J Oral Maxillofac Surg, 2002. **60**(9): p. 1032-7.

106. Kalpakci, K.N., et al., *An interspecies comparison of the temporomandibular joint disc.* J Dent Res, 2011. **90**(2): p. 193-8.

107. Shortkroff, S. and M. Spector, *Isolation and in vitro proliferation of chondrocytes, tenocytes, and ligament cells.* Methods Mol Med, 1999. **18**: p. 195-203.

108. Scapino, R.P., *The posterior attachment: its structure, function, and appearance in TMJ imaging studies. Part 1.* J Craniomandib Disord, 1991. **5**(2): p. 83-95.

109. Scapino, R.P., *The posterior attachment: its structure, function, and appearance in TMJ imaging studies. Part 2.* J Craniomandib Disord, 1991. **5**(3): p. 155-66.

110. Westesson, P.L., et al., *Cryosectional observations of functional anatomy of the temporomandibular joint.* Oral Surg Oral Med Oral Pathol, 1989. **68**(3): p. 247-51.

111. Swartz, M.A. and M.E. Fleury, *Interstitial flow and its effects in soft tissues.* Annu Rev Biomed Eng, 2007. **9**: p. 229-56.

112. Li, K.W., et al., *Gene regulation ex vivo within a wrap-around tendon.* Tissue Eng, 2006. **12**(9): p. 2611-8.

113. Spalazzi, J.P., et al., *Mechanoactive scaffold induces tendon remodeling and expression of fibrocartilage markers.* Clin Orthop Relat Res, 2008. **466**(8): p. 1938-48.

114. Benjamin, M. and J.R. Ralphs, *Fibrocartilage in tendons and ligaments--an adaptation to compressive load.* J Anat, 1998. **193 (Pt 4)**: p. 481-94.

115. Vanderploeg, E.J., et al., *Oscillatory tension differentially modulates matrix metabolism and cytoskeletal organization in chondrocytes and fibrochondrocytes.* J Biomech, 2004. **37**(12): p. 1941-52.

116. Gillbe, G.V., *The function of the disc of the temporomandibular joint.* J Prosthet Dent, 1975. **33**(2): p. 196-204.

117. Basalo, I.M., et al., *Cartilage interstitial fluid load support in unconfined compression following enzymatic digestion.* J Biomech Eng, 2004. **126**(6): p. 779-86.

118. Derby, M.A. and J.E. Pintar, *The histochemical specificity of Streptomyces hyaluronidase and chondroitinase ABC.* Histochem J, 1978. **10**(5): p. 529-47.

119. Katta, J., et al., *The effect of glycosaminoglycan depletion on the friction and deformation of articular cartilage.* Proc Inst Mech Eng H, 2008. **222**(1): p. 1-11.

120. Korhonen, R.K., et al., *Fibril reinforced poroelastic model predicts specifically mechanical behavior of normal, proteoglycan depleted and collagen degraded articular cartilage.* J Biomech, 2003. **36**(9): p. 1373-9.

121. Henninger, H.B., et al., *Effect of sulfated glycosaminoglycan digestion on the transverse permeability of medial collateral ligament.* J Biomech, 2010. **43**(13): p. 2567-73.

122. Ruhland, C., et al., *The glycosaminoglycan chain of decorin plays an important role in collagen fibril formation at the early stages of fibrillogenesis.* FEBS J, 2007. **274**(16): p. 4246-55.

123. Danielson, K.G., et al., *Targeted disruption of decorin leads to abnormal collagen fibril morphology and skin fragility.* J Cell Biol, 1997. **136**(3): p. 729-43.

124. Corsi, A., et al., *Phenotypic effects of biglycan deficiency are linked to collagen fibril abnormalities, are synergized by decorin deficiency, and mimic Ehlers-Danlos-like changes in bone and other connective tissues.* J Bone Miner Res, 2002. **17**(7): p. 1180-9.

125. Dolwick, M.F., *The temporomandibular joint: normal and abnormal anatomy*, in *Internal Derangements of the Temporomandibular Joint*, C.A. Helms, R.W. Katzberg, and M.F. Dolwick, Editors. 1983, Radiology Research and Education Foundation: San Francisco, CA. p. 1-14.

126. Wong, M.E., K.D. Allen, and K.A. Athanasiou, *Tissue Engineering of the Temporomandibular Joint*, in *Tissue Engineering and Artificial Organs*, B.J. K., Editor. 2006, CRC Press: Boca Raton, FL.

127. Werner, J.A., B. Tillmann, and A. Schleicher, *Functional anatomy of the temporomandibular joint. A morphologic study on human autopsy material.* Anat Embryol, 1991. **183**(1): p. 89-95.

128. Jagger, R.G., J.F. Bates, and S. Kopp, *Temporomandibular Joint Dysfunction: Essentials.* 1994, Oxford: Butterworth-Heinemann Ltd.

129. Gallo, L.M., et al., *Stress-field translation in the healthy human temporomandibular joint.* J Dent Res, 2000. **79**(10): p. 1740-6.

130. Detamore, M.S. and K.A. Athanasiou, *Motivation, characterization, and strategy for tissue engineering the temporomandibular joint disc.* Tissue Eng, 2003. **9**(6): p. 1065-87.

131. Mabuchi, K., et al., *The effect of additive hyaluronic acid on animal joints with experimentally reduced lubricating ability.* J Biomed Mater Res, 1994. **28**(8): p. 865-70.

132. Athanasiou, K.A., et al., *Tissue engineering of temporomandibular joint cartilage*. 2009: Morgan & Claypool.

133. Berkovitz, B.K. and H. Robertshaw, *Ultrastructural quantification of collagen in the articular disc of the temporomandibular joint of the rabbit.* Arch Oral Biol, 1993. **38**(1): p. 91-5.

134. Carvalho, R.S., E.H. Yen, and D.M. Suga, *The effect of growth on collagen and glycosaminoglycans in the articular disc of the rat temporomandibular joint.* Arch Oral Biol, 1993. **38**(6): p. 457-66.

135. Taguchi, N., S. Nakata, and T. Oka, *Three-dimensional observation of the temporomandibular joint disk in the rhesus monkey.* J Oral Surg, 1980. **38**(1): p. 11-5.

136. Berkovitz, B.K., *Crimping of collagen in the intra-articular disc of the temporomandibular joint: a comparative study.* J Oral Rehabil, 2000. **27**(7): p. 608-13.

137. Chin, L.P., F.D. Aker, and K. Zarrinnia, *The viscoelastic properties of the human temporomandibular joint disc.* J Oral Maxillofac Surg, 1996. **54**(3): p. 315-8.

138. Wang, L. and M.S. Detamore, *Tissue engineering the mandibular condyle.* Tissue Eng, 2007. **13**(8): p. 1955-71.

139. Singh, M. and M.S. Detamore, *Biomechanical properties of the mandibular condylar cartilage and their relevance to the TMJ disc.* J Biomech, 2009. **42**(4): p. 405-17.

140. Mizuno, I., et al., *The fine structure of the fibrous zone of articular cartilage in the rat mandibular condyle.* Shika Kiso Igakkai Zasshi, 1990. **32**(1): p. 69-79.

141. Appleton, J., *The ultrastructure of the articular tissue of the mandibular condyle in the rat.* Arch Oral Biol, 1975. **20**(12): p. 823-6.

142.   Copray, J.C. and R.S. Liem, *Ultrastructural changes associated with weaning in the mandibular condyle of the rat.* Acta Anat (Basel), 1989. **134**(1): p. 35-47.

143.   Silva, D.G. and J.A. Hart, *Ultrastructural observations on the mandibular condyle of the guinea pig.* J Ultrastruct Res, 1967. **20**(3): p. 227-43.

144.   Bibb, C.A., A.G. Pullinger, and F. Baldioceda, *The relationship of undifferentiated mesenchymal cells to TMJ articular tissue thickness.* J Dent Res, 1992. **71**(11): p. 1816-21.

145.   Bibb, C.A., A.G. Pullinger, and F. Baldioceda, *Serial variation in histological character of articular soft tissue in young human adult temporomandibular joint condyles.* Arch Oral Biol, 1993. **38**(4): p. 343-52.

146.   Blackwood, H.J., *Growth of the mandibular condyle of the rat studied with tritiated thymidine.* Arch Oral Biol, 1966. **11**(5): p. 493-500.

147.   Klinge, R.F., *The structure of the mandibular condyle in the monkey (Macaca mulatta).* Micron, 1996. **27**(5): p. 381-7.

148.   Pietila, K., et al., *Comparison of amounts and properties of collagen and proteoglycans in condylar, costal and nasal cartilages.* Cells Tissues Organs, 1999. **164**(1): p. 30-6.

149.   Delatte, M., et al., *Primary and secondary cartilages of the neonatal rat: the femoral head and the mandibular condyle.* Eur J Oral Sci, 2004. **112**(2): p. 156-62.

150.   Mizoguchi, I., et al., *An immunohistochemical study of regional differences in the distribution of type I and type II collagens in rat mandibular condylar cartilage.* Arch Oral Biol, 1996. **41**(8-9): p. 863-9.

151.   Teramoto, M., et al., *Effect of compressive forces on extracellular matrix in rat mandibular condylar cartilage.* J Bone Miner Metab, 2003. **21**(5): p. 276-86.

152. de Bont, L.G., et al., *Spatial arrangement of collagen fibrils in the articular cartilage of the mandibular condyle: a light microscopic and scanning electron microscopic study.* J Oral Maxillofac Surg, 1984. **42**(5): p. 306-13.

153. Luder, H.U. and H.E. Schroeder, *Light and electron microscopic morphology of the temporomandibular joint in growing and mature crab-eating monkeys (Macaca fascicularis): the condylar articular layer.* Anat Embryol (Berl), 1990. **181**(5): p. 499-511.

154. Singh, M. and M.S. Detamore, *Tensile properties of the mandibular condylar cartilage.* J Biomech Eng, 2008. **130**(1): p. 011009.

155. Shibata, S., et al., *Ultrastructural observation on matrix fibers in the condylar cartilage of the adult rat mandible.* Bull Tokyo Med Dent Univ, 1991. **38**(4): p. 53-61.

156. Mao, J.J., F. Rahemtulla, and P.G. Scott, *Proteoglycan expression in the rat temporomandibular joint in response to unilateral bite raise.* J Dent Res, 1998. **77**(7): p. 1520-8.

157. Roth, S., et al., *Specific properties of the extracellular chondroitin sulphate proteoglycans in the mandibular condylar growth centre in pigs.* Arch Oral Biol, 1997. **42**(1): p. 63-76.

158. Kantomaa, T. and P. Pirttiniemi, *Changes in proteoglycan and collagen content in the mandibular condylar cartilage of the rabbit caused by an altered relationship between the condyle and glenoid fossa.* Eur J Orthod, 1998. **20**(4): p. 435-41.

159. Del Santo, M., Jr., et al., *Age-associated changes in decorin in rat mandibular condylar cartilage.* Arch Oral Biol, 2000. **45**(6): p. 485-93.

160. Kang, H., et al., *[Tensile mechanics of mandibular condylar cartilage].* Hua Xi Kou Qiang Yi Xue Za Zhi, 2000. **18**(2): p. 85-7.

161. Tanaka, E., et al., *Dynamic shear behavior of mandibular condylar cartilage is dependent on testing direction.* J Biomech, 2008. **41**(5): p. 1119-23.

162. Tanaka, E., et al., *Biomechanical response of condylar cartilage-on-bone to dynamic shear.* J Biomed Mater Res A, 2008. **85**(1): p. 127-32.

163. Tanaka, E., et al., *Dynamic compressive properties of the mandibular condylar cartilage.* J Dent Res, 2006. **85**(6): p. 571-5.

164. Hu, K., et al., *Regional structural and viscoelastic properties of fibrocartilage upon dynamic nanoindentation of the articular condyle.* J Struct Biol, 2001. **136**(1): p. 46-52.

165. Kuboki, T., et al., *Viscoelastic properties of the pig temporomandibular joint articular soft tissues of the condyle and disc.* J Dent Res, 1997. **76**(11): p. 1760-9.

166. Singh, M. and M.S. Detamore, *Stress relaxation behavior of mandibular condylar cartilage under high-strain compression.* J Biomech Eng, 2009. **131**(6): p. 061008.

167. Webster, T.J., *Nanophase ceramics: The future orthopedic and dental implant material,* in *Advances in chemical engineering,* J.Y. Ying, Editor. 2001, Academic Press. p. 125-166.

168. Zhang, L. and T.J. Webster, *Nanotechnology and nanomaterials: Promises for improved tissue regeneration.* Nanotoday 2009. **4**(1): p. 66-80.

169. Kaplan, F.S., et al., *Form and function of bone,* in *Orthopaedic basic science,* S.P. Simon, Editor. 1994, American Academy of Orthopaedic Surgeons. p. 127-185.

170. Giesen, E.B., et al., *Changed morphology and mechanical properties of cancellous bone in the mandibular condyles of edentate people.* J Dent Res, 2004. **83**(3): p. 255-9.

171. Giesen, E.B., et al., *Mechanical properties of cancellous bone in the human mandibular condyle are anisotropic.* J Biomech, 2001. **34**(6): p. 799-803.

172. Schwartz-Dabney, C.L. and P.C. Dechow, *Variations in cortical material properties throughout the human dentate mandible.* Am J Phys Anthropol, 2003. **120**(3): p. 252-77.

173. Nomura, T., et al., *Micromechanics/structure relationships in the human mandible.* Dent Mater, 2003. **19**(3): p. 167-73.

174. van Ruijven, L.J., et al., *Prediction of mechanical properties of the cancellous bone of the mandibular condyle.* J Dent Res, 2003. **82**(10): p. 819-23.

175. Solberg, W.K., *Epidemiology, incidence and prevalence of temporomandibular disorders: a review,* in *Diagnosis and Management of Temporomandibular Disorders,* D. Laskin, et al., Editors. 1983, American Dental Association: Chicago, IL. p. 30-39.

176. Milam, S.B. and J.P. Schmitz, *Molecular biology of temporomandibular joint disorders: proposed mechanisms of disease.* J Oral Maxillofac Surg, 1995. **53**(12): p. 1448-54.

177. Zarb, G.A. and G.E. Carlsson, *Temporomandibular disorders: osteoarthritis.* J Orofac Pain, 1999. **13**(4): p. 295-306.

178. Hinton, R., et al., *Osteoarthritis: diagnosis and therapeutic considerations.* Am Fam Physician, 2002. **65**(5): p. 841-8.

179. Tanaka, E., et al., *Vascular endothelial growth factor plays an important autocrine/paracrine role in the progression of osteoarthritis.* Histochem Cell Biol, 2005. **123**(3): p. 275-81.

180. Vasconcelos, B.C., et al., *Surgical treatment of temporomandibular joint ankylosis: follow-up of 15 cases and literature review.* Med Oral Patol Oral Cir Bucal, 2009. **14**(1): p. E34-8.

181. Forssell, H. and E. Kalso, *Application of principles of evidence-based medicine to occlusal treatment for temporomandibular disorders: are there lessons to be learned?* J Orofac Pain, 2004. **18**(1): p. 9-22; discussion 23-32.

182. Nicolakis, P., et al., *An investigation of the effectiveness of exercise and manual therapy in treating symptoms of TMJ osteoarthritis.* Cranio, 2001. **19**(1): p. 26-32.

183. Toller, P.A., *Use and misuse of intra-articular corticosteroids in treatment of temporomandibular joint pain.* Proc R Soc Med, 1977. **70**(7): p. 461-3.

184. Shi, Z.D., et al., *[Comparative study on effects of sodium hyaluronate and prednisolone injections on experimental temporomandibular joint osteoarthritis of rabbits].* Zhongguo Xiu Fu Chong Jian Wai Ke Za Zhi, 2002. **16**(1): p. 5-10.

185. Holmlund, A., G. Hellsing, and T. Wredmark, *Arthroscopy of the temporomandibular joint. A clinical study.* Int J Oral Maxillofac Surg, 1986. **15**(6): p. 715-21.

186. Mercuri, L.G., *Surgical management of TMJ arthritis* in *TMDs, an evidence-based approach to diagnosis and treatment*, G.C.S. Laskin D. M., Hylander W. L., Editor. 2006, Quintessence: Chicago. p. 455-468.

187. Feinberg, S.E. and P.E. Larsen, *The use of a pedicled temporalis muscle-pericranial flap for replacement of the TMJ disc: preliminary report.* J Oral Maxillofac Surg, 1989. **47**(2): p. 142-6.

188. Wolford, L.M., O. Reiche-Fischel, and P. Mehra, *Changes in temporomandibular joint dysfunction after orthognathic surgery.* J Oral Maxillofac Surg, 2003. **61**(6): p. 655-60; discussion 661.

189. Trumpy, I.G. and T. Lyberg, *In vivo deterioration of proplast-teflon temporomandibular joint interpositional implants: a scanning electron microscopic and energy- dispersive X-ray analysis.* J Oral Maxillofac Surg, 1993. **51**(6): p. 624-9.

190. Almarza, A.J. and K.A. Athanasiou, *Effects of initial cell seeding density for the tissue engineering of the temporomandibular joint disc.* Ann Biomed Eng, 2005. **33**(7): p. 943-50.

191. Almarza, A.J. and K.A. Athanasiou, *Effects of hydrostatic pressure on TMJ disc cells.* Tissue Eng, 2006. **12**(5): p. 1285-94.

192. Bean, A.C., A.J. Almarza, and K.A. Athanasiou, *Effects of ascorbic acid concentration on the tissue engineering of the temporomandibular joint disc.* Proc Inst Mech Eng [H], 2006. **220**(3): p. 439-47.

193. Allen, K.D. and K.A. Athanasiou, *Scaffold and growth factor selection in temporomandibular joint disc engineering.* J Dent Res, 2008. **87**(2): p. 180-5.

194. Johns, D.E. and K.A. Athanasiou, *Improving culture conditions for temporomandibular joint disc tissue engineering.* Cells Tissues Organs, 2007. **185**(4): p. 246-57.

195. Allen, K.D. and K.A. Athanasiou, *Effect of passage and topography on gene expression of temporomandibular joint disc cells.* Tissue Eng, 2007. **13**(1): p. 101-10.

196. Allen, K.D., K. Erickson, and K.A. Athanasiou, *The effects of protein-coated surfaces on passaged porcine TMJ disc cells.* Arch Oral Biol, 2008. **53**(1): p. 53-9.

197. Allen, K.D. and K.A. Athanasiou, *Growth factor effects on passaged TMJ disk cells in monolayer and pellet cultures.* Orthod Craniofac Res, 2006. **9**(3): p. 143-52.

198. Johns, D.E., M.E. Wong, and K.A. Athanasiou, *Clinically relevant cell sources for TMJ disc engineering.* J Dent Res, 2008. **87**(6): p. 548-52.

199. Johns, D.E. and K.A. Athanasiou, *Growth factor effects on costal chondrocytes for tissue engineering fibrocartilage.* Cell Tissue Res, 2008. **333**(3): p. 439-47.

200. Anderson, D.E. and K.A. Athanasiou, *Passaged goat costal chondrocytes provide a feasible cell source for temporomandibular joint tissue engineering.* Ann Biomed Eng, 2008. **36**(12): p. 1992-2001.

201. Anderson, D.E. and K.A. Athanasiou, *A comparison of primary and passaged chondrocytes for use in engineering the temporomandibular joint.* Arch Oral Biol, 2009. **54**(2): p. 138-45.

202. Hoben, G.M., E.J. Koay, and K.A. Athanasiou, *Fibrochondrogenesis in two embryonic stem cell lines: effects of differentiation timelines.* Stem Cells, 2008. **26**(2): p. 422-30.

203. Hoben, G.M., V.P. Willard, and K.A. Athanasiou, *Fibrochondrogenesis of hESCs: growth factor combinations and cocultures.* Stem Cells Dev, 2009. **18**(2): p. 283-92.

204. Wang, L., et al., *Effect of initial seeding density on human umbilical cord mesenchymal stromal cells for fibrocartilage tissue engineering.* Tissue Eng Part A, 2009. **15**(5): p. 1009-17.

205. Wang, L. and M.S. Detamore, *Insulin-like growth factor-I improves chondrogenesis of predifferentiated human umbilical cord mesenchymal stromal cells.* J Orthop Res, 2009. **27**(8): p. 1109-15.

206. Deng, Y., J.C. Hu, and K.A. Athanasiou, *Isolation and chondroinduction of a dermis-isolated, aggrecan-sensitive subpopulation with high chondrogenic potential.* Arthritis Rheum, 2007. **56**(1): p. 168-76.

207. Puelacher, W.C., et al., *Temporomandibular joint disc replacement made by tissue-engineered growth of cartilage.* J Oral Maxillofac Surg, 1994. **52**(11): p. 1172-7.

208. Hu, J.C. and K.A. Athanasiou, *A self-assembling process in articular cartilage tissue engineering.* Tissue Eng, 2006. **12**(4): p. 969-79.

209. Natoli, R.M., et al., *Effects of multiple chondroitinase ABC applications on tissue engineered articular cartilage.* J Orthop Res, 2009.

210. Deschner, J., B. Rath-Deschner, and S. Agarwal, *Regulation of matrix metalloproteinase expression by dynamic tensile strain in rat fibrochondrocytes.* Osteoarthritis Cartilage, 2006. **14**(3): p. 264-72.

211. Takigawa, M., et al., *Studies on chondrocytes from mandibular condylar cartilage, nasal septal cartilage, and spheno-occipital synchondrosis in culture. I. Morphology, growth, glycosaminoglycan synthesis, and responsiveness to bovine parathyroid hormone (1-34).* J Dent Res, 1984. **63**(1): p. 19-22.

212. Tsubai, T., Y. Higashi, and J.E. Scott, *The effect of epidermal growth factor on the fetal rabbit mandibular condyle and isolated condylar fibroblasts.* Arch Oral Biol, 2000. **45**(6): p. 507-15.

213. Fuentes, M.A., et al., *Regulation of cell proliferation in rat mandibular condylar cartilage in explant culture by insulin-like growth factor-1 and fibroblast growth factor-2.* Arch Oral Biol, 2002. **47**(9): p. 643-54.

214. Bailey, M.M., et al., *A comparison of human umbilical cord matrix stem cells and temporomandibular joint condylar chondrocytes for tissue engineering temporomandibular joint condylar cartilage.* Tissue Eng, 2007. **13**(8): p. 2003-10.

215. Ogawa, T., et al., *Localization and inhibitory effect of basic fibroblast growth factor on chondrogenesis in cultured mouse mandibular condyle.* J Bone Miner Metab, 2003. **21**(3): p. 145-53.

216. Delatte, M.L., et al., *Growth regulation of the rat mandibular condyle and femoral head by transforming growth factor-{beta}1, fibroblast growth factor-2 and insulin-like growth factor-I.* Eur J Orthod, 2005. **27**(1): p. 17-26.

217. Wang, L. and M.S. Detamore, *Effects of growth factors and glucosamine on porcine mandibular condylar cartilage cells and hyaline cartilage cells for tissue engineering applications.* Arch Oral Biol, 2009. **54**(1): p. 1-5.

218. Wang, L., M. Lazebnik, and M.S. Detamore, *Hyaline cartilage cells outperform mandibular condylar cartilage cells in a TMJ fibrocartilage tissue engineering application.* Osteoarthritis Cartilage, 2009. **17**(3): p. 346-53.

219. Chang, J., et al., *Application of alginate three-dimensional culture system for in vitro culture of mandibular condylar chondrocytes from human osteoarthritic temporomandibular joint.* Zhonghua Kou Qiang Yi Xue Za Zhi, 2002. **37**(4): p. 246-8.

220. Suzuki, S., K. Itoh, and K. Ohyama, *Local administration of IGF-I stimulates the growth of mandibular condyle in mature rats.* J Orthod, 2004. **31**(2): p. 138-43.

221. Delatte, M., et al., *Growth stimulation of mandibular condyles and femoral heads of newborn rats by IGF-I.* Arch Oral Biol, 2004. **49**(3): p. 165-75.

222. Zhang, L., et al., *Nanomaterials for improved orthopedic and bone tissue engineering applications*, in *Advanced biomaterials: Fundamentals, processing and applications*, B. Basu, D. Katti, and A. Kumar, Editors. 2009, John Wiley & Sons Inc. p. 205-241.

223. Weng, Y., et al., *Tissue-engineered composites of bone and cartilage for mandible condylar reconstruction.* J Oral Maxillofac Surg, 2001. **59**(2): p. 185-90.

224. Alhadlaq, A. and J.J. Mao, *Tissue-engineered neogenesis of human-shaped mandibular condyle from rat mesenchymal stem cells.* J Dent Res, 2003. **82**(12): p. 951-6.

225. Alhadlaq, A., et al., *Adult stem cell driven genesis of human-shaped articular condyle.* Ann Biomed Eng, 2004. **32**(7): p. 911-23.

226. Alhadlaq, A. and J.J. Mao, *Tissue-engineered osteochondral constructs in the shape of an articular condyle.* J Bone Joint Surg Am, 2005. **87**(5): p. 936-44.

227. Chen, F., et al., *Bone graft in the shape of human mandibular condyle reconstruction via seeding marrow-derived osteoblasts into porous coral in a nude mice model.* J Oral Maxillofac Surg, 2002. **60**(10): p. 1155-9.

228. Ueki, K., et al., *The use of polylactic acid/polyglycolic acid copolymer and gelatin sponge complex containing human recombinant bone morphogenetic protein-2 following condylectomy in rabbits.* J Craniomaxillofac Surg, 2003. **31**(2): p. 107-14.

229. Abukawa, H., et al., *Formation of a mandibular condyle in vitro by tissue engineering.* J Oral Maxillofac Surg, 2003. **61**(1): p. 94-100.

230. Schek, R.M., et al., *Engineered osteochondral grafts using biphasic composite solid free-form fabricated scaffolds.* Tissue Eng, 2004. **10**(9-10): p. 1376-85.

231. Schek, R.M., et al., *Tissue engineering osteochondral implants for temporomandibular joint repair.* Orthod Craniofac Res, 2005. **8**(4): p. 313-9.

232. Hollister, S.J., et al., *An image-based approach for designing and manufacturing craniofacial scaffolds.* Int J Oral Maxillofac Surg, 2000. **29**(1): p. 67-71.

233. Smith, M.H., et al., *Computed tomography-based tissue-engineered scaffolds in craniomaxillofacial surgery.* Int J Med Robot, 2007. **3**(3): p. 207-16.

234. Hollister, S.J., et al., *Engineering craniofacial scaffolds.* Orthod Craniofac Res, 2005. **8**(3): p. 162-73.

235. Adamopoulos, O. and T. Papadopoulos, *Nanostructured bioceramics for maxillofacial applications.* J Mater Sci Mater Med, 2007. **18**(8): p. 1587-97.

236. Catledge, S.A., et al., *Nanostructured ceramics for biomedical implants.* J Nanosci Nanotechnol, 2002. **2**(3-4): p. 293-312.

237. Shin, M., H. Yoshimoto, and J.P. Vacanti, *In vivo bone tissue engineering using mesenchymal stem cells on a novel electrospun nanofibrous scaffold.* Tissue Eng, 2004. **10**(1-2): p. 33-41.

238. Srouji, S., et al., *Mandibular defect repair by TGF-beta and IGF-1 released from a biodegradable osteoconductive hydrogel.* J Craniomaxillofac Surg, 2005. **33**(2): p. 79-84.

239. Gothard, D., et al., *Engineering Embryonic Stem Cell Aggregation Allows an Enhanced Osteogenic Differentiation In Vitro.* Tissue Eng Part C Methods, 2009.

240. Darling, E.M. and K.A. Athanasiou, *Articular cartilage bioreactors and bioprocesses.* Tissue Eng, 2003. **9**(1): p. 9-26.

241. Hoben, G.M., E.J. Koay, and K.A. Athanasiou, *Fibrochondrogenesis in two embryonic stem cell lines: Effects of differentiation timelines.* Stem Cells, 2007. **In press**.

242. Rao, B.M. and P.W. Zandstra, *Culture development for human embryonic stem cell propagation: molecular aspects and challenges.* Curr Opin Biotechnol, 2005. **16**(5): p. 568-76.

243. Thomson, J.A., et al., *Embryonic stem cell lines derived from human blastocysts.* Science, 1998. **282**(5391): p. 1145-7.

244. Jaenisch, R., *Human cloning - the science and ethics of nuclear transplantation.* N Engl J Med, 2004. **351**(27): p. 2787-91.

245. Civin, C.I. and M.S. Rao, *How many human embryonic stem cell lines are sufficient? A U.S. perspective.* Stem Cells, 2006. **24**(4): p. 800-3.

246. Khoo, M.L., et al., *Growth and differentiation of embryoid bodies derived from human embryonic stem cells: effect of glucose and basic fibroblast growth factor.* Biol Reprod, 2005. **73**(6): p. 1147-56.

247. Johnstone, B., et al., *In vitro chondrogenesis of bone marrow-derived mesenchymal progenitor cells.* Exp Cell Res, 1998. **238**(1): p. 265-72.

248. Mackay, A.M., et al., *Chondrogenic differentiation of cultured human mesenchymal stem cells from marrow.* Tissue Eng, 1998. **4**(4): p. 415-28.

249. Yoo, J.U., et al., *The chondrogenic potential of human bone-marrow-derived mesenchymal progenitor cells.* J Bone Joint Surg Am, 1998. **80**(12): p. 1745-57.

250. Levenberg, S., et al., *Differentiation of human embryonic stem cells on three-dimensional polymer scaffolds.* Proc Natl Acad Sci U S A, 2003. **100**(22): p. 12741-6.

251. Toh, W.S., et al., *Effects of culture conditions and bone morphogenetic protein 2 on extent of chondrogenesis from human embryonic stem cells.* Stem Cells, 2007. **25**(4): p. 950-60.

252. Koay, E.J., G.M. Hoben, and K.A. Athanasiou, *Tissue Engineering with Chondrogenically-differentiated Human Embryonic Stem Cells.* Stem Cells, 2007.

253. Kim, M.S., et al., *Musculoskeletal differentiation of cells derived from human embryonic germ cells.* Stem Cells, 2005. **23**(1): p. 113-23.

254. Hwang, N.S., et al., *Chondrogenic differentiation of human embryonic stem cell-derived cells in arginine-glycine-aspartate-modified hydrogels.* Tissue Eng, 2006. **12**(9): p. 2695-706.

255. Hwang, N.S., et al., *Effects of three-dimensional culture and growth factors on the chondrogenic differentiation of murine embryonic stem cells.* Stem Cells, 2006. **24**(2): p. 284-91.

256. zur Nieden, N.I., et al., *Induction of chondro-, osteo- and adipogenesis in embryonic stem cells by bone morphogenetic protein-2: effect of cofactors on differentiating lineages.* BMC Dev Biol, 2005. **5**(1): p. 1.

257. Hegert, C., et al., *Differentiation plasticity of chondrocytes derived from mouse embryonic stem cells.* J Cell Sci, 2002. **115**(Pt 23): p. 4617-28.

258. Kramer, J., et al., *Embryonic stem cell-derived chondrogenic differentiation in vitro: activation by BMP-2 and BMP-4.* Mech Dev, 2000. **92**(2): p. 193-205.

259. Nakayama, N., et al., *Macroscopic cartilage formation with embryonic stem-cell-derived mesodermal progenitor cells.* J Cell Sci, 2003. **116**(Pt 10): p. 2015-28.

260. Warzecha, J., et al., *Sonic hedgehog protein promotes proliferation and chondrogenic differentiation of bone marrow-derived mesenchymal stem cells in vitro.* J Orthop Sci, 2006. **11**(5): p. 491-6.

261. Enomoto-Iwamoto, M., et al., *Hedgehog proteins stimulate chondrogenic cell differentiation and cartilage formation.* J Bone Miner Res, 2000. **15**(9): p. 1659-68.

262. Estes, B.T., A.W. Wu, and F. Guilak, *Potent induction of chondrocytic differentiation of human adipose-derived adult stem cells by bone morphogenetic protein 6.* Arthritis Rheum, 2006. **54**(4): p. 1222-32.

263. Hennig, T., et al., *Reduced chondrogenic potential of adipose tissue derived stromal cells correlates with an altered TGFbeta receptor and BMP profile and is overcome by BMP-6.* J Cell Physiol, 2007. **211**(3): p. 682-91.

264. Indrawattana, N., et al., *Growth factor combination for chondrogenic induction from human mesenchymal stem cell.* Biochem Biophys Res Commun, 2004. **320**(3): p. 914-9.

265. Vats, A., et al., *Chondrogenic differentiation of human embryonic stem cells: the effect of the micro-environment.* Tissue Eng, 2006. **12**(6): p. 1687-97.

266. Richardson, S.M., et al., *Intervertebral disc cell-mediated mesenchymal stem cell differentiation.* Stem Cells, 2006. **24**(3): p. 707-16.

267. Le Visage, C., et al., *Interaction of human mesenchymal stem cells with disc cells: changes in extracellular matrix biosynthesis.* Spine, 2006. **31**(18): p. 2036-42.

268. Vanderploeg, E.J., C.G. Wilson, and M.E. Levenston. *Immunolocalization of typle VI collagen in the bovine meniscus* in *52 nd Annual Meeting of the Orthopaedic Research Society.* 2006. Chicago, IL.

269. Wildey, G.M. and C.A. McDevitt, *Matrix protein mRNA levels in canine meniscus cells in vitro.* Arch Biochem Biophys, 1998. **353**(1): p. 10-5.

270. Carvalho, H.F., et al., *Identification, content, and distribution of type VI collagen in bovine tendons.* Cell Tissue Res, 2006. **325**(2): p. 315-24.

271. Quarto, R., et al., *Modulation of commitment, proliferation, and differentiation of chondrogenic cells in defined culture medium.* Endocrinology, 1997. **138**(11): p. 4966-76.

272. Graycar, J.L., et al., *Human transforming growth factor-beta 3: recombinant expression, purification, and biological activities in comparison with transforming growth factors-beta 1 and -beta 2.* Mol Endocrinol, 1989. **3**(12): p. 1977-86.

273. Ng, E.S., et al., *Forced aggregation of defined numbers of human embryonic stem cells into embryoid bodies fosters robust, reproducible hematopoietic differentiation.* Blood, 2005. **106**(5): p. 1601-3.

274. Burridge, P.W., et al., *Improved human embryonic stem cell embryoid body homogeneity and cardiomyocyte differentiation from a novel V-96 plate aggregation system highlights interline variability.* Stem Cells, 2007. **25**(4): p. 929-38.

275. Ataliotis, P., *Platelet-derived growth factor A modulates limb chondrogenesis both in vivo and in vitro.* Mech Dev, 2000. **94**(1-2): p. 13-24.

276. Majumdar, M.K., et al., *Isolation, characterization, and chondrogenic potential of human bone marrow-derived multipotential stromal cells.* J Cell Physiol, 2000. **185**(1): p. 98-106.

277. Barbero, A., et al., *Expansion on specific substrates regulates the phenotype and differentiation capacity of human articular chondrocytes.* J Cell Biochem, 2006. **98**(5): p. 1140-9.

278. Rosner, B., *Fundamentals of Biostatistics.* 5th ed. 2000, Pacific Grove, CA: Brooks/Cole.

279. Kawaguchi, J., P.J. Mee, and A.G. Smith, *Osteogenic and chondrogenic differentiation of embryonic stem cells in response to specific growth factors.* Bone, 2005. **36**(5): p. 758-69.

280. Alvarez, J., et al., *TGFbeta2 mediates the effects of hedgehog on hypertrophic differentiation and PTHrP expression.* Development, 2002. **129**(8): p. 1913-24.

281. Heberlein, U., T. Wolff, and G.M. Rubin, *The TGF beta homolog dpp and the segment polarity gene hedgehog are required for propagation of a morphogenetic wave in the Drosophila retina.* Cell, 1993. **75**(5): p. 913-26.

282. Murtaugh, L.C., J.H. Chyung, and A.B. Lassar, *Sonic hedgehog promotes somitic chondrogenesis by altering the cellular response to BMP signaling.* Genes Dev, 1999. **13**(2): p. 225-37.

283. Sekiya, I., et al., *Comparison of effect of BMP-2, -4, and -6 on in vitro cartilage formation of human adult stem cells from bone marrow stroma.* Cell Tissue Res, 2005. **320**(2): p. 269-76.

284. Sekiya, I., et al., *In vitro cartilage formation by human adult stem cells from bone marrow stroma defines the sequence of cellular and molecular events during chondrogenesis.* Proc Natl Acad Sci U S A, 2002. **99**(7): p. 4397-402.

285. Hwang, N.S., et al., *Morphogenetic signals from chondrocytes promote chondrogenic and osteogenic differentiation of mesenchymal stem cells.* J Cell Physiol, 2007. **212**(2): p. 281-4.

286. Richmon, J.D., et al., *Effect of growth factors on cell proliferation, matrix deposition, and morphology of human nasal septal chondrocytes cultured in monolayer.* Laryngoscope, 2005. **115**(9): p. 1553-60.

287. Pound, J.C., et al., *Strategies to promote chondrogenesis and osteogenesis from human bone marrow cells and articular chondrocytes encapsulated in polysaccharide templates.* Tissue Eng, 2006. **12**(10): p. 2789-99.

288. Rousche, K.T. and C.B. Knudson, *Temporal expression of CD44 during embryonic chick limb development and modulation of its expression with retinoic acid.* Matrix Biol, 2002. **21**(1): p. 53-62.

289. Knudson, C.B., et al., *The chondrocyte pericellular matrix: a model for hyaluronan-mediated cell-matrix interactions.* Biochem Soc Trans, 1999. **27**(2): p. 142-7.

290. Knudson, C.B., *Hyaluronan and CD44: strategic players for cell-matrix interactions during chondrogenesis and matrix assembly.* Birth Defects Res C Embryo Today, 2003. **69**(2): p. 174-96.

291. Grogan, S.P., et al., *Identification of markers to characterize and sort human articular chondrocytes with enhanced in vitro chondrogenic capacity.* Arthritis Rheum, 2007. **56**(2): p. 586-95.

292. Guilak, F. and V.C. Mow, *The mechanical environment of the chondrocyte: a biphasic finite element model of cell-matrix interactions in articular cartilage.* J Biomech, 2000. **33**(12): p. 1663-73.

293. Wang, N., J.P. Butler, and D.E. Ingber, *Mechanotransduction across the cell surface and through the cytoskeleton.* Science, 1993. **260**(5111): p. 1124-7.

294. Titushkin, I. and M. Cho, *Modulation of cellular mechanics during osteogenic differentiation of human mesenchymal stem cells.* Biophys J, 2007. **93**(10): p. 3693-702.

295. Darling, E.M., et al., *Viscoelastic properties of human mesenchymally-derived stem cells and primary osteoblasts, chondrocytes, and adipocytes.* J Biomech, 2008. **41**(2): p. 454-64.

296. Darling, E.M., S. Zauscher, and F. Guilak, *Viscoelastic properties of zonal articular chondrocytes measured by atomic force microscopy.* Osteoarthritis Cartilage, 2006. **14**(6): p. 571-9.

297. Sato, M., et al., *Application of the micropipette technique to the measurement of cultured porcine aortic endothelial cell viscoelastic properties.* J Biomech Eng, 1990. **112**(3): p. 263-8.

298. Koay, E.J., A.C. Shieh, and K.A. Athanasiou, *Creep indentation of single cells.* J Biomech Eng, 2003. **125**(3): p. 334-41.

299. Leipzig, N.D. and K.A. Athanasiou, *Unconfined creep compression of chondrocytes.* J Biomech, 2005. **38**(1): p. 77-85.

300. McBeath, R., et al., *Cell shape, cytoskeletal tension, and RhoA regulate stem cell lineage commitment.* Dev Cell, 2004. **6**(4): p. 483-95.

301. Carter, D.R., et al., *The mechanobiology of articular cartilage development and degeneration.* Clin Orthop Relat Res, 2004(427 Suppl): p. S69-77.

302. Schumann, D., et al., *Mechanobiological conditioning of stem cells for cartilage tissue engineering.* Biomed Mater Eng, 2006. **16**(4 Suppl): p. S37-52.

303. Terraciano, V., et al., *Differential response of adult and embryonic mesenchymal progenitor cells to mechanical compression in hydrogels.* Stem Cells, 2007. **25**(11): p. 2730-8.

304. Wu, C.C., et al., *Synergism of biochemical and mechanical stimuli in the differentiation of human placenta-derived multipotent cells into endothelial cells.* J Biomech, 2008. **41**(4): p. 813-21.

305. Koay, E.J., G.M. Hoben, and K.A. Athanasiou, *Tissue engineering with chondrogenically differentiated human embryonic stem cells.* Stem Cells, 2007. **25**(9): p. 2183-90.

306. Shieh, A.C. and K.A. Athanasiou, *Dynamic compression of single cells.* Osteoarthritis Cartilage, 2007. **15**(3): p. 328-34.

307. Leipzig, N.D. and K.A. Athanasiou, *Static compression of single chondrocytes catabolically modifies single-cell gene expression.* Biophys J, 2008. **94**(6): p. 2412-22.

308. Koay, E.J., G. Ofek, and K.A. Athanasiou, *Effects of TGF-beta1 and IGF-I on the compressibility, biomechanics, and strain-dependent recovery behavior of single chondrocytes.* J Biomech, 2008. **41**(5): p. 1044-52.

309. Itskovitz-Eldor, J., et al., *Differentiation of human embryonic stem cells into embryoid bodies compromising the three embryonic germ layers.* Mol Med, 2000. **6**(2): p. 88-95.

310. Pawlowski, A., et al., *Cell fractions from rat rib growth cartilage. Biochemical characterization of matrix molecules.* Exp Cell Res, 1986. **164**(1): p. 211-22.

311. Min, B.H., et al., *Characterization of subpopulated articular chondrocytes separated by Percoll density gradient.* In Vitro Cell Dev Biol Anim, 2002. **38**(1): p. 35-40.

312. Wong, M. and R.S. Tuan, *Interactive cellular modulation of chondrogenic differentiation in vitro by subpopulations of chick embryonic calvarial cells.* Dev Biol, 1995. **167**(1): p. 130-47.

313. Zhang, S.C., et al., *In vitro differentiation of transplantable neural precursors from human embryonic stem cells.* Nat Biotechnol, 2001. **19**(12): p. 1129-33.

314. Patella, V., et al., *Human heart mast cells. Isolation, purification, ultrastructure, and immunologic characterization.* J Immunol, 1995. **154**(6): p. 2855-65.

315. Shieh, A.C. and K.A. Athanasiou, *Biomechanics of single zonal chondrocytes.* J Biomech, 2006. **39**(9): p. 1595-602.

316. Leipzig, N.D., S.V. Eleswarapu, and K.A. Athanasiou, *The effects of TGF-beta1 and IGF-I on the biomechanics and cytoskeleton of single chondrocytes.* Osteoarthritis Cartilage, 2006.

317. Rosenberg, L., *Chemical basis for the histological use of safranin O in the study of articular cartilage.* J Bone Joint Surg Am, 1971. **53**(1): p. 69-82.

318. Angele, P., et al., *Cyclic hydrostatic pressure enhances the chondrogenic phenotype of human mesenchymal progenitor cells differentiated in vitro.* J Orthop Res, 2003. **21**(3): p. 451-7.

319. Taqvi, S. and K. Roy, *Influence of scaffold physical properties and stromal cell coculture on hematopoietic differentiation of mouse embryonic stem cells.* Biomaterials, 2006. **27**(36): p. 6024-31.

320. Blain, E.J., et al., *Disassembly of the vimentin cytoskeleton disrupts articular cartilage chondrocyte homeostasis.* Matrix Biol, 2006. **25**(7): p. 398-408.

321. Brown, P.D. and P.D. Benya, *Alterations in chondrocyte cytoskeletal architecture during phenotypic modulation by retinoic acid and dihydrocytochalasin B-induced reexpression.* J Cell Biol, 1988. **106**(1): p. 171-9.

322. Loty, S., et al., *Cytochalasin D induces changes in cell shape and promotes in vitro chondrogenesis: a morphological study.* Biol Cell, 1995. **83**(2-3): p. 149-61.

323. Vinall, R.L., S.H. Lo, and A.H. Reddi, *Regulation of articular chondrocyte phenotype by bone morphogenetic protein 7, interleukin 1, and cellular context is dependent on the cytoskeleton.* Exp Cell Res, 2002. **272**(1): p. 32-44.

324. Trickey, W.R., T.P. Vail, and F. Guilak, *The role of the cytoskeleton in the viscoelastic properties of human articular chondrocytes.* J Orthop Res, 2004. **22**(1): p. 131-9.

325. Mow, V.C. and A. Ratcliffe, *Structure and function of articular cartilage and meniscus*, in *Basic Orthopaedic Biomechanics*, V.C. Mow and W.C. Hayes, Editors. 1997, Lippincott-Raven: Philadelphia. p. 113-177.

326. Adams, J.D., U. Kim, and H.T. Soh, *Multitarget magnetic activated cell sorter.* Proc Natl Acad Sci U S A, 2008. **105**(47): p. 18165-70.

327. Fickert, S., J. Fiedler, and R.E. Brenner, *Identification of subpopulations with characteristics of mesenchymal progenitor cells from human osteoarthritic cartilage using triple staining for cell surface markers.* Arthritis Res Ther, 2004. **6**(5): p. R422-32.

328. AufderHeide, A.C. and K.A. Athanasiou, *Mechanical stimulation toward tissue engineering of the knee meniscus.* Ann Biomed Eng, 2004. **32**(8): p. 1161-74.

329. Freeman, P.M., et al., *Chondrocyte cells respond mechanically to compressive loads.* J Orthop Res, 1994. **12**(3): p. 311-20.

330. Alexopoulos, L.G., L.A. Setton, and F. Guilak, *The biomechanical role of the chondrocyte pericellular matrix in articular cartilage.* Acta Biomater, 2005. **1**(3): p. 317-25.

331. D'Andrea, P., et al., *Intercellular Ca2+ waves in mechanically stimulated articular chondrocytes.* Biorheology, 2000. **37**(1-2): p. 75-83.

332. Trickey, W.R., G.M. Lee, and F. Guilak, *Viscoelastic properties of chondrocytes from normal and osteoarthritic human cartilage.* J Orthop Res, 2000. **18**(6): p. 891-8.

333. Zhang, L., J. Hu, and K.A. Athanasiou, *The role of tissue engineering in articular cartilage repair and regeneration.* Crit Rev Biomed Eng, 2009. **37**(1-2): p. 1-57.

334. Hollander, A.P., S.C. Dickinson, and W. Kafienah, *Stem cells and cartilage development: complexities of a simple tissue.* Stem Cells, 2010. **28**(11): p. 1992-6.

335. Toh, W.S., E.H. Lee, and T. Cao, *Potential of Human Embryonic Stem Cells in Cartilage Tissue Engineering and Regenerative Medicine.* Stem Cell Rev, 2010.

336. Koay, E.J. and K.A. Athanasiou, *Hypoxic chondrogenic differentiation of human embryonic stem cells enhances cartilage protein synthesis and biomechanical functionality.* Osteoarthritis Cartilage, 2008. **16**(12): p. 1450-6.

337. Koay, E.J. and K.A. Athanasiou, *Development of serum-free, chemically defined conditions for human embryonic stem cell-derived fibrochondrogenesis.* Tissue Eng Part A, 2009. **15**(8): p. 2249-57.

338. Hwang, N.S., et al., *In vivo commitment and functional tissue regeneration using human embryonic stem cell-derived mesenchymal cells.* Proc Natl Acad Sci U S A, 2008. **105**(52): p. 20641-6.

339. Hwang, N.S., et al., *Enhanced chondrogenic differentiation of murine embryonic stem cells in hydrogels with glucosamine.* Biomaterials, 2006. **27**(36): p. 6015-23.

340. Toh, W.S., et al., *Cartilage repair using hyaluronan hydrogel-encapsulated human embryonic stem cell-derived chondrogenic cells.* Biomaterials, 2010. **31**(27): p. 6968-80.

341. Hwang, N.S., S. Varghese, and J. Elisseeff, *Derivation of chondrogenically-committed cells from human embryonic cells for cartilage tissue regeneration.* PLoS One, 2008. 3(6): p. e2498.

342. Oldershaw, R.A., et al., *Directed differentiation of human embryonic stem cells toward chondrocytes.* Nat Biotechnol, 2010. **28**(11): p. 1187-94.

343. Hwang, Y.S., J.M. Polak, and A. Mantalaris, *In vitro direct chondrogenesis of murine embryonic stem cells by bypassing embryoid body formation.* Stem Cells Dev, 2008. **17**(5): p. 971-8.

344. Huey, D.J., J.C. Hu, and K.A. Athanasiou, *Chondrogenically-tuned expansion enhances the cartilaginous matrix forming capabilities of primary, adult, leporine chondrocytes in the self-assembly modality.* Tissue Eng, 2011. **In Press**.

345. Gunja, N.J., et al., *Effects of agarose mould compliance and surface roughness on self-assembled meniscus-shaped constructs.* J Tissue Eng Regen Med, 2009. **3**(7): p. 521-30.

346. Huey, D.J. and K.A. Athanasiou, *Maturational growth of self-assembled, functional menisci as a result of TGF-beta1 and enzymatic chondroitinase-ABC stimulation.* Biomaterials, 2011. **32**(8): p. 2052-8.

347. Riekstina, U., et al., *Embryonic stem cell marker expression pattern in human mesenchymal stem cells derived from bone marrow, adipose tissue, heart and dermis.* Stem Cell Rev, 2009. **5**(4): p. 378-86.

348. Gang, E.J., et al., *SSEA-4 identifies mesenchymal stem cells from bone marrow.* Blood, 2007. **109**(4): p. 1743-51.

349. Loeser, R.F., et al., *Integrin expression by primary and immortalized human chondrocytes: evidence of a differential role for alpha1beta1 and alpha2beta1 integrins in mediating chondrocyte adhesion to types II and VI collagen.* Osteoarthritis Cartilage, 2000. **8**(2): p. 96-105.

350. Imabayashi, H., et al., *Redifferentiation of dedifferentiated chondrocytes and chondrogenesis of human bone marrow stromal cells via chondrosphere formation with expression profiling by large-scale cDNA analysis.* Exp Cell Res, 2003. **288**(1): p. 35-50.

351. Mandl, E.W., et al., *Serum-free medium supplemented with high-concentration FGF2 for cell expansion culture of human ear chondrocytes promotes redifferentiation capacity.* Tissue Eng, 2002. **8**(4): p. 573-80.

352. Yokoyama, A., et al., *FGF2 and dexamethasone increase the production of hyaluronan in two-dimensional culture of elastic cartilage-derived cells:*

in vitro analyses and in vivo cartilage formation. Cell Tissue Res, 2007. **329**(3): p. 469-78.

353.   Jakob, M., et al., *Specific growth factors during the expansion and redifferentiation of adult human articular chondrocytes enhance chondrogenesis and cartilaginous tissue formation in vitro.* J Cell Biochem, 2001. **81**(2): p. 368-77.

354.   Martin, I., et al., *Mammalian chondrocytes expanded in the presence of fibroblast growth factor 2 maintain the ability to differentiate and regenerate three-dimensional cartilaginous tissue.* Exp Cell Res, 1999. **253**(2): p. 681-8.

355.   Murakami, S., et al., *Up-regulation of the chondrogenic Sox9 gene by fibroblast growth factors is mediated by the mitogen-activated protein kinase pathway.* Proc Natl Acad Sci U S A, 2000. **97**(3): p. 1113-8.